Abnormalization of Tumor Vessels to Improve the Efficacy of Chemotherapy

Ann L. B. Seynhaeve

Abnormalization of Tumor Vessels to Improve the Efficacy of Chemotherapy

Abnormaliseren van tumor vaten voor een efficiëntere chemotherapie

THESIS
to obtain the degree of Doctor from the
Erasmus University Rotterdam
by command of the rector magnificus
Prof.dr. S.W.J. Lamberts
and according to the decision of the Doctorate Board

The public defence shall be held on
5 november 2008 at 9.45 hours
by

Ann Lucienne Bertha Seynhaeve
born at Kortrijk – Belgium

DOCTORAL COMMITEE

Promotor:	Prof.dr. A.M.M. Eggermont
Other Members:	Prof.dr. L.H.J. Looijenga Prof.dr.ir. M. de Jong Prof.dr. G. Storm
Copromotor:	Dr. T.L.M. ten Hagen

Garfield: "The most active thing about me is my imagination"
Einstein: "Imagination is more importation than knowledge"

Contents

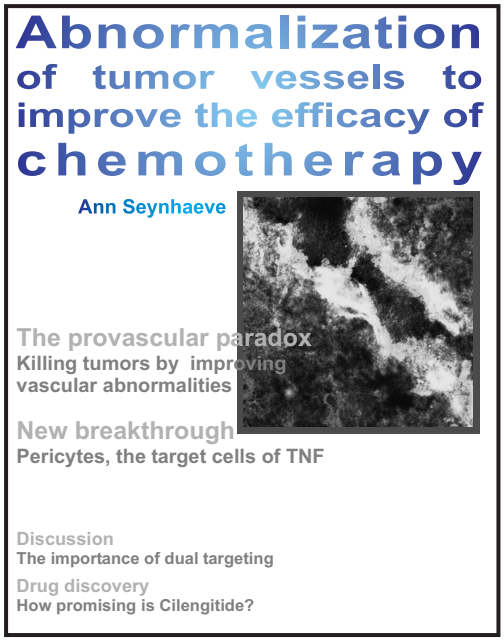

"The typical and normal characteristics of the vasculature is not present in the abnormal vasculature and can if manipulated develop further towards abnormality and provide a porte d'entrée for chemotherapeutic drugs."
- Dr. T.L.M. ten Hagen

Part 1 - Vascular abnormalization: tumor response

Part 2 - Vascular abnormalization: *In vitro* study

Part 3 - Vascular abnormalization: *In vivo* study

Part 4 - General discussion

Also

General introduction

Chapter 1

General introduction

Additional information

General introduction

INTRODUCTION TO THE THESIS

The antitumor effects of chemotherapeutics *in vitro* are often not matched by antitumor effects *in vivo* after systemic administration of these agents in animal models or in patients. Achieving an adequate drug concentration at the tumor site is a major challenge as drugs are dilated after systemic administration and rapidly cleared by liver and kidney. Dose-escalation is limited by toxicity to normal tissues, such as bone marrow, liver, kidney, hart, gastrointestinal track and the neural system. Pathophysiologic properties of tumor and the tumor-associated vasculature provide a number of barriers to adequate drug uptake at the tumor site. High interstitial fluid pressure (IFP), functional and non-functional tumor vessels and inadequate blood supply makes the intratumoral drug distribution and drug uptake very heterogeneous [1]. The amount of drug reaching the tumor cell is therefore insufficient to eradicate the tumor. There are however additional important targets for antitumor agents. Tumors consist of tumor cells and tumor stroma; endothelial cells (ECs), pericytes, immune cells and matrix composition These components are just as important in tumor biology and provide important targets for anticancer therapy.

The organization of normal blood vessels. Blood vessels consist of an endothelial cell lining surrounded by vascular mural cells (smooth muscle cells or pericytes), and a basal membrane enveloping both cells. ECs form the inner lining of a blood vessel providing a dynamic barrier between the underlying tissue and the blood. They regulate blood flow, thrombosis, thrombolysis and platelet adherence and play a key role in immune and inflammatory reactions by interacting with leucocytes. ECs can vary between organs and between arteries and veins not only expressing different markers but also responding differently to the same stimuli [2-4]. In established vessels adhesion between neighboring ECs is made by three types of junctional adhesions: adherens junctions, tight junctions and gap junctions [5]. Vascular endothelial (VE) cadherin, the primary component of the adherens junctions, is a member of the cadherin membrane receptor family involved in the calcium-dependent homophilic cell-cell interactions of its extracellular domain and is strictly located at the intercellular junctions of ECs. Intracellularly VE-cadherin is connected to the actin cytoskeleton via several catenin proteins, like α-catenin, β-catenin, γ-catenin (also referred to as plakoglobin) and p120. Mice were generated that lack VE-cadherin expression or express a mutant VE-cadherin lacking the beta-catenin cytoplasmic binding site to define the role of VE-cadherin *in vivo*. Both mutations lead to embryonic lethality within the early days of development due to lack of vessel development suggesting that VE-cadherin and its association with beta-catenin is requires for sprouting and adherens of ECs during early angiogenesis [6,7].

Smooth muscle cells and pericytes are assumed to belong to the same lineage. However, a good distinction is often difficult because some vessels, like arterioles and venules, have mural cells with properties between smooth muscle cells and pericytes. Also, there is no single common marker available to define a pericyte. Desmin, alpha smooth muscle actin and the high-molecular-weight melanoma-associated antigen (the mouse derivate is called NG2) are proteins used to identify pericytes but the expression varies between species, organs and pathological conditions [8,9]. The smooth muscle cells can be distinguished from the pericytes through their position in relation to the vessels. Vascular smooth muscle cells are not in direct contact with the ECs but are separated from the endothelium by the basal membrane. Pericytes are embedded in the basal lamina and make direct contact with the ECs by peg-socket contact and junctions [10-14]. There is still a lot controversy about the exact role of the pericytes. They have been suggested to sup-

press endothelial proliferation without having a role during the initial steps in angiogenesis. However reports have been published of pericytes lying in front of a sprouting endothelial cell [15].

Surrounding the vascular cells is the basal membrane, a self-assembled complex sheet-like structure providing structural support and regulating cell behavior. It consists of about 50 proteins although type IV collagen, laminin, heparan-sulphate proteoglycans and nidogen/entactin are the dominant components. Different isoforms of these proteins, quantity and assembly provides specificity making the composition of the basal membrane unique in each tissue [16-19]. ECs adhere to the underlying extracellular matrix (ECM) by a diverse family of integrins. Integrins are glycoproteins, consisting of an α- and a β-subunit, which forms heterodimeric receptors for the extracellular matrix. There are 18 α- and 8 β-units and each formed integrin has a unique set of ECM ligands. αVβ3, one of the most important integrins in ECs adhesion binds to fibronectin, collagen, vitronectin, and fibrinogen whereas αVβ5 binds predominantly to vitronectin [20]. The αV integrins are important in the formation of new blood vessels. They appear to be de-novo induced and activated on tumor angiogenic endothelia [21] and promote endothelial cell attachment, spreading, survival, proliferation and locomotion [22-25]. αV integrins, in particular αVβ3 and αVβ5, have been considered as therapeutic targets to inhibit angiogenesis [21].

The organization of tumor blood vessels. Tumor-associated vasculature (TAV) is "abnormal" in many aspects in comparison to normal vessels. The TAV display a lack of hierarchical branching organization in which the recognizable features of arterioles, capillaries and venules is lost. Vessels are tortuous and unevenly dilated. As a result, tumor blood flow is chaotic, can be stationary and even change direction. This leads to hypoperfusion, hypoxia and acidosis in solid tumors. Tumor-associated ECs are disorganized with irregular shape, sometime even overlapping each other or displaying fenestrae [26]. These intracellular openings make the vessel highly permeable and allow passage of macromolecules across the vasculature. Also, vesicles can form at the luminal side of the ECs fusing with the abluminal membrane releasing the content in the subendothelial space. The transcellular pathway is also mediated by vesiculo-vacuolar organelles (VVOs) [27-29]. These are clusters of interconnecting vacuoles in the cytoplasm of an EC transporting molecules form the luminal plasma membrane to the abluminal side. Permeability increase subsequently results in an increased IFP. This overall rise in IFP is further enhanced by the absence of functional lymphatics, typical in the tumor environment. Pericytes have long been neglected as important in angiogenesis and even believed to be absent in the tumor vasculature. However, pericytes are present in the tumor microenvironment and like the ECs, they have bizarre features not found in other conditions. In general, tumor-associated pericytes are irregularly scattered, sometimes overlapping other pericytes and loosely associated with the vessel endothelium. They display several extensions along the endothelium or into the tumor stroma occasionally contacting other vessels [30]. Also, the basal membrane has a loose association with ECs and pericytes, irregular thickness and extensions into the stroma [31]. The TAV varies greatly among tumor types. Eberhard quantified maturation in glioblastoma and 5 different carcinoma's and found that microvessel pericyte coverage ranges form 10 to 20 % in glioblastoma and renal cell carcinoma to approximately 65 % in mammary and colon carcinomas [32]

The antiangiogenic and antivascular approach. In 1971 Folkman proposed that inhibition of the development of newly formed tumor blood vessels would be an attractive new approach in cancer treatment [33]. Starving the tumor to death by depriving it from the inflow of nutrients with the use of vascular targeting agents was in theory a strait forward approach. Putting the theory in practice proved not so simple, but this idea leads to several strategies focusing on the specific pathway or characteristics of the TAV. First, the antiangiogenesis strategies interfere with the formation of new tumor blood vessel formation. Growth factors are important in this process

and vascular endothelial growth factor (VEGF) is believed to be the most important factor. It is an important mitogen for vascular ECs, mediates secretion and activation of enzymes that contributes to the degradation of the extracellular matrix and increases vascular permeability [34-37]. One prominent success in antiangiogenic cancer therapy is bevacizumab (Avastin), an antibody that neutralizes the activity of all isoforms of the VEGF-A molecule. [38]. Pre-clinical studies have shown that anti-VEGF therapy besides prohibiting vessel growth, also improve the integrity of remaining vessels bringing them to a more "normalized" structure. Pericytes are recruited especially to the tumor vessels and not to the normal vasculature. Alongside reinforcing the vessels with pericytes, matrix metalloproteinases are produced reducing the abnormal thick multilayer basal membrane. This is then followed by a reduction in IFP and an increase in oxygenation that leads to a better penetration of co-administered chemo- or radiotherapy [39,40]. Evidence for this normalization strategy has also been demonstrated recently in glioblastoma patients treated with AZD2171 (cediranab), a tyrosine kinase inhibitor of VEGF receptors. Daily administration of the inhibitor induced vascular normalization within 24 hours and lasted at least 28 days [41].

A second approach is to cause direct damage of the established tumor vasculature by vascular disrupting agents (VDAs). Although the VDAs have often been grouped with the antiangiogenic agents their working mechanism is quite different. In contrast to the antiangiogenic agents that prevent formation of new blood vessels, the VDAs target the already established TAV by destroying the endothelial lining. This causes shutdown of blood flow, deprivation of oxygen and nutrients resulting in massive tumor necrosis. This concept was formally proposed when Denekamp *et al*. suggested that the high proliferation rate of the tumor-associated ECs could be a potential target [42]. They demonstrated that occlusion of the blood supply in a subcutaneously implanted tumor resulted in tumor regression and long-term tumor control. VDAs can be divided in ligand bound and small molecules agents. Ligand bound VDAs are usually antibodies or peptides directed against a marker selectively upregulated on tumor-associated ECs and requires an intensive knowledge and identification of suitable targets on the (human) tumor endothelium [43]. In contradiction, small molecule VDAs subdivided in tubulin-binding agents and flavonoids have no specific selectivity. Because of the high turnover in the tumor endothelium, these dividing immature ECs rely on their tubulin cytoskeleton network to maintain shape and integrity. Tubulin-binding VDAs inhibit tubulin polymerization and change the shape of the ECs. These changes dramatically alters vascular permeability and blood flow inducing hemorrhage and coagulation [44,45]. The antivascular effects of flavoids are mediated via the release of vasoactive components like TNF, serotonin and nitric oxide leading to apotosis of ECs, increased permeability and IFP resulting in vascular collapse and tumor necrosis [46-49]

The provascular approach. In contrast to the other strategies that both attack the vasculature this approach is rather counter-intuitive. In this strategy the choice of a chemotherapeutic agent depends on its efficacy in killing the tumor cells. However, as mentioned above reaching the appropriate toxic levels at the site of the tumor cells is a major problem. For successful treatment the chemotherapeutic drug has to be accompanied by an agent that does not necessarily have a toxic effect but serves as a facilitator to improve the bioavalability of the drug. Agents such as TNF, histamine and interleukin-2 have been demonstrated to increase the intratumoral concentration of chemotherapy [50-55]. Especially the use of TNF has been very successful and many studies have been performed to elucidate its mechanism. The isolated limb perfusion (ILP) is a treatment for malignancies of the extremities in which the tumor-bearing extremity is isolated form the patient's circulatory system, connected to a heart-lung machine and perfused with cytotoxic agents. This achieves very high loco-regional drug levels with minimal systemic exposure to the drug and thus no systemic toxicity. The combination of TNF and melphalan in the ILP results in an increased tumor response in patients with in-transit melanoma metastases or locally advanced soft-tissue

sarcomas compared to ILP with melphalan alone without the toxic side effects. [56]. These results led to the approval of TNF by the European Medicine Evaluation Agency and TNF-based ILP has become the standard treatment for patients with in-transit melanoma and non-resectable sarcomas of the extremities. The majority of the patients can thus be spared an amputation [57,58]. We observed that with the administration of TNF there is an increased accumulation of the cytotoxic drug in the tumor [59,60]. Histopathologically, hemorrhagic necrosis was found after perfusion with both drugs. Almost directly after perfusion, platelet aggregation and damage to the ECs was found. It has also been showed previously that leucocytes play an important roll in the tumor response [61]. Systemic treatment with low-dose TNF in combination with liposomal encapsulated doxorubicin (Doxil) in tumor-bearing animals resulted in an improved tumor response compared to treatment with Doxil alone [50,62]. In this setting low-dose TNF administration lead to enhanced extravasation of liposomes in the tumor microenvironment, based on an increase in the leakiness of the TAV. TNF-induced enhanced accumulation of the liposomes in the tumor appears to be crucial for the observed response.

AIM OF THE THESIS

The aim of this thesis is to improve the delivery of cytotoxic agents to the tumor cells and to explain the mechanism behind this process. For this we use two agents with different targets; vasoactive agents that target the tumor-associated vasculature and chemotherapy that kills the tumor cells. Two vasoactive agents, TNF and Cilengitide are investigated in combination with the cytotoxic agents, melphalan, doxorubicin or Doxil. We studied the effects on ECs, pericytes and extracellular matrix as well as the interactions between the blood components, peripheral blood mononuclear cells and endothelial cells en the 4D kinetics of the uptake of the chemotherapeutic agents at the tumor site. A better insight in these processes will lead to the design of improved treatment regimens and more effective therapies for cancer patients.

OUTLINE OF THE THESIS

In the first part, the tumor response of two vasoactive agents, TNF and Cilengitde is investigated. In **chapter 2** we study the antitumor activity after systemic treatment with TNF and Doxil in osteosarcoma-bearing rats. Previous experiments in soft tissue sarcoma-bearing rats showed impressive tumor response with this combination accompanied by augmented accumulation of the chemotherapeutic drug. Therefore, this treatment needs to be evaluated in tumor types with a different origin and structure. **Chapter 3** describes the antitumor activity of Cilengitide, a cyclic inhibitor of αV integrins in clinical development as an antiangiogenic agent, in the melphalan-based ILP setting in soft tissue sarcoma-bearing rats. We investigate the effect of this inhibitor of ECs *in vitro* as well as *in vivo* and evaluate the capacity of Cilengitide to augment the intratumoral drug concentrations as we have observed after administration of TNF.

In the second part of this thesis the effect of TNF on endothelial cells is studied *in vitro*. In **Chapter 4** we investigate the ECs integrity and measure cell growth, cell morphology, permeability. We combine TNF with other important factors as interferon-gamma and peripheral blood mononuclear cells (PBMC) and look at endogenous produced factors that could be responsible for the observed effects. In the following two chapters, based on the changes in vascular integrity as observed in the experiments described in the previous chapter, we focus in more detail on the cell to matrix (**chapter 5**) and cell to cell adhesion (**chapter 6**). In chapter 5 endogenous produced matrix metalloproteinase-2 and -9 that contribute to the degradation of the endothelial layer is studied and in chapter 6 we study the effect of TNF on the increased permeability and the presence of the adherent junction protein VE-cadherin.

In the third part, we focus on the mechanism and action of TNF in the locoregional and systemic treatment in combination with conventional chemotherapy *in vivo*. **Chapter 7** describes the early changes in the tumor microenvironment during and directly after TNF-based ILP, which could explain the improved tumor response. We investigate the effect of TNF on the vasculature and immune cell infiltration using histology and also evaluate the expression of several cytokines in the tumor tissue. In **chapter 8** we use the dorsal skin-fold chamber with a B16BL6 tumor to elucidate the systemic effect of TNF and tumor distribution of free and liposomal chemotherapy in more detail. As observed in previous experiments TNF increased the intratumoral Doxil concentration. However, the exact location of the drug was still unknown. Using intravital microscopy we study the liposomal distribution inside the tumor in more detail. In **chapter 9** we investigate whether or not addition of systemic low-dose TNF in combination with Doxil would have similar effects on different tumors. For this we use four tumors with differences in their vascular properties. Besides the evaluation of tumor response we also investigate the correlation between these vascular differences and the observed response.

REFERENCES

1.Jain RK. Barriers to drug delivery in solid tumors. Sci Am. 1994: 271(1), 58-65.

2.Deng DX, Tsalenko A, Vailaya A, Ben Dor A, Kundu R, Estay I et al. Differences in vascular bed disease susceptibility reflect differences in gene expression response to atherogenic stimuli. Circ Res. 2006: 98(2), 200-208.

3.Takase B, Uehata A, Akima T, Nagai T, Nishioka T, Hamabe A et al. Endothelium-dependent flow-mediated vasodilation in coronary and brachial arteries in suspected coronary artery disease. Am J Cardiol. 1998: 82(12), 1535-1538.

4.Kalogeris TJ, Kevil CG, Laroux FS, Coe LL, Phifer TJ, and Alexander JS. Differential monocyte adhesion and adhesion molecule expression in venous and arterial endothelial cells. Am J Physiol. 1999: 276(1 Pt 1), L9-L19.

5.Bazzoni G and Dejana E. Endothelial cell-to-cell junctions: molecular organization and role in vascular homeostasis. Physiol Rev. 2004: 84(3), 869-901.

6.Navarro P, Ruco L, and Dejana E. Differential localization of VE- and N-cadherins in human endothelial cells: VE-cadherin competes with N-cadherin for junctional localization. J Cell Biol. 1998: 140(6), 1475-1484.

7.Carmeliet P, Lampugnani MG, Moons L, Breviario F, Compernolle V, Bono F et al. Targeted deficiency or cytosolic truncation of the VE-cadherin gene in mice impairs VEGF-mediated endothelial survival and angiogenesis. Cell. 1999: 98(2), 147-157.

8.Nehls V and Drenckhahn D. Heterogeneity of microvascular pericytes for smooth muscle type alpha-actin. J Cell Biol. 1991: 113(1), 147-154.

9.Kurz H, Lauer D, Papoutsi M, Christ B, and Wilting J. Pericytes in experimental MDA-MB231 tumor angiogenesis. Histochem Cell Biol. 2002: 117(6), 527-534.

10.Fujimoto K. Pericyte-endothelial gap junctions in developing rat cerebral capillaries: a fine structural study. Anat Rec. 1995: 242(4), 562-565.

11.Larson DM, Carson MP, and Haudenschild CC. Junctional transfer of small molecules in cultured bovine brain microvascular endothelial cells and pericytes. Microvasc Res. 1987: 34(2), 184-199.

12.Cuevas P, Gutierrez-Diaz JA, Reimers D, Dujovny M, Diaz FG, and Ausman JI. Pericyte endothelial gap junctions in human cerebral capillaries. Anat Embryol (Berl). 1984: 170(2), 155-159.

13.Carlson EC. Fenestrated subendothelial basement membranes in human retinal capillaries. Invest Ophthalmol Vis Sci. 1989: 30(9), 1923-1932.

14.Diaz-Flores L, Gutierrez R, Varela H, Rancel N, and Valladares F. Microvascular pericytes: a review of their morphological and functional characteristics. Histol Histopathol. 1991: 6(2), 269-286.

15.Nehls V, Denzer K, and Drenckhahn D. Pericyte involvement in capillary sprouting during angiogenesis in situ. Cell Tissue Res. 1992: 270(3), 469-474.

16.Hallmann R, Horn N, Selg M, Wendler O, Pausch F, and Sorokin LM. Expression and function of laminins in the embryonic and mature vasculature. Physiol Rev. 2005: 85(3), 979-1000.

17.Yurchenco PD and O'Rear JJ. Basal lamina assembly. Curr Opin Cell Biol. 1994: 6(5), 674-681.
18.Erickson AC and Couchman JR. Still more complexity in mammalian basement membranes. J Histochem Cytochem. 2000: 48(10), 1291-1306.
19.Tunggal P, Smyth N, Paulsson M, and Ott MC. Laminins: structure and genetic regulation. Microsc Res Tech. 2000: 51(3), 214-227.
20.Stupack DG and Cheresh DA. Get a ligand, get a life: integrins, signaling and cell survival. J Cell Sci. 2002: 115(Pt 19), 3729-3738.
21.Alghisi GC and Ruegg C. Vascular integrins in tumor angiogenesis: mediators and therapeutic targets. Endothelium. 2006: 13(2), 113-135.
22.Brooks PC, Montgomery AM, Rosenfeld M, Reisfeld RA, Hu T, Klier G et al. Integrin alpha v beta 3 antagonists promote tumor regression by inducing apoptosis of angiogenic blood vessels. Cell. 1994: 79(7), 1157-1164.
23.Brooks PC, Clark RA, and Cheresh DA. Requirement of vascular integrin alpha v beta 3 for angiogenesis. Science. 1994: 264(5158), 569-571.
24.Cheresh DA. Structural and functional properties of ganglioside antigens on human tumors of neuroectodermal origin. Surv Synth Pathol Res. 1985: 4(2), 97-109.
25.Seftor RE, Seftor EA, Gehlsen KR, Stetler-Stevenson WG, Brown PD, Ruoslahti E et al. Role of the alpha v beta 3 integrin in human melanoma cell invasion. Proc Natl Acad Sci U S A. 1992: 89(5), 1557-1561.
26.Hashizume H, Baluk P, Morikawa S, McLean JW, Thurston G, Roberge S et al. Openings between defective endothelial cells explain tumor vessel leakiness. Am J Pathol. 2000: 156(4), 1363-1380.
27.Feng D, Nagy JA, Dvorak AM, and Dvorak HF. Different pathways of macromolecule extravasation from hyperpermeable tumor vessels. Microvasc Res. 2000: 59(1), 24-37.
28.Rippe B, Rosengren BI, Carlsson O, and Venturoli D. Transendothelial transport: the vesicle controversy. J Vasc Res. 2002: 39(5), 375-390.
29.Feng D, Nagy JA, Hipp J, Pyne K, Dvorak HF, and Dvorak AM. Reinterpretation of endothelial cell gaps induced by vasoactive mediators in guinea-pig, mouse and rat: many are transcellular pores. J Physiol. 1997: 504 (Pt 3), 747-761.
30.Morikawa S, Baluk P, Kaidoh T, Haskell A, Jain RK, and McDonald DM. Abnormalities in pericytes on blood vessels and endothelial sprouts in tumors. Am J Pathol. 2002: 160(3), 985-1000.
31.Baluk P, Morikawa S, Haskell A, Mancuso M, and McDonald DM. Abnormalities of basement membrane on blood vessels and endothelial sprouts in tumors. Am J Pathol. 2003: 163(5), 1801-1815.
32.Eberhard A, Kahlert S, Goede V, Hemmerlein B, Plate KH, and Augustin HG. Heterogeneity of angiogenesis and blood vessel maturation in human tumors: implications for antiangiogenic tumor therapies. Cancer Res. 2000: 60(5), 1388-1393.
33.Folkman J. Tumor angiogenesis: therapeutic implications. N Engl J Med. 1971: 285(21), 1182-1186.
34.Ferrara N. Role of vascular endothelial growth factor in physiologic and pathologic angiogenesis: therapeutic implications. Semin Oncol. 2002: 29(6 Suppl 16), 10-14.
35.Yuan F, Chen Y, Dellian M, Safabakhsh N, Ferrara N, and Jain RK. Time-dependent vascular regression and permeability changes in established human tumor xenografts induced by an anti-vascular endothelial growth factor/vascular permeability factor antibody. Proc Natl Acad Sci U S A. 1996: 93(25), 14765-14770.
36.Zucker S, Mirza H, Conner CE, Lorenz AF, Drews MH, Bahou WF et al. Vascular endothelial growth factor induces tissue factor and matrix metalloproteinase production in endothelial cells: conversion of prothrombin to thrombin results in progelatinase A activation and cell proliferation. Int J Cancer. 1998: 75(5), 780-786.
37.Dvorak HF, Brown LF, Detmar M, and Dvorak AM. Vascular permeability factor/vascular endothelial growth factor, microvascular hyperpermeability, and angiogenesis. Am J Pathol. 1995: 146(5), 1029-1039.
38.Hurwitz H, Fehrenbacher L, Novotny W, Cartwright T, Hainsworth J, Heim W et al. Bevacizumab plus irinotecan, fluorouracil, and leucovorin for metastatic colorectal cancer. N Engl J Med. 2004: 350(23), 2335-2342.
39.Tong RT, Boucher Y, Kozin SV, Winkler F, Hicklin DJ, and Jain RK. Vascular normalization by vascular endothelial growth factor receptor 2 blockade induces a pressure gradient across the vasculature and improves drug penetration in tumors. Cancer Res. 2004: 64(11), 3731-3736.

40.Winkler F, Kozin SV, Tong RT, Chae SS, Booth MF, Garkavtsev I et al. Kinetics of vascular normalization by VEGFR2 blockade governs brain tumor response to radiation: role of oxygenation, angiopoietin-1, and matrix metalloproteinases. Cancer Cell. 2004: 6(6), 553-563.
41.Batchelor TT, Sorensen AG, di Tomaso E, Zhang WT, Duda DG, Cohen KS et al. AZD2171, a pan-VEGF receptor tyrosine kinase inhibitor, normalizes tumor vasculature and alleviates edema in glioblastoma patients. Cancer Cell. 2007: 11(1), 83-95.
42.Denekamp J and Hobson B. Endothelial-cell proliferation in experimental tumours. Br J Cancer. 1982: 46(5), 711-720.
43.Thorpe PE. Vascular targeting agents as cancer therapeutics. Clin Cancer Res. 2004. 10(2):415-427.
44.Dark GG, Hill SA, Prise VE, Tozer GM, Pettit GR, and Chaplin DJ. Combretastatin A-4, an agent that displays potent and selective toxicity toward tumor vasculature. Cancer Res. 1997: 57(10), 1829-1834.
45.Iyer S, Chaplin DJ, Rosenthal DS, Boulares AH, Li LY, and Smulson ME. Induction of apoptosis in proliferating human endothelial cells by the tumor-specific antiangiogenesis agent combretastatin A-4. Cancer Res. 1998: 58(20), 4510-4514.
46.Mahadevan V, Malik ST, Meager A, Fiers W, Lewis GP, and Hart IR. Role of tumor necrosis factor in flavone acetic acid-induced tumor vasculature shutdown. Cancer Res. 1990: 50(17), 5537-5542.
47.Zhao L, Ching LM, Kestell P, and Baguley BC. The antitumour activity of 5,6-dimethylxanthenone-4-acetic acid (DMX-AA) in TNF receptor-1 knockout mice. Br J Cancer. 2002: 87(4), 465-470.
48.Baguley BC, Zhuang L, and Kestell P. Increased plasma serotonin following treatment with flavone-8-acetic acid, 5,6-dimethylxanthenone-4-acetic acid, vinblastine, and colchicine: relation to vascular effects. Oncol Res. 1997: 9(2), 55-60.
49.Thomsen LL, Baguley BC, and Wilson WR. Nitric oxide: its production in host-cell-infiltrated EMT6 spheroids and its role in tumour cell killing by flavone-8-acetic acid and 5,6-dimethylxanthenone-4-acetic acid. Cancer Chemother Pharmacol. 1992: 31(2), 151-155.
50.Brouckaert P, Takahashi N, van Tiel ST, Hostens J, Eggermont AM, Seynhaeve AL et al. Tumor necrosis factor-alpha augmented tumor response in B16BL6 melanoma-bearing mice treated with stealth liposomal doxorubicin (Doxil) correlates with altered Doxil pharmacokinetics. Int J Cancer. 2004: 109(3), 442-448.
51.Brunstein F, Rens J, van Tiel ST, Eggermont AM, and ten Hagen TL. Histamine, a vasoactive agent with vascular disrupting potential, improves tumour response by enhancing local drug delivery. Br J Cancer. 2006: 95(12), 1663-1669.
52.Brunstein F, Hoving S, Seynhaeve AL, van Tiel ST, Guetens G, de Bruijn EA et al. Synergistic antitumor activity of histamine plus melphalan in isolated limb perfusion: preclinical studies. J Natl Cancer Inst. 2004: 96(21), 1603-1610.
53.de Wilt JH, Manusama ER, van Tiel ST, van Ijken MG, ten Hagen TL, and Eggermont AM. Prerequisites for effective isolated limb perfusion using tumour necrosis factor alpha and melphalan in rats. Br J Cancer. 1999: 80(1-2), 161-166.
54.Hoving S, Brunstein F, aan de Wiel-Ambagtsheer G, van Tiel ST, de Boeck G, de Bruijn EA et al. Synergistic antitumor response of interleukin 2 with melphalan in isolated limb perfusion in soft tissue sarcoma-bearing rats. Cancer Res. 2005: 65(10), 4300-4308.
55.Manusama ER, Stavast J, Durante NM, Marquet RL, and Eggermont AM. Isolated limb perfusion with TNF alpha and melphalan in a rat osteosarcoma model: a new anti-tumour approach. Eur J Surg Oncol. 1996: 22(2), 152-157.
56.Lienard D, Ewalenko P, Delmotte JJ, Renard N, and Lejeune FJ. High-dose recombinant tumor necrosis factor alpha in combination with interferon gamma and melphalan in isolation perfusion of the limbs for melanoma and sarcoma. J Clin Oncol. 1992: 10(1), 52-60.
57.Rossi CR, Mocellin S, Pilati P, Foletto M, Nitti D, and Lise M. TNFalpha-based isolated perfusion for limb-threatening soft tissue sarcomas: state of the art and future trends. J Immunother. 2003: 26(4), 291-300.
58.Eggermont AM, Brunstein F, Grunhagen D, and ten Hagen TL. Regional treatment of metastasis: role of regional perfusion. State of the art isolated limb perfusion for limb salvage. Ann Oncol. 2004: 15 Suppl 4, iv107-iv112.
59.de Wilt JH, ten Hagen TL, de Boeck G, van Tiel ST, de Bruijn EA, and Eggermont AM. Tumour necrosis factor alpha increases melphalan concentration in tumour tissue after isolated limb perfusion. Br J Cancer. 2000: 82(5), 1000-1003.
60.van der Veen AH, de Wilt JH, Eggermont AM, van Tiel ST, Seynhaeve AL, and ten Hagen TL. TNF-alpha augments intratumoural concentrations of doxorubicin in TNF-alpha-based isolated limb perfusion in rat sarcoma models and enhances anti-tumour effects. Br J Cancer. 2000: 82(4), 973-980.

61.Manusama ER, Nooijen PT, Stavast J, de Wilt JH, Marquet RL, and Eggermont AM. Assessment of the role of neutrophils on the antitumor effect of TNFalpha in an in vivo isolated limb perfusion model in sarcoma-bearing brown Norway rats. J Surg Res. 1998: 78(2), 169-175.
62.ten Hagen TL, Seynhaeve AL, van Tiel ST, Ruiter DJ, and Eggermont AM. Pegylated liposomal tumor necrosis factor-alpha results in reduced toxicity and synergistic antitumor activity after systemic administration in combination with liposomal doxorubicin (Doxil) in soft tissue sarcoma-bearing rats. Int J Cancer. 2002: 97(1), 115-120.

Part 1 - Vascular abnormalization tumor response

Chapter 2 **TNF augments tumor response to Doxil**
Saske Hoving, Ann L.B. Seynhaeve, Sandra T. van Tiel, Alexander M.M. Eggermont, and Timo L.M. ten Hagen
Anticancer Drugs. 2005: 16(6), 667-674

Chapter 3 **Cilengitide augments tumor response to melphalan**
Timo L.M. ten Hagen, Ann L.B. Seynhaeve, Gisela aan de Wiel-Ambagtsheer, Ernst A. de Bruijn, Sandra T. van Tiel, Curzio Ruegg, Michael Meyring, Matthias Grell, Simon L. Goodman, and Alexander M.M. Eggermont
Submitted for publication

About the authors (in alphabetical order)
Gisela aan de Wiel-Ambagtsheer; Department of Surgical Oncology, Erasmus MC-Daniel den Hoed Cancer Center, Rotterdam, The Netherlands - **Ernst A. de Bruijn**; Department of Experimental Oncology, University of Leuven, Leuven, Belgium - **Alexander M.M. Eggermont**; Department of Surgical Oncology, Erasmus MC-Daniel den Hoed Cancer Center, Rotterdam, The Netherlands - **Simon L. Goodman**; Therapeutic Area Oncology, Merck KGaA, Darmstadt, Germany. - **Matthias Grell**; Therapeutic Area Oncology, Merck KGaA, Darmstadt, Germany - **Timo L.M. ten Hagen**; Department of Surgical Oncology, Erasmus MC-Daniel den Hoed Cancer Center, Rotterdam, The Netherlands - **Saske Hoving**; Department of Surgical Oncology, Erasmus MC-Daniel den Hoed Cancer Center, Rotterdam, The Netherlands - **Michael Meyring**; Institute of Drug Metabolism and Pharmacokinetics, Merck KGaA, Grafing, Germany- **Curzio Ruegg**; Division of Experimental Oncology, Centre Pluridisciplinaire d'Oncologie and Swiss Institute for Experimental Cancer Research-NCCR Molecular Oncology, Lausanne, Switzerland - **Ann L.B. Seynhaeve**; Department of Surgical Oncology, Erasmus MC-Daniel den Hoed Cancer Center, Rotterdam, The Netherlands - **Sandra T. van Tiel**; Department of Surgical Oncology, Erasmus MC-Daniel den Hoed Cancer Center, Rotterdam, The Netherlands.

Chapter 2

Addition of low-dose TNFα to systemic treatment with Stealth liposomal doxorubicin (Doxil) improved antitumor activity in osteosarcoma-bearing rats

Saske Hoving
Ann L.B. Seynhaeve
Sandra T. van Tiel
Alexander M.M. Eggermont
Timo L.M. ten Hagen

Anticancer Drugs. 2005: 16(6), 677-674

Research Article

Addition of low-dose TNFα to systemic treatment with Stealth liposomal doxorubicin (Doxil) improved antitumor activity in osteosarcoma-bearing rats

Saske Hoving, Ann L.B. Seynhaeve, Sandra T. van Tiel, Alexander M.M. Eggermont, and Timo L.M. ten Hagen

Department of Surgical Oncology, Erasmus MC-Daniel den Hoed Cancer Center, Rotterdam, The Netherlands

ARTICLE INFORMATION

Anticancer Drugs. 2005: 16(6), 667-674

ACKNOWLEDGMENTS

TNF was a generous gift from Dr. G. Adolf and Doxil was kindly provided by Dr. P. Working. The work was funded by grant DDHK 2000-2224 of the Dutch Cancer Society.

ABSTRACT

Improved efficacy of Doxil (Stealth liposomal doxorubicin) compared to free doxorubicin has been demonstrated in the treatment of several tumor types. We have shown that addition of a low-dose tumor necrosis factor-alpha (TNF) to systemic Doxil administration dramatically improved tumor response in the highly vascularized rat soft tissue sarcoma BN175. Whether a similar enhanced efficacy can be achieved in less vascularized tumors is uncertain. We therefore examined the effect of systemic administration of Doxil in combination with low-dose TNF in intermediate vascularized osteosarcoma-bearing rats (ROS-1). Small fragments of the osteosarcoma were implanted subcutaneously in the lower limb. Treatment was started when the tumors reached an average diameter of 1 cm. Rats were treated with 5 intravenous injections at 4 day interval with Doxil or doxorubicin and TNF. Systemic treatment with Doxil resulted in a better tumor growth delay than free doxorubicin, but with progressive diseases in all animals. The 3.5-fold augmented accumulation of Doxil compared to free doxorubicin presumably explains the enhanced tumor regression. Addition of low-dose TNF augmented the antitumor activity of Doxil, although no increased drug uptake was found compared to Doxil alone. *In vitro* studies showed that ROS-1 is sensitive to TNF, but systemic treatment with TNF alone did not result in a tumor growth delay. Furthermore we demonstrated that treatment with Doxil alone or with TNF resulted in massive coagulative necrosis of tumor tissue. In conclusion, combination therapy of Doxil and low-dose TNF seems attractive for the treatment of highly vascularized tumors but also of intermediate vascularized tumors like the osteosarcoma.

INTRODUCTION

Encapsulation of anticancer agents in liposomes offers a potential means of manipulating drug distribution to improve antitumor efficacy and reduce toxicity. Stealth liposomes are sterically stabilized liposomes that contain methoxypolyethylene glycol (MPEG). Because of their small size, long circulation time, and reduced interaction with formed elements of the blood, these liposomes tend to accumulate in tumors,

presumably due to leakage through the often-compromised tumor vasculature [1-8]. Doxil (Stealth liposomal doxorubicin) is effective in the treatment of several -tumor types, including advanced or metastatic soft tissue sarcoma [9], AIDS-related Kaposi's sarcoma [10], metastatic breast cancer [11] and epithelial ovarian cancer [12].

Pre-clinical and clinical studies have shown impressive improvement of the antitumor activity of melphalan and doxorubicin in local treatment of different tumor types when TNF was co-administered [13-18]. We demonstrated that the basis for the synergy is, on one hand a significant enhancement of tumor selective melphalan and doxorubicin uptake and on the other hand the subsequent destruction of tumor vasculature caused by TNF [19,20].

Successful application of TNF for systemic treatment of tumors however is seriously hampered by its severe toxicity and therefore only low dosages can be administered [21,22]. In previous studies we showed that systemic co-administration of Doxil and low-dose TNF resulted in a pronounced tumor response in both rat and mice tumor models. In soft tissue sarcoma-bearing rats systemic treatment with Doxil in combination with low-dose TNF improved the antitumor activity dramatically resulting in a tumor response (complete or partial regression) in most of the animals. Repeated injection of Doxil combined with TNF resulted in augmented accumulation of the drug in tumor tissue, which could explain the observed synergistic antitumor effect [23]. When B16BL6 melanoma-bearing mice were injected with Doxil combined with TNF, also an increased drug accumulation was found compared to liposomes alone [24]. TNF increases the leakiness of the vasculature by increasing the gaps between the endothelial lining in the tumor, possibly explaining the augmented accumulation after extravasation of liposomes [25,26].

We evaluate in the experiments described here whether the use of TNF in combination with Doxil not only results in synergistic antitumor response in the highly vascularized soft tissue sarcoma but also in the less vascularized osteosarcoma.

EXPERIMENTAL PROCEDURES

Agents. Human recombinant tumor necrosis factor-alpha with a specific activity of $5x10^7$ IU/mg was kindly provided by Dr. G. Adolf (Bender Wien GmbH) and stored at a concentration of 2 mg/ml at -80°C or under liquid nitrogen. Endotoxin levels (LAL) were below 0.6 EU/mg. Pegylated liposomal doxorubicin (Doxil) was kindly provided by Dr. P. Working (ALZA Corporation). Doxorubicin hydrochloride (adriblastina) was purchased from Pharmachemie BV.

Animals and tumor model. Male inbred WAG/RIJ rats were used for the osteosarcoma model (ROS-1). This tumor originated spontaneously in the tibia of a rat. Rats were obtained from Harlan-CPB and weighing 250-300 gram. Rats were fed a standard laboratory diet *ad libitum*. Small fragments (3 mm) of the syngeneic ROS-1 sarcoma or the soft tissue sarcoma BN175 were implanted subcutaneously in the right hind leg as previously described [27]. Tumor growth was recorded by caliper measurement and tumor volume calculated using the formula $0.4 \times (A^2 \times B)$ (where B represents the largest diameter and A the diameter perpendicular to B). Rats were sacrificed if tumor diameter exceeded 25 mm or at the end of the experiments. Animal studies were done in accordance with protocols approved by the committee on Animal Research of the Erasmus MC, Rotterdam, the Netherlands.

Treatment protocol. Treatment was started when the ROS-1 tumors reached an average diameter of 9-11 mm. The rats were randomized into the following 6 groups: placebo liposomes (sham), TNF, doxorubicin, Doxil, doxorubicin plus TNF and Doxil plus TNF. Rats were injected 5 times i.v. with an interval of 4 days between the injections; first dose of 4.5 mg/kg Doxil or doxorubicin and 1.0 mg/kg for consecutive doses. TNF was given at a concentration of 15 µg/kg for all 5 doses. When rats were treated with doxorubicin or Doxil combined with TNF, these agents were injected separately, shortly after each other. The classification of tumor response was: progressive disease (PD) = increase of tumor volume (> 25%) over a 20 day period;

no change (NC) = tumor volume equal to volume as start of treatment (in a range of - 25% and + 25%); partial remission (PR) = decrease of tumor volume (- 25 and -90 %); complete remission (CR) = tumor volume less than 10% of initial volume.

Measurement of doxorubicin accumulation in tumor tissue. The effect of TNF on Doxil accumulation in ROS-1 tumors was investigated. After 3 injections the tumor size of rats treated with Doxil in combination with TNF started to differ from the tumor size of rats in the other groups and for this reason we decided to compare doxorubicin tumor uptake not later than this time point. Rats received 3 injections of doxorubicin or Doxil with or without TNF with an interval of 4 days between the injections as described in the treatment protocol. Tumors were excised 24 hours after the last injection and tissues were analyzed for doxorubicin and its fluorescent metabolites as previously described [28]. Briefly, tumors were incubated in acidified isopropanol (0.075 N HCl in 90% isopropanol) for 24 hours at 4°C and after that the tumors were homogenized (PRO200 homogenizer with 10 mm generator, Pro Scientific), centrifuged for 30 min at 2500 rpm and supernatants were harvested. A Hitachi F4500 fluorescence spectrometer (excitation 472 nm and emission 590 nm) was used for measurement of the samples. A standard curve was prepared with known concentrations of doxorubicin diluted in acidified isopropanol. All measurements were repeated after addition of an internal doxorubicin standard.

Histology. Rats were treated with placebo liposomes, TNF, Doxil or Doxil plus TNF. When the tumors reached an average diameter of 17 ± 1 mm, they were excised and fixed in 4% formaldehyde and embedded in paraffin. Tissue sections of 4 µm were cut and stained with hematoxylin and eosin, examined on a Leica DM-RXA and photographed using a Sony DXC950 camera. At least 3 different tumors in each experimental group were subjected to blind evaluation.

Immunohistochemistry. Untreated BN175 and ROS-1 tumors with a diameter of 9-11 mm were excised and immediately frozen in liquid nitrogen. Immunohistochemical studies were performed on acetone-fixed 7 µm cryostat sections. The tumor sections were fixed for 30 min with 4% formaldehyde and after rinsing with PBS, the endogenous peroxidase activity was blocked by incubation for 5 min in methanol/3% H_2O_2. The slides were incubated for 1 hour with mouse anti rat CD31 (1:50; Becton Dickinson) diluted in 5% rat serum/PBS. Thereafter, sections were washed with PBS and incubated for 1 hour with goat anti mouse peroxidase-labeled antibody (1:100; DAKO) diluted in 5% rat serum/PBS. After rinsing with PBS, positive cells were revealed by immunoperoxidase reaction with DAB solution (DAB-kit, DAKO) and counterstained lightly with haematoxylin (Sigma). The sections were examined on a Leica DM-RXA and photographed using a Sony 3CCD DXC 950 camera. The number of vessels and the area of vessels per field of interest were measured in calibrated digital images (Research Assistant 3.0, RVC). For quantification of the microvessel density (MVD) 6 representative fields of interest per slide, 3 sections of 4 individual tumors were examined.

***In vitro* cytotoxicity assay.** The rat osteosarcoma ROS-1 cells were maintained in MEM supplemented with 10% FCS and 0.1% penicilline-streptomycine. Media and supplements were obtained from Life Technologies. ROS-1 cells were plated in 96-well plates (Costar BV) at a final concentration of $1x10^4$ cells per well and allowed to grow for 24 hours. Cells were incubated at 37°C in 5% CO_2 for 72 hours in the presence of various concentrations of TNF, doxorubicin and Doxil. The range of final drug concentrations was 0.1 - 10 µg/ml for TNF, 0.001 - 100 µg/ml doxorubicin and 0.05 - 1000 µg/ml Doxil. Growth of tumor cells was measured using the sulphorhodamine-B assay (SRB, Sigma) according to the method of Skehan [29]. In short, cells were washed twice with phosphate buffered saline, incubated with 10% trichloric acetic acid (1 hour, 4°C) and washed again. Cells were stained with 0.4%

SRB (15-30 min), washed with 1% acetic acid and were allowed to dry. Protein bound SRB was dissolved in TRIS (10 mM, pH 9.4). The optical density (O.D.) was read at 540 nm. Tumor cell growth was calculated using the formula: cell growth = (O.D. test well/O.D. control) x 100 percent.

***In vitro* assessment of doxorubicin uptake in tumor cells.** Intracellular doxorubicin levels in osteosarcoma ROS-1 cells were measured by flowcytometry to determine whether the observed *in vitro* toxicity correlated with cellular uptake of doxorubicin. ROS-1 cells were plated in 24-well plates at a final concentration of $5x10^4$ cells per well and allowed to growth for 24 hours. Doxorubicin, Doxil and TNF, diluted in MEM supplement with 10 % FCS, were added to the wells, after which cells were incubated for 10, 30, 60 and 120 min. The final drug concentration in the wells for all 3 drugs was 0, 0.1, 1.0 and 10 µg/ml. After incubation, cells were washed to discard non-incorporated drug and treated with trypsin-EDTA for 2 min. The cell suspensions were washed twice in medium and resuspended in PBS. Cellular uptake was measured on a Becton Dickinson FACScan using Cell Quest software on Apple Macintosh computer. Excitation was set at 488 nm and emission at 530 nm.

Statistical analysis. Results were evaluated for statistical significance with the Mann Whitney U test. P-values below 0.05 were considered statistically significant. Calculations were performed on a personal computer using GraphPad Prism v3.0 and SPSS v10.0 for Windows 2000.

RESULTS

The combination of low-dose TNF and Doxil results in strong antitumor response. To evaluate the antitumor activity of Doxil in combination with low-dose TNF, osteosarcoma-bearing rats were treated with a total of 5 injections of doxorubicin or Doxil with or without TNF. Treatment with doxorubicin resulted in a slight delay in tumor growth, with progressive diseases in all animals (**Fig. 1**). Progressive disease was also seen in all animals treated with Doxil, but with a better tumor growth delay than doxorubicin. Addition of TNF to the Doxil treatment enhanced the antitumor response, resulting in a response rate of 50% (partial plus complete response). In contrast, addition of TNF to doxorubicin treatment did not improve the antitumor response. Treatment with TNF alone had no antitumor effect. No obvious systemic toxicity was observed in any of the treatments.

Necrosis is observed after treatment with TNF and Doxil. Histopathological examination was performed on tumors with the same size, shortly after regrowth occurred. Treatment of the rats with Doxil and Doxil in combination with TNF resulted in severe tumor necrosis and extensive cell death (**Fig. 2**). Massive coagulative necrosis of 68% of the tumor area was seen in Doxil treated tumors and 40% in the Doxil plus TNF treated tumors. Less necrosis was seen in rats treated with placebo liposomes or TNF (10 and 17%, respectively). In all 4 groups infiltrated polymorph nuclear cells (PMN) were detected.

Addition of TNF did not increase intratumoral drug concentration. To investigate whether the observed beneficial effect of TNF on the Doxil treatment was due to an increased liposome extravasation into tumor tissue, doxorubicin concentrations in tumors after 3 treatments were determined. Doxorubicin levels in tumors were 3.5-fold higher when Doxil was injected compared to doxorubicin, although not significantly (**Fig. 3**). Addition of TNF did not induce a further accumulation of Doxil and TNF had also no effect on the tumor uptake of free doxorubicin.

ROS-1 tumors contain fewer vessels compared to BN175. Quantification of the microvessel density (MVD) was performed by immunohistochemical staining of endothelial cells in frozen BN175 and ROS-1 tumor sections. The number of vessels as well as the total tumor vessel area was measured. The area per vessel was computed by dividing the total vessel area

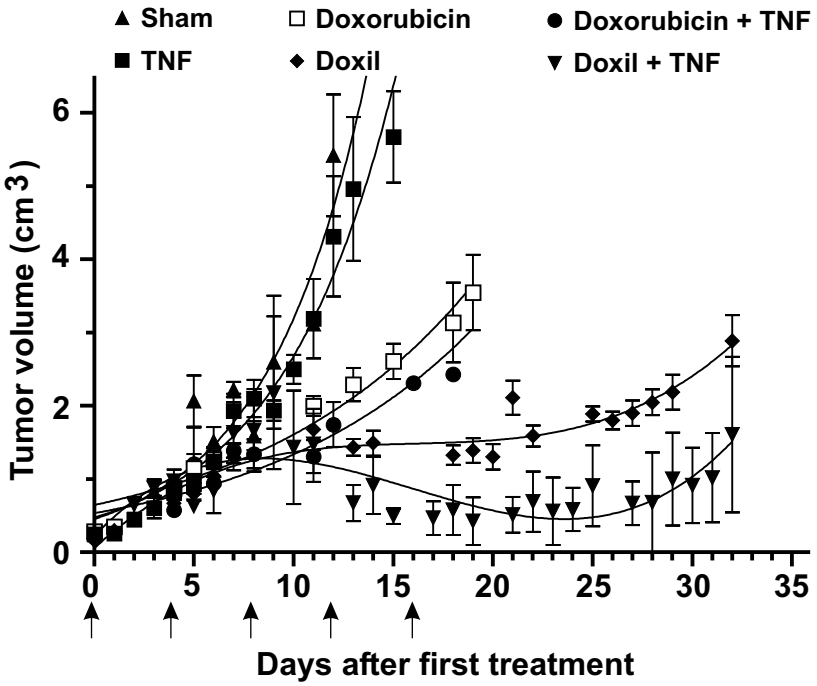

Figure 1. Addition of TNF improves the antitumor effect of Doxil in ROS-1 osteosarcoma-bearing rats. Rats were injected 5 times i.v. with an interval of 4 days between the injections (arrows). Chemotherapy or TNF alone had hardly any effect on the tumor growth. Combination of doxorubicin with TNF reduced tumor growth but the most impressive results were obtained with the treatment of Doxil in combination with TNF. Data points represent tumor volumes ± SD of 6 to 8 individual animals.

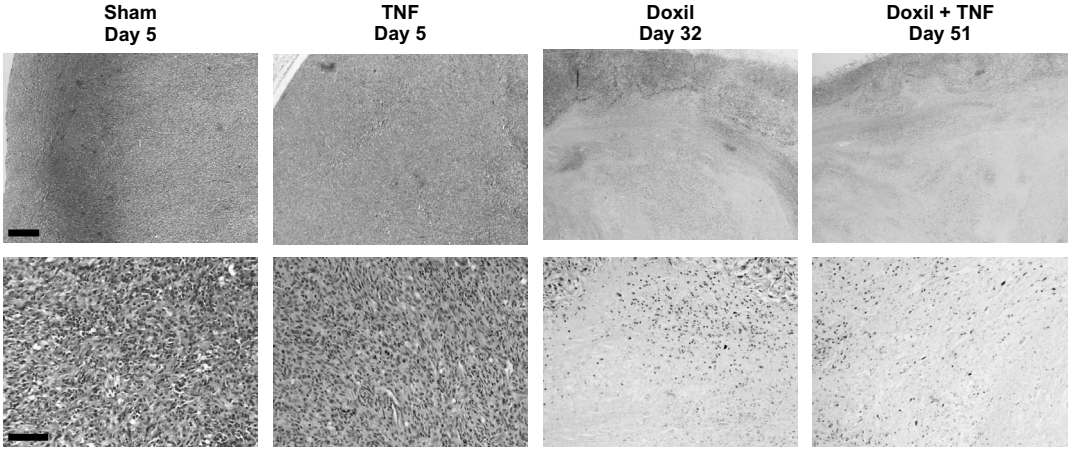

Figure 2. Massive necrosis is observed after Doxil treatment. Paraffin sections of the osteosarcoma after systemic treatment were stained with haematoxylin-eosin. Sham and TNF-treated tumors hardly showed any necrosis when the tumors reached a size of 17 mm. Necrosis was observed in Doxil treated tumors that was further enhanced with the addition of TNF. Scale bar apply for upper pictures, 500 µm. Scale bar apply for lower pictures, 100 µm. (See color section for a full-color version.)

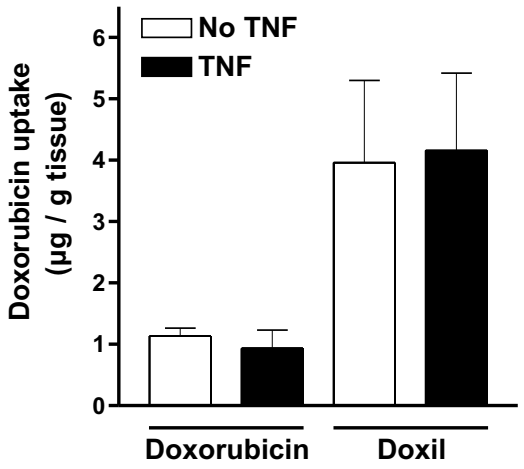

Figure 3. Addition of TNF does not increase intratumoral doxorubicin levels. Doxorubicin levels in tumors after systemic administration of 3 injection of doxorubicin or Doxil with or without TNF were measured. Significant more doxorubicin was observed intratumoral when administered in liposomal formulation compared to free drug. However addition of TNF did not increase the accumulation of doxorubicin or Doxil. Columns represent µg doxorubicin per g tumor tissue ± SD of 3 to 6 individual animals.

by the number of vessels. The number of vessels in the BN175 tumor was 2.9 times higher than in the ROS-1 tumor (**Fig. 4a**), although the vessels had the same size (**Fig. 4b** and **Fig. 4c**).

Addition of TNF did not increase cytotoxicity on ROS-1 cells *in vitro.* *In vitro* experiments were performed to define whether direct cytotoxicity contributed to the improved tumor response of Doxil in combination with TNF. Figure 5 shows that exposure of ROS-1 tumor cells to doxorubicin resulted in a dose dependent cell growth inhibition, with an IC_{50} of 3.8 µg/ml. Doxil appeared to be less cytotoxic to osteosarcoma cells with an IC_{50} of 25.7 µg/ml. ROS-1 cells were moderately sensitive to TNF with a maximum growth inhibition of 32% at 10 µg/ml TNF. Addition of TNF to doxorubicin or Doxil had no effect on the cytotoxicity of the antitumor agents; comparable IC_{50} values were found (**Fig. 5a** and **Fig. 5b**).

Addition of TNF did not change uptake of Doxil or doxorubicin in tumor cells *in vitro.* We examined if TNF augmented the intracellular accumulation of doxorubicin or Doxil, which could explain the improved tumor response. Increased intracellular concentrations of doxorubicin or Doxil were observed when incubated with increasing concentrations of doxorubicin or Doxil (ranging 0.1 to 10 µg/ml) and increasing time (ranging 10 to 120 min). Addition of TNF up to 10 µg/ml did not result in an increased uptake of doxorubicin or Doxil (data not shown).

DISCUSSION

In the present study we demonstrated that Stealth liposomal doxorubicin (Doxil) resulted in a better tumor growth delay than free doxorubicin in osteosarcoma-bearing rats. However, tumor control was not achieved as progressive disease was observed in all animals. Addition of low-dose TNF augmented the antitumor activity of Doxil resulting in a response rate of 50%. These experiments are in agreement with earlier studies where we demonstrated that TNF improved the antitumor activity of Doxil in a rat soft tissue sarcoma and a mouse melanoma model [23,30].

Transport of small drugs across the blood vessel wall involves diffusion whereas transport of macromolecules involves convection. Diffusion is the random motion of small molecules. Convection is mediated by the movement of fluid [31-34]. In highly vascularized tumors more tumor cells will be reached by the chemotherapeutics. In general, tumor vessels are more permeable than normal vessels and the maximum size of particles that can cross the tumor vessel wall is called the pore cutoff size. There is a large variance in cutoff sizes in different tumor types. Vessels of some, but not all, primary brain tumors are nearly impermeable, while in other tumors cutoff pore sizes between 100 nm and 1.2 µm are found. Vascular permeability may depend on tumor type and microenvironment and increases with tumor size. It is believed that not the microvessel density is the limiting factor of macromolecule

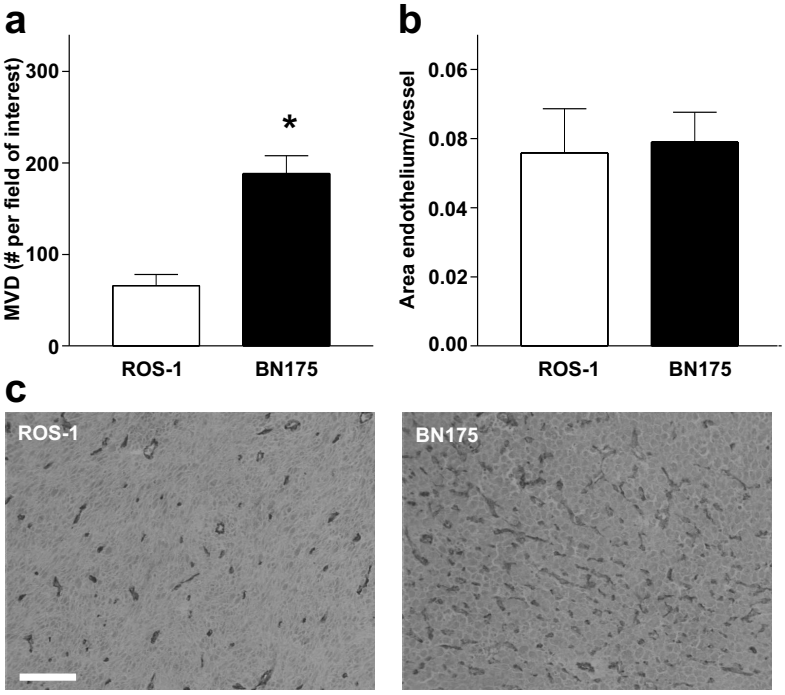

Figure 4. Structural differences between ROS-1 osteosarcoma and BN175 soft tissue sarcoma. (**a**) The microvessel density (MVD, number of vessels per field of interest at magnification 40x) of untreated ROS-1 and BN175 tumors of 9-11 mm in diameter was assessed by immunohistochemical staining for CD31. The BN175 tumor had 2.9 times more vessels than the ROS-1 tumor. Columns represent MVD ± SEM of 3 sections of 4 individual tumors; *, $P < 0.05$. (**b**) The vessels of the BN175 and ROS-1 tumors had the same size. Columns represent area endothelium per vessel per field of interest ± SEM of 3 sections of 4 individual tumors. (**c**) Untreated tumor sections of ROS-1 and BN175 of 8-10 mm in diameter were stained for CD31. BN175 showed much more tumor vessels compared to ROS-1. Scale bar apply for all images, 100 µm.

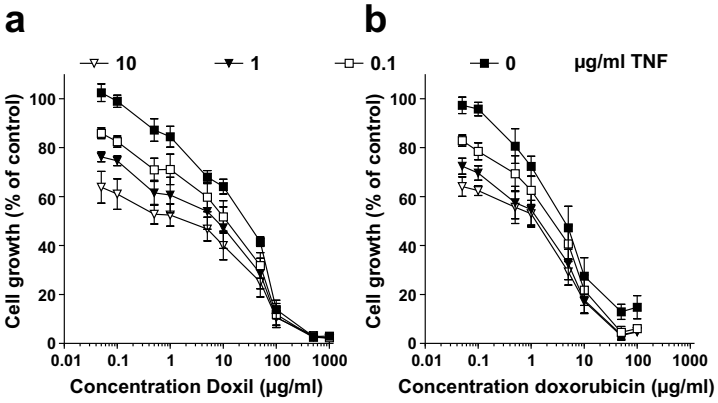

Figure 5. No synergistic effect of TNF is observed *in vitro*. (**a**) In vitro growth of ROS-1 tumor cells with Doxil with varies concentrations of TNF showed that cells were moderate sensitive to TNF alone. Exposure to Doxil resulted in a dose dependent cell growth reduction but addition of TNF had no effect of the antitumor activity of Doxil. (**b**) The same observations with doxorubicin were observed. Addition of TNF did not increase the cytotoxic effect of doxorubicin. Doxorubicin was found more cytotoxic to ROS-1 tumor cells compared to Doxil. Data points represent percentage cell growth compared to control treated cells ± SEM of 2 treatments in 3 individual experiments.

drug delivery to solid tumors, but the permeability of the tumor vessels [35,36].

Several studies have shown that encapsulation of anticancer agents in liposomes can reduce systemic toxicity while retaining or even improving *in vivo* efficacy [1,4,7,37]. Doxil is effective in the treatment of several tumor types, including advanced or metastatic soft tissue sarcoma [38], AIDS-related Kaposi's sarcoma [39], metastatic breast cancer [40] and epithelial ovarian cancer [41]. Stealth liposomes have a long circulation time and tend to accumulate in tumors, presumably due to leakage through the tumor vasculature [1,3,4,6-8,42]. In the present study we showed that systemic treatment with Doxil resulted in a better tumor growth delay than free doxorubicin and that the 3.5-fold increased drug accumulation could explain the observed enhanced antitumor effect. The antitumor activity of Doxil in the osteosarcoma model is comparable to the antitumor activity in the soft tissue sarcoma BN175, although *in vitro* studies showed a clear difference. BN175 cells are 10 times more sensitive to Doxil than ROS-1 cells [23]. Four times more Doxil is found in ROS-1 tumor tissue than in the BN175 tumor after 3 i.v. injections of Doxil alone. Most likely this indicates that the tumor vessels of the ROS-1 tumor are more permeable than the vessels of the BN175 tumor.

Previously we reported on the improved antitumor activity of systemically injected Doxil when combined with low-dose TNF in soft tissue sarcoma-bearing rats. Repeated injections of Doxil plus TNF resulted in augmented tumor uptake of doxorubicin, which could explain the observed enhanced antitumor effect [23]. Also in the B16BL6 melanoma-bearing mice an augmented accumulation of Doxil is seen when combined with TNF. TNF likely increases the leakiness of the vasculature by increasing the gaps between the endothelial lining in the tumor, possibly explaining the augmented accumulation after extravasation of liposomes [25,43].

In the present study we did not observe an increased drug accumulation when Doxil was combined with TNF in the osteosarcoma ROS-1 model. TNF has an effect on tumor endothelial cells and the ROS-1 tumor is less vascularized than the BN175 tumor. Although in TNF-based isolated hepatic perfusions a highly vascularized tumor results in a good tumor response and *vice versa*, no such effect was found in the TNF-based ILP. Both the BN175 and the ROS-1 tumor showed a synergistic antitumor response when TNF is added to the ILP [18,44].

In vitro studies demonstrated a higher sensitivity of the osteosarcoma cells for TNF as compared to the BN175 cells. The dose of TNF used in the systemic treatment is probably too low to have an effect on its own, but may switch the balance to a better response when combined with Doxil. Also, administration of TNF may trigger local production of TNF and other cytokines improving tumor response when combined with Doxil.

We found less coagulative necrosis in tumor tissue after treatment with Doxil and TNF than with Doxil alone. We think this is due to the fact that the tumors were excised at the same size. As the tumors from Doxil plus TNF treated rats regressed more they also regrew more to gain the same size as the Doxil alone treated tumors. We demonstrated for the first time that TNF augments the antitumor activity of Doxil not only in highly vascularized tumors like the soft tissue sarcoma BN175, but also in the intermediate vascularized ROS-1. These findings confirm the promising role for TNF as enhancer of systemic therapy of solid tumors with Stealth liposomes.

REFERENCES

1.Allen TM, Newman MS, Woodle MC, Mayhew E, and Uster PS. Pharmacokinetics and anti-tumor activity of vincristine encapsulated in sterically stabilized liposomes. Int J Cancer. 1995: 62(2), 199-204.

2.Gabizon A and Papahadjopoulos D. Liposome formulations with prolonged circulation time in blood and enhanced uptake by tumors. Proc Natl Acad Sci U S A. 1988: 85(18), 6949-6953.

3.Gabizon A and Martin F. Polyethylene glycol-coated (pegylated) liposomal doxorubicin. Rationale for use in solid tumours. Drugs. 1997: 54 Suppl 4, 15-21.

4.Lasic DD. Doxorubicin in sterically stabilized liposomes. Nature. 1996: 380(6574), 561-562.

5.Maeda H, Fang J, Inutsuka T, and Kitamoto Y. Vascular permeability enhancement in solid tumor: various factors, mechanisms involved and its implications. Int Immunopharmacol. 2003: 3(3), 319-328.
6.Mayer LD, Cullis PR, and Bally MB. Designing therapeutically optimized liposomal anticancer delivery systems: lessons from conventional liposomes. 2002: (4.2), 231-257.
7.Papahadjopoulos D, Allen TM, Gabizon A, Mayhew E, Matthay K, Huang SK et al. Sterically stabilized liposomes: improvements in pharmacokinetics and antitumor therapeutic efficacy. Proc Natl Acad Sci U S A. 1991: 88(24), 11460-11464.
8.Wu NZ, Da D, Rudoll TL, Needham D, Whorton AR, and Dewhirst MW. Increased microvascular permeability contributes to preferential accumulation of Stealth liposomes in tumor tissue. Cancer Res. 1993: 53(16), 3765-70.
9.Judson I, Radford JA, Harris M, Blay JY, van Hoesel Q, Le Cesne A et al. Randomised phase II trial of pegylated liposomal doxorubicin (DOXIL/CAELYX) versus doxorubicin in the treatment of advanced or metastatic soft tissue sarcoma: a study by the EORTC Soft Tissue and Bone Sarcoma Group. Eur J Cancer. 2001: 37(7), 870-877.
10.Northfelt DW, Dezube BJ, Thommes JA, Miller BJ, Fischl MA, Friedman-Kien A et al. Pegylated-liposomal doxorubicin versus doxorubicin, bleomycin, and vincristine in the treatment of AIDS-related Kaposi's sarcoma: results of a randomized phase III clinical trial. J Clin Oncol. 1998: 16(7), 2445-2451.
11.O'Brien ME, Wigler N, Inbar M, Rosso R, Grischke E, Santoro A et al. Reduced cardiotoxicity and comparable efficcy in a phase III trial of pegylated liposomal doxorubicin HCl (CAELYX/Doxil) versus conventional doxorubicin for first-line treatment of metastatic breast cancer. Ann Oncol. 2004: 15(3), 440-449.
12.Stebbing J and Gaya A. Pegylated liposomal doxorubicin (Caelyx) in recurrent ovarian cancer. Cancer Treat Rev. 2002: 28(2), 121-125.
13.Bickels J, Manusama ER, Gutman M, Eggermont AM, Kollender Y, Abu-Abid S et al. Isolated limb perfusion with tumour necrosis factor-alpha and melphalan for unresectable bone sarcomas of the lower extremity. Eur J Surg Oncol. 1999: 25(5), 509-514.
14.Eggermont AM, Schraffordt KH, Lienard D, Kroon BB, van Geel AN, Hoekstra HJ et al. Isolated limb perfusion with high-dose tumor necrosis factor-alpha in combination with interferon-gamma and melphalan for nonresectable extremity soft tissue sarcomas: a multicenter trial. J Clin Oncol. 1996: 14(10), 2653-2665.
15.Eggermont AM, Schraffordt KH, Klausner JM, Kroon BB, Schlag PM, Lienard D et al. Isolated limb perfusion with tumor necrosis factor and melphalan for limb salvage in 186 patients with locally advanced soft tissue extremity sarcomas. The cumulative multicenter European experience. Ann Surg. 1996: 224(6), 756-764.
16.Lienard D, Lejeune FJ, and Ewalenko P. In transit metastases of malignant melanoma treated by high dose rTNF alpha in combination with interferon-gamma and melphalan in isolation perfusion. World J Surg. 1992: 16(2), 234-240.
17.Olieman AF, Lienard D, Eggermont AM, Kroon BB, Lejeune FJ, Hoekstra HJ et al. Hyperthermic isolated limb perfusion with tumor necrosis factor alpha, interferon gamma, and melphalan for locally advanced nonmelanoma skin tumors of the extremities: a multicenter study. Arch Surg. 1999: 134(3), 303-307.
18.van der Veen AH, de Wilt JH, Eggermont AM, van Tiel ST, Seynhaeve AL, and ten Hagen TL. TNF-alpha augments intratumoural concentrations of doxorubicin in TNF-alpha-based isolated limb perfusion in rat sarcoma models and enhances anti-tumour effects. Br J Cancer. 2000: 82(4), 973-980.
19.de Wilt JH, ten Hagen TL, de Boeck G, van Tiel ST, de Bruijn EA, and Eggermont AM. Tumour necrosis factor alpha increases melphalan concentration in tumour tissue after isolated limb perfusion. Br J Cancer. 2000: 82(5), 1000-1003.
20.Eggermont AM, Schraffordt KH, Lienard D, Kroon BB, van Geel AN, Hoekstra HJ et al. Isolated limb perfusion with high-dose tumor necrosis factor-alpha in combination with interferon-gamma and melphalan for nonresectable extremity soft tissue sarcomas: a multicenter trial. J Clin Oncol. 1996: 14(10), 2653-2665.
21.Tracey KJ, Beutler B, Lowry SF, Merryweather J, Wolpe S, Milsark IW et al. Shock and tissue injury induced by recombinant human cachectin. Science. 1986: 234(4775), 470-474.
22.Spriggs DR, Sherman ML, Michie H, Arthur KA, Imamura K, Wilmore D et al. Recombinant human tumor necrosis factor administered as a 24-hour intravenous infusion. A phase I and pharmacologic study. J Natl Cancer Inst. 1988: 80(13), 1039-1044.
23.ten Hagen TL, van der Veen AH, Nooijen PT, van Tiel ST, Seynhaeve AL, and Eggermont AM. Low-dose tumor necrosis factor-alpha augments antitumor activity of stealth liposomal doxorubicin (DOXIL) in soft tissue sarcoma-bearing rats. Int J Cancer. 2000: 87(6), 829-37.

24.Brouckaert P, Takahashi N, van Tiel ST, Hostens J, Eggermont AM, Seynhaeve AL et al. Tumor necrosis factor-alpha augmented tumor response in B16BL6 melanoma-bearing mice treated with stealth liposomal doxorubicin (Doxil) correlates with altered Doxil pharmacokinetics. Int J Cancer. 2004: 109(3), 442-448.

25.Brett J, Gerlach H, Nawroth P, Steinberg S, Godman G, and Stern D. Tumor necrosis factor/cachectin increases permeability of endothelial cell monolayers by a mechanism involving regulatory G proteins. J Exp Med. 1989: 169(6), 1977-1991.

26.Partridge CA, Horvath CJ, Del Vecchio PJ, Phillips PG, and Malik AB. Influence of extracellular matrix in tumor necrosis factor-induced increase in endothelial permeability. Am J Physiol. 1992: 263(6 Pt 1), L627-L633.

27.Manusama ER, Nooijen PT, Stavast J, Durante NM, Marquet RL, and Eggermont AM. Synergistic antitumour effect of recombinant human tumour necrosis factor alpha with melphalan in isolated limb perfusion in the rat. Br J Surg. 1996: 83(4), 551-555.

28.Mayer LD, Tai LC, Ko DS, Masin D, Ginsberg RS, Cullis PR et al. Influence of vesicle size, lipid composition, and drug-to-lipid ratio on the biological activity of liposomal doxorubicin in mice. Cancer Res. 1989: 49(21), 5922-5930.

29.Skehan P, Storeng R, Scudiero D, Monks A, McMahon J, Vistica D et al. New colorimetric cytotoxicity assay for anticancer-drug screening. J Natl Cancer Inst. 1990: 82(13), 1107-1112.

30.Brouckaert P, Takahashi N, van Tiel ST, Hostens J, Eggermont AM, Seynhaeve AL et al. Tumor necrosis factor-alpha augmented tumor response in B16BL6 melanoma-bearing mice treated with stealth liposomal doxorubicin (Doxil) correlates with altered Doxil pharmacokinetics. Int J Cancer. 2004: 109(3), 442-448.

31.Boucher Y, Baxter LT, and Jain RK. Interstitial pressure gradients in tissue-isolated and subcutaneous tumors: implications for therapy. Cancer Res. 1990: 50(15), 4478-4484.

32.Yuan F. Transvascular drug delivery in solid tumors. Semin Radiat Oncol. 1998: 8(3), 164-175.

33.Dvorak HF, Nagy JA, Dvorak JT, and Dvorak AM. Identification and characterization of the blood vessels of solid tumors that are leaky to circulating macromolecules. Am J Pathol. 1988: 133(1), 95-109.

34.Jain RK. Transport of molecules, particles, and cells in solid tumors. Annu Rev Biomed Eng. 1999: 1, 241-263.

35.Hobbs SK, Monsky WL, Yuan F, Roberts WG, Griffith L, Torchilin VP et al. Regulation of transport pathways in tumor vessels: role of tumor type and microenvironment. Proc Natl Acad Sci U S A. 1998: 95(8), 4607-12.

36.Yuan F, Dellian M, Fukumura D, Leunig M, Berk DA, Torchilin VP et al. Vascular permeability in a human tumor xenograft: molecular size dependence and cutoff size. Cancer Res. 1995: 55(17), 3752-3756.

37.Sparano JA and Winer EP. Liposomal anthracyclines for breast cancer. Semin Oncol. 2001: 28(4 Suppl 12), 32-40.

38.Judson I, Radford JA, Harris M, Blay JY, van Hoesel Q, Le Cesne A et al. Randomised phase II trial of pegylated liposomal doxorubicin (DOXIL/CAELYX) versus doxorubicin in the treatment of advanced or metastatic soft tissue sarcoma: a study by the EORTC Soft Tissue and Bone Sarcoma Group. Eur J Cancer. 2001: 37(7), 870-877.

39.Northfelt DW, Dezube BJ, Thommes JA, Miller BJ, Fischl MA, Friedman-Kien A et al. Pegylated-liposomal doxorubicin versus doxorubicin, bleomycin, and vincristine in the treatment of AIDS-related Kaposi's sarcoma: results of a randomized phase III clinical trial. J Clin Oncol. 1998: 16(7), 2445-2451.

40.O'Brien ME, Wigler N, Inbar M, Rosso R, Grischke E, Santoro A et al. Reduced cardiotoxicity and comparable efficacy in a phase III trial of pegylated liposomal doxorubicin HCl (CAELYX/Doxil) versus conventional doxorubicin for first-line treatment of metastatic breast cancer. Ann Oncol. 2004: 15(3), 440-449.

41.Stebbing J and Gaya A. Pegylated liposomal doxorubicin (Caelyx) in recurrent ovarian cancer. Cancer Treat Rev. 2002: 28(2), 121-125.

42.Newman MS, Colbern GT, Working PK, Engbers C, and Amantea MA. Comparative pharmacokinetics, tissue distribution, and therapeutic effectiveness of cisplatin encapsulated in long-circulating, pegylated liposomes (SPI-077) in tumor-bearing mice. Cancer Chemother Pharmacol. 1999: 43(1), 1-7.

43.Partridge CA, Horvath CJ, Del Vecchio PJ, Phillips PG, and Malik AB. Influence of extracellular matrix in tumor necrosis factor-induced increase in endothelial permeability. Am J Physiol. 1992: 263(6 Pt 1), L627-L633.

44.Manusama ER, Stavast J, Durante NM, Marquet RL, and Eggermont AM. Isolated limb perfusion with TNF alpha and melphalan in a rat osteosarcoma model: a new anti-tumour approach. Eur J Surg Oncol. 1996: 22(2), 152-157.

Chapter 3

The integrin inhibitor Cilengitide augments tumor response in loco-regional therapy with melphalan

Timo L.M. ten Hagen
Ann L.B. Seynhaeve
Gisela aan de Wiel-Ambagtsheer
Ernst A. de Bruijn
Sandra T. van Tiel
Curzio Ruegg
Michael Meyring
Matthias Grell
Simon L. Goodman
Alexander M.M. Eggermont

Submitted for publication

Research article

The integrin inhibitor Cilengitide augments tumor response in loco-regional therapy with melphalan

Timo L.M. ten Hagen[1], Ann L.B. Seynhaeve[1], Gisela aan de Wiel-Ambagtsheer[1], Ernst A. de Bruijn[2], Sandra T. van Tiel[1], Curzio Ruegg[3], Michael Meyring[4], Matthias Grell[5], Simon L. Goodman[5], and Alexander M.M. Eggermont[1].

[1]Department of Surgical Oncology, Erasmus MC, Rotterdam, The Netherlands, [2]Department of Experimental Oncology, University of Leuven, Leuven, Belgium, [3]Division of Experimental Oncology, Centre Pluridisciplinaire d'Oncologie and Swiss Institute for Experimental Cancer Research-NCCR Molecular Oncology, Lausanne, Switzerland, [4]Insitute of Drug Metabolism and Pharmacokinetics, Merck KGaA, Grafing, Germany and [5]Therapeutic Area Oncology, Merck KGaA, Darmstadt, Germany.

ARTICLE INFORMATION

Submitted for publication

ACKNOWLEDGMENTS

The authors thank Diane Hahn for valuable technical assistance and Dr. Kirsten Kullak of Boehringer Ingelheim for the provision of TNF.

ABSTRACT

Isolated limb perfusion (ILP) with tumor necrosis factor-alpha (TNF) and the antitumor drug melphalan, is successfully used to treat patients with advanced bulky melanoma and sarcoma of the limbs. However, the intrinsic toxicity of TNF led us to explore alternative drugs that might synergize with chemotherapy in this setting. Cilengitide (EMD 121974) is a cyclic inhibitor of αV integrins in clinical development as an antiangiogenic agent. In this study, we show that Cilengitide strongly enhances the antitumor effects of melphalan in soft tissue sarcoma-bearing rats treated by ILP. Interestingly, and in notable contrast to previous *in vivo* antitumor studies with αV inhibitors, Cilengitide acts in a time frame in the hours immediately bordering the ILP. Cilengitide triggers a strong increase in the concentration of melphalan within the tumor and increased death of tumor associated endothelial cell, but did not affect non-tumoral tissues. As Cilengitide has a low toxicity these data indicate its possible use in combination with chemotherapy in more demanding settings, such as organ perfusion and systemic administration, for the treatment of advanced solid tumors.

INTRODUCTION

Growth of solid tumors depends strongly on tumor angiogenesis, the formation of new blood vessels in the tumor microenvironment [1]. Adhesion receptors of the integrin family are the main endothelial cell adhesion molecules binding to the underlying extracellular matrix (ECM). The αV integrins are important in the formation of new blood vessels. They appear to be de-novo induced and activated on tumor angiogenic endothelia [2] and promote endothelial cell attachment, spreading, survival, proliferation and locomotion [3-10]. αV integrins, in particular αVβ3 and αVβ5, have been considered as therapeutic targets to inhibit angiogenesis [2]. Cilengitide is a cyclic pentapeptide inhibitor of αVβ3 and αVβ5 integrins, and blocks growth factors- and tumor-driven angiogenesis [11]. The isolated limb perfusion (ILP) is a surgical procedure used in the clinic for rescue therapy of distributed malignant melanoma and soft tissue sarcoma and has a high success rate [12,13]. In this model, the tumor response depends on the combination of the

alkylating reagent melphalan with the anti-neovascular activity of tumor necrosis factor-alpha (TNF). We have shown that TNF augments the influx of the cytotoxic agents into the tumor compartment, likely due to increased vascular permeability and reduction of the intratumoral pressure [14-16]. Also, in animal isolated organ perfusions we showed a beneficial effect of TNF in combination with chemotherapy [17,18]. However, the severe local toxicity prevents the effective use of TNF either during organ perfusion or for systemic administration in humans. Since Cilengitide can disrupt the endothelial cell layer of angiogenic vessels, we hypothesized that at early time point's disruption of the endothelial cells could result in an increased vascular permeability and enhanced melphalan accumulation in the tumor, as we showed for TNF. Therefore we investigated whether perturbation of the tumor-vascular compartment by Cilengitide could affect melphalan-based ILP and improve antitumor response.

EXPERIMENTAL METHODS

Agents. Cilengitide (EMD 121974; cyclic(Arg-Gly-Asp-D-Phe-(N-Methyl)-Valine) in physiological saline (15 mg/ml; 25.5 mM) and EMD 66203 (cyclic(Arg-Gly-Asp-D-Phe-Valine; c(RGDfV)) in physiological saline (15 mg/ml; 26 mM) were kindly provided by Merck KGaA, Darmstadt, FRG, and further diluted in saline or appropriate culture medium. Melphalan (Alkeran) was purchased from GlaxoSmithKline BV and diluted in PBS to a concentration of 2 mg/ml. Recombinant human tumor necrosis factor-alpha (TNF; 2 mg/ml; specific activity $6x10^7$ U/mg; endotoxin < 1 units (EU) per mg protein) was kindly provided by Boehringer Ingelheim.

Animals and tumor model. Male inbred Brown Norway rats (Harlan-CPB, the Netherlands) were used at a weight of 250-300 g, and were fed a standard laboratory diet *ad libitum*. Small fragments (1 mm^3) of the syngeneic BN175 soft tissue sarcoma were implanted subcutaneously in the right hind leg just above the ankle as previously described [19]. Rats were sacrificed when tumor diameter exceeded 25 mm or at the end of the experiment. All animal studies were done in accordance with protocols approved by the committee on Animal Research of the Erasmus MC, Rotterdam, the Netherlands.

Treatment protocol. After implantation tumors were allowed to grow to a diameter of 12-14 mm and rats were randomly assigned to the different treatment groups as listed in table 1. The treatment schedules for the different groups are depicted in figure 1 (**Fig. 1**). Rats were injected i.p. with Cilengitide (50 mg/kg) or saline 2 hours before and 3 hours after ILP. During ILP Cilengitide (500 µg, 170 µM), melphalan (40 µg, 8 µg/ml) and/or TNF (50 µg, 10 µg/ml) were added to the circuit containing a total volume of 5 ml Haemaccel (Behring Pharma).

Isolated limb perfusion. The perfusion technique was performed as described previously [19]. Isoflurane (Pharmachemie) was used as inhalation anesthesia during the operation. The femoral vessels were approached through an incision parallel to the inguinal ligament after systemic heparin administration of 50 IU (Leo Pharmaceutical Products) to prevent coagulation. The femoral artery and vein were cannulated with silastic tubing (0.30 mm inner diameter, 0.64 mm outer diameter; 0.64 mm inner diameter, 1.19 mm outer diameter, respectively; Dow Corning, Ann Arbor, MI). Applying a tourniquet around the groin temporarily occluded the collaterals. An oxygenation reservoir filled with 5 ml Haemaccel and a low-flow roller pump (Watson Marlow type 505 U, Falmouth) were included into the circuit. Cilengitide, melphalan and TNF were added as bolus to the circuit reservoir. The roller pump circulated the perfusate at a flow of 2.4 ml/min for 30 min. It is important to note that in this study the ILP with melphalan and/or TNF lasted only 20 min, as a pre-perfusion with Cilengitide or sham of 10 min was given. This was in contrast to previous studies in which we performed perfusion with TNF and melphalan for the full 30 min. A washout with 5 ml oxygenated Haemaccel was performed at the end of the perfusion. During

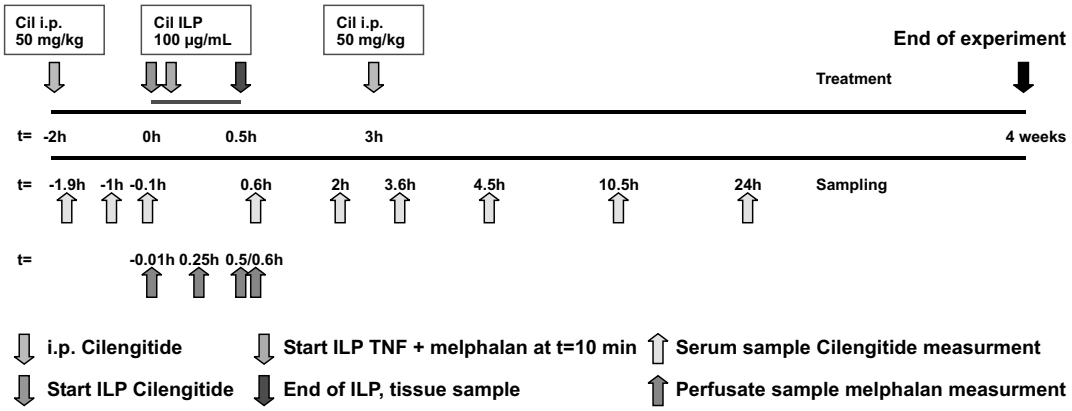

Figure 1. Time-line of Cilengitide treatment and sample collection. (See color section for a full-color version.)

ILP and washout, the hind leg was kept at a constant temperature of 38-39°C by a warm-water mattress applied around the leg. Limb function was subsequently monitored daily to assess treatment and drug related local toxicity.

Assessment of tumor response. Tumor growth was recorded daily by caliper measurement and tumor volume calculated using the formula 0.4 x (A^2 x B) (where B represents the largest diameter and A the diameter perpendicular to B). The classification of tumor response was: progressive disease (PD) = increase of tumor volume (>25%); no change (NC) = tumor volume equal to volume during perfusion (in a range of -25% and + 25%); partial remission (PR) = decrease of tumor volume (-25% and -90%); complete remission (CR) = tumor volume less than 10% of initial volume. Response rate (RR) is partial remission and complete remission.

Histopathology staining. Directly after ILP, tumors were excised, stored in formalin, and embedded in paraffin. Four µm sections were cut and stained with hematoxylin and eosin using standard procedures. Three or four different tumors in each experimental group were subjected to blinded evaluation. At least 6 slides were examined from each tumor. The sections were examined on a Leica DM-RXA light microscope and photographed using a Sony 3CCD DXC 950 camera.

Drug pharmacokinetics. During the treatment protocol depicted in figure 1 serum and perfusate samples were collected from at least 3 rats as indicated. At the end of perfusion directly after washout, tumor and part of the hind limb muscle were excised. Samples were immediately frozen in liquid nitrogen to stop metabolism of melphalan, and stored at -80°C.

Tissue and perfusate concentrations of melphalan. Tumor and muscle tissues were homogenized in 2 ml acetonitrile (Pro 200 homogenizer, Pro Scientific) and centrifuged at 2500 g. Melphalan was measured in these supernatants, serum and perfusate samples by gas chromatography-mass spectrometry (GC-MS) as described earlier by Tjaden and de Bruijn [20]. p-(Bis(2-chloroethyl)amino)-phenylacetic methyl ester was used as internal standard.

Cilengitide pharmacokinetics. The levels of Cilengitide in serum were measured using liquid chromatography with tandem mass spectrometric detection (LC-MS/MS) as described elsewhere [21]. The cyclic peptide c(RGDfV) was used as an internal standard. Stocks solutions of c(RGDfV) were prepared in acetonitrile/methanol/water (1:1:1, v/v/v) and further diluted with methanol/water (2:98, v/v). Sample aliquots were mixed with internal standard solution (1:80, v/v), extracted over an Oasis HLB column (50x1 mm; Waters), and resolved on a reversed phase column (LiChroCart 30-2 Puro-

spher, RP8e; Merck KGaA) on a gradient from 100% (0.1%) formic acid to 10% (0.1%) formic acid/90% acetonitrile (v/v). Detection was carried out by multiple reaction monitoring in the positive ion mode using an API-3000 mass spectrometer (Applied Biosystems). Mass transitions of $M+H^+$ m/z 589 to 312 and m/z 575 to 312 (precursor and product ions) were used for Cilengitide and internal standard c(RGDfV), respectively.

Endothelial apoptosis. Apoptotic cell death was detected by TUNEL staining with a commercially available DNA end-labeling kit (In Situ Cell Death-detection Kit, Fluorescein labeled, Roche). Tumor tissues were also stained for the presence of endothelial cells to differentiate between apoptosis of the endothelium and apoptosis of tumor cells. Acetone-fixed frozen sections were post-fixed in 4% paraformaldehyde for 30 min and incubated for 1 hour with mouse anti rat CD31PE (1:50; Becton Dickinson). After washing with PBS the sections were again fixed in 4% paraformaldehyde for 10 min and permeabilized with 0.1% Triton X-100 in 0.1% sodium citrate for 2 min on ice. The slides were then incubated with the TUNEL mixture for 1 hour at 37°C, mounted with mounting medium containing polyvinyl alcohol (Mowiol 4-88, Fluka) and 2.5% (w/v) DABCO (Sigma), examined on a Leica DM-RXA microscope and photographed using a Sony 3CCD DXC 950 camera.

Culture conditions. Cells isolated from the BN175 tumor cells were maintained in culture in RPMI-1640 (Lonza) supplemented with 10% fetal calf serum (Lonza). Human umbilical vein endothelial cells (HUVEC) were isolated by collagenase digestion using the method described by Jaffe [22] and cultured in HUVEC medium containing human endothelial-SFM (Invitrogen), 20% heat-inactivated newborn calf serum (Lonza), 10% heat-inactivated human serum (Lonza), 20 ng/ml human recombinant basic Fibroblast Growth Factor (Peprotech EC Ltd), 100 ng/ml human recombinant Epidermal Growth Factor (Peprotech EC Ltd). Each isolate was derived from an individual umbilical vein and used for experiments at passage 5 or 6. For all experiments, unless mentioned otherwise, HUVEC were cultured on plates coated with vitronectin (1 µg/ml; Promega), fibronectin (10 µg/ml; Roche Diagnostics) or gelatin (10 mg/ml; Sigma) in a concentration of $6x10^3$ cells in 100 µl per well for a 96 well-plate (Corning BV) and $3x10^4$ cells in 500 µl per well for a 24 well-plate (Corning BV) and allowed to adhere for 24 hours. BN175 cells were cultured in similar concentrations on untreated plates. Cells were incubated at 37°C in 5% CO_2.

Integrin expression and inhibition of adhesion by Cilengitide. To identify the integrin usage and sensitivity to Cilengitide of rat integrins on the BN175 tumor cells, cell-attachment and attachment-inhibition assays were performed as described before [23]. In brief, $2.5x10^4$ BN175 cells per well in RPMI-1640 medium supplemented with 0.5% bovine serum albumin were allowed to adhere for 1 hour at 37°C on plates coated with the ECM molecules human plasma fibronectin, vitronectin, fibrinogen, collagen type I (Serva), collagen type IV (Sigma), or laminin I (Sigma), before washing and quantification by assay for lysozomal hexosaminidase against an external standard curve. The assays were performed in the presence or absence of 1 mM Mn^{2+} ions to reveal the presence of expressed but non-activated integrins. For adhesion inhibition assays, plates were coated with vitronectin (2 µg/ml) and $2.5x10^4$ cells per well suspended in culture medium were allowed to adhere for 1 hour in the presence of serially diluted Cilengitide and c(RGDfV), before washing and quantification of attached cells.

***In vitro* response of endothelial cells and tumor cells to Cilengitide.** HUVEC and BN175 cells were cultured in a 96 well-plate for 72 hours in the continuous presence of various concentrations of Cilengitide and melphalan. Cell growth was measured using the sulphorhodamine-B (SRB) assay according to the method of Skehan [24]. In short, cells were washed twice with PBS, fixed with 10% trichloric acetic acid (1 hour, 4°C) and washed again.

Cells were stained with 0.4% SRB (Sigma) for 15-30 min, washed with 1% acetic acid and were allowed to dry. Protein bound SRB was dissolved in TRIS (10 mM, pH 9.4). The optical density (O.D.) was read at 540 nm. Cell growth was calculated using the formula: cell growth = (O.D. test well/O.D. control) x 100 percent. The drug concentration reducing the absorbance to 50% of the control (IC_{50}) was determined from the growth curves. The experiments were repeated at least 5 times.

***In vitro* apoptosis assay.** HUVEC in a 24 well-plate were incubated with 50, 5, 0.5 or 0 µg/ml Cilengitide for 5 and 60 min. Detached cells were collected from the supernatant and attached cells were harvested by mild trypsinization. Early apoptosis was detected by annexin V and necrosis/late apoptosis with propidium iodide staining, according to the manufacturer's instructions (Vybrant Apoptosis Assay kit #3, Molecular Probes). Cells were immediately analyzed by flow-cytometry (FACScan, Becton Dickinson) and data analysis was performed using WinMDI 2.7 (Freeware, Joseph Trotter, Scripps Research Institute). Alternatively, apoptosis was also detected using YO-PRO-1 (Molecular Probes). At the end of the incubation period, detached cells were removed, HUVEC medium containing YO-PRO-1 (0.5 µM) was added to the well with the remaining adherent cells, and incubated for 15 min at 37°C. Fluorescence was then visualized using an inverted Zeiss Axiovert 100M microscope and captured with an Axiocam HRc digital camera, using AxioVision v4.0 software.

Morphology and permeability changes *in vitro*. HUVEC in a 24 well-plate were incubated with 50, 5, 0.5 or 0 µg/ml Cilengitide and after 0.5, 1, 2, 4, 8 and 24 hours morphological cell changes were examined with a 10x N.A. 0.30 Plan-Neofluar objective lens using an inverted Zeiss Axiovert 100M microscope equipped with an Axiocam HRc digital camera using AxioVision v4.0 software (Carl Zeiss). Alternatively, HUVEC were plated in 500 µL Cilengitide containing HUVEC medium at a concentration of 3x104 cells per well in a coated 24 well-plate. After 0.5, 1, 2, 4, 8 and 24 hours the adherence of the cells was examined microscopically.

To evaluate the transendothelial monolayer-permeability, HUVEC were plated in a coated transwell (Corning BV; 0.4 µm pore size, 6.5 mm diameter, polyester filters) at a density of 1.2x104 cells per well. In the lower compartment, 1 ml of HUVEC medium was added. Two days after seeding a confluent monolayer had formed, non-adhering cells were removed and the medium was replaced with 200 µl of 50, 5, 0.5 or 0 µg/ml Cilengitide together with 50 µl fluorescein (0.5 mg/ml, Sigma). At 0.25, 0.5, 1, 2, 4, 8 and 24 hours, 50 µl medium of the lower chamber was taken and fluorescence was measured at excitation 490 nm and emission 530 nm, in a Victor^2 1410 multilabel counter (Wallac). Induction of permeability was indicated by a higher concentration of fluorescein in the lower chamber of the transwell relative to untreated controls.

Statistical analysis. *In vitro* results were evaluated for statistical significance with the Mann-Whitney U-test. Synergy of Cilengitide, melphalan and TNF was tested as described before [25]. Briefly, the tumor-response-ratio was calculated by dividing the tumor volume at day 5 and 8 with the volume at day 0. The ratio of Cilengitide alone plus melphalan alone was compared with the ratio of Cilengitide plus melphalan (Mann-Whitney U-test). Response rates were subjected to analysis-of-variance and post hoc to the least significant difference multiple comparison test. All statistical tests were two-sided and P values less than 0.05 were considered as statistically significant. Calculations were performed on a personal computer using GraphPad Prism v3.0 and SPSS v11.0 for Windows 2000.

RESULTS

The combination of Cilengitide and melphalan results in a strong tumor response. The anti-vascular agent TNF is applied only during the brief period of perfusion during ILP, and yet, it strongly enhances the antitumor activity of melphalan [14,26]. Based on this experi-

Table 1. Treatment groups and tumor response of BN175 soft tissue sarcoma bearing rats after ILP with Cilengitide, TNF and melphalan.

Group[a]	Therapy regimen		Tumor response[d]					
	i.p injections[b]	in perfusate[c]	PD	SD	PR	CR	RR	n
1	Sham	Sham	9	1			0	10
2	Sham	Cilengitide	4				0	4
3	Cilengitide	Sham	7				0	7
4	Cilengitide	Cilengitide	14				0	14
5	Sham	TNF	9	1	1	1	17%	12
6	Cilengitide	TNF	5				0	5
7	Sham	Cilengitide+TNF	6				0	6
8	Cilengitide	Cilengitide+TNF*	5				0	5
9	Cilengitide	Cilengitide+TNF	10			2	16%	12
10	Sham	melphalan	9	2	1		8%	12
11	Cilengitide	melphalan	5		1		17%	6
12	Sham	Cilengitide+melphalan	3				0	3
13	Cilengitide	Cilengitide+melphalan	2	1	2	8	77%	13
14	Sham	TNF+melphalan	7	2	1	2	25%	12
15	Cilengitide	TNF+melphalan			3	3	100%	6
16	Sham	Cilengitide+TNF+melphalan	2	1	2	1	50%	6
17	Cilengitide	Cilengitide+TNF+melphalan	2	0	3	8	85%	13
18	Cilengitide before ILP	Cilengitide+TNF+melphalan	3**	1	1		20%	5
19	Cilengitide after ILP	TNF+melphalan	3		1	1	40%	5

Note: animals were treated as depicted in the time line in figure 1.

[a] Group numbers refer to table 1.

[b] Rats were injected i.p. 2 hours before and 3 hours after ILP with Cilengitide as described in the experimental procedures.

[c] ILP was started with sham or Cilengitide and after 10 min melphalan or TNF was added.

[d] Tumor response is classified as described in the experimental procedures: PD, progressive disease; SD, stable disease; PR, partial response; CR, complete response in absolute numbers; RR, response rate (PR plus CR) in percentage.

* In this group TNF was added directly with Cilengitide at the beginning of the perfusion. In contrast with the other groups, in which TNF and/or melphalan was present for 20 min, TNF was present in this group for the full 30 min in the perfusate.

** Although initially a response was observed rapid regrowth occurred showing PD at day 10.

ence, we investigated whether the antiangiogenic agent Cilengitide might also work in such a short time scale. To test the activity of Cilengitide in a combination with chemotherapy for the treatment of tumors in ILP, rats bearing established and rapidly growing syngeneic soft tissue sarcoma in the hind limb were perfused with Cilengitide combined with melphalan and TNF under different regimens (**Table 1** and **Fig. 2**). In the first set of experiments Cilengitide was administered to animals pre- and post-ILP by i.p injection and during ILP with melphalan, to maximally saturate available αV integrins. This protocol gave a response rate (RR) of 77%, with 8/13 complete and 2/13 partial responders (group 13), with a response on tumor volume for at least 12 days. This treatment was much more effective than ILP with melphalan plus TNF (group 14, RR of 25%) and ILP with melphalan (group 10, RR of 8%) without any addition of Cilengitide. ILP and i.p. treatment with Cilengitide alone (group 4, RR of 0%) had no effect (statistics are presented in **Supplementary Table 1** and **Supplementary Table 2**). We could show a statistically significant synergy between Cilengitide (when injected i.p. and given during ILP) and melphalan ($P < 0.05$;

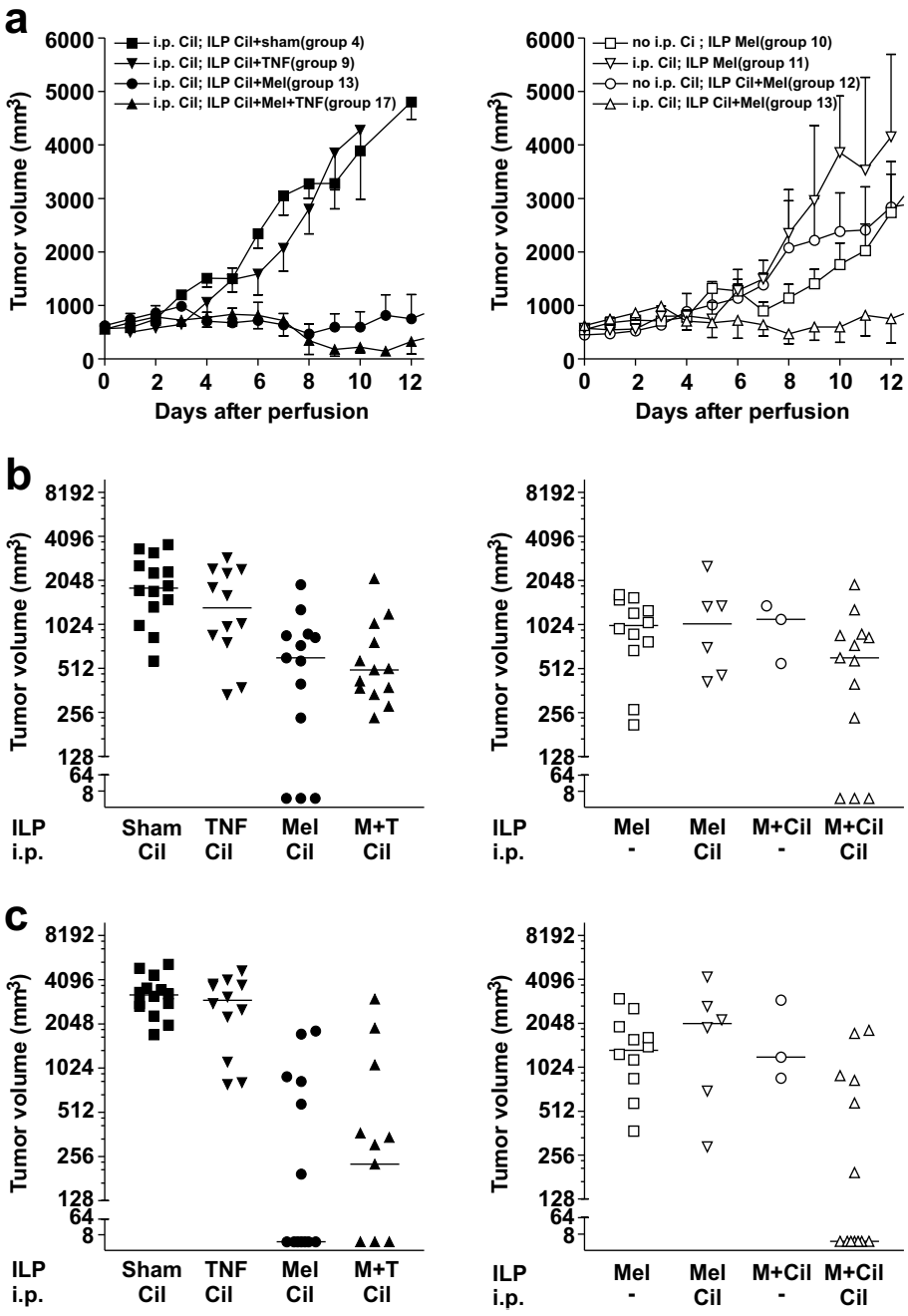

Figure 2. Tumor response in rats treated with Cilengitide in combination with melphalan-based isolated limb perfusion. (**a**) BN175 tumor growth was measured daily after treatment as depicted in figure 1. In the left graphs all rats received Cilengitide (Cil) as i.p. injection and as bolus in the perfusate. In right graphs different regiments of Cilengitide with melphalan were used. Tumor volumes of individual animals at 5 days (**b**) and 8 days (**c**) after i.p. with Cilengitide and ILP with Cilengitide, melphalan (M or Mel) and TNF (T). These results show that Cilengitide-melphalan combination results in a strong tumor response. Data points represent tumor volume ± SD; number of rats is indicated in table 1.

Supplementary Table 1. Statistical analysis of tumor response

Group[a]	Therapy regimen		Group[a]			
	i.p injection[b]	in perfusate[c]	4	9	13	17
1	Sham	Sham	0.237	0.633	0.000	0.000
4	Cilengitide	Cilengitide		0.134	0.000	0.000
9	Cilengitide	Cilengitide +TNF			0.002	0.002
13	Cilengitide	Cilengitide + melphalan				0.930
17	Cilengitide	Cilengitide + TNF + melphalan				

Note: animals were treated as depicted in the time line in figure 1.

[a] Group numbers refer to table 1.

[b] Rats were injected i.p. 2 hours before and 3 hours after ILP with Cilengitide as described in the experimental procedures

[c] ILP was started with sham or Cilengitide and after 10 min melphalan or TNF was added

Supplementary Table 2. Statistical analysis of tumor volumes

Group[a]	Therapy regimen		Group[d]						
	i.p injection[b]	in perfusate[c]	4	9	10	11	12	13	17
4	Cilengitide	Cilengitide	X	0.198	0.005	0.058	0.078	0.000	0.000
9	Cilengitide	Cilengitide+TNF	0.504	X	0.204	0.512	0.564	0.000	0.014
10	Sham	melphalan	0.002	0.049	X	0.925	1.000	0.002	0.004
11	Cilengitide	melphalan	0.039	0.190	0.615	X	0.796	0.007	0.022
12	Sham	Cilengitide+melphalan	0.059	0.312	0.815	1.00	X	0.042	0.069
13	Cilengitide	Cilengitide+melphalan	0.000	0.012	0.060	0.188	0.251	X	0.939
17	Cilengitide	Cilengitide + TNF + melphalan	0.000	0.000	0.073	0.114	0.122	0.398	X

Note: animals were treated as depicted in the time line in figure 1.

[a] Group numbers refer to table 1.

[b] Rats were injected i.p. 2 hours before and 3 hours after ILP with Cilengitide as described in the experimental procedures

[c] ILP was started with sham or Cilengitide and after 10 min melphalan or TNF was added.

[d] Upper right corner statistical analysis at day 5 and lower left corner at day 8.

Cilengitide or melphalan given alone versus Cilengitide plus melphalan treatment).

In a second set of experiments Cilengitide was only administered during ILP or as an i.p. injection before and after the ILP only. Injection of Cilengitide i.p. improved tumor response in a melphalan-based ILP (group 11) to 17%, while administration only during ILP with melphalan (group 12) did not affect tumor-response. In a third set of experiments Cilengitide was given in combination with a melphalan plus TNF-based ILP. Addition of Cilengitide to a TNF-plus-melphalan ILP resulted in a very good response rate of 85% (group 17). To obtain the best response Cilengitide had to be given i.p. before and after ILP and in the perfusate during the perfusion. In contrast to the combination with melphalan, Cilengitide had a much weaker impact on TNF-based perfusion (groups 7-9), suggesting that Cilengitide and TNF may both affect the same target, namely tumor endothelial cells, each to an already maximal extend. Treatment of the rats with Cilengitide alone (i.e. i.p. or during ILP, group 2, 3 and 4) had no effect on tumor progression. Importantly, a perfusion with melphalan plus TNF for the full 30 minutes as previously routinely conducted, results in a tumor response of around 75%, indicating that the time frame of exposure affects response rate. No gross toxicity related to the applied high systemic and local doses of Cilengitide was seen (data not shown).

The combination of Cilengitide and melphalan results in loss of endothelial integrity and hemorrhage. While administration of melphalan alone during the ILP had minimal effect on the tumor-associated vasculature, combined administration of Cilengitide and melphalan dramatically affected the endothelial integrity of tumor blood vessels. Immunohistological analysis of perfused tumors, removed immediately after ILP, revealed a clear disruption of the endothelial layer. Endothelial cells detached from the vessel wall in tumors treated with Cilengitide in combination with melphalan, while administration of melphalan alone had no such effect (**Fig. 3a** and **Fig 3b**). These results were confirmed by TUNEL stain-

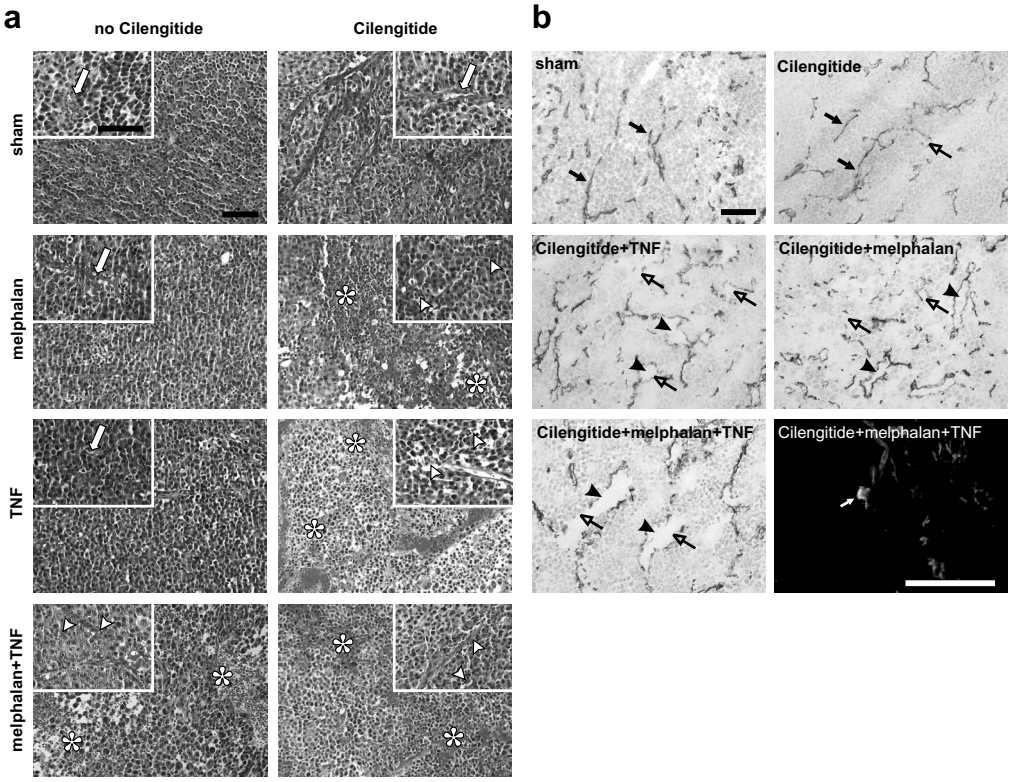

Figure 3. Histopathology of BN175 tumor after Cilengitide treatment in combination with a melphalan-based ILP. (**a**) Tumors were excised immediately after treatment for histological evaluation. Left panel, H&E staining was performed on tumors of all groups and showed no effect on tumor cells and tumor vasculature (open arrow) when animals were treated with sham, melphalan or TNF alone. Confirming previous results, ILP with melphalan plus TNF resulted in marked vascular damage (arrow head), which was accompanied by hemorrhage and edema (asterisk). Right panel, administration of Cilengitide alone had no noticeable effect on tumor histology or on tumor-associated vasculature (open arrow). However, when Cilengitide was combined with melphalan, TNF or melphalan plus TNF massive vascular destruction (open arrow) and hemorrhage (asterik) were observed. (**b**) Damage to the tumor-associated vasculature is visualized by CD31 staining. Tumors were removed at the end of the treatment, frozen and processed for immunohistochemistry as described in the experimental procedures. Perfusion with Cilengitide alone had marginal effect on tumor vessel integrity or diameter (closed arrow), while treatment with a combination of Cilengitide with melphalan, TNF or melphalan plus TNF resulted in profound loss of vascular integrity (open arrow) and widening of the vascular lumen (arrow head). Endothelial cell apoptosis is shown after treatment with Cilengitide plus melphalan and TNF by TUNEL staining. The photograph (lower right panel) demonstrates apoptotic tumor cells (green), endothelial cells (red) and apoptotic endothelial cells (yellow, arrow). Scale bar apply for all images, 100 µm. (See color section for a full-color version.)

ing showing apoptosis of intratumoral endothelial cells when Cilengitide was administered (**Fig. 3b,** lower right panel). Large areas of tumor necrosis were observed in all combination protocols involving Cilengitide; Cilengitide with melphalan, Cilengitide with TNF and Cilengitide with melphalan plus TNF. Although ILP with TNF plus Cilengitide resulted in abundant tumor necrosis there was no translation in a clinical tumor response. These observations show that combination with a chemotherapeutic agent is crucial for achieving clinical tumor regression in this model. Minimal apoptosis or hemorrhage was found in non-tumor tissue (data not shown).

The addition of Cilengitide increases intratumoral melphalan concentrations. To investigate whether improved tumor response to melphalan in combination with Cilengitide involved enhanced drug delivery in the tumor, we measured intratumoral levels of melphalan. After ILP with melphalan alone on average 0.6 µg ± 0.2 melphalan per g tumor tissue was found, which was augmented 3.2 (1.9 ± 0.1 µg/g; $P < 0.01$) to 7-fold (4.2 ± 2.0 µg/g; $P < 0.05$) by the addition of Cilengitide, depending on dosing schedule (**Fig. 4a**). Cilengitide did not affect the accumulation of melphalan in the muscle tissue of the perfused leg. These results are consistent with our previous observations in TNF-based ILP, whereby TNF increased melphalan accumulation in tumor tissue through an effect on vascular permeability, while leaving permeability in normal tissue unaffected [27].

The combination with melphalan has no influence on the systemic pharmacokinetics of Cilengitide. To evaluate the systemic Cilengitide levels, Cilengitide was administered i.p. before ILP and in the perfusate during ILP in combination with melphalan and/or TNF. Blood samples were collected during treatment as depicted in figure 1. Systemic Cilengitide levels reached around 20 µg/ml (35 µM) within 10 min after i.p. administration and continued to rise to approximately 40 µg/ml (70 µM) in the first hour (**Fig. 4b**). Thereafter systemic Cilengitide levels in serum dropped with an elimination half-life of 2.1 hours. The administration of Cilengitide during ILP did not affect systemic levels as a relatively low concentration was used and a thorough washout was applied at the end of the perfusion. Data fitted a one-phase exponential decay with a goodness of fit of 0.93. The ILP, whether with Cilengitide, TNF, melphalan or combinations thereof, did not influence the systemic pharmacokinetics of Cilengitide.

Cilengitide disrupts cell adhesion mediated by αVβ3 and αVβ5 integrins and increases cell death and permeability *in vitro*. In contrast to the well-characterized integrin profiles of endothelial cells, BN175 rat sarcoma have yet to be characterized for their adhesion properties. We investigated the interaction of BN175 cells with αV ligands vitronectin, fibronectin and fibrinogen, and with non-αV ligands collagens type I and IV and laminin, and the sensitivity of this attachment to Cilengitide. BN175 cells attached and spread strongly on vitronectin, fibronectin and laminin I, but poorly on collagens and fibrinogen. Even when the integrin activator Mn^{2+} was added, collagen adhesion remained on background and adhesion to vitronectin increased strongly. Addition of Mn^{2+} caused only a weak increase of adhesion to fibrinogen (**Fig. 5a**). This profile indicates that αVβ5 is the principal vitronectin receptor, and that low amounts of αVβ3 in a weakly activated state are also present on BN175 cells. Adhesion to vitronectin was strongly inhibited by Cilengitide with an IC_{50} of approximately 2 µg/ml (4 µM), and by the related analogue c(RGDfV) with an IC_{50} of 9 µg/ml (16 µM) (**Fig. 5b**). These data are consistent with αVβ5 dependent adhesion to vitronectin [23,28]. Adhesion on fibronectin was likely principally mediated by α5β1. Laminin I adhesion was likely mediated by α6β1. Lack of adhesion to collagen reveals no active α1β1 or α2β1 receptors.

To test whether the observed synergy between melphalan and Cilengitide was a direct effect on endothelial cells or tumor cells, cultured endothelial cells (i.e. HUVEC) and BN175 cells were exposed to Cilengitide and melphalan

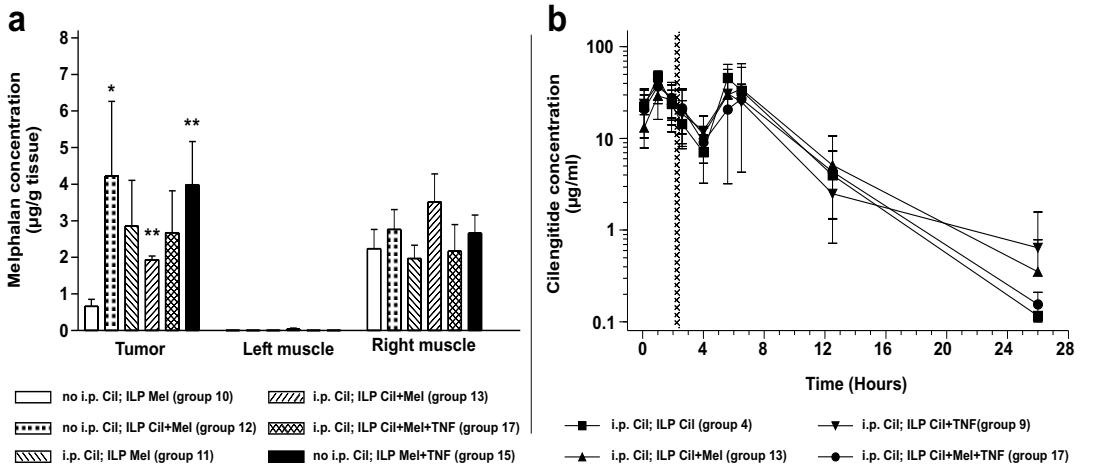

Figure 4. Tumor accumulation and phamacokinetics (**a**) Tumoral accumulation of melphalan after treatment with Cilengitide and melphalan-based isolated limb perfusion. Immediately after the end of the ILP and washout, tumor and muscle of the perfused limb (right) and non-perfused limb (left) were excised, weighted and snap-frozen. Melphalan content was measured as described in the experimental procedures. Both addition of Cilengitide to the perfusion as well as i.p. pre-treatment augmented accumulation of melphalan in the tumor. Accumulation in adjacent skin was not significantly affected. Columns represent µg melphalan per gram tissue ± SD of 6 individual animals; *, $P < 0.05$ *versus* group 10; **, $P < 0.001$ *versus* group 10. (**b**) Pharmacokinetics of Cilengitide in serum of rats during treatment as depicted in figure 1. Blood samples were collected and Cilengitide concentration determined as described in the experimental procedures. Cilengitide was injected 2 hours before and 3 hours after the ILP. Hexed region indicate perfusion period. Serum concentrations increase sharply after i.p. injection followed by a single phase clearance with a half life of 2.1 hours. Perfusion with Cilengitide did not affect Cilengitide levels in the blood due to the isolated procedure and thorough washout. Also addition of TNF, melphalan or TNF plus melphalan did not affect Cilengitide pharmacokinetics. Data points represent µg Cilengitide per ml ± SD of 3 individual animals.

or TNF, and combinations thereof. The addition of melphalan to Cilengitide increased cell death of both BN175 cells and HUVEC (**Fig. 5c**), but addition of TNF had no effect (**Supplementary Fig. 1a**). Endothelial cells on vitronectin were more sensitive to Cilengitide than cells cultured on fibronectin. αV integrins, which mediate attachment to vitronectin, and especially αVβ3, provide a survival signal to endothelial cells which, when disrupted, may stimulate their apoptosis [2]. Endothelial cells grown on the matrix components vitronectin and fibronectin and exposed to Cilengitide underwent apoptosis and necrosis, especially when grown on the obligate αV ligand vitronectin, closely correlating with the above-described assay ($P < 0.01$; **Supplementary Fig. 1b** and **Supplementary Fig. 1c**). This cell death was secondary to cell detachment, since cells that remained adherent during Cilengitide treatment stained negative for apoptosis (YO-PRO-1), and YO-PRO-1 positive cells were only observed among already detached cells, indicating that cell-death followed rather then preceded Cilengitide-induced detachment (data not shown). As a disruption of the vascular lining was observed *in vivo* following Cilengitide-ILP by histology we speculated that the increase in melphalan in the tumor was a result of an improved intratumoral delivery.

To test whether Cilengitide affected endothelial permeability directly, HUVEC monolayers were exposed to Cilengitide. Within 30 min, a time frame relevant for the ILP, endothelial permeability increased 3.5-fold when cultures were exposed to 50 µg/ml Cilengitide, which is below the maximum theoretical level reached during the ILP (100 µg/ml) ($P < 0.05$;

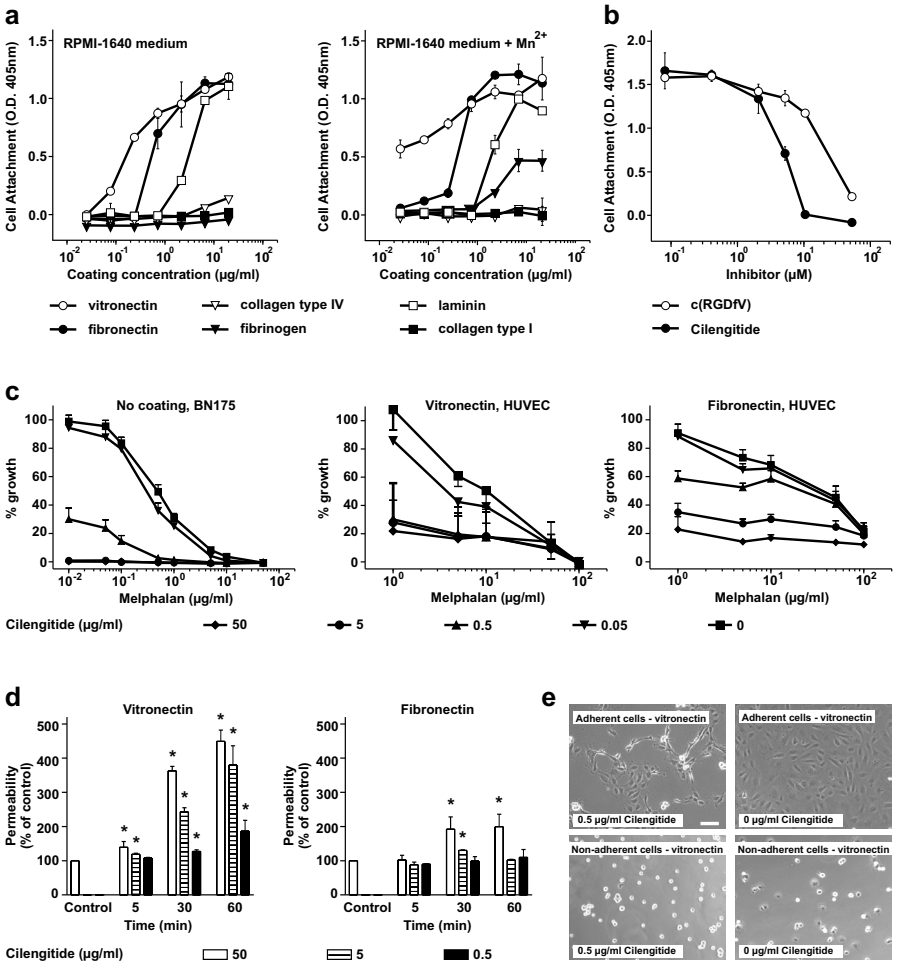

Figure 5. *In vitro* effects of Cilengitide on BN175 tumor cells and HUVEC. (**a**) Attachment characteristics of BN175 cells. BN175 cells were allowed to attach for 1 hour to surfaces coated with the indicated concentrations of ECM molecules vitronectin, fibronectin, fibrinogen, laminin, collagen type I or collagen type IV in RPMI or RPMI with supplemented 1 mM Mn^{2+}. (**b**) BN175 cells were allowed to attach for 1 hour to vitronectin in the presence of the indicated concentrations of Cilengitide or c(RGDfV). Data points represent cell attachment (100% cell attachment was equivalent to OD 1.5) ± SEM of 3 individual experiments in duplicate. (**c**) BN175 tumor cells and HUVEC were exposed to Cilengitide alone or combined with melphalan for a period of 72 hours and cell content was evaluated. A dose response of Cilengitide on BN175 cells was observed which appeared to interact with melphalan, showing higher toxicity of melphalan when Cilengitide was added. Comparable activity was observed when HUVEC were exposed to Cilengitide combined with melphalan. HUVEC appeared more sensitive to Cilengitide when grown on vitronectin compared to fibronectin. Data points represent cell growth ± SEM of at least 3 individual experiments in duplicate. (**d**) HUVEC were cultured as a confluent monolayer in a transwell chamber and exposed to Cilengitide. Permeability of the endothelial layer was determined by measuring the trans-endothelial diffusion of fluorescein over time. Exposure of endothelial cells to Cilengitide augmented vascular permeability within 30 min especially when cells were cultured on vitronectin. Columns represent percentage permeability compared to control treated cells ± SEM of at least 3 individual experiments in duplicate; *, $P < 0.05$ *versus* control. (**e**) HUVEC seeded on vitronectin, were exposed to Cilengitide directly (non-adherent) or after 24 hours of culturing (adherent) and morphology was studied 1 hour after Cilengitide exposure. Cilengitide caused HUVEC detachment in adherent cells and also inhibited adhesion. Scale bar apply for all images, 100 µm.

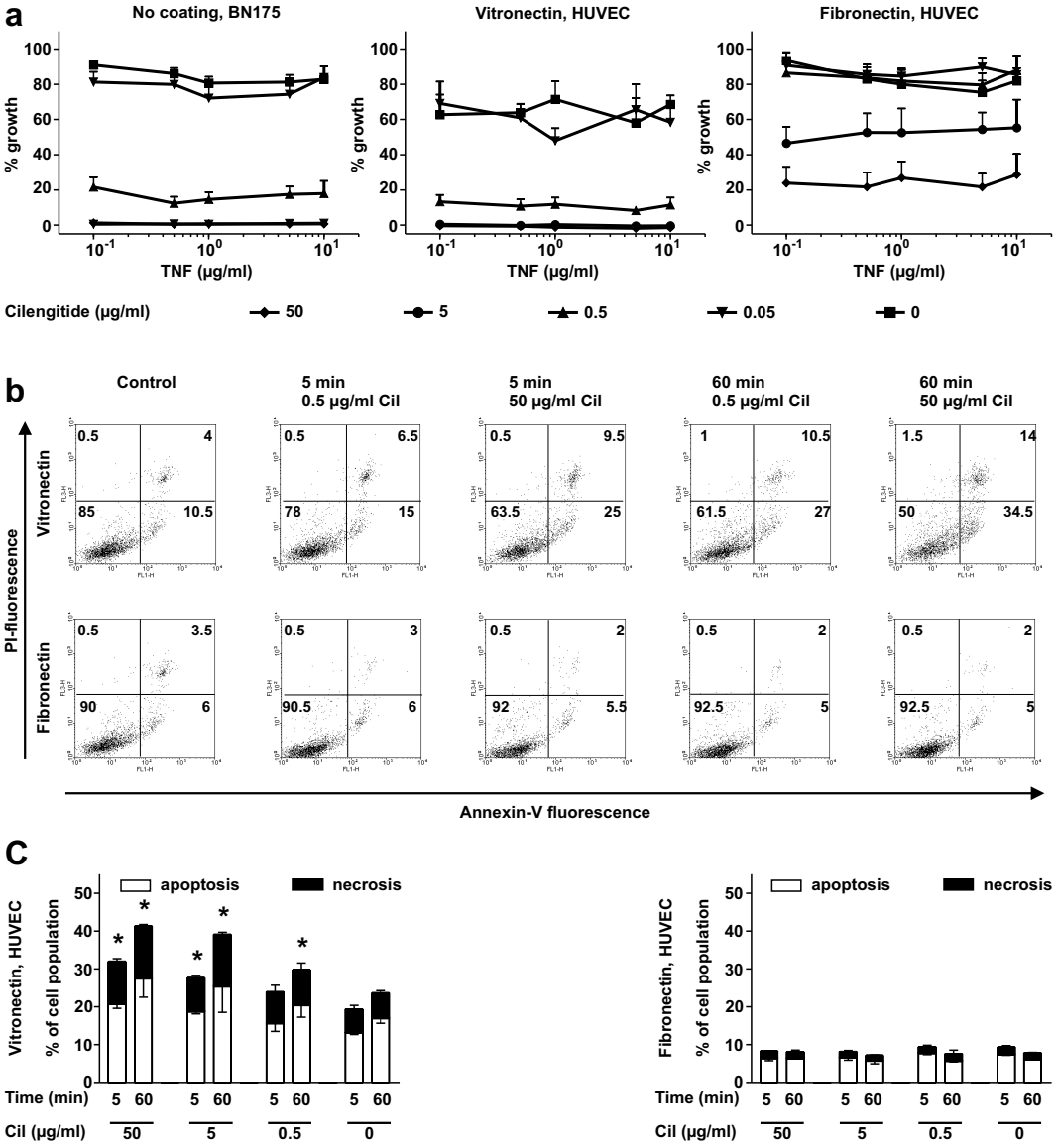

Supplementary Figure 1. Effect of Cilengitide on BN175 tumor cells and HUVEC. (**a**) BN175 tumor cells and HUVEC were exposed to Cilengitide combined with TNF for a period of 72 hours and cell content was evaluated. TNF appeared to have no direct effect on the BN175 cells and HUVEC or the toxicity profile of Cilengitide. Data points represent cell growth ± SEM of at least 3 individual experiments in duplicate. (**b**) Representative FACS data of Cilengitide-induced apoptosis in HUVEC grown on vitronectin or fibronectin in a time frame of 5 and 60 min. The number in each quadrant represent percentage cells. (**c**) Quantification of apoptosis (Annexin V positive cells) and necrosis (Annexin V and PI positive cells) is depicted. More apoptosis and necrosis after addition of Cilengitide (Cil) was observed when HUVEC were grown on vitronectin. Columns represent cell population ± SEM of 3 individual experiments in duplicate; *, $P < 0.01$ *versus* 0 µg/ml Cilengitide of the same time period.

Fig. 5d). Permeability continued to increase to a maximum of 5-fold in 1 hour. At a Cilengitide concentration of 0.5 µg/ml we found that the endothelial cell morphology was already changed, and that cells detached when grown on vitronectin (**Fig. 5e**). HUVEC that were exposed to Cilengitide directly did not adhere to vitronectin, confirming that vitronectin receptors on HUVEC were fully inhibited by Cilengitide (**Fig 5e**, **Supplementary Fig. 2** and **Supplementary Table 3**).

DISCUSSION

The tumor vasculature is considered as an excellent target in cancer treatment. Tumor endothelial cells have a distinctive phenotype that allows their targeting to achieve antitumor effects directly or in combination with chemotherapy. Integrin αVβ3 and αVβ5 are highly expressed on activated endothelial cells of the tumor neovasculature, while their expression is low on quiescent endothelia. Therefore, these integrins have been proposed as an attractive therapeutic target [3,29-31]. Prevention of the binding of the integrins αVβ3 and αVβ5 to ECM ligands can result in endothelial cell apoptosis [32,33]. Further support for the importance of αV-integrin on tumor endothelia comes from studies employing specific antibodies. The anti-αV-integrin antibody 17E6 inhibits melanoma development [23], while the αVβ3-antibody LM609 inhibits growth and invasion of tumors and inhibits angiogenesis in a CAM assay [3,4,29]. Animal studies demonstrated that addition of Cilengitide to radioimmunotherapy improved treatment efficacy in an experimental breast cancer model, apparently by targeting

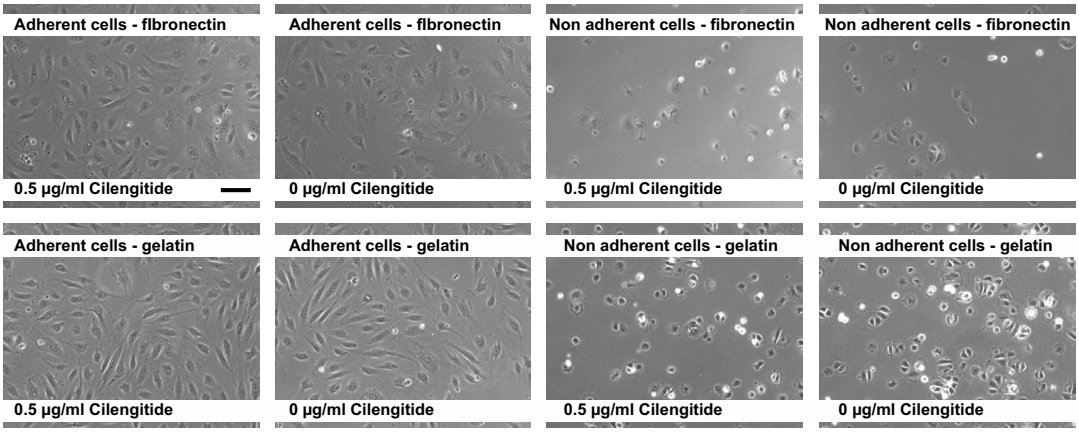

Supplementary Figure 2. Effect of Cilengitide on the adherence of HUVEC. HUVEC seeded on fibronectin and gelatin, were exposed to Cilengitide directly (non-adherent) or after 24 hours of culturing (adherent) and morphology was studied 1 hour after Cilengitide exposure. Cilengitide caused some HUVEC detachment in adherent cells and also inhibited adhesion on fibronectin coating but had no effect on the adherence on gelatin. Scale bar apply for all images, 100 µm.

Supplementary table 3. Percentage non-adherent cells on different coatings.

Coating	Cilengitide (µg/ml)			
	50	5	0.5	0
Vitronectin	99.5 ± 0.9*	85.5 ± 9.2*	77.0 ± 29*	11.2 ± 0.5
Fibronectin	55.3 ± 13.9*	36.7 ± 20.1	30.7 ± 7.4	17.1 ± 4.0
Gelatin	28.0 ± 0.5	21.4 ± 2.7	16.6 ± 4.0	20.4 ± 3.1

Note: HUVEC were plated in Cilengitide containing HUVEC medium in wells coated with different ECM. One hour after plating cells photographs were taken and adherent and non-adherent cells were counted. Data represent percentage non-adherent cells ± SD of 3 individual experiments. *, $P < 0.05$ *versus* 0 µg/ml Cilengitide.

both tumor cells and endothelia, since apoptosis of both populations was increased in the combination groups [34,35]. Furthermore, treatment with a related αVβ3 antagonist diminished the severity of arthritis, in association with increased endothelial cell apoptosis in angiogenic blood vessels [36], and blocked neo-angiogenesis in ophthalmological models [37,38]. Cilengitide is currently being evaluated in clinical phase I/II trials for glioblastoma acute myeloid leukaemia, metastatic melanoma and prostate cancer [39-41].

As Cilengitide can interfere with endothelial cell adhesion and trigger endothelial cell apoptosis in neovasculature, we tested whether its addition to a melphalan-based ILP treatment of established solid tumors could improve tumor response. Here we demonstrate that a Cilengitide-melphalan combination treatment results in a strong antitumor response with a 77% overall response rate (partial plus complete responders) while treatment with Cilengitide or melphalan alone resulted respectively in a very limited response rate of 0 and 8%. Many other studies have shown that blockade of αV-integrins can slow tumor growth, usually in immune-suppressed xenograft models, and typically in multiple repeat doses, usually daily [42-44]. In marked contrast, in this study, large, well established, syngeneic, orthotopic tumors were exposed only briefly to Cilengitide in combination with melphalan. The synergistic effect of Cilengitide on the classical alkylating agent melphalan in this short term, and arguably highly realistic model were notable. Our results show that pre-loading the animals with Cilengitide is crucial for synergy, suggesting that saturation of the integrins may pre-sensitize target cells to the cytotoxic activity of melphalan. Our parallel histological studies show that Cilengitide rapidly disrupts the endothelia of the tumor vasculature, while leaving the normal vasculature intact, resulting in massive intratumoral hemorrhage. *In vitro* we observed Cilengitide-induced anchorage-dependent cells death (anoikis), in line with previous results [42]. These observations are consistent with our previous results using TNF-based isolated perfusions [26]. Moreover, as seen when TNF was used in ILP, addition of Cilengitide also augmented the accumulation of melphalan within the tumor [14,15]. At least two mechanisms induced by Cilengitide can be considered for this effect: a) an increased leakiness of the tumor vasculature or b) an improved perfusion of the tumor. The first hypothesis is supported by the intratumoral hemorrhage observed *in vivo* in Cilengitide-treated animals, and by the increased permeability of an endothelial monolayer that is induced by Cilengitide *in vitro*. For the second hypothesis there is to date no experimental support.

The *in vitro* experiments described here indicate that a direct effect of Cilengitide on tumor cells may also contribute to its antitumor effect Tumor cell kill is observed *in vitro* at a relative low Cilengitide concentration. As single agent Cilengitide inhibits brain-tumor growth [44] and has been reported to stabilize disease progression in advanced head and neck cancer [45]. Effects on endothelial cells may also affect local tumor progression. Cilengitide can inhibit endothelial cell invasion in 3D ECM gels, and vascular endothelial growth factor and basic fibroblast growth factor-induced differentiation [28]. However, in our study we do not observe a direct effect of Cilengitide on tumor growth. This might be due to the unique and short exposure of the tumor to Cilengitide in our experimental model, in contrast to the repeated/prolonged exposure in other studies. The histology clearly shows that treatment with Cilengitide alone had no effect on tumor cells or endothelial cells. These results are in contrast with the *in vitro* observation showing detachment of endothelial cells by Cilengitide. We hypothesize that either the effect of Cilengitide is milder *in vivo* due to reduced dose level and duration of exposure, or due to the engagement by endothelial cells and tumor cells of integrins other than αVβ3 and αVβ5. Our *in vitro* data shows, however, that Cilengitide enhances the cytotoxic activity of melphalan, which may very well explain the observed tumor response *in vivo*.

In conclusion, our results show that addition of Cilengitide augments the activity of co-administered melphalan in the local treat-

ment of established experimental sarcoma. This increased antitumor effect may involve at least three Cilengitide-dependent effects: a) increased accumulation of melphalan in the tumor, b) sensitization of tumor cells to the antitumor effect of melphalan, c) sensitization of endothelial cells to the cytotoxic activity of melphalan. These results also corroborate a critical role of integrin αVβ3 and αVβ5 for the integrity and survival or angiogenic tumor vessels. Previously we reported comparable results with the cytokine TNF in combination with melphalan. Thus the present data indicate that Cilengitide may substitute for the biological activity of TNF in this therapy. Since Cilengitide, in contrast to TNF, has no dose limiting toxicity in patients [21] the strong sensitizing effect combined with low toxicity indicates a great potential for Cilengitide, in systemic treatment settings in combination with chemotherapy.

REFERENCES

1.Carmeliet P. Angiogenesis in health and disease. Nat Med. 2003: 9(6), 653-660.

2.Alghisi GC and Ruegg C. Vascular integrins in tumor angiogenesis: mediators and therapeutic targets. Endothelium. 2006: 13(2), 113-135.

3.Brooks PC, Clark RA, and Cheresh DA. Requirement of vascular integrin alpha v beta 3 for angiogenesis. Science. 1994: 264(5158), 569-571.

4.Brooks PC, Montgomery AM, Rosenfeld M, Reisfeld RA, Hu T, Klier G et al. Integrin alpha v beta 3 antagonists promote tumor regression by inducing apoptosis of angiogenic blood vessels. Cell. 1994: 79(7), 1157-1164.

5.Cheresh DA. Structural and functional properties of ganglioside antigens on human tumors of neuroectodermal origin. Surv Synth Pathol Res. 1985: 4(2), 97-109.

6.Panetti TS and McKeown-Longo PJ. The alpha v beta 5 integrin receptor regulates receptor-mediated endocytosis of vitronectin. J Biol Chem. 1993: 268(16), 11492-11495.

7.Seftor RE, Seftor EA, Gehlsen KR, Stetler-Stevenson WG, Brown PD, Ruoslahti E et al. Role of the alpha v beta 3 integrin in human melanoma cell invasion. Proc Natl Acad Sci U S A. 1992: 89(5), 1557-1561.

8.Wickham TJ, Mathias P, Cheresh DA, and Nemerow GR. Integrins alpha v beta 3 and alpha v beta 5 promote adenovirus internalization but not virus attachment. Cell. 1993: 73(2), 309-319.

9.Panetti TS and McKeown-Longo PJ. Receptor-mediated endocytosis of vitronectin is regulated by its conformational state. J Biol Chem. 1993: 268(16), 11988-11993.

10.de Boer HC, de Groot PG, Bouma BN, and Preissner KT. Ternary vitronectin-thrombin-antithrombin III complexes in human plasma. Detection and mode of association. J Biol Chem. 1993: 268(2), 1279-1283.

11.Smith JW. Cilengitide Merck. Curr Opin Investig Drugs. 2003: 4(6), 741-745.

12.Eggermont AM, de Wilt JH, and ten Hagen TL. Current uses of isolated limb perfusion in the clinic and a model system for new strategies. Lancet Oncol. 2003: 4(7), 429-437.

13.Lienard D, Ewalenko P, Delmotte JJ, Renard N, and Lejeune FJ. High-dose recombinant tumor necrosis factor alpha in combination with interferon gamma and melphalan in isolation perfusion of the limbs for melanoma and sarcoma. J Clin Oncol. 1992: 10(1), 52-60.

14.de Wilt JH, ten Hagen TL, de Boeck G, van Tiel ST, de Bruijn EA, and Eggermont AM. Tumour necrosis factor-alpha increases melphalan concentration in tumour tissue after isolated limb perfusion. Br J Cancer. 2000: 82(5), 1000-1003.

15.van der Veen AH, de Wilt JH, Eggermont AM, van Tiel ST, Seynhaeve AL, and ten Hagen TL. TNF-alpha augments intratumoural concentrations of doxorubicin in TNF-alpha-based isolated limb perfusion in rat sarcoma models and enhances anti-tumour effects. Br J Cancer. 2000: 82(4), 973-980.

16.Seynhaeve AL, Hoving S, Schipper D, Vermeulen CE, aan de Wiel-Ambagtsheer G, van Tiel ST et al. Tumor Necrosis Factor {alpha} Mediates Homogeneous Distribution of Liposomes in Murine Melanoma that Contributes to a Better Tumor Response. Cancer Res. 2007: 67(19), 9455-9462.

17.van der Veen AH, Seynhaeve AL, Breurs J, Nooijen PT, Marquet RL, and Eggermont AM. In vivo isolated kidney perfusion with tumour necrosis factor alpha (TNF-alpha) in tumour-bearing rats. Br J Cancer. 1999: 79(3-4), 433-439.

18.van Etten B, de Vries MR, van Ijken MG, Lans TE, Guetens G, Ambagtsheer G et al. Degree of tumour vascularity correlates with drug accumulation and tumour response upon TNF-alpha-based isolated hepatic perfusion. Br J Cancer. 2003: 88(2), 314-319.

19.de Wilt JH, Manusama ER, van Tiel ST, van Ijken MG, and ten Hagen TL, Eggermont AM. Prerequisites for effective isolated limb perfusion using tumour necrosis factor alpha and melphalan in rats. Br J Cancer. 1999: 80(1-2), 161-166.

20.Tjaden UR and de Bruijn EA. Chromatographic analysis of anticancer drugs. J Chromatogr. 1990: 531, 235-294.
21.Eskens FA, Dumez H, Hoekstra R, Perschl A, Brindley C, Bottcher S et al. Phase I and pharmacokinetic study of continuous twice weekly intravenous administration of Cilengitide (EMD 121974), a novel inhibitor of the integrins alphavbeta3 and alphavbeta5 in patients with advanced solid tumours. Eur J Cancer. 2003: 39(7), 917-926.
22.Jaffe EA, Nachman RL, Becker CG, and Minick CR. Culture of human endothelial cells derived from umbilical veins. Identification by morphologic and immunologic criteria. J Clin Invest. 1973: 52(11), 2745-2756.
23.Mitjans F, Sander D, Adan J, Sutter A, Martinez JM, Jaggle CS et al. An anti-alpha v-integrin antibody that blocks integrin function inhibits the development of a human melanoma in nude mice. J Cell Sci. 1995: 108 (Pt 8), 2825-2838.
24.Skehan P, Storeng R, Scudiero D, Monks A, McMahon J, Vistica D et al. New colorimetric cytotoxicity assay for anticancer-drug screening. J Natl Cancer Inst. 1990: 82(13), 1107-1112.
25.Brunstein F, Hoving S, Seynhaeve AL, van Tiel ST, Guetens G, de Bruijn EA et al. Synergistic antitumor activity of histamine plus melphalan in isolated limb perfusion: preclinical studies. J Natl Cancer Inst. 2004: 96(21), 1603-1610.
26.Hoving S, Seynhaeve AL, van Tiel ST, aan de Wiel-Ambagtsheer G, de Bruijn EA, Eggermont AM et al. Early destruction of tumor vasculature in tumor necrosis factor-alpha-based isolated limb perfusion is responsible for tumor response. Anticancer Drugs. 2006: 17(8), 949-959.
27.ten Hagen TL, Eggermont AM, and Lejeune FJ. TNF is here to stay--revisited. Trends Immunol. 2001: 22(3), 127-129.
28.Nisato RE, Tille JC, Jonczyk A, Goodman SL, and Pepper MS. alphav beta 3 and alphav beta 5 integrin antagonists inhibit angiogenesis in vitro. Angiogenesis. 2003: 6(2), 105-119.
29.Brooks PC, Stromblad S, Klemke R, Visscher D, Sarkar FH, and Cheresh DA. Antiintegrin alpha v beta 3 blocks human breast cancer growth and angiogenesis in human skin. J Clin Invest. 1995: 96(4), 1815-1822.
30.Varner JA, Brooks PC, and Cheresh DA. REVIEW: the integrin alpha V beta 3: angiogenesis and apoptosis. Cell Adhes Commun. 1995: 3(4), 367-374.
31.Max R, Gerritsen RR, Nooijen PT, Goodman SL, Sutter A, Keilholz U et al. Immunohistochemical analysis of integrin alpha vbeta3 expression on tumor-associated vessels of human carcinomas. Int J Cancer. 1997: 71(3), 320-324.
32.Malik RK. Regulation of apoptosis by integrin receptors. J Pediatr Hematol Oncol. 1997: 19(6), 541-545.
33.Scatena M, Almeida M, Chaisson ML, Fausto N, Nicosia RF, and Giachelli CM. NF-kappaB mediates alphavbeta3 integrin-induced endothelial cell survival. J Cell Biol. 1998: 141(4), 1083-1093.
34.Burke PA, DeNardo SJ, Miers LA, Lamborn KR, Matzku S, and DeNardo GL. Cilengitide targeting of alpha(v)beta(3) integrin receptor synergizes with radioimmunotherapy to increase efficacy and apoptosis in breast cancer xenografts. Cancer Res. 2002: 62(15), 4263-4272.
35.Burke PA, DeNardo SJ, Miers LA, Kukis DL, and DeNardo GL. Combined modality radioimmunotherapy. Promise and peril. Cancer. 2002: 94(4 Suppl), 1320-1331.
36.Storgard CM, Stupack DG, Jonczyk A, Goodman SL, Fox RI, and Cheresh DA. Decreased angiogenesis and arthritic disease in rabbits treated with an alphavbeta3 antagonist. J Clin Invest. 1999: 103(1), 47-54.
37.Fu Y, Ponce ML, Thill M, Yuan P, Wang NS, and Csaky KG. Angiogenesis inhibition and choroidal neovascularization suppression by sustained delivery of an integrin antagonist, EMD478761. Invest Ophthalmol Vis Sci. 2007: 48(11), 5184-5190.
38.Santulli RJ, Kinney WA, Ghosh S, Decorte BL, Liu L, Tuman RW et al. Studies with an orally bioavailable alpha V integrin antagonist in animal models of ocular vasculopathy: retinal neovascularization in mice and retinal vascular permeability in diabetic rats. J Pharmacol Exp Ther. 2008: 324(3), 894-901.
39.Beekman KW, Colevas AD, Cooney K, Dipaola R, Dunn RL, Gross M et al. Phase II evaluations of cilengitide in asymptomatic patients with androgen-independent prostate cancer: scientific rationale and study design. Clin Genitourin Cancer. 2006: 4(4), 299-302.
40.Stupp R and Ruegg C. Integrin inhibitors reaching the clinic. J Clin Oncol. 2007: 25(13), 1637-1638.
41.MacDonald TJ, Stewart CF, Kocak M, Goldman S, Ellenbogen RG, Phillips P et al. Phase I clinical trial of cilengitide in children with refractory brain tumors: Pediatric Brain Tumor Consortium Study PBTC-012. J Clin Oncol. 2008: 26(6), 919-924.
42.Taga T, Suzuki A, Gonzalez-Gomez I, Gilles FH, Stins M, Shimada H et al. alpha v-Integrin antagonist EMD 121974 induces apoptosis in brain tumor cells growing on vitronectin and tenascin. Int J Cancer. 2002: 98(5), 690-697.
43.Yamada S, Bu XY, Khankaldyyan V, Gonzales-Gomez I, McComb JG, and Laug WE. Effect of the angiogenesis inhibitor Cilengitide (EMD 121974) on glioblastoma growth in nude mice. Neurosurgery. 2006: 59(6), 1304-1312.

44.MacDonald TJ, Taga T, Shimada H, Tabrizi P, Zlokovic BV, Cheresh DA et al. Preferential susceptibility of brain tumors to the antiangiogenic effects of an alpha(v) integrin antagonist. Neurosurgery. 2001: 48(1), 151-157.
45.Raguse JD, Gath HJ, Bier J, Riess H, Oettle H. Cilengitide (EMD 121974) arrests the growth of a heavily pretreated highly vascularised head and neck tumour. Oral Oncol. 2004: 40(2), 228-230

Part 2 - Vascular abnormalization

In vitro study

Chapter 4 **TNF induces changes in endothelial cell morphology**
Ann L.B. Seynhaeve, Cindy E. Vermeulen, Alexander.M.M. Eggermont, and Timo L.M. ten Hagen
Cell Biochemistry and Biophysics. 2006: 44(1), 157-170

Chapter 5 **MMP-9 after TNF-induction causes loss of endothelial integrity**
Ann L.B. Seynhaeve, Debby Schipper, Alexander M.M. Eggermont, and Timo L.M. ten Hagen
Submitted for publication

Chapter 6 **VE-cadherin degradation in TNF-induced endothelial changes**
Ann L.B. Seynhaeve, Debby Schipper, Alexander M.M. Eggermont, and Timo L.M. ten Hagen
In preparation

About the authors (in alphabetical order)
Alexander M.M. Eggermont; Department of Surgical Oncology, Erasmus MC-Daniel den Hoed Cancer Center, Rotterdam, The Netherlands - **Timo L.M. ten Hagen**; Department of Surgical Oncology, Erasmus MC-Daniel den Hoed Cancer Center, Rotterdam, The Netherlands – **Debby Schipper**; Department of Surgical Oncology, Erasmus MC-Daniel den Hoed Cancer Center, Rotterdam, The Netherlands – **Ann L.B. Seynhaeve**; Department of Surgical Oncology, Erasmus MC-Daniel den Hoed Cancer Center, Rotterdam, The Netherlands – **Cindy E. Vermeulen**; Department of Surgical Oncology, Erasmus MC-Daniel den Hoed Cancer Center, Rotterdam, The Netherlands

Chapter 4

Cytokines and vascular permeability: An *in vitro* study on human endothelial cells in relation to TNFα primed peripheral blood mononuclear cells

Ann L.B. Seynhaeve
Cindy E. Vermeulen
Alexander M.M. Eggermont
Timo L.M. ten Hagen

Cell Biochemistry and Biophysics. 2006: 44(1), 157-170

Research article

Cytokines and vascular permeability: An *in vitro* study on human endothelial cells in relation to TNFα primed peripheral blood mononuclear cells

Ann L.B. Seynhaeve, Cindy E. Vermeulen, Alexander.M.M. Eggermont, and Timo L.M. ten Hagen

Department of Surgical Oncology, Erasmus MC-Daniel den Hoed Cancer Center, Rotterdam, The Netherlands

ARTICLE INFORMATION

Cell Biochemistry and Biophysics. 2006: 44(1), 157-169

ABSTRACT

Tumor response is strongly enhanced by addition of tumor necrosis factor-alpha (TNF) to chemotherapy in local-regional perfusion. TNF primarily targets the endothelial lining of the tumor-associated vasculature, thereby improving permeability of the vascular bed. This augments uptake of the co-administered chemotherapeutic drug in the tumor. *In vitro*, however the high-dose TNF used had no direct effect on endothelial cells, indicating that other factors, most likely TNF-induced, are involved in the antivascular activities observed *in vivo*. This is supported by *in vivo* studies in our laboratory in which depletion of leukocytes resulted in loss of the antivascular activity of TNF. The present study examined the role of peripheral blood mononuclear cells (PBMC) on endothelial cells by exposing them to TNF, interferon-gamma (IFN) and PBMC. We observed morphological changes of the endothelial cells when exposed to TNF in combination with IFN. Endothelial cells became elongated and gaps between the cells appeared. Addition of PBMC enhanced these alterations even further. The endothelial layer became disrupted with highly irregularly shaped cells displaying large gap formations. PBMC also contributed to an increased permeability of the endothelial layer without augmenting apoptosis. Replacing PBMC by interleukin-1beta (IL-1ß) produced similar effect with regard to inhibition of cell growth, morphological changes and induction of apoptosis. Blocking IL-1ß with a neutralizing antibody diminished the effects inflicted of PBMC. These observations indicate that endogenously produced IL-1ß by primed PBMC plays an important role in the antivascular effect of TNF.

INTRODUCTION

The success of the clinical isolated limb perfusion programs to treat in-transit melanoma metastases and limb threatening soft tissue sarcomas with a combination of tumor necrosis factor-alpha (TNF) and chemotherapeutic drugs has launched investigations into the mechanisms behind the synergistic antitumor effects observed [1-3]. In our laboratory we have demonstrated that addition of TNF leads to an enhanced accumulation of melphalan or doxorubicin in the tumor in various isolated limb perfusion (ILP) models [4,5]. In the systemic setting, TNF enhances the tumor accumulation

of long circulating liposomal drugs, resulting in synergistic antitumor effects [6,7].

Clinical and experimental studies demonstrate that TNF primarily targets the endothelial lining of the tumor-associated vasculature (TAV) [8,9]. Angiograms of patients receiving a TNF-based ILP demonstrated complete disruption of the TAV. Histological studies after ILP showed extravasation of erythrocytes and hemorrhagic necrosis, resulting from endothelial cell degeneration and loss of endothelial integrity, which could be linked to high-dose TNF that is used in the ILP [10]. Strikingly, also in low-dose systemic treatment TNF dramatically improved tumor response without obvious damage to the endothelial lining. Taken together, these results indicate that TNF-induced vascular permeability was critical for the tumor response observed.

The response of endothelial cells to TNF and another important cytokine; interferon-gamma (IFN) has been extensively studied. These cytokines are known to inhibit the proliferation of endothelial cells [11,12], to increase the permeability of the endothelial layer [13], to inhibit the αVß3 mediated endothelial cell adhesion to the extracellular matrix [14], to augment neutrophil transmigration [15,16] and to induce morphological changes [17] *in vitro*. However, *in vitro* TNF inflicts only minor changes in endothelial cells, and tumor cells appear quite insensitive to TNF. Also, *in vivo*, TNF alone in high concentrations does not induce tumor regression after an ILP.

An important *in vivo* observation is the necessity of leukocytes during TNF-based ILP to obtain the typical synergistic tumor response. This could also explain the lack of response of endothelial cells to TNF alone *in vitro* [18]. These observations place interaction of TNF with leukocytes at the center of the synergistic tumor response observed. In this study, we investigate the interaction of TNF and peripheral blood mononuclear cells (PBMC) in mediating endothelial cell morphology changes, which could explain the synergy observed. In particular we focus on PBMC-produced factors, which contribute to the increased permeability of the endothelial cell lining.

EXPERIMENTAL PROCEDURES

Agents. Recombinant human Tumor necrosis factor-alpha (TNF) and recombinant human Interferon-gamma (IFN) were kindly provided by Dr. G. Adolf (Boehringer Ingelheim GmbH). TNF had a specific activity of $5x10^7$ U/mg as determined in the murine LM cell assay [19]. Endotoxin levels were < 1.25 units (EU) per mg protein. IFN had a specific activity of $2.5x10^7$ U/mg as determined in an HLA-DR assay. Recombinant human interleukin-1beta (IL-1ß) was purchased from Peprotech EC Ltd. As determined by stimulation of thymidine uptake by murine C3H/HeJ thymocytes, the ED_{50} was ≤ 0.1 ng/ml, corresponding to a specific activity of ≥ $1x10^7$ U/mg. Endotoxin levels were less than 1 EU per µg protein. Goat anti human interleukin-1beta (anti IL-1ß) was purchased from R&D systems. As determined by the LAL method, endotoxin levels were less than < 0.01 EU per µg. Melphalan (Alkeran, 50 mg per vial) was purchased from GlaxoSmithKline BV and diluted in phosphate buffered saline to a concentration of 2 mg/ml. Doxorubicin (Adriablastina) was purchased from Pharmachemie BV in a concentration of 2 mg/ml.

Cells and cultured conditions. Human umbilical vein endothelial cells (HUVEC) were isolated by collagenase digestion using the method described by Jaffe *et al* [20]. Each isolate was derived from an individual umbilical vein and used for experiments at passage 5. HUVEC were cultured in HUVEC medium containing human endothelial-serum free medium (Invitrogen), 20% heat inactivated newborn calf serum (Cambrex), 10% heat inactivated human serum (Cambrex), 20 ng/ml human recombinant basic fibroblast growth factor (Peprotech EC Ltd), 100 ng/ml human recombinant epidermal growth factor (Peprotech EC Ltd) in fibronectin (Roche Diagnostics) coated flasks. HUVEC had the characteristic cobblestone morphology and tested positive for CD31. Human peripheral blood mononuclear cells (PBMC) were isolated from healthy donors using the Vacutainer CPT Mononuclear Cell Preparation Tubes with sodium heparin (Becton Dickinson). PBMC were washed with phosphate buffered

saline and counted with trypan blue to determine the viable cell concentration. PBMC, at a final concentration of $120x10^4$ PBMC/ml, were used in all experiments.

Assessment of toxicity towards endothelial cells. HUVEC were plated to 96 well multiplates (Corning BV), coated with fibronectin, at a final concentration of $6x10^3$ cells per well and allowed to grow for 24 hours. TNF, IFN, doxorubicin and melphalan were added to the wells and incubated for 72 hours. The range of final drug concentration was 0.6 ng/ml - 15 µg/ml. The endothelial cells were also incubated for 72 hours with combinations of cytokines and cytotoxic agents. As a control, cells were incubated with HUVEC medium alone. Growth of endothelial cells was measured using the sulphorhodamine B protein stain assay (SRB) according to the method of Skehan [21]. Briefly, cells were washed with PBS, incubated with 10% trichloric acetic acid (1 hour, 4ºC) and washed in distilled water. Cells were then stained for 15 min with SRB (Sigma), washed with 1% acetic acid and allowed to dry. Protein bound SRB was dissolved in 10 mM Tris buffer and optical density (O.D.) was measured at 540 nm. Cell growth was calculated using the formula: percentage cell growth = (O.D. test well/O.D. control well) x 100 percent. HUVEC exposed to the concentrations of TNF and IFN indicated in the results section were co-incubated with PBMC. Prior to addition of the drug, a plate (0 hour) was washed, fixated and used as 100% growth. Every 24 hours after addition of the agents, up to 144 hours, a plate was washed carefully 3 times to remove PBMC, fixated and stained using the SRB method. In order to test the necessity of cell-cell interaction between endothelial cells and PBMC, a transwell system was used. HUVEC were plated in fibronectin coated 24 well multiplates (Corning BV) at a final concentration of $3x10^4$ cells per well and allowed to grow for 24 hours. A transwell with pores of 0.4 µm (Millipore) was placed into 600 µl HUVEC medium containing TNF with or without IFN. In the transwell, PBMC in 300 µl were added. To establish the role of IL-1ß, HUVEC were incubated with TNF, IFN and IL-1ß or exposed to TNF, IFN, PBMC in the presence of a neutralizing antibody against IL-1ß for 144 hours. After 144 hours the plate was washed, fixated and stained using the SRB method. Cells incubated with only HUVEC medium were used as 100% growth.

Morphological changes. HUVEC were plated in fibronectin coated 24 well multiplates at a final concentration of $3x10^4$ cells per well and allowed to grow for 24 hours. The cells were incubated with TNF and IFN at dosage range mentioned in the results section, in combination with respectively PBMC, IL-1ß or PBMC in the presence of neutralizing antibodies to IL-1ß. After 24, 72 and 144 hours, morphological cell changes were examined with a 10x N.A. 0.30 Plan-Neofluar objective lens using an inverted Zeiss Axiovert 100M microscope equipped with an Axiocam digital camera (Carl Zeiss). Cell elongation was measured and expressed as the ratio of the length of the major cell axis to the width perpendicular to the length. Ten cells and at least four independent incubations were determined. In addition, gap formation was determined for each treatment. The cell-free area was outlined and the gap formation was calculated using the formula: percentage cell-free area = (cell-free area/total area) x 100 percent. All measurements were done using the AxioVision 3.0 software.

Immunofluorescence. HUVEC were plated on to fibronectin coated cover glass at a final concentration of $3x10^4$ cells per glass and allowed to grow for 24 hours. The cells were incubated with HUVEC medium, 10 µg/ml TNF in combination with 0.001 µg/ml IFN or 10 µg/ml TNF in combination with 0.001 µg/ml IFN and PBMC. After 144 hours of incubation, cells were rinsed in PBS and fixed with 3.6% paraformaldehyde for 10 min at room temperature. Cells were permeabilized with 0.1% Triton X-100 for 10 min at room temperature, and aspecific binding sites were blocked with 1% BSA in PBS for 10 min at room temperature. Cells were stained with Alexa Fluor 568 phalloidin (1:400; Molecular Probes) for the detection of F-actin (20 min, room temperature) and

mounted with vectashield (Vector laboratories) mixed with DAPI (Molecular Probes) in order to stain cell nuclei. Cells were examined using a Leica DMRX-A microscope and images taken with a Sony DXC 950 camera.

Western blot. HUVEC, PBMC and HUVEC co-cultured with PBMC were stimulated with 10 µg/ml TNF combined with 0.001 - 0.1 µg/ml IFN for 48 hours. After stimulation, supernatant was collected to determine the presence of endogenous IL-1ß. Reduced samples were separated by electrophoresis in a 15% SDS-polyacrilamide gel and transferred to a PVDF membrane (BioRad). Following transfer, the membranes were blocked with MPBS (5% milk powder in PBS/0.05% tween-20) and incubated overnight with goat anti human IL-1ß (1:1500; R&D systems) in MPBS. After washing, the membrane was incubated with rabbit anti goat biotin (1:1500; Southern Biotechnology) in MPBS. Bound biotin was incubated with alkaline-phosphatase-streptavidin complex (BioRad), and this in turn stained with BCIP/NBT liquid substrate (BioRad). The staining was stopped with 2 mM EDTA.

Apoptosis assay. Two methods were used for the detection of apoptosis: first, FACS analysis using annexin V (for apoptotic cells) and propidium iodide (PI, necrotic cells) to screen all cells (adherent and detached), and secondly, YO-PRO-1 for detection of apoptotic adherent cells. To avoid detection of apoptotic PBMC, these were added in a transwell system (Millipore). HUVEC were incubated with combinations of 10 µg/ml TNF, 0.001 µg/ml IFN, 0.01 µg/ml IL-1ß and PBMC. After incubation for 24, 72 or 144 hours, detached cells were collected from the supernatant and living cells were harvested by mild trypsinization and washed with PBS. Early apoptosis was detected using the annexin V kit, according to the manufacturer's instructions (Vybrant Apoptosis Assay kit #3, Molecular Probes). Cells were immediately analyzed by flowcytometry (FACScan, Becton Dickinson). Data analysis was performed using WinMDI 2.7 (Freeware, Joseph Trotter, Scripps Research Institute). Alternatively, apoptosis was also detected using the monomeric cyanine nucleic acid stain YO-PRO-1 (Molecular probes). At the end of the incubation period of the HUVEC, detached cells were removed. HUVEC medium with YO-PRO-1, in a final concentration of 0.5 µM, was added to the well with the remaining adherent cells and incubated for 15 min at 37°C. Fluorescence was visualized using an inverted Zeiss Axiovert 100M microscope and captured with an Axiocam digital camera, using AxioVision v3.0 software.

Endothelial cell permeability assay. HUVEC were plated in a transwell (0.4 µm pore size, 6.5 mm diameter, polyester filters; Corning BV), coated with fibronectin, at a density of $2.5x10^4$ cells per well. After culture for 24 hours, the medium in the upper chamber was replaced with medium containing combinations of TNF, IFN, PBMC, IL-1ß, anti IL-1ß or HUVEC medium during 24, 72 and 144 hours. To measure permeability, FITC-BSA in a concentration of 50 µg/well was added to the upper chamber. After the indicated incubation time the FITC fluorescence at the lower chamber was read using a fluorescence plate reader (Wallac Victor^2, Perkin Elmer).

Statistical analysis. The Mann-Whitney U-test was used in all statistical analysis. P values below 0.05 were considered statistically significant.

RESULTS

Morphological changes in endothelial cells in relation to activated PBMC. A crucial observation raised the question how TNF affects the endothelial lining of tumor vessels. When leukocytes were depleted we observed impaired tumor response to TNF-based ILP [18]. Secondly, IFN has been added in several studies because of synergistic antitumor activity when combined with TNF, although its beneficial effect is still debated [22]. Therefore, we tested the effect of a combination of TNF and IFN on endothelial cells. HUVEC were incubated with TNF, IFN, melphalan or doxorubicin for 72 hours. TNF or IFN alone had only a negligible

effect on the endothelial cells. Incubation of HUVEC with melphalan or doxorubicin resulted in a dose related cytotoxicity with an IC_{50} of respectively 40 µg/ml and 0.2 µg/ml (data not shown). When HUVEC were exposed to TNF or IFN in combination with melphalan or doxorubicin the IC_{50} of these drugs were not altered, indicating a lack of synergy between the cytokines and the cytotoxic agents (data not shown). Even when TNF, IFN and melphalan were combined no synergy could be observed (data not shown). These results demonstrate a clear lack of direct activity of TNF and IFN on endothelial cells. Therefore, we tried to establish the role of leukocytes in TNF-based tumor therapy. HUVEC were exposed to TNF, IFN and PBMC during 144 hours and effect on cell growth was determined. Addition of PBMC to TNF and IFN inflicted strong cell growth reduction of HUVEC and eventually cell death, which was not observed with TNF and IFN alone (**Fig. 1a**). TNF levels between 10 and 0.1 µg/ml have been tested resulting in comparable but less pronounced effects for the lower concentrations. Photographs were taken to examine the morphology of the cells after incubation (**Fig. 1b**). Under normal culture conditions endothelial cells form a monolayer of cobblestone-like cells. Exposure of HUVEC to TNF resulted in slight elongation of the cells, whereas incubation with 0.001 µg/ml IFN alone or PBMC alone had no effect on cell morphology. Combination of 10 µg/ml TNF with 0.001 µg/ml IFN resulted in more pronounced morphological changes. Cells became more elongated and gaps between the cells became visible. Dramatic disruption of the HUVEC monolayer resulted from exposure to 10 µg/ml TNF, 0.001 µg/ml IFN and PBMC. Exposure of HUVEC to 10 µg/ml TNF in combination with 0.1 µg/ml IFN resulted in the formation of elongated cells and even larger gaps, addition of PBMC further increased these observed effects. These differences in gap formation and cell elongation were confirmed by measurements of cell-free area and the cell shape ratio (**Table 1**). Addition of PBMC to 10 µg/ml TNF and IFN, 0.1 µg/ml as well as 0.001 µg/ml, resulted in significant changes in length to width ratio and cell-free area compared to incubations in which PBMC were not added.

Cytoskeletal changes in HUVEC exposed to TNF, IFN and PBMC. Control endothelial cells treated with HUVEC medium showed actin fibers highly concentrated at the periphery of the cell, ending in dense points. When cells were treated with 10 µg/ml TNF in combination with 0.001 µg/ml IFN, cells became elongated and enlarged, which was not further enhanced with higher dose of IFN (0.1 µg/ml). The cellular alignment corresponded with alignment of actin fibers. More stretched actin fibers were seen in the center of the cell while actin was diminished at the periphery. The dense actin points, observed in cells treated with HUVEC medium, seemed lowered, although also the number of cells is decreased. Addition of 10 µg/ml TNF in combination with 0.001 µg/ml IFN and PBMC resulted in stretching of the actin fibers and bleb formation, which could possibly indicate loss of membrane integrity (Fig. 2).

Identification of IL-1ß as a crucial soluble factor for HUVEC morphology. To determine the role of PBMC in the above-observed endothelial morphology changes we evaluated whether a cell-cell interaction was necessary for this process or if a soluble factor could be identify. Incubation of endothelial cells with TNF, IFN and PBMC was performed in a transwell system to avoid contact between endothelial cells and PBMC by physical separation of the cells while soluble factors are not blocked. Comparable growth curve and morphological changes were obtained as when endothelial cells were in contact with the PBMC (data not shown). These results indicate that a soluble factor is responsible for the observed results. To determine possible soluble factors derived from PBMC, western blot analysis was performed. After analysis of the supernatant of PBMC and/or HUVEC stimulated with above-mentioned cytokines, it was shown that both PBMC and HUVEC produced soluble IL-1ß in response to TNF irrespective of the IFN concentration (**Fig. 3**). To test the hypothesis that IL-1ß is responsible for the effects observed in cell growth

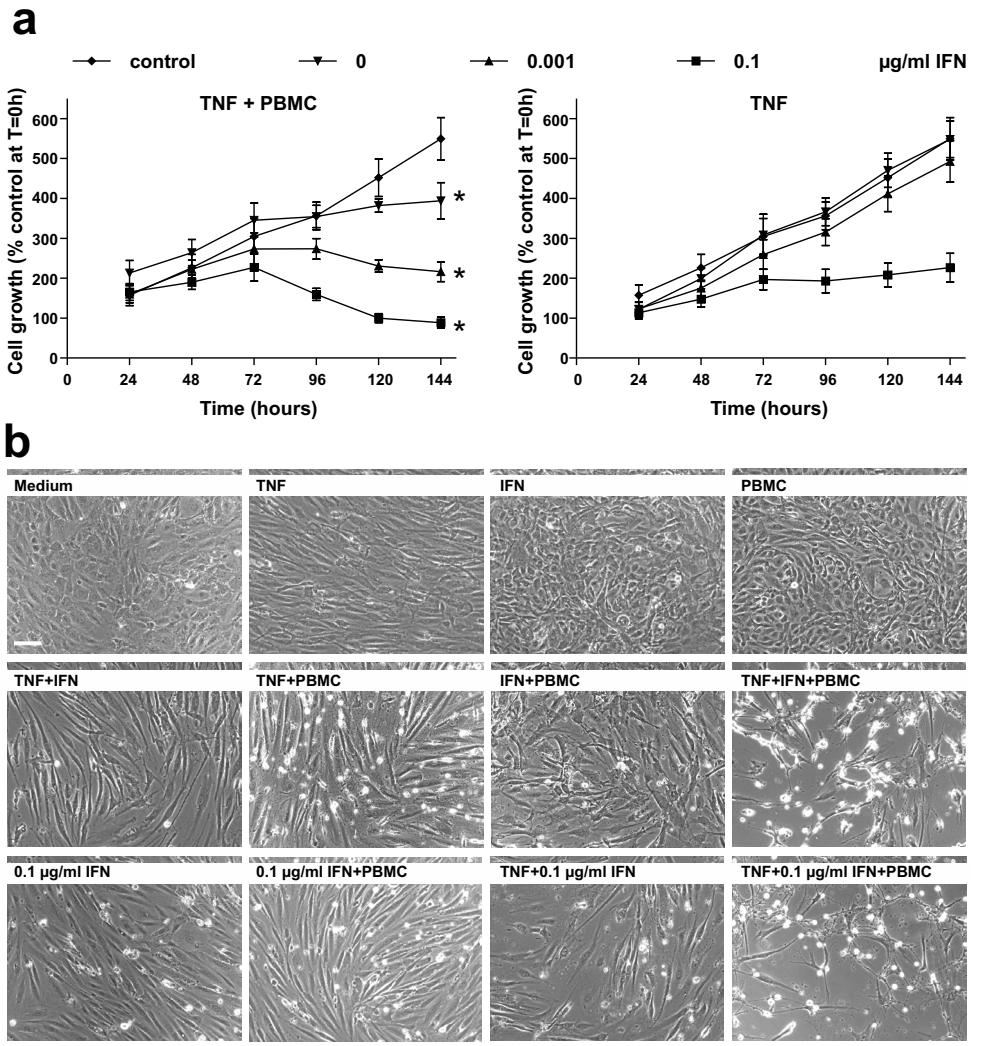

Figure 1. The morphology of HUVEC changes after incubation of primed-PBMC. (**a**) Cell growth of HUVEC, incubated with 10 µg/ml TNF and PBMC (left graph), and 10 µg/ml TNF (right graph) in combination with 0.1 µg, 0.001 µg, and 0 µg IFN per ml was measured in course of time. Cells incubated with medium alone were used as a control. Cells incubated with TNF and 0.1 µg/ml IFN showed cell growth stabilization whereas a concentration of 0.001 µg/ml IFN had no effect on cell growth. PBMC greatly enhanced the cell growth inhibitory effect of TNF and IFN, resulting even in cell death. Data points represent percentage cell growth compared to control treated cells at 0 hour ± SEM of at least 2 treatments of 5 individual experiments; *, $P < 0.05$, cells incubated for 144 hours with PBMC *versus* cells incubated without PBMC. (**b**) Photographs of HUVEC taken 144 hours after incubation with 10 µg/ml TNF, 0.001 µg/ml IFN (indicated as IFN) or 0.1 µg/ml IFN and PBMC. Typical cobblestone structure of the monolayer after incubated with only medium is shown. Incubation with TNF resulted in elongation and alignment of the cells. When IFN (0.001 µg/ml) or PBMC was administered no morphological changes were observed. Treatment of cells with TNF and IFN (0.001 µg/ml), TNF and PBMC, or IFN (0.001 µg/ml) and PBMC resulted in increased elongation of the HUVEC and slight gap formation. These changes further expanded when incubated with a combination of TNF, IFN (0.001 µg/ml) and PBMC. A higher dose of IFN (0.1 µg/ml) alone showed already elongation of the cells, which was not changed when PBMC were added. Further elongation and gap formation was seen when combined with TNF and, TNF and PBMC. Scale bar apply for all images, 100 µm.

Table 1. Effect of PBMC on cell elongation and gap formation.

Incubation	Medium		PBMC	
	Length to width ratio[a]	Cell-free area (%)[b]	Length to width ratio[a]	Cell-free area (%)[b]
Medium	1.5 ± 0.2	0	2.3 ± 0.8	1 ± 1
TNF	5.4 ± 0.4	1 ± 1	10.5 ± 2.5*	14 ± 13#
0.001 µg/ml IFN	1.9 ± 0.2	0	2.9 ± 0.4	0
TNF + 0.001 µg/ml IFN	6.4 ± 0.4	10 ± 9	16.5 ± 2.3*	39 ± 21#
0.1 µg/ml IFN	4.3 ± 0.3	0	6.4 ± 0.4*	0
TNF + 0.1 µg/ml IFN	11.9 ± 2.2	38 ± 25	26.1 ± 2.8*	78 ± 14#

Note: HUVEC were incubated during 144 hours. Concentrations used were 10 µg/ml TNF and 0.1 µg/ml or 0.001 µg/ml IFN.

[a] Ratio of major and minor axes was measured to determine the cell elongation. Data represent length to width ratio ± SEM of 10 cells per treatment of at least 4 individual experiments; *, $P < 0.05$, cells incubated without PBMC *versus* cells incubated with corresponding cytokines and PBMC

[b] Cell-free area, as a percent of the total area, was calculated to verify the gap formation. Data represent percentage cell free area ± SD of at least 4 individual experiments; #, $P < 0.05$, cells incubated without PBMC *versus* cells incubated with corresponding cytokines and PBMC.

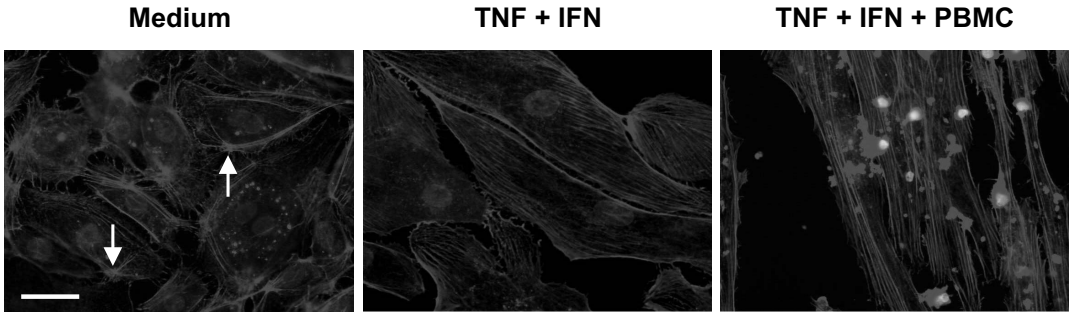

Figure 2. The cytoskeleton changes after incubation of primed PBMC. Staining for F-actin (red) and DAPI (blue) after incubation of HUVEC as described in the experimental procedures. Untreated cells revealed actin mainly localized at the periphery of the cell and clustering to form actin rich points (arrow). Cells treated with TNF (10 µg/ml) in combination with IFN (0.001 µg/ml) showed a decrease in peripheral actin and actin fibers oriented in the long axis of the cell. Cells treated with a combination of TNF, IFN and PBMC showed further elongation of actin fibers. Scale bar apply for all images, 50 µm. (See color section for a full-color version.)

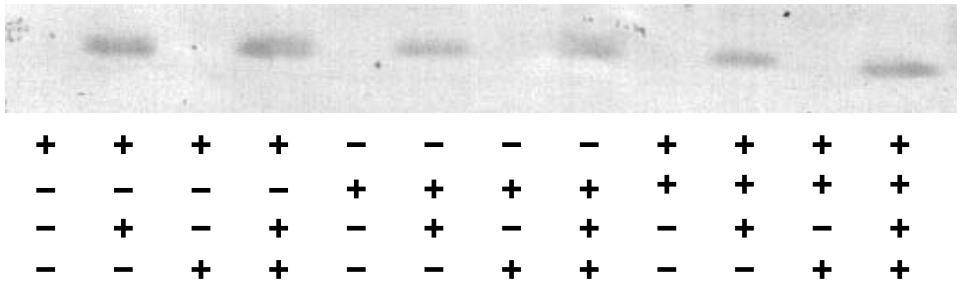

Figure 3. Incubation with TNF leads to production of IL-1ß. Western blot analysis of endogenous IL-1ß production by HUVEC and PBMC as described in the experimental procedures. Cells, PBMC as well as HUVEC that were incubated with TNF produced endogenous IL-1ß. IFN had no effect on production of IL-1ß.

and morphological changes two approaches were performed. First, endothelial cells were exposed to TNF and IFN in combination with IL-1ß. Second, production of IL-1ß by PBMC after stimulation with TNF, IFN and PBMC was blocked with a neutralizing antibody. After 144 hours, cell growth was measured (**Table 2**). Replacement of PBMC with 0.01 µg/ml IL-1ß evoked comparable HUVEC growth reduction. Moreover, comparable morphological changes of HUVEC were observed, indicating IL-1ß as a critical PBMC-derived factor in TNF mediated endothelial disruption. Looking at cell-free area, 10 µg/ml TNF in combination with 0.001 µg/ml IFN and PBMC showed comparable gap formation as TNF in combination with IFN and 0.01 µg/ml IL-1ß, namely 39 ± 22% and 26 ± 9% (**Fig. 4a**). Combining TNF and IFN with PBMC or IL-1ß-induced comparable degree of cell elongation, respectively 16.5 ± 2.3 and 14.5 ± 2.3 (**Fig. 4b**). When endogenous IL-1ß was blocked in cells treated with 10 µg/ml TNF in combination with 0.001 µg/ml IFN and PBMC, cell-free area (5 ± 5%) as well as length to width ratio (7.9 ± 2.5) was strongly diminished and comparable to exposure with TNF and IFN alone (10 ± 9% for cell-free area and 6.4 ± 0.4 for length to width ratio). When a concentration of 0.1 µg/ml IFN was used the same effects were observed. PBMC, in a combination with TNF and IFN, could be replaced by IL-1ß, with regard to induction of cell-free area (78 ± 14% for PBMC *versus* 71 ± 16% for IL-1ß) and cell elongation (26.1 ± 2.8 for PBMC *versus* 23.5 ± 3.3 for IL-1ß) (data not shown). Importantly, incubation of HUVEC with 0.001 µg/ml IFN and 0.01 µg/ml IL-1ß resulted in more elongated and aligned cells than when incubated with 0.001 µg/ml IFN and PBMC (**Fig 4c**). This is in line with the results of the western blot showing that IFN does not induce production of IL-1ß. Secondly, especially the combination of IFN and IL-1ß seems responsible for the observed morphological changes. This could also be confirmed by inhibition of endogenous IL-1ß. Blocking endogenous IL-1ß, with 1 µg/ml anti IL-1ß, in cells that were incubated with 10 µg/ml TNF, 0.001 µg/ml IFN and PBMC reversed the PBMC inflicted effects. Addition of anti IL-ß to TNF plus IFN did not change the response of HUVEC indicating that PBMC are the most likely source of IL-ß (data not shown). That TNF is the stimulator of the production of IL-1ß was confirmed by blocking endogenous IL-1ß. In cells incubated with 10 µg/ml TNF combined with PBMC and anti IL-1ß a reduction in cell elongation was observed.

TNF and IFN-induced apoptosis in HUVEC. To exclude the possibility that the observed effect on HUVEC were related to induction of apoptosis, we tested for cell death using annexin V and YO-PRO-1. Exposure of HUVEC to TNF and IFN resulted in 24 ± 2% apoptosis in 72 hours, which did not increase further over the next 72 hours. Addition of PBMC or IL-1ß had no further effect (apoptosis respectively 26 ± 2% and 20 ± 3%) (**Fig. 5a**). YO-PRO-1 pictures revealed that adherent cells incubated with 10 µg/ml TNF and 0.001 µg/ml IFN remained viable (**Fig. 5b,** left photographs) Similar pictures were seen when cells were incubated with 10

Table 2. Effect of IL-1ß on HUVEC growth.

Incubation	Cell growth (% of control)[a]			
	Medium	PBMC	IL-1ß	PBMC+IL-1ß
TNF	95 ± 2	72 ± 9	56 ± 6*	81 ± 9**
IFN	90 ± 3	58 ± 8*	58 ± 4*	83 ± 9**
TNF+IFN	78 ± 4	48 ± 7*	42 ± 3*	84 ± 5**

Note: HUVEC were incubated with 10 µg/ml TNF, 0.001 µg/ml IFN, 0.01 µg/ml IL-1ß and 1 µg/ml anti IL-1ß for 144 hours. HUVEC incubated with HUVEC medium only were used as controls and set as 100 percent cell growth.

[a] Percentage cell growth of HUVEC exposed to given factors as compared to HUVEC cultured in HUVEC medium only. Data represent percentage cell growth compared to HUVEC medium treated cells ± SEM of 2 treatments of at least 3 individual experiments; *, $P < 0.05$, cells incubated with PBMC or IL-1ß *versus* medium; **, $P < 0.05$, cells incubated with anti IL-1ß *versus* cells incubated with IL-1ß or PBMC.

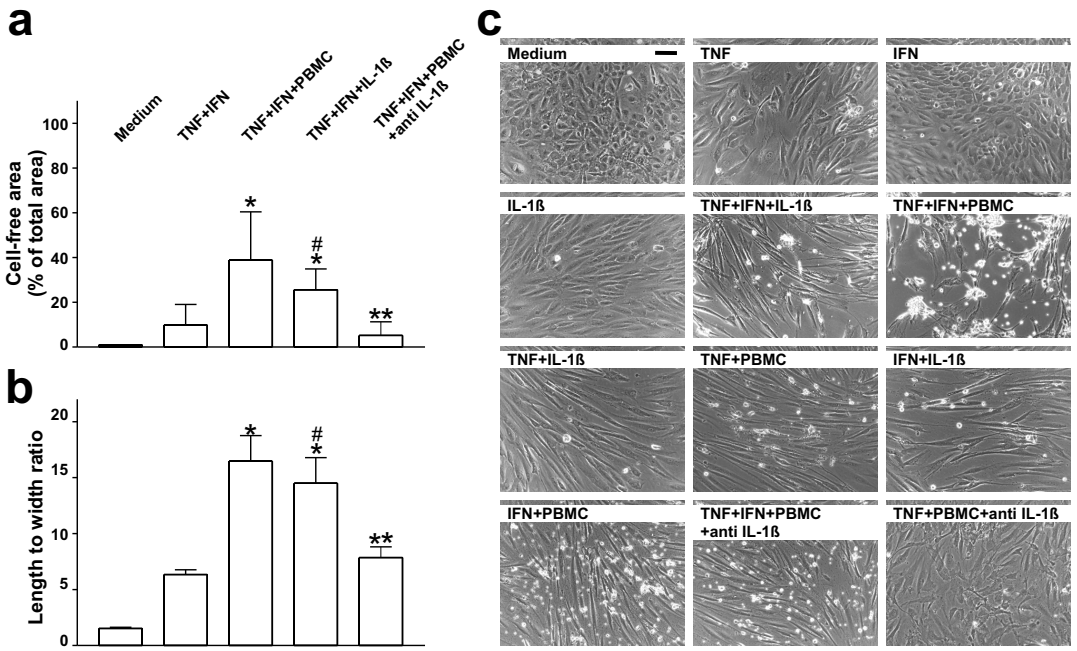

Figure 4. Endogenous produced IL-1ß is responsible for TNF-induced morphological changes. (**a**) Cell-free area, as function of gap formation and (**b**) length to width ratio, representative for cell elongation, after 144 hours incubated with 10 µg/ml TNF, 0.001 µg/ml IFN, PBMC, 0.01 µg/ml IL-1ß or anti IL-1ß, were calculated. Cell-free area and length to width ratio were significantly augmented when PBMC were added. Replacing PBMC by IL-1ß resulted in a similar increase. Blocking endogenous IL-1ß with the neutralizing antibody in cells reversed the effects. Columns represent percentage cell-free area ± SD of at least 4 individual experiments and length to width ratio ± SEM of 10 cells per treatment of at least 4 individual experiments; *, $P < 0.05$, cell-free area or length to width ratio cells incubated with TNF in combination with IFN *versus* cells incubated with TNF in combination with IFN and PBMC or IL-1ß; **, not significant *versus* cells incubated with TNF in combination with IFN; #, not significant *versus* cells incubated with TNF in combination with IFN and PBMC. (**c**) Represented photographs were taken 144 hours after incubation. Exposure to HUVEC medium, TNF, IFN or IL-1ß resulted at most in some elongation of the cells. Exposure of HUVEC to TNF, IFN and IL-1ß combined inflicted strong morphology changes and gap formation comparable to the combination of TNF, IFN and PBMC. Likewise, addition of IL-1ß to TNF inflicted comparable results when TNF was combined with PBMC. However, whereas addition of IL-1ß to IFN inflicted a strong response this was not seen when IFN and PBMC were added. Blocking of endogenous IL-1ß with 1 µg/ml anti IL-1ß reversed the strong morphological changes inflicted by TNF, IFN and PBMC. This was also observed when anti IL-1ß was added to HUVEC incubated with 10 µg/ml TNF and PBMC. Scale bar apply for all images, 100 µm.

µg/ml TNF in combination with 0.001 µg/ml IFN and PBMC (**Fig. 5b**, right photographs) or 0.01 µg/ml IL-1ß (data not shown).

Augmentation of endothelial permeability by TNF and IFN. To assess the importance of our findings for the clinical setting, i.e. augmentation of drug accumulation in tumor tissue by increasing permeability of the tumor vascular bed, we tested the effect of TNF, IFN and PBMC on the permeability of a HUVEC monolayer. Exposure of the HUVEC monolayer to TNF and IFN for 24 hours until 72 hours had no effect on FITC-BSA transfers irrespective of the presence of PBMC (data not shown). However, at 144 hours of incubation permeability increased 2-fold for TNF in combination with IFN and a 6-fold increase was observed for the combination of TNF, IFN and PBMC (**Fig. 6**). Replacing PBMC with IL-1ß resulted in similar permeabil-

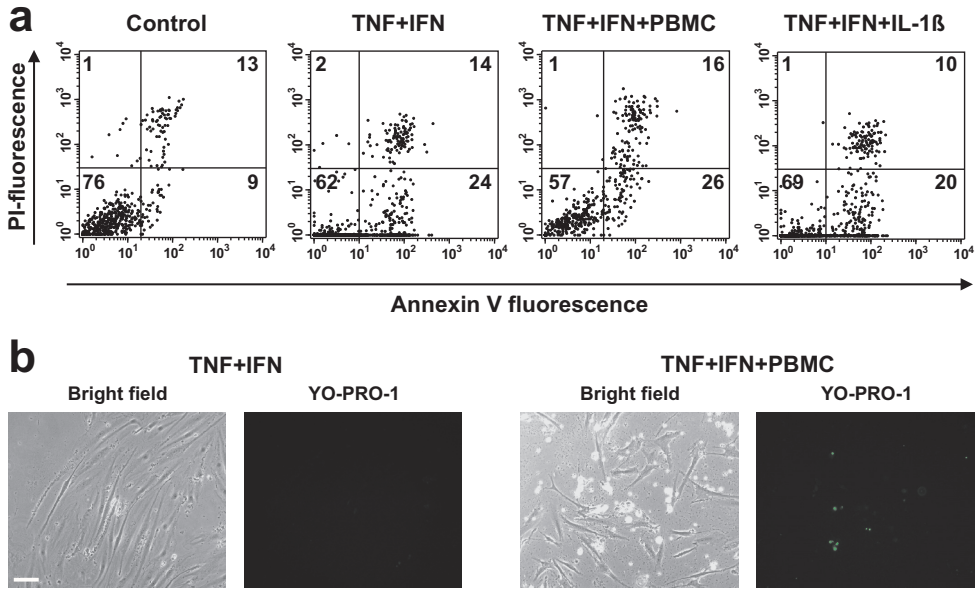

Figure 5. No change in apoptosis is found after addition of PBMC. Apoptosis was detected using PI and annexin V or YO-PRO-1 after 144 hours of incubation. (**a**) Viable cells are negative for PI and annexin V, apoptotic cells are positive for annexin V and necrotic cells are double positive for PI and annexin V. Numbers in each quadrant represent percentage cells. No significance was observed between the different incubations. (**b**) YO-PRO-1 pictures revealed that adherent cells after incubation with TNF (10 µg/ml) in combination with IFN (0.001 µg/ml) showed no apoptosis. Addition of PBMC gave no increase in apoptosis of adherent cells. Scale bar apply for all images, 100 µm.

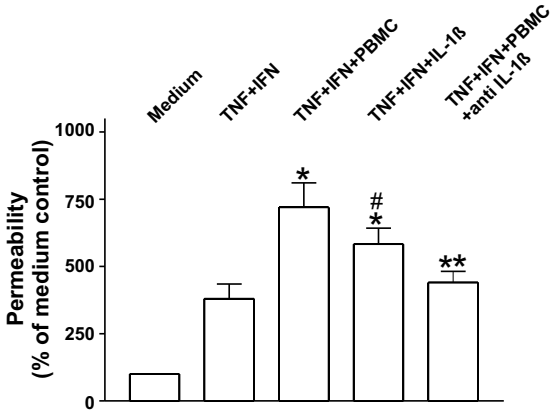

Figure 6. Permeability of the endothelial layer increases after 144 hours of incubation. Permeability changes after 144 hours with 10 µg/ml TNF, 0.001 µg/ml IFN, PBMC, 0.01 µg/ml IL-1ß or 1 µg/ml anti IL-1ß were detected. Addition of PBMC to TNF and IFN showed significant increase in permeability. Replacing PBMC with IL-1ß also resulted in increased permeability, whereas blocking endogenous IL-1ß reversed the effects. Columns represent percentage permeability increase compared to medium treated cells ± SD of 3 individual experiments; *, $P < 0.05$, permeability in cells incubated with TNF in combination with IFN *versus* cells incubated with TNF in combination with IFN and PBMC or IL-1ß; **, not significant *versus* cells incubated with TNF in combination with IFN; #, not significant *versus* cells incubated with TNF in combination IFN and PBMC.

ity increase. Addition of anti IL-1ß reduced the permeability increase by TNF in combination of IFN and PBMC back to the level of TNF in combination with IFN. These results indicate a striking indirect effect of TNF on the vascular permeability through induction of IFN and IL-1ß production by PBMC.

DISCUSSION

Previously, we showed that both in local regional setting as well as in systemic approaches addition of high-dose TNF to chemotherapy dramatically improves drug accumulation in the solid tumor resulting in profound tumor responses [4,5,7,23]. An important activity of this TNF-based therapy is an alteration of the pathophysiology of the solid tumor. Here, we report that high-dose TNF, especially in combination with IFN, induces morphological changes of endothelial cells; the cells become elongated and gap formation between the cells occurs. Importantly, these morphologic changes are much more pronounced when PBMC are added. Cells become further elongated, therefore intensifying gap formation that contributes to an increased permeability. The addition of PBMC turned the endothelial cells sensitive to lower concentrations of IFN. We demonstrate that PBMC-derived IL-1ß is responsible for this effect. It seems that IFN has a direct effect on endothelial cell growth but hardly on endothelial cell morphology, which is enhanced by IL-1ß. Beside that, we observe minimal changes in cell growth and percentage apoptosis. These observations indicate that the cascade initiated by high-dose TNF rather induce a change in endothelial cell morphology, resulting in formation of gaps and augmented vascular permeability than apoptosis of the endothelial cells. We observed that TNF has its effect on confluent endothelial cell monolayer and we speculate that the permeability change is not due to a decreased cell proliferation but to alterations in cell morphology.

It has been reported that stimulation of endothelial cells is associated with reduction and redistribution of extra- and intracellular proteins [14,24-28]. These proteins, like actin, are important in maintaining cell integrity and shape. Other proteins are crucial for contact of endothelial cells to the extracellular matrix. After stimulation of endothelial cells focal adhesion points are disrupted and cells detach from the matrix. Disruption of anchorage of endothelial cells to matrix components through integrins initiates anoikis. Although we saw no major induction of cell death, cells have to detach from the matrix in order to migrate and stretch. From our results we conclude that the TNF-induced cascade predominantly resulted in alteration of cell-cell and cell-matrix interaction and not a disruption of this contact.

Components of adherens and tight junctions, like occludin, cadherin and ZO-1, are downregulated within stimulated cells and contact between two neighboring cells is breached [29-33]. Redistribution of the actin cytoskeleton, detachment of the cells, and loss of contact are associated with the increased permeability of an endothelial monolayer when it is stimulated with cytokines [34-36]. We show here that the addition of PBMC even further expands the morphological changes of the endothelial cells, which is associated with actin redistribution, and therefore further increasing permeability. The permeability increase is most likely associated with the altered morphology and gap formation but may also result from the induction of vesiculo-vascuolar organelles (VVOs) [37]. As we recently showed that histamine also improves tumor response by augmenting vascular leakage, this is currently under investigation, as histamine is known to induce VVOs [38].

Furthermore, TNF is a mediator for recruitment of leukocytes and participates in the production of numerous endogenous factors, like IL-1ß, IL-2, IL-4, IL-6, IL-8 and IFNγ [39-42]. Moreover, we demonstrate that addition of IL-1ß to a combination of TNF and IFN could mimic the morphological changes observed when PBMC was added. We hypothesize that IL-1ß plays an important part in the process of TNF-induced morphological alterations of endothelial cells. Western blot analysis showed that TNF is essential for the production on IL-1ß, indicating an indirect effect of TNF towards the endothelial cells.

It has been shown that within a few hours after perfusion infiltration of erythrocytes, polymorphnuclear cells and platelets start to aggregate whereas macrophages invade the tumor later, after approximately 7 days. Lymphocytes start to infiltrate the tumor 6 to 7 days after perfusion [10,43]. Although after perfusion a wash out is performed, removing cytokines and cytotoxic agents, macrophages and lymphocytes are likely to produce a steady state of TNF, IFN and interleukins, which could have a continuous effect on the tumor vasculature. It has been described that tumor infiltrating lymphocytes are producing cytokines like TNF and IFN after treatment [44-46]. Angiograms of fast growing sarcomas revealed that a few weeks after perfusion the tumor-associated vasculature is eradicated [47], indicating that only one boost of high-dose exogenous TNF triggers mechanisms, which have an impact for extended periods of time. Further investigation is performed to understand the short-term effects of TNF on the endothelial cells.

Our data indicates that high-dose TNF inflicts endothelial damage through the induction of IFN and PBMC-derived IL-1ß. However, although we hypothesis IL-1ß as a major factor also other PBMC-derived factors are likely involved. Mainly inhibition of proliferation and severe alterations in morphology over longer periods are observed. The role of PBMC, in this model, is predominantly the intensification of

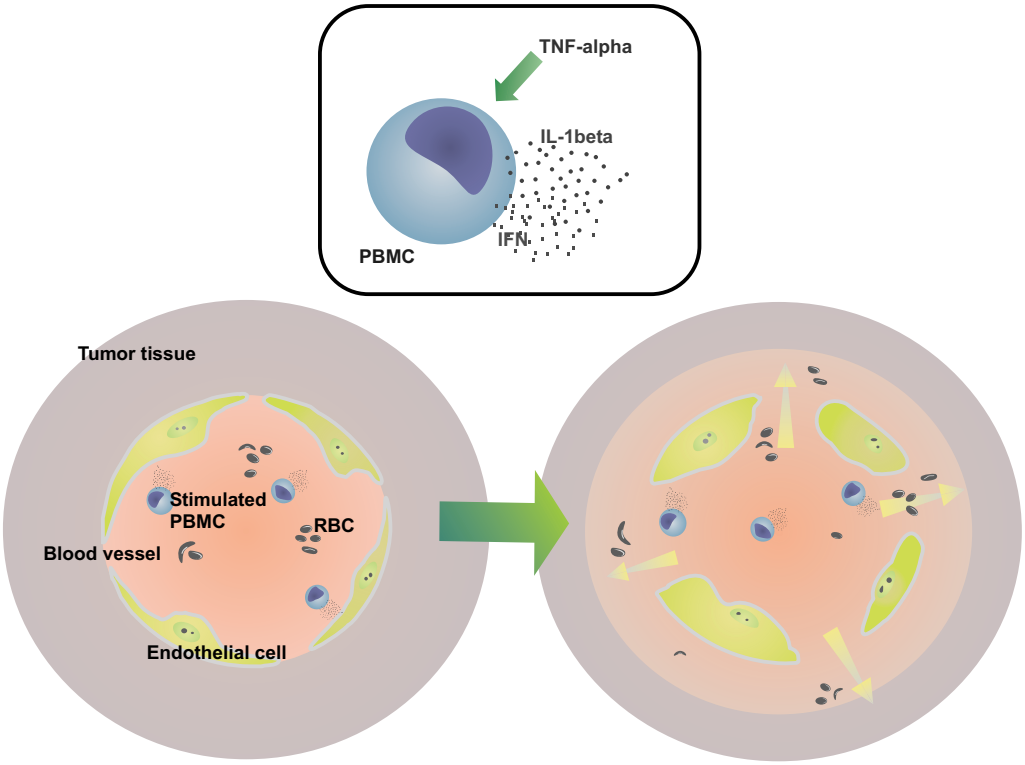

Figure 7. Proposed mechanism of TNF-mediated changes in tumor vascular permeability leading to augmented local drug accumulation in high-dose TNF combination therapy. Here we show that TNF, added in combination with cytotoxic agents, activate PBMC to produce IL-1ß and IFN. Mainly IFN and IL-1ß are responsible for the induction of morphological changes of the endothelial lining of the tumor-associated vasculature, thereby increasing vascular permeability. This enhances infiltration of blood cells and improves drug accumulation in the surrounding tumor tissue. (See color section for a full-color version.)

the morphological changes and permeability of the endothelial barrier. Translated to the *in vivo* situation (**Fig. 7**) this increased permeability participates on one side in an augmented leakage of co-administered chemotherapeutic in the tumor. On the other side recruitment of PBMC, provides continuous production of endogenous cytokines, contributing to the destruction of tumor vessels and necrosis of the tumor.

REFERENCES

1.Lienard D, Ewalenko P, Delmotte JJ, Renard N, and Lejeune FJ. High-dose recombinant tumor necrosis factor alpha in combination with interferon gamma and melphalan in isolation perfusion of the limbs for melanoma and sarcoma. J Clin Oncol. 1992: 10(1), 52-60.

2.Eggermont AM, Schraffordt KH, Lienard D, Kroon BB, van Geel AN, Hoekstra HJ et al. Isolated limb perfusion with high-dose tumor necrosis factor-alpha in combination with interferon-gamma and melphalan for nonresectable extremity soft tissue sarcomas: a multicenter trial. J Clin Oncol. 1996: 14(10), 2653-2665.

3.Eggermont AM. TNF registered in Europe: does TNF get a second chance? J Immunother. 2000: 23(4), 505-506.

4.de Wilt JH, ten Hagen TL, de Boeck G, van Tiel ST, de Bruijn EA, and Eggermont AM. Tumour necrosis factor alpha increases melphalan concentration in tumour tissue after isolated limb perfusion. Br J Cancer. 2000: 82(5), 1000-1003.

5.van der Veen AH, de Wilt JH, Eggermont AM, van Tiel ST, Seynhaeve AL, and ten Hagen TL. TNF-alpha augments intratumoural concentrations of doxorubicin in TNF-alpha-based isolated limb perfusion in rat sarcoma models and enhances anti-tumour effects. Br J Cancer. 2000: 82(4), 973-980.

6.Brouckaert P, Takahashi N, van Tiel ST, Hostens J, Eggermont AM, Seynhaeve AL et al. Tumor necrosis factor-alpha augmented tumor response in B16BL6 melanoma-bearing mice treated with stealth liposomal doxorubicin (Doxil) correlates with altered Doxil pharmacokinetics. Int J Cancer. 2004: 109(3), 442-448.

7.ten Hagen TL, van der Veen AH, Nooijen PT, van Tiel ST, Seynhaeve AL, and Eggermont AM. Low-dose tumor necrosis factor-alpha augments antitumor activity of stealth liposomal doxorubicin (DOXIL) in soft tissue sarcoma-bearing rats. Int J Cancer. 2000: 87(6), 829-837.

8.ten Hagen TL and Eggermont AM. Manipulation of the tumour-associated vasculature to improve tumour therapy. J Liposome Res. 2002: 12(1-2), 149-154.

9.Lejeune FJ, Ruegg C, and Lienard D. Clinical applications of TNF-alpha in cancer. Curr Opin Immunol. 1998: 10(5), 573-580.

10.Nooijen PT, Manusama ER, Eggermont AM, Schalkwijk L, Stavast J, Marquet RL et al. Synergistic effects of TNF-alpha and melphalan in an isolated limb perfusion model of rat sarcoma: a histopathological, immunohistochemical and electron microscopical study. Br J Cancer. 1996: 74(12), 1908-1915.

11.Mauerhoff T, Belfiore A, Pujol-Borrell R, and Bottazzo GF. Growth inhibition of human endothelial cells by human recombinant tumor necrosis factor alpha and -gamma. Tumori. 1994: 80(4), 301-305.

12.Norioka K, Borden EC, and Auerbach R. Inhibitory effects of cytokines on vascular endothelial cells: synergistic interactions among -gamma, tumor necrosis factor-alpha, and interleukin-1. J Immunother. 1992: 12(1), 13-18.

13.Burke-Gaffney A and Keenan AK. Does TNF-alpha directly increase endothelial cell monolayer permeability? Agents Actions. 1993: 38, C83-C85.

14.Ruegg C, Yilmaz A, Bieler G, Bamat J, Chaubert P, and Lejeune FJ. Evidence for the involvement of endothelial cell integrin alphaVbeta3 in the disruption of the tumor vasculature induced by TNF and IFN-gamma. Nat Med. 1998: 4(4), 408-414.

15.Korpelainen EI, Gamble JR, Smith WB, Goodall GJ, Qiyu S, Woodcock JM et al. The receptor for interleukin 3 is selectively induced in human endothelial cells by tumor necrosis factor alpha and potentiates interleukin 8 secretion and neutrophil transmigration. Proc Natl Acad Sci U S A. 1993: 90(23), 11137-11141.

16.Luu NT, Rainger GE, and Nash GB. Kinetics of the different steps during neutrophil migration through cultured endothelial monolayers treated with tumour necrosis factor-alpha. J Vasc Res. 1999: 36(6), 477-485.

17.Yilmaz A, Bieler G, Spertini O, Lejeune FJ, and Ruegg C. Pulse treatment of human vascular endothelial cells with high doses of tumor necrosis factor and interferon-gamma results in simultaneous synergistic and reversible effects on proliferation and morphology. Int J Cancer. 1998: 77(4), 592-599.

18.Manusama ER, Nooijen PT, Stavast J, de Wilt JH, Marquet RL, and Eggermont AM. Assessment of the role of neutrophils on the antitumor effect of TNFalpha in an in vivo isolated limb perfusion model in sarcoma-bearing brown Norway rats. J Surg Res. 1998: 78(2), 169-175.

19.Kramer SM and Carver ME. Serum-free in vitro bioassay for the detection of tumor necrosis factor. J Immunol Methods. 1986: 93(2), 201-206.

20.Jaffe EA, Nachman RL, Becker CG, and Minick CR. Culture of human endothelial cells derived from umbilical veins. Identification by morphologic and immunologic criteria. J Clin Invest. 1973: 52(11), 2745-2756.

21.Skehan P, Storeng R, Scudiero D, Monks A, McMahon J, Vistica D et al. New colorimetric cytotoxicity assay for anticancer-drug screening. J Natl Cancer Inst. 1990: 82(13), 1107-1112.

22.Takahashi N, Fiers W, and Brouckaert P. Anti-tumor activity of tumor necrosis factor in combination with interferon-gamma is not affected by prior tolerization. Int J Cancer. 1995: 63(6), 846-854.

23.van Ijken MG, van Etten B, de Wilt JH, van Tiel ST, ten Hagen TL, and Eggermont AM. Tumor necrosis factor-alpha augments tumor effects in isolated hepatic perfusion with melphalan in a rat sarcoma model. J Immunother. 2000: 23(4), 449-455.

24.Schnittler HJ, Schneider SW, Raifer H, Luo F, Dieterich P, Just I et al. Role of actin filaments in endothelial cell-cell adhesion and membrane stability under fluid shear stress. Pflugers Arch. 2001: 442(5), 675-687.

25.Gao B, Saba TM, and Tsan MF. Role of alpha(v)beta(3)-integrin in TNF-alpha-induced endothelial cell migration. Am J Physiol Cell Physiol. 2002: 283(4), C1196-C1205.

26.Lim MJ, Chiang ET, Hechtman HB, and Shepro D. Inflammation-induced subcellular redistribution of VE-cadherin, actin, and gamma-catenin in cultured human lung microvessel endothelial cells. Microvasc Res. 2001: 62(3), 366-382.

27.Goldblum SE, Ding X, and Campbell-Washington J. TNF-alpha induces endothelial cell F-actin depolymerization, new actin synthesis, and barrier dysfunction. Am J Physiol. 1993: 264(4 Pt 1), C894-C905.

28.Kohno K, Hamanaka R, Abe T, Nomura Y, Morimoto A, Izumi H et al. Morphological change and destabilization of beta-actin mRNA by tumor necrosis factor in human microvascular endothelial cells. Exp Cell Res. 1993: 208(2), 498-503.

29.Coyne CB, Vanhook MK, Gambling TM, Carson JL, Boucher RC, and Johnson LG. Regulation of airway tight junctions by proinflammatory cytokines. Mol Biol Cell. 2002: 13(9), 3218-3234.

30.Wachtel M, Bolliger MF, Ishihara H, Frei K, Bluethmann H, and Gloor SM. Down-regulation of occludin expression in astrocytes by tumour necrosis factor (TNF) is mediated via TNF type-1 receptor and nuclear factor-kappaB activation. J Neurochem. 2001: 78(1), 155-162.

31.Mankertz J, Tavalali S, Schmitz H, Mankertz A, Riecken EO, Fromm M et al. Expression from the human occludin promoter is affected by tumor necrosis factor alpha and interferon gamma. J Cell Sci. 2000: 113 (Pt 11), 2085-2090.

32.Kniesel U and Wolburg H. Tight junctions of the blood-brain barrier. Cell Mol Neurobiol. 2000: 20(1), 57-76.

33.Wright TJ, Leach L, Shaw PE, and Jones P. Dynamics of vascular endothelial-cadherin and beta-catenin localization by vascular endothelial growth factor-induced angiogenesis in human umbilical vein cells. Exp Cell Res. 2002: 280(2), 159-168.

34.Friedl J, Puhlmann M, Bartlett DL, Libutti SK, Turner EN, Gnant MF et al. Induction of permeability across endothelial cell monolayers by tumor necrosis factor (TNF) occurs via a tissue factor-dependent mechanism: relationship between the procoagulant and permeability effects of TNF. Blood. 2002: 100(4), 1334-1339.

35.Nooteboom A, van der Linden CJ, and Hendriks T. Tumor necrosis factor-alpha and interleukin-1beta mediate endothelial permeability induced by lipopolysaccharide-stimulated whole blood. Crit Care Med. 2002: 30(9), 2063-2068.

36.Petrache I, Birukova A, Ramirez SI, Garcia JG, and Verin AD. The Role of the Microtubules in Tumor Necrosis Factor-{alpha}-Induced Endothelial Cell Permeability. Am J Respir Cell Mol Biol. 2003: 28(5), 574-581.

37.Dvorak AM and Feng D. The vesiculo-vacuolar organelle (VVO). A new endothelial cell permeability organelle. J Histochem Cytochem. 2001: 49(4):419-432.

38.Brunstein F, Hoving S, Seynhaeve AL, van Tiel ST, Guetens G, de Bruijn EA et al. Synergistic antitumor activity of histamine plus melphalan in isolated limb perfusion: preclinical studies. J Natl Cancer Inst. 2004: 96(21), 1603-1610.

39.Ahlberg R, MacNamara B, Andersson M, Zheng C, Svensson A, Holm G et al. Stimulation of T-cell cytokine production and NK-cell function by IL-2, IFN-alpha and histamine treatment during remission of non-Hodgkin's lymphoma. Hematol J. 2003: 4(5), 336-341.

40.Andersson U, Andersson J, Lindfors A, Wagner K, Moller G, and Heusser CH. Simultaneous production of interleukin 2, interleukin 4 and interferon-gamma by activated human blood lymphocytes. Eur J Immunol. 1990: 20(7), 1591-1596.

41.Luo Y, Chen X, and O'Donnell MA. Role of Th1 and Th2 cytokines in BCG-induced IFN-gamma production: cy-

tokine promotion and simulation of BCG effect. Cytokine. 2003: 21(1), 17-26.
42.Nilsen EM, Johansen FE, Jahnsen FL, Lundin KE, Scholz T, Brandtzaeg P et al. Cytokine profiles of cultured microvascular endothelial cells from the human intestine. Gut. 1998: 42(5), 635-642.
43.Renard N, Lienard D, Lespagnard L, Eggermont A, Heimann R, and Lejeune F. Early endothelium activation and polymorphonuclear cell invasion precede specific necrosis of human melanoma and sarcoma treated by intravascular high-dose tumour necrosis factor alpha (rTNF alpha). Int J Cancer. 1994: 57(5), 656-663.
44.Ramesh R, Marrogi AJ, Munshi A, Abboud CN, and Freeman SM. In vivo analysis of the ‚bystander effect': a cytokine cascade. Exp Hematol. 1996: 24(7), 829-838.
45.Barth RJJ, Mule JJ, Spiess PJ, and Rosenberg SA. Interferon gamma and tumor necrosis factor have a role in tumor regressions mediated by murine CD8+ tumor-infiltrating lymphocytes. J Exp Med. 1991: 173(3), 647-658.
46.Sadanaga N, Nagoshi M, Lederer JA, Joo HG, Eberlein TJ, and Goedegebuure PS. Local secretion of IFN-gamma induces an antitumor response: comparison between T cells plus IL-2 and IFN-gamma transfected tumor cells. J Immunother. 1999: 22(4), 315-323.
47.Eggermont AM, de Wilt JH, and ten Hagen TL. Current uses of isolated limb perfusion in the clinic and a model system for new strategies. Lancet Oncol. 2003: 4(7), 429-437.

Chapter 5

Endothelial cell derived MMP-9 cause loss of endothelial cell integrity through interleukin-1beta produced by TNF-primed peripheral blood mononuclear cells

Ann L.B. Seynhaeve
Debby Schipper
Alexander M.M. Eggermont
Timo L.M. ten Hagen

Submitted for publication

Research article

Endothelial cell derived MMP-9 cause loss of endothelial cell integrity through interleukin-1beta produced by TNF-primed peripheral blood mononuclear cells

Ann L.B. Seynhaeve, Debby Schipper, Alexander M.M. Eggermont, and Timo L.M. ten Hagen

Department of Surgical Oncology, Erasmus MC-Daniel den Hoed Cancer Center, Rotterdam, the Netherlands

ARTICLE INFORMATION

Submitted for publication

ACKNOWLEDGMENTS

The authors thank Sanja Stevanović and Paul Wennekendonk for their technical assistance and Dr. K. Kullak of Boehringer Ingelheim GmbH for the generous supply of TNF.

ABSTRACT

The importance of combining chemotherapy and antivascular or antiangiogenic therapy has been underscored by a number of studies. We and others demonstrated the synergistic interaction between chemotherapy and tumor necrosis factor-alpha (TNF) in solid tumor treatment. TNF facilitates an augmented accumulation of the co-administered chemotherapeutic specifically in tumor tissue. The factors involved in the TNF-mediated vascular response are largely unknown. Here we show that TNF-induced production of interleukin-1beta by peripheral blood mononuclear cells triggers the endothelial cells to produce matrix metalloproteinase-9, which is responsible for changes in endothelial morphology and permeability. These data indicate that TNF indirectly affects endothelial permeability through degradation of the matrix.

INTRODUCTION

Addition of tumor necrosis factor-alpha (TNF) to chemotherapy results in dramatic improvement of tumor response in patients with intransit melanoma metastases and limb threatening soft tissue sarcomas [1-4]. Two previous findings provided important information on the activity of TNF. First, when TNF is added an augmented accumulation of the co-administered drug (e.g. melphalan or doxorubicin) is observed. Secondly, for TNF to be active leukocytes are indispensable [8,9]. Within a few hours after TNF administration extravasation of erythrocytes, infiltration of polymorphonuclear cells and platelet aggregation occurs. Macrophages and lymphocytes invaded the tumor 6 to 7 days after perfusion. *In vitro* endothelial cells appeared quite insensitive to TNF, whereas in the presence of peripheral blood mononuclear cells (PBMC) disruption of the endothelial monolayer was observed. Endothelial cells became elongated, intensifying gap formation that engenders increased permeability. Further investigations revealed that these observed effects were induced by PBMC-derived interleukin-1beta (IL-1ß) [10]. Loss of endothelial integrity could result from, first the disruption of the adhesive interaction between neighboring endothelial cells and secondly from disruption of interaction between cell and extracellular matrix. Degradation of the basal membrane and extracellular matrix involves the participation of proteolytic enzymes, like metalloproteinases (MMPs). MMP-2 and MMP-9 are produced by stromal cells and cleaves substrates, such as laminin and type IV collagen, which are over expressed in the basal lamina in tumors [11-14].

In our system the interaction between two cell types, HUVEC and PBMC, is investigated. We looked at the production and the biological role of MMPs and tried to identify which cell type produces the necessary MMPs in this co-culture. Here we show that TNF interacts with

peripheral blood mononuclear cells and endothelial cells, in coalition with other cytokines, like interferon-gamma (IFN) and IL-1ß, mediating MMP production. From the enhanced MMP production matrix degradation results inflicting morphologic changes of the endothelial cell and increased endothelial permeability.

EXPERIMENTAL PROCEDURES

Agents. Recombinant human Tumor necrosis factor-alpha (TNF) and recombinant human Interferon-gamma (IFN) were kindly provided by Boehringer Ingelheim GmbH. TNF had a specific activity of $5x10^7$ U/mg as determined in the murine LM cell assay. Endotoxin levels were < 1.25 units (EU) per mg protein. IFN had a specific activity of $2.5x10^7$ U/mg as determined in an HLA-DR assay. Recombinant human interleukin-1beta (IL-1ß) was purchased from Peprotech EC Ltd. As determined by stimulation of thymidine uptake by murine C3H/HeJ thymocytes, the ED_{50} was ≤ 0.1 ng/ml, corresponding to a specific activity of ≥ $1x10^7$ U/mg. Endotoxin levels were less than 1 EU per µg protein. Goat anti human interleukin-1beta (anti IL-1ß) was purchased from R&D systems. As determined by the LAL method, endotoxin levels were less than 10 ng/ml. GM6001 (Ilomastat), a broad spectrum MMP inhibitor was purchased from Chemicon and N-actelylcysteine (NAC) from Pharmachemie BV. Active Human MMP-2 and MMP-9 enzymes were purchased from Calbiochem.

Cells and cultured conditions. Human umbilical vein endothelial cells (HUVEC) were isolated by collagenase digestion using the method described by Jaffe *et al* [15]. Each isolate was derived from an individual umbilical vein and used for experiments at passage 5 or 6. HUVEC were cultured in HUVEC medium containing human endothelial-serum free medium (Invitrogen), 20% heat inactivated newborn calf serum (Lonza), 10% heat inactivated human serum (Lonza), 20 ng/ml human recombinant basic fibroblast growth factor (Peprotech EC Ltd), 100 ng/ml human recombinant epidermal growth factor (Peprotech EC Ltd) on fibronectin (Roche Diagnostics) coated flasks. HUVEC had the characteristic cobblestone morphology and tested positive for CD31. For all experiments, with the exception of western blot, cells were cultured, after plating, in serum-poor HUVEC medium (Human endothelial-SFM, 5% heat inactivated human serum, 20 ng/ml human recombinant basic fibroblast growth factor and 100 ng/ml human recombinant epidermal growth factor). For western blot experiments, cells were cultured in serum-free HUVEC medium (human endothelial-SFM, 20 ng/ml human recombinant basic fibroblast growth factor and 100 ng/ml human recombinant epidermal growth factor). Apart from a slower growth rate there were no changes in sensitivity towards the added drugs. Human peripheral blood mononuclear cells (PBMC) were isolated from healthy donors using the Vacutainer CPT Mononuclear Cell Preparation Tubes with sodium heparin (Becton Dickinson). PBMC were washed with phosphate buffered saline and counted with trypan blue to determine the viable cell concentration. PBMC, at a final concentration of $120x10^4$ PBMC/ml, were used in all experiments.

Stimulation of endothelial cells. HUVEC were plated in 24 wells multiplate (Corning BV), coated with fibronectin, at a final concentration of $3x10^4$ cells per well. After 24 hours, cells were washed and supernatant was replaced with serum-poor HUVEC medium containing 10 µg/ml TNF, 0.1 µg/ml IFN, PBMC or 0.01 µg/ml IL-1ß. To block production by endogenous IL-1ß, HUVEC were pretreated for 3 hours with a neutralizing antibody for IL-1ß and additionally co-cultured with the cytokines and PBMC. GM6001, an inhibitor for MMP-1, 2, 3, 8 and 9, was added in a concentration of 25 µM and N-acteylcysteine, which is known to inhibit particularly MMP-2 and 9, in a concentration of 12.5 mM. For western blot analysis the same concentrations TNF, IFN and PBMC in serum-free HUVEC medium were used. HUVEC were also incubated with active human MMP-2 and MMP-9 enzyme. Unless mentioned otherwise, incubation time was 144 hours in a humidified atmosphere at 37°C and 5% CO_2.

Assessment of growth and morphology changes of endothelial cells. Growth of endothelial cells was measured using a Sulphorhodamine B protein stain assay (SRB, Sigma) according to the method of Skehan [16]. As a control, endothelial cells incubated with only HUVEC medium were used. Briefly, cells were incubated with 10% trichloric acetic acid (1 hour, 4°C), stained for 15 min with SRB, washed with 1% acetic acid and allowed to dry. Protein bound SRB was dissolved in 10 mM Tris buffer, and the optical density (O.D.) was measured at 540 nm. Cell growth was calculated using the formula: percentage cell growth = (O.D. test well/O.D. control well) x 100 percent. Morphological cell changes were examined with a 10x NA 0.30 plan-neofluar objective lens using an inverted Zeiss Axiovert 100M microscope equipped with an Axiocam digital camera (Carl Zeiss). Cell elongation was measured and expressed as the ratio of the length of the major cell axis to the width perpendicular to the length. Ten cells and at least four independent incubations were determined. In addition, gap formation was determined. The cell-free area was outlined and gap formation was calculated using the formula: percentage cell-free area = (cell-free area/total area) x 100 percent. Al measurements were done using the AxioVision 3.0 software.

Sample preparation. After HUVEC incubation, supernatant was collected and centrifuged to pellet detached cells and PBMC. To ensure that the supernatants were derived from equal cell numbers, for each experimental condition, DNA content was measured (CyQuant Cell Proliferation Assay Kit, Molecular Probes). Bacteriophage λDNA, included in the kit, was used as standard. In general, 5 to 20 µl of supernatant was loaded on the gel, corresponding to 1000 ng/ml DNA.

Preparation of cell lysates. After indicated incubations, adherent cells were washed and harvested by scraping the cells into a small volume of lysis buffer (20 mM Tris-HCl (pH 8.8), 125 mM NaCl, 1% triton X-100). Extracts were incubated on ice for 30 min and clarified by microcentrifuge at 20,000g for 10 min. Protein concentration of lysate was determined using the Advanced Protein Assay Reagent (Cytoskeleton).

Gelatin zymography. MMP-9 and MMP-2 activity were analysed by zymography. Under non-reducing conditions, samples were electrophoresed on a 10% polyacrilamide gel containing 1% gelatin (Sigma). Following electrophoresis, gels were washed with 2.5% triton X-100 and incubated in MMP-development buffer (50 mM Tris-HCl (pH 8.8), 5 mM $CaCl_2$) for 24 hours at 37°C. Gels were stained during 5 hours with 0.5% Coomassie Blue R250 (Sigma) and destained in 45% methanol:45% distilled H_2O:10% acetic acid. Protein identity was confirmed using a MMP-9 and MMP-2 standard (Chemicon). All zymographic MMP activities were inhibited by the metal chelator EDTA, confirming their identity as MMP. Computerized densitometry was used to evaluate enzymatic activity (ImageJ 1.31v, Wayne Rasband).

Western blot analysis. Proteins in the supernatant were precipitated using ice-cold aceton at –20°C for at least 1 hour and dried overnight. The pelleted proteins were resuspended, electrophoresed under reducing conditions on a 10% polyacrilamide gel and transferred to a PVDF membrane (BioRad). Following transfer, the membranes were blocked with MPBS (5% milkpowder in PBS/0.05% tween-20) and incubated overnight with mouse anti human MMP-1 or mouse anti human MMP-3 at 4°C (1:100; Calbiochem) in MPBS. After washing, the membrane was incubated with goat anti mouse biotin (1:1500; Southern Biotechnology) in MPBS. Bound biotin was incubated with alkaline-phosphatase-streptavidin complex (BioRad) and this in turn stained with BCIP/NBT liquid substrate (Roche Diagnostics).

Enzyme-linked immunoabsorbant assay. Total MMP-1, MMP-2, MMP-3 and MMP-9 content in the supernatant were determined using a commercial ELISA kit according to the manufacturer's instruction. Quantikine Human

MMP-2 and MMP-9 were purchased from R&D systems and MMP-1 and MMP-3 Biotrak ELISA system from Amersham Biosciences.

RESULTS

Endothelial MMP-9 expression after stimulation with TNF, IFN and PBMC. Exposure of HUVEC to TNF or IFN alone, as well as combined failed to induce MMP-9. However, production of MMP-9 was significantly enhanced when endothelial cells were stimulated with TNF (10 µg/ml) in combination of IFN (0.1 µg/ml) and PBMC (**Fig. 1a**). These observations were confirmed by ELISA (**Supplementary Fig. 1a**). Lowering the IFN dose to 0.001 µg/ml resulted in comparable MMP-9 expression (data not shown). MMP-2 was continuously expressed and responded poorly to stimulators, which is known from the literature, and corresponded with ELISA (data not shown). Intracellular MMP-9 production, latent as well as active, was observed in cells exposed to TNF in combination with PBMC and increased further when IFN was added (**Fig. 1b**). To distinguish PBMC-derived MMPs from MMPs produced by endothelial cells, we removed the supernatant, including PBMC and cytokines after 72 hours of incubation. The endothelial cells were incubated for an additional 72 hours with fresh

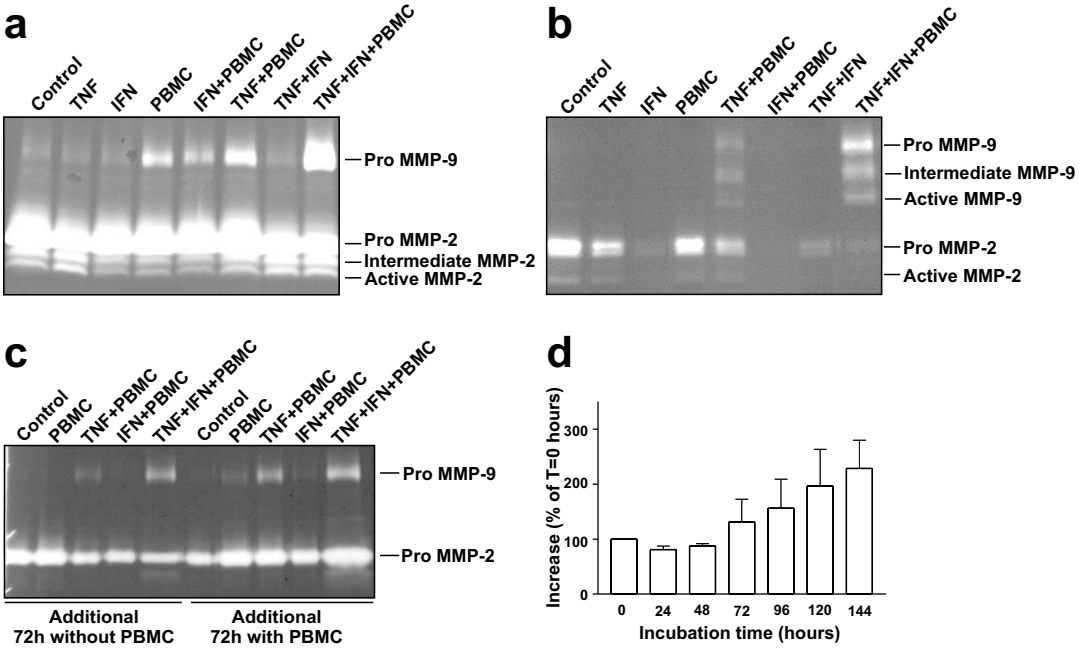

Figure 1. MMP-9 expression is increased after HUVEC stimulation with TNF, IFN and PBMC. (**a**) Supernatant of HUVEC incubated for 144 hours with TNF, IFN and PBMC were assessed by gelatin zymography. MMP-9 expression was significantly increased when HUVEC were exposed to TNF, IFN and PBMC. (**b**) Zymography of HUVEC lysate was also implemented and revealed that HUVEC incubated with TNF, IFN and PBMC produce a large amount of MMP-9. (**c**) Additional zymographs were performed to identify that MMP are predominantly EC-derived. HUVEC were incubated with cytokines in combination with PBMC for 72 hours. After 72 hours supernatant was replaced with cytokines alone (left) or with cytokines in combination with PBMC (right) for an additional 72 hours. HUVEC initially incubated with TNF, IFN and PBMC continued to produce MMP-9 after PBMC were removed. (**d**) HUVEC were exposed to TNF, IFN and PBMC for 24 hours. Supernatant was replaced with medium and every 24 hours a sample was taken and zymography performed. MMP-9 band densities were quantified by densitometry and showed that HUVEC continues to produce MMP-9. Columns represent percentage densitrometric increase ± SD of 3 individual experiments. The cell treated with TNF in combination with IFN and PBMC for the initial 24 hours was set at 0 hours.

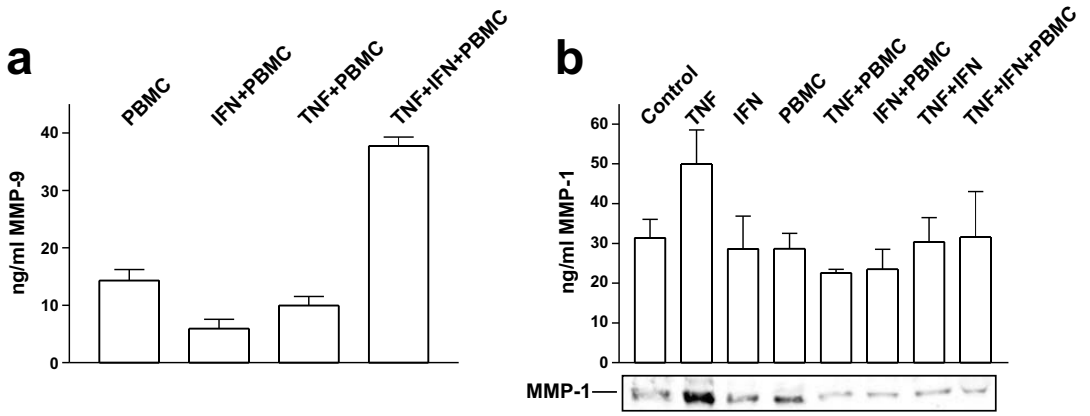

Supplementary Figure 1. MMP-9 expression is increased, but MMP-1 is not after HUVEC stimulation with TNF, IFN and PBMC. (a) ELISA of supernatant of HUVEC incubated for 144 hours with TNF, IFN and PBMC revealed a increase in MMP-9 production. (**b**) ELISA and Western blot of these samples for MMP-1 showed no significant changes. Columns represent ng MMP per ml ± SEM of 2 treatments of 3 individual experiments.

medium and respective cytokines but without PBMC. As a reference, cells were incubated with fresh medium with cytokines and PBMC (**Fig. 1c**). The endothelial cells appeared to produce equal amounts of MMP-9 irrespective of the incubation conditions or sequence. This indicates that particularly endothelial cells are responsible for the production of MMP-9. Priming of HUVEC for 24 hours with TNF combined with IFN and PBMC resulted in continuous production of MMP-9 (**Fig. 1d**) and MMP-2 (data not shown) till 144 hours. PBMC incubated with medium, TNF or IFN alone or TNF combined with IFN produced an equivalent amount of MMP-9 and MMP-2 (data not shown). These experiments confirmed that, in a co-culture of HUVEC and PBMC, the endothelial cells are the main source of MMP-9. The zymography revealed a constitutive band at approximately 45 kDa possibly resulting from MMP-1 or MMP-3 activity. We assayed the production of MMP-1 with ELISA and western blot (**Supplementary Fig. 1b**). MMP-1 secretion was only increased with the addition of TNF. Stimulation of HUVEC with other combinations did not induce MMP-1 production. We could not detect any measurable levels of MMP-3 with western blot (data not shown). With ELISA, we detected levels of MMP-3 in a range from 500 pg/ml to 1000 pg/ml, however, these were not affected by the different stimuli (data not shown).

Identification of IL-1ß as a crucial factor for the production of MMP-2 and -9. Previously, we identified PMBC-derived IL-1ß as a crucial factor in TNF-mediated morphology and permeability changes of endothelial cells [10] (**Fig. 2a**). Therefore, we examined the role of endogenous produced IL-1ß in TNF-evoked MMP production in endothelial cells. First, endothelial cells were exposed to TNF and IFN in combination with IL-1ß. Second, endogenous production of IL-1ß by PBMC was blocked with a neutralizing antibody. IL-1ß alone failed to induce MMP-9 production. However, similar MMP-9 levels were produced by endothelial cells when stimulated by TNF combined with PBMC as with TNF combined with IL-1ß. The results indicate that PBMC can be replaced by IL-1ß. Moreover, the MMP-9 production was further enhanced by IFN (**Fig. 2b**). The MMP-2 production is not affected by IL-1ß (data not shown). Pre-incubation of endothelial cells for 3 hours with anti IL-1ß and subsequently stimulated with TNF combined with IFN and PBMC resulted in a prominent decline in MMP-9 production (**Fig. 2c**). These data demonstrate the importance of IL-1ß in MMP-9 production. Next to that, the results indicate that endothe-

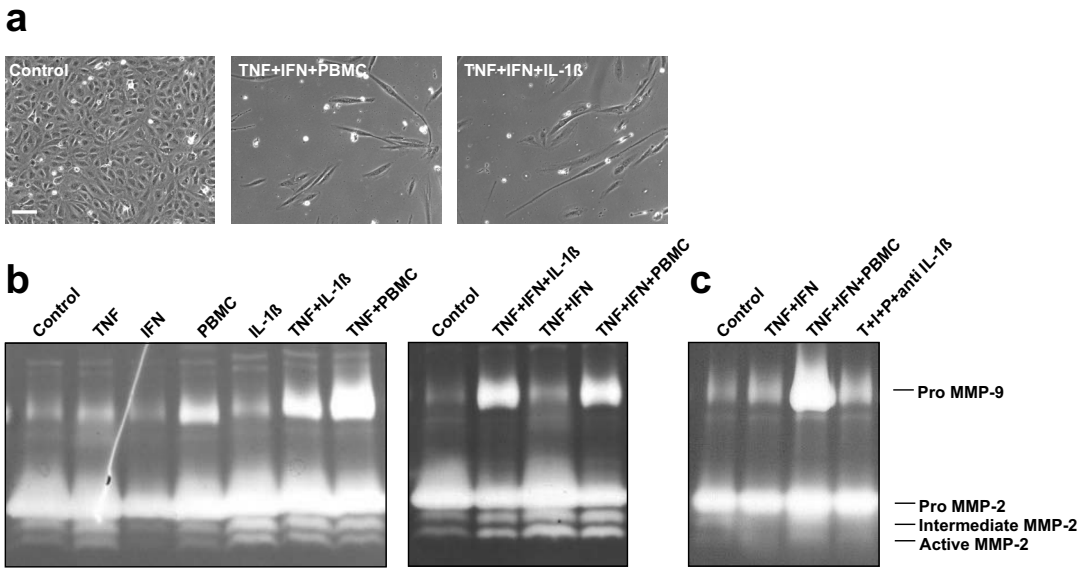

Figure 2. Identification of IL-1ß as the mediator of EC-derived MMP-9 production. (**a**) Photographs of HUVEC were taken 144 hours after incubation with TNF, IFN and PBMC. Typical cobblestone structure of the monolayer after incubated with only medium is shown. Incubation with TNF, IFN and PBMC resulted in pronounced elongation of the cells and gap formation. When PBMC were replaced with IL-1ß the inflicted morphology changes were comparable. Scale bar apply for all images, 100 µm. (**b**) Gelatinase activity was determined in supernatant of HUVEC incubated with TNF, IFN, PBMC or IL-1ß. Representative zymographs are shown and revealed that HUVEC stimulated with IL-1ß in combination with TNF (left zymography) or with TNF and IFN (right zymography) produce large amounts of MMP-9. (**c**) Prior to treatment of the HUVEC with TNF (T) in combination with IFN (I) and PBMC (P), a neutralizing antibody against IL-1ß (1 µg/ml) was added to the culture. Blocking of endogenous produced IL-1ß strongly reduced the MMP-9 production.

lial-derived MMP-9 is essential for the observed effects and not MMP-9 produced by PBMC.

Morphological changes and survival of HUVEC after MMP inhibition. We investigated the effect of MMPs on endothelial cell morphology changes and growth. For this purpose, we used two different inhibitors, GM6001, a broad spectrum MMP-inhibitor and N-acetylcysteine (NAC), an inhibitor for MMP-2 and MMP-9. Gelatin zymography (**Fig. 3a**) and densitrometric analysis (**Supplementary Table 1**) revealed a decrease in MMP-9 and MMP-2 production when inhibitors were added. The MMP-9 production of HUVEC treated with TNF in combination with IFN and PBMC decreased 6-fold when N-acetylcysteine was added. Densitrometric analysis of zymography showed a 10-fold decrease in MMP-9 gelatinase activity by N-acetylcysteine in HUVEC incubated with TNF in combination with IFN and IL-1ß (**Fig. 3b**). Under normal culture conditions endothelial cells formed a typical cobblestone monolayer (**Fig. 3c**). Exposure to N-acetylcysteine had no effect on the cells, while GM6001 induced a slight stretching of the cells (data not shown). Endothelial cells cultured with TNF combined with IFN and PBMC showed a fibroblast-like resemblance and large gaps between the cells became visible. Also, the gap formation in the endothelial layer incubated with TNF combined with IFN and IL-1ß was markedly reduced when MMP production was inhibited with N-acetylcysteine. Although, we observed no changes in cell elongation we found a significantly reduced gap formation when MMP activity was suppressed with either N-acetylcysteine (**Table 1**) or GM6001 (data not shown). MMP inhibition causes survival in cells treated with TNF in combination with IFN and TNF in combina-

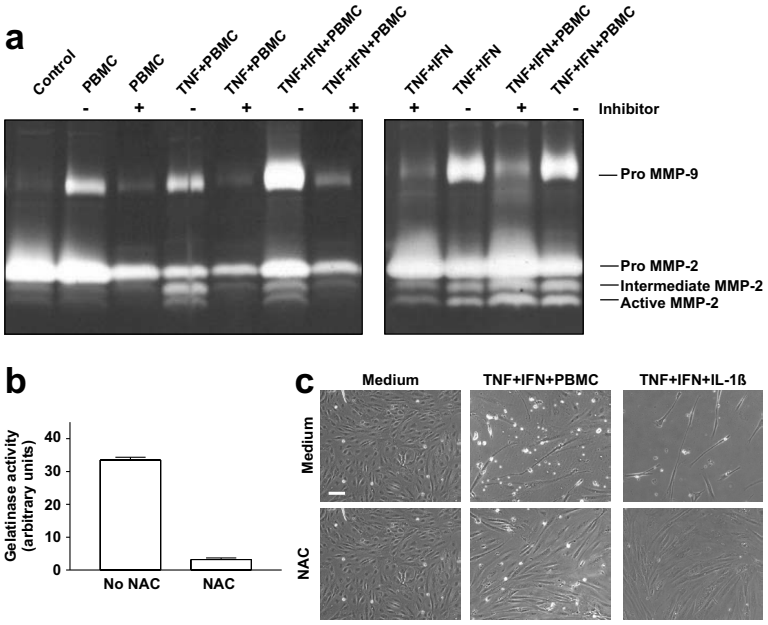

Figure 3. MMP-inhibitors reduces the TNF-induced effects on HUVEC growth and morphology. (**a**) Supernatant of HUVEC treated with MMP-inhibitor N-acetylcysteine (left zymography) or GM6001 (right zymography) were evaluated with zymography and showed a reduction in gelatinase activity when MMP-inhibitors were added. (**b**) Densitrometric analysis of the MMP-9 band in zymography of supernatant taken from HUVEC incubated with TNF, IFN and IL-1ß showed that MMP-9 production is also significantly decreased when N-acetylcysteine (NAC) was added. Colums represent arbitrary units ± SD of 3 individual experiments. (**c**) Photographs of HUVEC were taken 144 hours after incubation with TNF (T), IFN (I), PBMC (P) or IL-1ß and the MMP-inhibitor N-acetylcysteine. Cells incubated with TNF, IFN and PBMC showed again the morphological changes as before. Blocking MMP production with N-acetylcysteine decreased these changes, especially gap formation, significantly Scale bar apply for all images, 100 µm.

Supplementary table 1. Densitometric analysis of MMP-9 and MMP-2 activity in HUVEC conditioned medium.

Incubation	MMP-9 activity (fold-increase of control)		MMP-2 activity (fold-increase of control)	
	Medium	NAC	Medium	NAC
Medium	1	0.5 ± 0.4	1	0.6 ± 0.1*
TNF	1.3 ± 0.5	0.2 ± 0.1*	1 ± 0.1	0.7 ± 0.1
IFN	1.1 ± 0.6	0.35 ± 0.3	1.1 ± 0.2	0.9 ± 0.2
PBMC	5.5 ± 4.7	0.92 ± 0.5	1.0 ± 0.1	0.9 ± 0.1
TNF + PBMC	16.9 ± 10.4	3.0 ± 1.5	1.3 ± 0.2	1.0 ± 0.2
IFN + PBMC	1.3 ± 0.5	0.4 ± 0.3	1.1 ± 0.1	0.7 ± 0.1
TNF + IFN	1.7 ± 0.2	0.3 ± 0.3*	1.9 ± 0.2	1.5 ± 0.2
TNF + IFN + PBMC	40.0 ± 22.1	6.0 ± 2.0*	5.2 ± 1.5	4.0 ± 0.5

Note: Huvec were incubated with 10 µg/ml TNF, 0.1 µg/ml IFN, PBMC and N-acetylcysteine for 144 hours and zymography of the supernatant was performed as described in the experimental procedures. Computerized densitometry were calculated to evaluate relative enzymatic activity using HUVEC medium as control. Data represent fold increase compared to HUVEC medium treated cells ± SD of at least 4 individual experiments; *, $P < 0.05$, cells incubated with medium *versus* N-acetylcysteine.

Table 1. Cell length to width ratio and cell-free area of HUVEC in the presence of MMP inhibitor N-acetylcysteine.

Incubation	Length to width ratio[a]		Cell-free area (%)[b]	
	Medium	NAC	Medium	NAC
Medium	1.3 ± 0.1	2.0 ± 0.4	0 ± 0.1	0 ± 0.1
TNF + IFN + PBMC	20.6 ± 2.1	13.5 ± 1.2	93.3 ± 3.8	9.9 ± 3.4*
TNF + IFN + IL-1ß	12.6 ± 1.8	11.0 ± 1.1	91.8 ± 2.1	21.1 ± 3.6*

Note: HUVEC were incubated with 10 µg/ml TNF, 0.1 µg/ml IFN and PBMC or 0.1 µg/ml IL-1ß. MMP activity was inhibited with N-acetylcysteine for 144 hours and morphological cell changes examined.

[a] Ratio of major and minor axes was measured to determine the cell elongation. Data represent length to width ratio ± SEM of 10 cells per treatment of at least 4 individual experiments.

[b] Cell-free area, as a percent of the total area, was calculated to verify the gap formation. Data represent percentage cell-free area ± SD of at least 4 individual experiments; *, $P < 0.05$, cells incubated with HUVEC medium *versus* N-acetylcysteine.

Table 2. Percentage survival of HUVEC in the presence of TNF, IFN, PBMC and the MMP inhibitors GM6001 and N-acetylcysteine.

Incubation	% Medium[a]	% GM6001[b]	ϰ	% NAC[b]	ϰ
TNF + PBMC	66.7 ± 1.9	59.2 ± 3.4	-7.5	88.3 ± 3.2*	21.6
TNF + 0,1 µg/ml IFN	28.4 ± 3.15	43.3 ± 5.5*	14.9	78.3 ± 7.2*	49.9
TNF + 0.001 µg/ml IFN	66.7 ± 3.7	73.9 ± 14.2	7.2	97.9 ± 8.9*	31.1
TNF + 0.1 µg/ml IFN + PBMC	20.7 ± 1.8	38.4 ± 7.3*	17.7	56.9 ± 4.3*	36.4
TNF + 0.001 µg/ml IFN + PBMC	37.2 ± 1.9	58.6 ± 9.3*	21.4	62.0 ± 4.0*	24.8

Note: HUVEC were incubated with 10 µg/ml TNF, IFN and PBMC. MMP activity was inhibited with GM6001 or N-acetylcysteine for 144 hours. HUVEC incubated with HUVEC medium only were used as controls and set as 100 percent cell growth.

[a] Percentage cell growth of HUVEC exposed to given factors as compared to HUVEC cultured with HUVEC medium only.

[b] Percentage cell growth of HUVEC exposed to given factors and MMP inhibitor as compared to HUVEC cultured with HUVEC medium only.

Data represent percentage cell growth compared to HUVEC medium treated cells ± SEM of 2 experiments of at least 4 individual experiments; *, $P < 0.05$, cells incubated with medium *versus* inhibitor.

[c] Survival gain or loss in the presence of GM6001 or N-acetylcysteine compared to cells treated without inhibitors.

tion with IFN and PBMC (**Table 2**). The data confirmed the observation that IL-1ß and endothelial-derived MMPs are key players in TNF-inflicted morphology and permeability changes of endothelial cells.

Effect of exogenous MMP on HUVEC morphology. To further indicate that these specific EC-derived MMPs are needed we stimulated HUVEC with exogenous MMP, at levels measured in the MMP-9 and MMP-2 ELISA. HUVEC stimulated with only MMP-2 or MMP-9 showed no changes compared to cells incubated with medium. Incubation of HUVEC with TNF in combination with IFN showed cell elongation and gap formation that was further increased with the addition of PBMC. However, when PBMC were replaced with MMP-2 or MMP-9 we noticed that the morphological changes were comparable to those seen in cells incubated with TNF and IFN (**Fig. 4a**). Looking at cell elongation, TNF in combination with IFN showed no change in length to width ratio as TNF in combination with IFN and MMP-2 or MMP-9 enzyme, namely 6.0 ± 0.7 for TNF plus IFN, and 9.4 ± 0.8 for TNF in combination with IFN plus MMP-2, and 8.8 ± 1.7 for TNF in combination with IFN plus MMP-9. Length to width ratio of HUVEC incubated with TNF in combination with IFN and PBMC (18.9 ± 1.3) or IL-

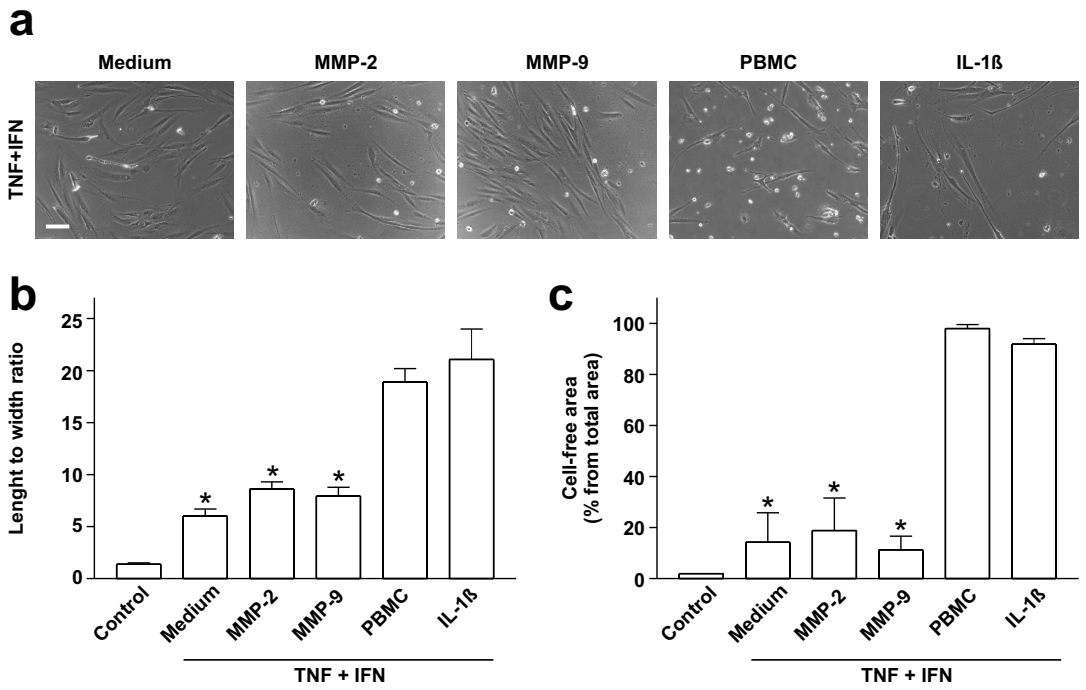

Figure 4. Exogenous MMPs has no effect on HUVEC morphology. (**a**) Photographs were taken of HUVEC incubated with TNF (T) and IFN (I) combined with PBMC (P), IL-1ß, MMP-2 or MMP-9. HUVEC incubated with TNF and IFN showed some cell elongation and gap formation that was further increased when PBMC were added. Replacing PBMC with active MMP-2 or MMP-9 enzyme did not induce these changes. Scale bar apply for all images, 100 µm. (**b**) Length to width ratio, representative for cell elongation, and (**c**) cell-free area, as function of gap formation, were calculated. Incubation with TNF and IFN increased cell elongation as well as gap formation compared to control. These effects were not further increased when MMP-2 or MMP-9 was added. However, addition of PBMC augmented cell elongation as well as gap formation. Columns represent length to width ratio ± SEM of 10 cells per treatment of at least 4 individual experiments and percentage cell-free area ± SD of at least 4 individual experiments; *, $P < 0.05$, cells incubated with medium, MMP-2 or MMP-9 *versus* cells incubated with PBMC.

1ß (22.5 ± 1.8) was significantly enlarged as compared to the other combinations (**Fig. 4b**). Also, cell-free area, as an indication for gap formation, in HUVEC incubated with TNF and IFN (14.3 ± 11.5%) was comparable with that of TNF in combination with IFN and MMP-2 (24.1 ± 19.3%) and TNF in combination with IFN and MMP-9 (11.0 ± 8.0%). Cell-free area was significantly higher in HUVEC exposed to TNF in combination with IFN and PBMC (97.9 ± 0.6%) or IL-1ß (91.8 ± 2.1%) (**Fig. 4c**). Exogenous MMP did not inflict the same morphological effects as seen in HUVEC incubated with TNF in combination with IFN and PBMC or in HUVEC incubated with TNF in combination with IFN and IL-1ß.

DISCUSSION

We have previously shown that TNF-mediated changes of the endothelial lining of the tumor-associated vasculature with TNF drastically improved tumor response through an augmented accumulation of the co-administered chemotherapeutic drug [16-18]. We also demonstrated that exposure of HUVEC to TNF combined with IFN and PBMC induced cell elongation and gap formation. The main PBMC-derived factor responsible for the observed changes is IL-1ß [10]. The morphology and permeability changes implicate degradation of the extracellular matrix (ECM) that is governed by activated MMPs. We found increased amounts of MMP-9 in supernatant and cell lysate of HUVEC stimulated

with TNF, IFN and PBMC, whereas production of MMP-1, MMP-2 and MMP-3 was not affected. Adding IL-1ß validated the importance of IL-1ß in the production of MMPs and blocking endogenous produced IL-1ß with a neutralizing antibody. Thus we concluded that IL-1ß triggers the endothelial cells to produce MMP-9. We established the biological relevance of increased activity of MMP-9 with the aid of MMP inhibitors. Inhibition of MMPs reversed the effect of TNF, IFN and PBMC on HUVEC. Cells were rescued, gap formation was reduced and permeability decreased significantly, indicating that MMP-9 plays an important role in these processes.

Overproduction of MMP-2 and -9 has been long recognized as a major contribution to the degradation of extracellular matrix in the tumor environment. They are not only involved in the mechanical removal of the proteins in the ECM but are also able to participate in the regulation of cell growth, apoptosis, angiogenesis, invasion and metastasis [19-21]. Elevated levels of gelatinases correlates with the aggressiveness of the tumor and is often associated with poor prognosis [22,23]. The current view is that gelatinases contribute positively in favor of tumor progression and therefore several MMP inhibitors are studied in clinical trials, although results have been disappointing thus far [24-26]. However, it seems likely that the breakdown of the ECM and the basal membrane renders the underlying tumor tissue more accessible for chemotherapeutic drug.

Addition of high-dose TNF to an isolated limb perfusion (ILP) with melphalan results in high response rates in patients with in-transit melanoma metastases and limb threatening soft tissue sarcomas and in four out of five patients amputation could be avoided [27-31]. Angiograms of sarcoma-bearing patients after TNF-based ILP demonstrated complete destruction of the tumor vascular bed, whereas the normal vessels were not affected [32]. In our laboratory, we demonstrated that addition of TNF leads to an enhanced accumulation of melphalan or doxorubicin specifically in the tumor in various ILP models [5,6]. This indicated that TNF primarily affects the tumor vasculature. Furthermore, systemic use of low-dose TNF in combination with Stealth liposomal doxorubicin (DOXIL) resulted as well in increased accumulation of cytotoxic drug in the tumor and therefore in significant improved tumor response [7,33,34]. In conclusion, we hypothesize that loss off endothelial cell integrity and increased permeability is of considerable importance in the treatment of solid tumors. MMPs have been reported to proteolyse cadherins, ß-catenin and occludin, which are important proteins in maintaining cell integrity [35-37]. Given that intercellular junctions represent a second significant target for MMPs, increased vascular permeability may also occur through destruction of the tight and adherens junctions that maintain the endothelial barrier. Cytokine-mediated induction of MMPs, leading to increased junctional reorganization, may be an important mechanism for increased permeability observed in ILP and liposomal treatment. Effects of cytokines and PBMC on junctional proteins are currently under investigation by us. Strikingly, addition of exogenous MMP did not simulate the effects we observed with endogenous produced MMPs. Also, MMP-9 appeared only as a zymogen in the supernatant, whereas the active form could be detected in the cell lysate. This indicates that location of the MMP is of crucial importance. We speculate that endothelial cell-associated MMPs, which are in close proximity to the underlining matrix are the source of proteolytic activity. Docking of MMPs on the cell surface provides a direct mechanism by which cells utilize the proteolytic activity on the ECM. Additionally, cell surface localized MMPs are also protected against most inhibitors. Paradoxically, MMP-2 in the cell lysate was decreased when IFN was added whereas in the supernatant MMP-2 was not affected. This could indicate that the role of MMP-2 is minimal in this setting.

As suggested in figure 5 (**Fig.5**) the present work supports a model in which endogenously produced IL-1ß by TNF-primed PBMC, stimulates endothelial cells to produce MMP-9, hereby causing degradation of the underlying ECM, resulting in loss of the integrity of the

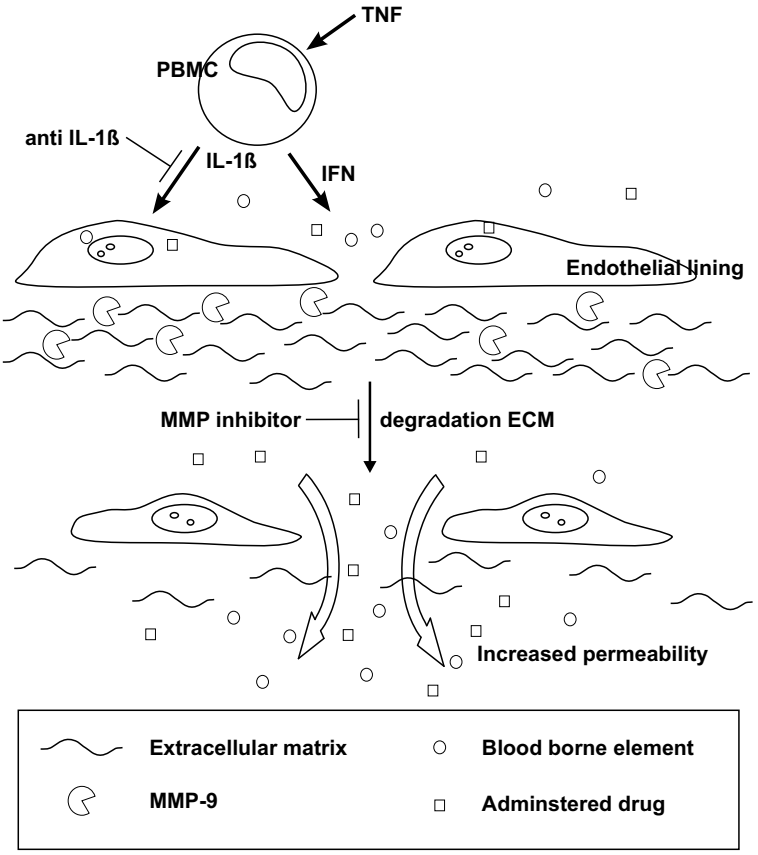

Figure 5. Proposed mechanism of IL-1ß-mediated production of MMP-9 by endothelial cells, leading to degradation of the extracellular matrix and increased endothelial permeability. TNF triggers PBMC to produce IL-1ß and IFN. These factors are responsible for the induction of the morphological changes of the endothelial lining. IL-1ß stimulates endothelial cells to produce MMP-9, presumably at the basal side, resulting in breakdown of the underlying extracellular matrix of tumor-associated vasculature, thereby increasing vascular permeability. This enhances infiltration of blood borne elements and improves drug accumulation in the surrounding tumor tissue.

endothelial lining subsequently increasing permeability of the tumor vessels.

REFERENCES

1.Eggermont AM, Schraffordt KH, Klausner JM, Kroon BB, Schlag PM, Lienard D et al. Isolated limb perfusion with tumor necrosis factor and melphalan for limb salvage in 186 patients with locally advanced soft tissue extremity sarcomas. The cumulative multicenter European experience. Ann Surg. 1996: 224(6), 756-764.

2.Eggermont AM, Schraffordt KH, Lienard D, Kroon BB, van Geel AN, Hoekstra HJ et al. Isolated limb perfusion with high-dose tumor necrosis factor-alpha in combination with interferon-gamma and melphalan for nonresectable extremity soft tissue sarcomas: a multicenter trial. J Clin Oncol. 1996: 14(10), 2653-2665.

3.Lejeune FJ, Ruegg C, and Lienard D. Clinical applications of TNF-alpha in cancer. Curr Opin Immunol. 1998: 10(5), 573-580.

4.Lienard D, Ewalenko P, Delmotte JJ, Renard N, and Lejeune FJ. High-dose recombinant tumor necrosis factor alpha in combination with interferon gamma and melphalan in isolation perfusion of the limbs for melanoma and sarcoma. J Clin Oncol. 1992: 10(1), 52-60.

5.van der Veen AH, de Wilt JH, Eggermont AM, van Tiel ST, Seynhaeve AL, and ten Hagen TL. TNF-alpha augments intratumoural concentrations of doxorubicin in TNF-alpha-

based isolated limb perfusion in rat sarcoma models and enhances anti-tumour effects. Br J Cancer. 2000: 82(4), 973-980.

6.de Wilt JH, ten Hagen TL, de Boeck G, van Tiel ST, de Bruijn EA, and Eggermont AM. Tumour necrosis factor alpha increases melphalan concentration in tumour tissue after isolated limb perfusion. Br J Cancer. 2000: 82(5), 1000-1003.

7.ten Hagen TL, van der Veen AH, Nooijen PT, van Tiel ST, Seynhaeve AL, and Eggermont AM. Low-dose tumor necrosis factor-alpha augments antitumor activity of stealth liposomal doxorubicin (DOXIL) in soft tissue sarcoma-bearing rats. Int J Cancer. 2000: 87(6), 829-837.

8.Manusama ER, Nooijen PT, Stavast J, de Wilt JH, Marquet RL, and Eggermont AM. Assessment of the role of neutrophils on the antitumor effect of TNFalpha in an in vivo isolated limb perfusion model in sarcoma-bearing brown Norway rats. J Surg Res. 1998: 78(2), 169-175.

9.Nooijen PT, Manusama ER, Eggermont AM, Schalkwijk L, Stavast J, Marquet RL et al. Synergistic effects of TNF-alpha and melphalan in an isolated limb perfusion model of rat sarcoma: a histopathological, immunohistochemical and electron microscopical study. Br J Cancer. 1996: 74(12), 1908-1915.

10.Seynhaeve AL, Vermeulen CE, Eggermont AM, and ten Hagen TL. Cytokines and vascular permeability: an in vitro study on human endothelial cells in relation to tumor necrosis factor-alpha-primed peripheral blood mononuclear cells. Cell Biochem Biophys. 2006: 44(1), 157-169.

11.Kobayashi T, Hattori S, and Shinkai H. Matrix metalloproteinases-2 and -9 are secreted from human fibroblasts. Acta Derm Venereol. 2003: 83(2), 105-107.

12.Hanemaaijer R, Koolwijk P, le Clercq L, de Vree WJ, and van Hinsbergh VW. Regulation of matrix metalloproteinase expression in human vein and microvascular endothelial cells. Effects of tumour necrosis factor alpha, interleukin 1 and phorbol ester. Biochem J. 1993: 296 (Pt 3), 803-809.

13.Egeblad M and Werb Z. New functions for the matrix metalloproteinases in cancer progression. Nat Rev Cancer. 2002: 2(3), 161-174.

14.Bjorklund M and Koivunen E. Gelatinase-mediated migration and invasion of cancer cells. Biochim Biophys Acta. 2005: 1755(1), 37-69.

15.Jaffe EA, Nachman RL, Becker CG, and Minick CR. Culture of human endothelial cells derived from umbilical veins. Identification by morphologic and immunologic criteria. J Clin Invest. 1973: 52(11), 2745-2756.

16.Skehan P, Storeng R, Scudiero D, Monks A, McMahon J, Vistica D et al. New colorimetric cytotoxicity assay for anticancer-drug screening. J Natl Cancer Inst. 1990: 82(13), 1107-1112.

17.ten Hagen TL and Eggermont AM. Manipulation of the tumour-associated vasculature to improve tumour therapy. J Liposome Res. 2002: 12(1-2), 149-154.

18.ten Hagen TL and Eggermont AM. Solid tumor therapy: manipulation of the vasculature with TNF. Technol Cancer Res Treat. 2003: 2(3), 195-203.

19.Foda HD and Zucker S. Matrix metalloproteinases in cancer invasion, metastasis and angiogenesis. Drug Discov Today. 2001: 6(9), 478-482.

20.Bergers G, Brekken R, McMahon G, Vu TH, Itoh T, Tamaki K et al. Matrix metalloproteinase-9 triggers the angiogenic switch during carcinogenesis. Nat Cell Biol. 2000: 2(10), 737-744.

21.Meyer E, Vollmer JY, Bovey R, and Stamenkovic I. Matrix metalloproteinases 9 and 10 inhibit protein kinase C-potentiated, p53-mediated apoptosis. Cancer Res. 2005: 65(10), 4261-4272.

22.Schmalfeldt B, Prechtel D, Harting K, Spathe K, Rutke S, Konik E et al. Increased expression of matrix metalloproteinases (MMP)-2, MMP-9, and the urokinase-type plasminogen activator is associated with progression from benign to advanced ovarian cancer. Clin Cancer Res. 2001: 7(8), 2396-2404.

23.Zeng ZS, Huang Y, Cohen AM, and Guillem JG. Prediction of colorectal cancer relapse and survival via tissue RNA levels of matrix metalloproteinase-9. J Clin Oncol. 1996: 14(12), 3133-3140.

24.Heath EI, O'Reilly S, Humphrey R, Sundaresan P, Donehower RC, Sartorius S et al. Phase I trial of the matrix metalloproteinase inhibitor BAY12-9566 in patients with advanced solid tumors. Cancer Chemother Pharmacol. 2001: 48(4), 269-274.

25.Hidalgo M and Eckhardt SG. Development of matrix metalloproteinase inhibitors in cancer therapy. J Natl Cancer Inst. 2001: 93(3), 178-193.

26.Sparano JA, Bernardo P, Stephenson P, Gradishar WJ, Ingle JN, Zucker S et al. Randomized phase III trial of marimastat versus placebo in patients with metastatic breast cancer who have responding or stable disease after first-line chemotherapy: Eastern Cooperative Oncology Group trial E2196. J Clin Oncol. 2004: 22(23), 4683-4690.

27.Bartlett DL, Ma G, Alexander HR, Libutti SK, and Fraker DL. Isolated limb reperfusion with tumor necrosis factor and melphalan in patients with extremity melanoma after failure of isolated limb perfusion with chemotherapeutics. Cancer. 1997: 80(11), 2084-2090.

28.Eggermont AM, Schraffordt KH, Klausner JM, Schlag PM, Kroon B, Gustafson B et al. Limb salvage by isolated limb perfusion with tumor necrosis factor alpha and melphalan for locally advanced extremity soft tissue sarcomas: results of 270 perfusions in 246 patients. Porceed ASCO. 1999: 11, 497.
29.Grunhagen DJ, Brunstein F, Graveland WJ, van Geel AN, de Wilt JH, and Eggermont AM. Isolated limb perfusion with tumor necrosis factor and melphalan prevents amputation in patients with multiple sarcomas in arm or leg. Ann Surg Oncol. 2005: 12(6), 473-479.
30.Lans TE, Grunhagen DJ, de Wilt JH, van Geel AN, and Eggermont AM. Isolated Limb Perfusions With Tumor Necrosis Factor and Melphalan for Locally Recurrent Soft Tissue Sarcoma in Previously Irradiated Limbs. Ann Surg Oncol. 2005.
31.Hohenberger P and Tunn PU. Isolated limb perfusion with rhTNF-alpha and melphalan for locally recurrent childhood synovial sarcoma of the limb. J Pediatr Hematol Oncol. 2003: 25(11), 905-909.
32.Eggermont AM, de Wilt JH, and ten Hagen TL. Current uses of isolated limb perfusion in the clinic and a model system for new strategies. Lancet Oncol. 2003: 4(7), 429-437.
33.Brouckaert P, Takahashi N, van Tiel ST, Hostens J, Eggermont AM, Seynhaeve AL et al. Tumor necrosis factor-alpha augmented tumor response in B16BL6 melanoma-bearing mice treated with stealth liposomal doxorubicin (Doxil) correlates with altered Doxil pharmacokinetics. Int J Cancer. 2004: 109(3), 442-448.
34.Hoving S, Seynhaeve AL, van Tiel ST, Eggermont AM, and ten Hagen TL. Addition of low-dose tumor necrosis factor-alpha to systemic treatment with STEALTH liposomal doxorubicin (Doxil) improved anti-tumor activity in osteosarcoma-bearing rats. Anticancer Drugs. 2005: 16(6), 667-674.
35.Sanceau J, Truchet S, and Bauvois B. Matrix metalloproteinase-9 silencing by RNA interference triggers the migratory-adhesive switch in Ewing's sarcoma cells. J Biol Chem. 2003: 278(38), 36537-36546.
36.Wu WB and Huang TF. Activation of MMP-2, cleavage of matrix proteins, and adherens junctions during a snake venom metalloproteinase-induced endothelial cell apoptosis. Exp Cell Res. 2003: 288(1), 143-157.
37.Siu MK, Lee WM, and Cheng CY. The interplay of collagen IV, tumor necrosis factor-alpha, gelatinase B (matrix metalloprotease-9), and tissue inhibitor of metalloproteases-1 in the basal lamina regulates Sertoli cell-tight junction dynamics in the rat testis. Endocrinology. 2003: 144(1), 371-387.

Chapter 6

TNF-primed peripheral blood mononuclear cells damage endothelial integrity via interleukin-1beta by degradation of VE-cadherin

Ann L.B. Seynhaeve
Debby Schipper
Alexander M.M. Eggermont
Timo L.M. ten Hagen

In preparation

Research article

TNF-primed peripheral blood mononuclear cells damage endothelial integrity via interleukin-1beta by degradation of VE-cadherin

Ann L.B. Seynhaeve, Debby Schipper, Alexander M.M. Eggermont, and Timo L.M. ten Hagen

Department of Surgical Oncology, Erasmus MC/Daniel den Hoed Cancer Center, Rotterdam, the Netherlands

ARTICLE INFORMATION

In preparation

ACKNOWLEDGMENTS

The authors thank Sangeeta Koendan-Panday for her technical assistance and Dr. K. Kullak of Boehringer Ingelheim GmbH for the generous supply of TNF.

ABSTRACT

Tumor necrosis factor-alpha (TNF) in combination with interferon-gamma (IFN) changes the integrity of the endothelial cell monolayer and this is further enhanced with the addition of peripheral blood mononuclear cells (PBMC). The enhanced effect of PBMC was mostly induced by the endogenous production if interleukin-1beta (IL-1ß) after TNF stimulation. VE-cadherin is an important protein in maintenance of the endothelial integrity. In this study we investigated the effect of TNF, IFN, PBMC and IL-1ß on the expression of VE-cadherin in human umbilical vein endothelial cells (HUVEC).

INTRODUCTION

Increased permeability of the tumor-associated vasculature is a feature observed when the proinflammatory cytokine TNF is used in the treatment of soft tissue sarcoma and melanoma. As a result of this enhance permeability more chemotherapeutic drug, like melphalan or doxorubicin, extravasate from the blood circulation into the tumor tissue resulting in an improved antitumor effects [1-3]. Normally, the use of TNF is limited because of the severe side effect when administered at the dose needed for a tumor effect. Our laboratory is specialised in two techniques in which TNF can be safely administered. First, high doses can be reached using an isolated limb perfusion (ILP) in which the blood circulation of the tumor-bearing extremity is isolated form the rest of the body. Second, systemic low dose TNF in the margin of the maximal tolerated dose can repeatedly be administrated. TNF or the chemotherapeutic agent as a single therapy gave poor results, the dual approach in which TNF changes the vascular permeability and the chemotherapeutic agent that kills the tumor cells results in an improved tumor response [4,7].

TNF activates the endothelium resulting in altered cell morphology, changes in adhesion expression and loss in barrier function [8,9]. The response of endothelial cells to TNF and another important cytokine; interferon-gamma (IFN) has been extensively studied. *In vitro*, these cytokines inhibit proliferation of endothelial cells, inhibits αVβ3-mediated adhesion to the extracellular matrix and induce morphological and permeability changes. These changes induced by TNF and IFN were further enhanced by the addition of peripheral blood mononuclear cells.

Adherens junctions act as important regulators in the integrity of endothelial cells by connecting neighbouring cells and are formed by transmembrane proteins belonging to the cadherin superfamily [10]. Endothelial cells express a cell-specific cadherin, vascular endothelial (VE) cadherin, also known as CD144 or cadherin-5.

It mediates a homophilic, calcium dependent adhesion with the VE-cadherin of an adjacent endothelial cell and the cytoplasmic domain interact with ß-catenin and plakoglobin that associates in turn with α-catenin linking the entire complex to the actin cytoskeleton [11].

In this study we investigate the effects of TNF, IFN and PBMC on the effect of VE-cadherin in endothelial cells to further illustrated the changes in vascular permeability.

EXPERIMENTAL PROCEDURES

Agents. Recombinant human Tumor necrosis factor-alpha (TNF) and recombinant human IFN gamma (IFN) were kindly provided by Boehringer-Ingelheim GmbH. TNF had a specific activity of 5 x 10^7 U/mg and endotoxin levels were < 1.25 U/mg protein. IFN had a specific activity of 2.5 x 10^7 U/mg and endotoxin levels were < 1 U/mg protein. Recombinant human interleukin-1beta (IL-1ß) was purchased from Peprotech EC Ltd with an activity of 1 x 10^7 U/mg and endotoxin levels were < 1U/µg protein.

Cells and cultured conditions. Human umbilical vein endothelial cells (HUVEC) were isolated by collagenase digestion using the method described by Jaffe *et al* [12]. Each isolate was derived from an individual umbilical vein and used for experiments at passage 5. HUVEC were cultured in HUVEC medium containing human endothelial-serum free medium (Invitrogen), 20% heat inactivated newborn calf serum (Lonza), 10% heat inactivated human serum (Lonza) 20 ng/ml human recombinant Basic Fibroblast Growth Factor (Peprotech EC Ltd), 100 ng/ml human recombinant Epidermal Growth Factor (Peprotech EC Ltd) in fibronectin (Roche Diagnostics) coated flasks. HUVEC had the characteristic cobblestone morphology and tested positive for CD-31.

Human peripheral blood mononuclear cells (PBMC) were isolated from healthy donors using the Vacutainer CPT Mononuclear Cell Preparation Tubes with sodium heparin (Becton Dickinson). PBMC were washed with phosphate buffered saline and counted with trypan blue to determine the viable cell concentration. PBMC, at a final concentration of 120x10^4 PBMC/ml, were used in all experiments.

Assessment of toxicity, apoptosis and permeability towards endothelial cells. HUVEC were plated in fibronectin-coated wells at a concentration of 6 x 10^4 cells per ml and allowed to grow for 24 hours. Combinations of TNF, IFN, IL-1ß and PBMC were added to the well and incubated for 72 and 144 hours. As a control, cells were incubated with HUVEC medium alone. Growth of endothelial cells was measured using the sulphorhodamine B (SRB, Sigma) protein stain assay, according to the method of Skehan [13]. Briefly, cells were washed with PBS, incubated with 10% trichloric acetic acid (1 hour, 4°C) and washed in distilled water. Cells were then stained for 15 min with SRB, washed with 1% acetic acid and allowed to dry. Protein bound SRB was dissolved in 10 mM Tris buffer and optial density (O.D.) was measured at 540 nm. Cell growth was calculated using the formula: percentage cell growth = (O.D. test well/O.D. control well) x 100 percent. For the apoptosis assay, detached cells in the supernatant were collected and living cells were harvested by mild trypsinization and washed with PBS. Early apoptosis was detected using the annexin V kit and necrosis by propidium iodide (PI), according to the manufacturer's instructions (Vybrant Apoptosis Assay kit #3, Molecular Probes). Cells were immediately analyzed by flowcytometry (FACScan, Becton Dickinson). Data analysis was performed using WinMDI 2.7 (Freeware, Joseph Trotter, Scripps Research Institute). To measure permeability, HUVEC were plated in the upper chamber of a transwell (0.4 µm pore size, 6.5 mm diameter, polyester filters; Corning BV), coated with fibronectin, at a density of 2.5x10^4 cells per transwell. When the cell established a rigid monolayer the medium in the upper chamber was replaced with medium containing combinations of TNF, IFN, IL-1ß and PBMC for 72 and 144 hours. To measure permeability, FITC-BSA in a concentration of 50 µg/well was added in the upper chamber. After the indicated incubation time, the upper chamber was removed and the FITC fluorescence at the lower

chamber was read using a fluorescence plate reader (Wallac Victor^2, Perkin Elmer).

Morphological changes. HUVEC were incubated with combinations of TNF, IFN, IL-1ß and PBMC. After 72 and 144 hours, morphological cell changes were examined with a 10x N.A. 0.30 Plan-Neofluar objective lens using an inverted Zeiss Axiovert 100M microscope equipped with an Axiocam digital camera (Carl Zeiss). Cell elongation was measured and expressed as the ratio of the length of the major cell axis to the width perpendicular to the length. Ten cells and at least four independent incubations were determined. In addition, gaps formation was determined for each treatment. The cell-free area was outlined and the gap formation was calculated using the formula: percentage cell-free area = (cell free area/total area) x 100 percent. Al measurements were done using the AxioVision 3.0 software.

Immunofluorescence. HUVEC were cultured in a final concentration of 6 x 10^4 cells per ml on a fibronectin coated cover glass and allowed to grow for 24 hours. The cells were incubated with HUVEC medium, 10 µg/ml TNF in combination with 0.001 µg/ml IFN or 10 µg/ml TNF in combination with 0.001 µg/ml IFN and PBMC. After 72 hours incubation, cells were rinsed in PBS and fixed with 3.6 % paraformaldehyde for 10 min at room temperature. Cells were permeabilized with 0.1% Triton X-100 for 10 min, and a-specific binding sites were blocked with 1% BSA in PBS for 10 min. Cells were stained with mouse anti human VE-cadherin (1:100; Chemicon) for 20 min followed by incubation with an Alexa Fluor conjugated goat anti mouse 488 secondary antibody (Molecular Probes) for another 20 min. After washing the cells were mounted with vectashield (Vector laboratories) mixed with DAPI (Molecular Probes) in order to stain cell nuclei. Cells were examined using a Leica DMRX-A microscope and images taken with a Sony DXC 950 camera.

Analysis of VE-cadherin expression by western blotting. HUVEC were incubated with combinations of TNF, IFN, IL-1ß and PBMC for 72 hours, washed with PBS to removed PBMC, scraped off in PBS using a cell scraper and collected. After pelleting down the cells, the pellet was dissolved in ice cold lysis buffer (20 mM Tris-HCl (pH 7.2), 100 mM NaCl, 1 mM EGTA, 1 mM EDTA, 1 mM PMSF, 2 µg/ml pepstatin, 2 µg/ml leupeptin, 2 µg/ml aprotonin), incubated for 1 hour on ice and centrifuged at 200 rcf. Centrifuging the supernatant at 25,000 rcf for 30 min separated the cytosolic and membrane-bound proteins. The supernatant with the cytosolic proteins was collected en stored at -20°C until further analysis. To remove any contaminating cytosolic proteins the pellet was washed with ice-cold lysis buffer and centrifuged at 25.000 rcf for 30 min. The pellet was resuspended in ice-cold extraction buffer (20 mM Tris-HCl (pH 7.4), 150 mM NaCl, 5 mM EDTA, 0.5% Igepal CA-630, 0.1% SDS, 1 mM PMSF, 2 µg/ml pepstatin, 2 µg/ml leupeptin, 2 µg/ml aprotonin), incubated for 1 hour on ice and centrifuged at 25.000 rcf for 30 min. The supernatant with the membrane-bound proteins was collected and stored at -20°C until further analysis. Protein concentration in the cytosolic and membrane fractions was determined with Compassion Plus reagent (Pierce) and 7 µg of protein was separated by electrophoreses in a 10% SDS-PAGE gel under reducing conditions and transferred to a polyvinylidene difluoride membrane (Bio-Rad). Membranes were blocked with MPBS (5% milk powder in PBS/0.05% tween-20) and incubated with mouse anti human VE-cadherin diluted in MPBS (1:200; Chemicon) overnight at 4°C. After washing, the membrane was incubated with goat anti mouse biotin diluted in MPBS (1:1500; Southern Biotechnology) for 1 hour at room temperature. Bound biotin was incubated with alkaline-phosphatase-streptavidin complex (Bio-Rad), and this in turn stained with BCIP/NBT liquid substrate (Bio-Rad). The staining was stopped with 2 mM EDTA.

Semi-quantitative RT-PCR. Total RNA was extracted from HUVEC incubated with combinations of TNF, IFN, IL-1ß and PBMC for 72 hours using TRIzol reagent as suggested by the manufacturer (Invitrogen). cDNA synthesis

was carried out by incubating 1.0 µg RNA with Omniscript Reverse Transcriptase (Qiagen) and oligo $d(T)_{16}$ (Invitrogen) for 1 hour at 42°C following heating for 5 min at 93°C to terminate the reaction. PCR reaction was performed with a Biometra T-gradient PCR machine on a reaction mix of 1.5 µl cDNA, 200 nM dNTP, 1,5 mM MgCl2, 50 pM of the sense and antisense primers and 0.5 U Titanium Taq DNA polymerase (Becton Dickinson) in PCR buffer to 50 µl final volume. The VE-cadherin primer (sense 5'-ACGACAACTGGCCTGTGTTCAC-3' and antisense 5'-TGCATCCACTGCTGTCACAGAG-3') was purchased from Invitrogen. ß2-microglobulin (sense 5'-CTCACGTCATCCAGCAGAGA-3' and antisense 5'-CGGCAGGCATACTCATCTTT-3') was used as an internal standard. For PCR we used the following parameters: initial denaturation at 94˚C for 5 min followed by a maximum of 40 cycles of 94˚C for 45 sec, annealing at 61.5 °C for 45 sec and extension 72˚C for 1 min. To obtain results from the exponential phase of the reaction every 2 cycles, 5 µl of PCR product was collected and the samples were separated on a 1.5% agarose gel, stained with ethidium bromide and photographed under ultraviolet light box. A 100-bp ladder was used as the standard. The threshold cycle was determined as the cycle where the visible band of a specific PCR product first appeared on the gel. The results were expressed as the cycle of first appearance of the band normalized with the cycle of first appearance of ß2-micorglobulin.

Statistical analysis. The Mann-Whitney U-test was used in all statistical analysis. P values below 0.05 were considered statistically significant.

RESULTS

TNF and IFN increase endothelial permeability that is further increased with the addition of PBMC. HUVEC were exposed to TNF, IFN, PBMC and IL-1ß during 72 and 144 hours and changes in growth and permeability were determined. The cytokines TNF and IFN as a single treatment gave no effect on the endothelial monolayer and reduction in cell growth was not observed (data not shown). Even the combination TNF and IFN gave no reduction in cell growth (85 ± 12%) demonstrating a lack of direct activity of these cytokines on endothelial cells. When HUVEC were incubated for 72 hours with TNF in combination with IFN and PBMC no significant difference in cell growth (90 ± 13%) could be observed. However, the additive effects of PBMC became apparent after 144 h of incubation resulting in a significant reduction in cell growth (47 ± 8%). This effect could also be observed when PBMC was replaced by IL-1ß. Incubation for 72 hours with TNF in combination with IFN and IL-1ß had no effect on cell growth (77 ± 15%) and significant induction of cell growth was observed 144 hours later (42 ± 3%) (**Fig. 1a**). There was a significant increase in endothelial permeability after exposure for 72 hours with TNF and IFN (152 ± 4%), TNF in combination with IFN and PBMC (163 ± 8%) or with IL-1ß (130 ± 4%). Further incubation of the endothelial cells increased permeability to a 7-fold increase after TNF in combination with IFN and PBMC and 6-fold increase in combination with IL-1ß (**Fig. 1b**). That endogenous produced IL-1ß after priming the PBMC is responsible for the effects has been shown in previous experiments. Neutralising the endogenous produced IL-1ß with an antibody brought the cell growth (84 ± 5 %) and permeability changes back to the level of TNF and IFN (data not shown). No significant changes in apoptosis was found after incubation with TNF and IFN compared to control and even addition of PBMC or IL-1ß had no influence on cell apoptosis indicating that morphological changes is the major effect for the increased permeability of the endothelial layer (data not shown).

TNF and IFN induce morphological changes in the endothelial monolayer. HUVEC under normal conditions form a cobblestone-like monolayer. Incubation with TNF alone resulted in a slight increase in cell elongation whereas IFN alone had no effect on the HUVEC (data not shown). The morphological phenotype of the HUVEC changed with the addition of TNF and IFN from this cobblestone monolayer to more

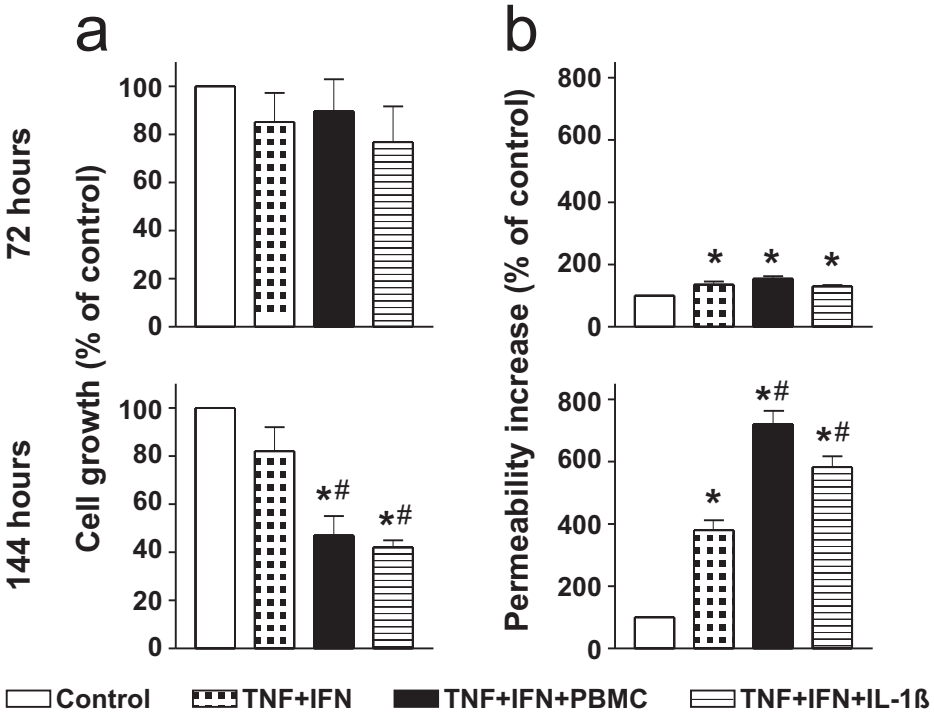

Figure 1. TNF and IFN increase growth reduction and endothelial permeability. (**a**) Cell growth of HUVEC incubated with 10 µg/ml TNF and 0.001 µg/ml IFN in combination with PBMC or IL-1ß after 72 or 144 hours. Seventy-two hours after incubation, no effect was observed. At 144 hours addition of PBMC or IL-1ß resulted in significant growth reduction. Columns represent percentage cell growth compared to control treated cells ± SEM of 5 individual experiments in duplicate; *, $P < 0.05$ *versus* control treated cells; #, $P < 0.05$ *versus* cells treated with TNF in combination with IFN. (**b**) Permeability changes of the endothelial layer were measured as described in the experimental procedures. Addition of TNF in combination with TNF increased permeability changes after 72 hours of incubation compared to control treated cells. At that time point PBMC or IL-1ß had no effect. The effect of PBMC or IL-1ß was observed 144 hours after incubation. Columns represent percentage permeability increase compared to control treated cells ± SEM of at least 3 individual experiments in duplicate; *, $P < 0.05$ *versus* control treated cells; #, $P < 0.05$ *versus* cells treated with TNF in combination with IFN.

stretched cells that was even further enhanced with the addition of PBMC or IL-1ß. Also gaps between the cells became visible with the addition of PBMC after 144 hours of incubation. These gaps were also observed when replacing PBMC with IL-1ß (**Fig. 2a**). Incubation after 72 hours with TNF in combination with IFN resulted in significant cell elongation compared to control treated HUVEC (7.5 ± 0.9 versus 1.4 ± 0.1). At this time point we observed no gap formation and the surface was for 96 ± 5% covered with endothelial cells. This cell elongation is apparently sufficient to induce moderate increase in permeability. Longer incubation had no effect on cell elongation, but increased contact loss between the cells, increasing gap formation slightly. At 72 hours, the addition of PBMC or IL-1ß had no effect on cell elongation and gap formation compared to TNF and IFN. However, after 144 hours cell elongation was drastically increased and the cells obtained a fibroblast like morphology with a length to width ratio of 16.4 ± 2.2 after addition of PBMC or 14.5 ± 2.3 after IL-1ß (**Fig. 2b**). Also the gap formation was significant increased resulting in a cell area of 61 ± 10% of the total area after incubation with TNF in combination with IFN and PBMC. Replacing PBMC with IL-

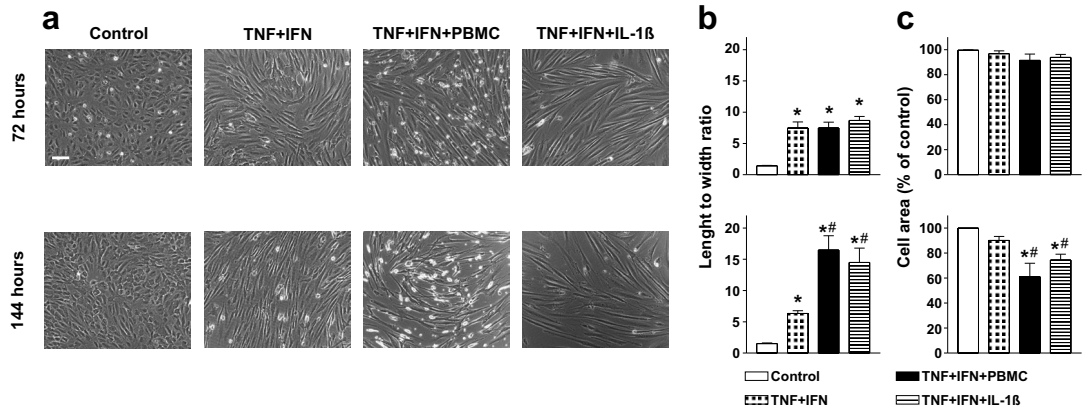

Figure 2. TNF and IFN induce morphological changes. (**a**) Photographs taken from HUVEC incubated with TNF, IFN and PBMC or IL-1ß for 72 or 144 hours. Scale bar apply to all images, 100 µm. (**b**) Length to width ratio and (**c**) cell area were measured after incubation for 72 or 144 hours. TNF and IFN increased cell elongation after 72 hours and addition of PBMC or IL-1ß had no effect. The additive effects were observed after 144 hours. Columns represent percentage cell-free area ± SD of at least 5 individual experiments and length to width ratio ± SEM of 10 cells per treatment of at least 4 individual experiments; *, $P < 0.05$ *versus* control treated cells; #, $P < 0.05$ *versus* cells treated with TNF in combination with IFN.

1ß reduced the cell area also significantly to 75 ± 4% (**Fig. 2c**).

TNF-primed PBMC and IL-1ß disrupts VE-cadherin at the membrane. Increased permeability and leakage of the vasculature is often the result of a disruption in the junction proteins between neighbouring cells. VE-cadherin is the major transmembrane protein in maintaining the integrity of the endothelial cell monolayer. Therefore we investigated the pattern of VE-cadherin in untreated HUVEC and HUVEC incubated with TNF, IFN in combination with PBMC or IL-1ß. Because the additional effects of PBMC or IL-1ß became apparent after 72 hours we chose this time point for the analysis. Immunofluoresent staining of VE-cadherin in untreated cells shows a uniform VE-cadherin staining pattern localised at the membrane of the cells. When cells were exposed to TNF and IFN, the staining pattern changed with some loss of cell-cell contacts and slight reduction of VE-cadherin staining at the membrane. With the addition of PBMC or IL-1ß staining of VE-cadherin was reduced drastically especially at sites with gap formation in with endothelial cells had lost contact with the neighbouring cell (**Fig. 3a**). Western blot analysis shows no significant change in overall expression of VE-cadherin in endothelial cells after exposure to TNF or IFN alone (data not shown) and also after incubation with TNF in combination with IFN, no significant reduction could be found. However, with the addition of PBMC or IL-1ß VE-cadherin levels were markedly reduced in the membrane fraction of the cells (**Fig. 3b**). PCR analysis of HUVEC after incubation indicates that the exposure to TNF and IFN does not reduce mRNA levels of VE-cadherin. Even with the addition of PBMC or IL-1ß no reduction is observed (**Fig. 4**). These data indicates that the production of VE-cadherin is not altered by PBMC or IL-1ß, but that the protein is degraded at the membrane resulting in gap formation and increased permeability. Because we observed a reduction in staining pattern in de VE-cadherin after TNF and IFN incubation and no reduction in protein level we believe that VE-cadherin proteins relocalize within the membrane thereby stimulating permeability changes. Addition of PBMC or IL-1ß then degrades these proteins.

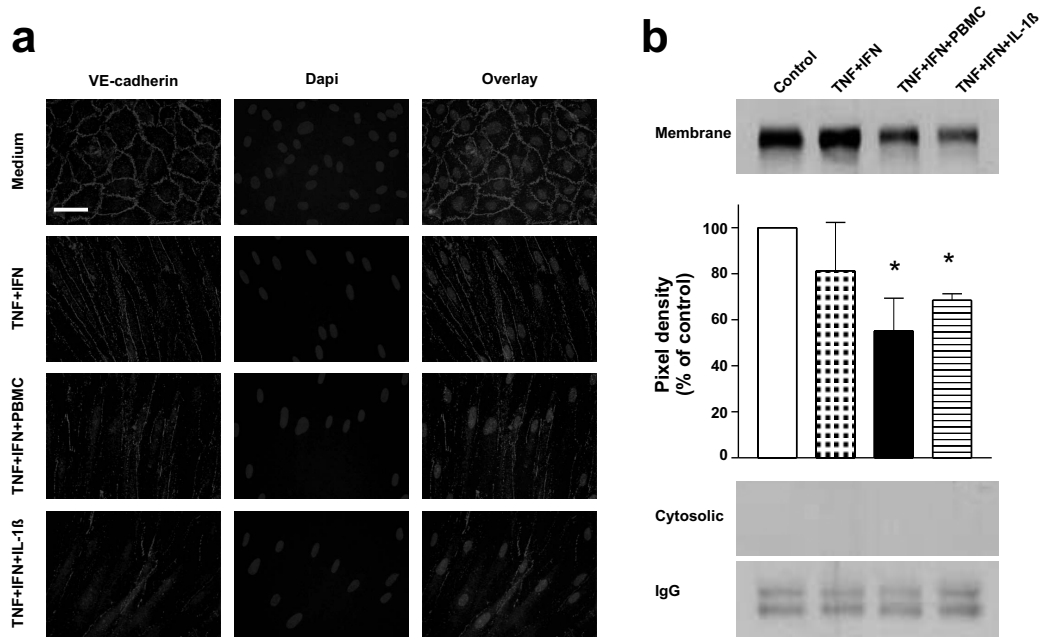

Figure 3. VE-cadherin is degraded at the cell membrane. (**a**) Staining for VE-cadherin and DAPI of HUVEC after incubation for 72 hours as described in the experimental procedures. Control treated cells show that VE-cadherin localized at cell-cell junctions between two cells. Incubating the cells with TNF and IFN resulted in a more speckled pattern of VE-cadherin. Addition of PBMC and IL-1ß further reduced VE-cadherin expression at the cell junctions. Scale bar apply for all images, 50 µm. (**b**) Western blotting show a significant decrease in the expression of VE-cadherin in the membrane fraction of HUVEC after incubation of TNF in combination with IFN and PBMC. Replacing PBMC with IL-1ß also significantly decreased the amount of VE-cadherin. Columns represent percentage pixel density compared to control ± SD of at least 4 individual experiments; *, $P < 0.05$ *versus* control treated cells. (See color section for a full-color version.)

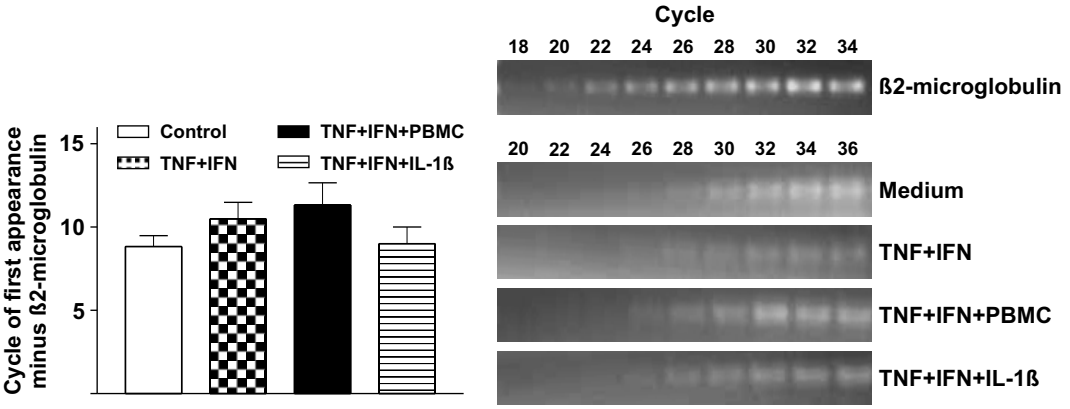

Figure 4. No change in the mRNA expression of VE-cadherin was observed. VE-cadherin mRNA expression in HUVEC incubated for 72 hours was investigated using semi-quantitative PCR. The mRNA expression did not change after incubation. The decrease protein expression at the membrane is not caused by an decrease in mRNA production. Columns represent the cycle of first appearance of the VE-cadherin band minus the first appearance of the ß2-microglobulin housekeeping gene ± SEM of 2 treatments of 3 individual experiments.

DISCUSSION

Previously we demonstrated that TNF in combination with IFN and PBMC induced permeability changes in endothelial cells and the effect of PBMC was mediated by endogenous produced IL-1ß after TNF-stimulation [9]. TNF alone has hardly any effect on endothelial cells and that has also been found by other researchers [14,15]. Other stimulators like IFN, PBMC, melanoma conditioned medium or hyperthermia, that mimic the tumor environment of conditions during ILP are required for TNF effects. Here we show that the additional effect of PBMC or IL-1ß starts after 3 days of incubation. When endothelial cells were exposed to TNF in combination with IFN a significant increase in flux of the macromolecule FITC-BSA was found, indicating a change in endothelial integrity.

VE-cadherin, the primary component of the adherens junctions, is a member of the cadherin membrane receptor family involved in the calcium-dependent homophilic cell-cell interactions of its extracellular domain and is strictly located at the intercellular junctions of endothelial cells. The extracellular binding between two VE-cadherin molecules mainly affects the initial cell-cell contacts during vessel development. The intracellular domain connects to the actin cytoskeleton through cytoplasmic interactions with catenin proteins, like α-catenin, β-catenin, γ-catenin (also referred to as plakoglobin) and p120. An increase in vascular permeability is in most occasions associated with a disruption if VE-cadherin [10, 16]. Furthermore, dynamic changes in membrane-associated VE-cadherin are also involved in the transmigration of leucocytes. It seems that VE-cadherin relocate and cluster together at the site of diapedesis [17-19]. Treatment of cells with TNF in combination with IFN results in degradation of VE-cadherin at the membrane that was further enhanced with the addition of PBMC. Replacing PBMC with IL-1ß also showed reduction of the protein.

However, these findings have little relevance to the ILP since TNF-induced effects *in vitro* requires longer exposure then is clinical used. In contrast, priming of polymorfnuclear cells instead of PBMC with TNF induced permeability changes within 30 min of incubation without no obvious gap-formation, cell elongation and cell number. However, degradation of VE-cadherin is observed within 30 min.

REFERENCES

1.de Wilt JH, ten Hagen TL, de Boeck G, van Tiel ST, de Bruijn EA, and Eggermont AM. Tumour necrosis factor alpha increases melphalan concentration in tumour tissue after isolated limb perfusion. Br J Cancer. 2000: 82(5), 1000-1003.

2.Seynhaeve AL, Hoving S, Schipper D, Vermeulen CE, aan de Wiel-Ambagtsheer G, van Tiel ST et al. Tumor Necrosis Factor {alpha} Mediates Homogeneous Distribution of Liposomes in Murine Melanoma that Contributes to a Better Tumor Response. Cancer Res. 2007: 67(19), 9455-9462.

3.van der Veen AH, de Wilt JH, Eggermont AM, van Tiel ST, Seynhaeve AL, and ten Hagen TL. TNF-alpha augments intratumoural concentrations of doxorubicin in TNF-alpha-based isolated limb perfusion in rat sarcoma models and enhances anti-tumour effects. Br J Cancer. 2000: 82(4), 973-980.

4.de Wilt JH, Manusama ER, van Tiel ST, van Ijken MG, ten Hagen TL, and Eggermont AM. Prerequisites for effective isolated limb perfusion using tumour necrosis factor alpha and melphalan in rats. Br J Cancer. 1999: 80(1-2), 161-166.

5.Hoving S, Seynhaeve AL, van Tiel ST, Eggermont AM, and ten Hagen TL. Addition of low-dose tumor necrosis factor-alpha to systemic treatment with STEALTH liposomal doxorubicin (Doxil) improved anti-tumor activity in osteosarcoma-bearing rats. Anticancer Drugs. 2005: 16(6), 667-674.

6.Manusama ER, Nooijen PT, Stavast J, Durante NM, Marquet RL, and Eggermont AM. Synergistic antitumour effect of recombinant human tumour necrosis factor alpha with melphalan in isolated limb perfusion in the rat. Br J Surg. 1996: 83(4), 551-555.

7.Hoving S, Seynhaeve AL, van Tiel ST, aan de Wiel-Ambagtsheer G, de Bruijn EA, Eggermont AM et al. Early destruction of tumor vasculature in tumor necrosis factor-alpha-based isolated limb perfusion is responsible for tumor response. Anticancer Drugs. 2006: 17(8), 949-959.

8.Ruegg C, Yilmaz A, Bieler G, Bamat J, Chaubert P, and Lejeune FJ. Evidence for the involvement of endothelial cell integrin alphaVbeta3 in the disruption of the tumor vasculature induced by TNF and IFN-gamma. Nat Med. 1998: 4(4), 408-414.

9.Seynhaeve AL, Vermeulen CE, Eggermont AM, and ten Hagen TL. Cytokines and vascular permeability: an in vitro study on human endothelial cells in relation to tumor necrosis factor-alpha-primed peripheral blood mononuclear cells. Cell Biochem Biophys. 2006: 44(1), 157-169.
10.Venkiteswaran K, Xiao K, Summers S, Calkins CC, Vincent PA, Pumiglia K et al. Regulation of endothelial barrier function and growth by VE-cadherin, plakoglobin, and beta-catenin. Am J Physiol Cell Physiol. 2002: 283(3), C811-C821.
11.Dejana E, Bazzoni G, and Lampugnani MG. Vascular endothelial (VE)-cadherin: only an intercellular glue? Exp Cell Res. 1999: 252(1), 13-19.
12.Jaffe EA, Nachman RL, Becker CG, and Minick CR. Culture of human endothelial cells derived from umbilical veins. Identification by morphologic and immunologic criteria. J Clin Invest. 1973: 52(11), 2745-2756.
13.Skehan P, Storeng R, Scudiero D, Monks A, McMahon J, Vistica D et al. New colorimetric cytotoxicity assay for anticancer-drug screening. J Natl Cancer Inst. 1990: 82(13), 1107-1112.
14.Friedl J, Turner E, and Alexander HR, Jr. Augmentation of endothelial cell monolayer permeability by hyperthermia but not tumor necrosis factor: evidence for disruption of vascular integrity via VE-cadherin down-regulation. Int J Oncol. 2003: 23(3), 611-616.
15.Menon C, Ghartey A, Canter R, Feldman M, and Fraker DL. Tumor necrosis factor-alpha damages tumor blood vessel integrity by targeting VE-cadherin. Ann Surg. 2006: 244(5), 781-791.
16.Andriopoulou P, Navarro P, Zanetti A, Lampugnani MG, and Dejana E. Histamine induces tyrosine phosphorylation of endothelial cell-to-cell adherens junctions. Arterioscler Thromb Vasc Biol. 1999: 19(10), 2286-2297.
17.Allport JR, Ding H, Collins T, Gerritsen ME, and Luscinskas FW. Endothelial-dependent mechanisms regulate leukocyte transmigration: a process involving the proteasome and disruption of the vascular endothelial-cadherin complex at endothelial cell-to-cell junctions. J Exp Med. 1997: 186(4), 517-527.
18.Allport JR, Muller WA, and Luscinskas FW. Monocytes induce reversible focal changes in vascular endothelial cadherin complex during transendothelial migration under flow. J Cell Biol. 2000: 148(1), 203-216.
19.Sandig M, Negrou E, and Rogers KA. Changes in the distribution of LFA-1, catenins, and F-actin during transendothelial migration of monocytes in culture. J Cell Sci. 1997: 110 (Pt 22), 2807-2818.

Part 3 - Vascular abnormalization

In vivo study

Chapter 7 **Destruction of tumor vasculature is responsible for response**
Saske Hoving, Ann L.B. Seynhaeve, Sandra T. van Tiel, Gisela aan de Wiel-Ambagtsheer, Ernst A. de Bruijn, Alexander M.M. Eggermont, and Timo L.M. ten Hagen
Anticancer Drugs. 2006: 17(8), 949-959

Chapter 8 **Homogenous distribution of liposomes is mediated by TNF**
Ann L.B. Seynhaeve, Saske Hoving, Debby Schipper, Cindy E. Vermeulen, Gisela aan de Wiel-Ambagtsheer, Sandra T. van Tiel, Alexander M.M. Eggermont, and Timo L.M. ten Hagen
Cancer Research. 2007: 67(19), 9455-9462

Chapter 9 **TNFR1 on pericytes correlates with TNF response**
Ann L.B. Seynhaeve, Saske Hoving, Debby Schipper, Alexander M.M. Eggermont, and Timo L.M. ten Hagen
Submitted for publication

About the authors (in alphabetical order)
Gisela aan de Wiel-Ambagtsheer; Department of Surgical Oncology, Erasmus MC-Daniel den Hoed Cancer Center, Rotterdam, The Netherlands - **Ernst A. de Bruijn**; Department of Experimental Oncology, University of Leuven, Leuven, Belgium - **Alexander M.M. Eggermont**; Department of Surgical Oncology, Erasmus MC-Daniel den Hoed Cancer Center, Rotterdam, The Netherlands - **Timo L.M. ten Hagen**; Department of Surgical Oncology, Erasmus MC-Daniel den Hoed Cancer Center, Rotterdam, The Netherlands - **Saske Hoving**; Department of Surgical Oncology, Erasmus MC-Daniel den Hoed Cancer Center, Rotterdam, The Netherlands - **Debby Schipper**; Department of Surgical Oncology, Erasmus MC-Daniel den Hoed Cancer Center, Rotterdam, The Netherlands – **Ann L.B. Seynhaeve**; Department of Surgical Oncology, Erasmus MC-Daniel den Hoed Cancer Center, Rotterdam, The Netherlands - **Sandra T. van Tiel**; Department of Surgical Oncology, Erasmus MC-Daniel den Hoed Cancer Center, Rotterdam, The Netherlands– **Cindy E. Vermeulen**; Department of Surgical Oncology, Erasmus MC-Daniel den Hoed Cancer Center, Rotterdam, The Netherlands

Chapter 7

Early destruction of tumor vasculature in TNF-based isolated limb perfusion is responsible for tumor response

Saske Hoving
Ann L.B. Seynhaeve
Sandra T. van Tiel
Gisela aan de Wiel-Ambagtsheer
Ernst A. de Bruijn
Alexander M.M. Eggermont
Timo L.M. ten Hagen

Anticancer Drugs. 2006; 17(8), 949-959

Research article

Early destruction of tumor vasculature in TNF-based isolated limb perfusion is responsible for tumor response

Saske Hoving[1], Ann L.B. Seynhaeve[1], Sandra T. van Tiel[1], Gisela aan de Wiel-Ambagtsheer[1], Ernst A. de Bruijn[2], Alexander M.M. Eggermont[1], and Timo L.M. ten Hagen[1]

[1]Department of Surgical Oncology, Erasmus MC, Rotterdam, The Netherlands, [2]Department of Experimental Oncology, University of Leuven, Leuven, Belgium

ARTICLE INFORMATION

Anticancer Drugs. 2006; 17(8), 949-959

ACKNOWLEGMENTS

The authors thank Joost Rens for his assistance with the IFP measurements, Cindy van Velthoven for the immunohistochemical studies. This study was supported by grant DDHK 2000-2224 of the Dutch Cancer Society and a grant of the Foundation "Stichting Erasmus Heelkundig Kankeronderzoek" and Dr. K. Kullak of Boehringer Ingelheim GmbH by means of generous supply of TNF.

ABSTRACT

Addition of high-dose TNF to melphalan-based isolated limb perfusion (ILP) enhances antitumor effects impressively. Unfortunately, the mechanism of action of TNF is still not fully understood. Here we investigated the effects of TNF on the tumor microenvironment and on secondary immunological events during and shortly after ILP in soft tissue sarcoma-bearing rats. Already during ILP softening of the tumor was observed. Co-administration of TNF in the ILP with melphalan induced a 6-fold enhanced drug accumulation of melphalan in the tumor compared to ILP with melphalan alone. Also, directly after perfusion with TNF plus melphalan, so already in a time-frame of 30 minutes, vascular destruction, erythrocyte extravasation and hemorrhage was detected. However, interstitial fluid pressure (IFP) and pH in the tumor were not altered by TNF and no clear immune effects, cellular infiltration and cytokine expression were observed. Taken together, these results indicate that TNF-induces rapid damage to the tumor vascular endothelial lining resulting in augmented drug accumulation. As other important parameters were not changed, e.g. IFP and pH, we speculate that the tumor vascular changes and concurrent hemorrhage and drug accumulation are the key explanations for the observed synergistic antitumor response.

INTRODUCTION

Isolated limb perfusion (ILP) with tumor necrosis factor-alpha (TNF) and melphalan, or in lesser extend with doxorubicin, is currently one of the therapies available for the treatment of patients with advanced bulky melanoma and sarcoma of the limbs and results in impressive enhancement of the response rates of over 80% in a great variety of tumors [1,2]. Effective tumor therapy with TNF requires high concentrations, a prerequisite that is limited by the toxicity of the cytokine. The development of the ILP allows locoregional high doses with minimal risk for systemic toxicity. Investigations to the exact mechanism of the synergistic effect between TNF and chemotherapy in ILP are still ongoing. At the histopathological level it was shown that 3 hours after ILP the effects of TNF in a ILP starts with intratumoral endothelial cell activation followed by over-expression of adhesion molecules, which in turn leads to polymorphonuclear leukocyte (PMN) homing, endothelium injury and finally coagulative and hemorrhagic necrosis [3,4].

We developed a TNF-based isolated limb perfusion models in rats, with similar results compared to the clinical setting, to gain further insight in the mechanisms underlying the ob-

served synergy [5,6]. In this animal model we also observed hemorrhagic necrosis, edema, extravasation of erythrocytes, infiltration of polymorphonuclear neutrophils and destruction of tumor vasculature 24 hours after perfusion [7]. The antitumor response is regulated by numerous factors, including cytokine production by tumor cells and other cell source of the tumor microenvironment (endothelial cells, fibroblasts, tumor infiltrating lymphocytes) and other cytotoxic factors, like nitric oxide. Performing an ILP with TNF in combination of melphalan in leukopenic rats we found that the synergistic TNF-effect was lost, indicating the importance of leukocytes in this model [8]. TNF induces the production of other cytokines (e.g. IL-1, IL-6 and IL-8) as well as cytotoxic factors (e.g. nitric oxide) by T lymphocytes, granulocytes and macrophages, which could mediate the tumor suppression. The complexity of the interaction of TNF with various immune modulators within the tumor microenvironment is yet not well defined [9-11].

These histopathological effects of TNF described thus far are relatively long after ILP. However, early vascular changes, i.e. directly at the end of the ILP procedure, are unknown. In this study we focus on the effects inflicted by TNF during and shortly after ILP.

EXPERIMENTAL PROCEDURES

Agents. Recombinant human tumor necrosis factor-alpha was provided by Boehringer Ingelheim GmbH with a specific activity of 5.8 x 10^7 U/mg as determined in the murine L-M cell assay [12]. Endotoxin levels were < 1.25 units (EU) per mg protein. TNF concentrations used were 50 µg in 5 ml perfusate. Melphalan (Alkeran, GlaxoSmithKline BV) was diluted in phosphate buffered saline to a concentration of 2 mg/ml. Concentrations used were 40 µg in 5 ml perfusate.

Animals and tumor model. Male inbred BN rats, weighing 250-300 gram, obtained from Harlan-CPB were used for isolated limb perfusions. Rats were fed a standard laboratory diet *ad libitum* and were housed under standard conditions. The experimental protocols adhered to the rules outlined in the "Dutch Animal Experimentation Act" (1977) and the published "Guidelines of the UKCCCR for the welfare of animals in experimental Neoplasia [13]. The committee on Animal Research of the Erasmus University Rotterdam, the Netherlands, approved the protocol. The rapidly growing and metastasizing BN175 soft tissue sarcoma, which is transplantable to the BN rat, was used. Fragments of 2-3 mm were implanted subcutaneous in the right hind limb, just above the ankle. Perfusion was performed at a tumor diameter of 13 ± 2 mm, approximately 7 days after implantation.

Isolated limb perfusion. The perfusion technique was performed as described previously [6]. Briefly, animals were anaesthetized with Ketalin (Apharmo) and Xylazin (Bayer B.V.). To prevent coagulation 50 IU of heparin was injected intravenously. To keep the rat's hind limb at a constant temperature of 38-39°C, a warm water mattress was applied. Temperature was measured with a temperature probe on the skin covering the tumor. The femoral artery and vein were cannulated with silastic tubing (0.012 inch inner diameter, 0.025 inch outer diameter; 0.025 inch inner diameter, 0.047 inch outer diameter respectively, Dow Corning). Collaterals were occluded by a groin tourniquet and isolation time started when the tourniquet was tightened. An oxygenation reservoir and a roller pump were included into the circuit. The perfusion solution was 5 ml Haemaccel (Behring Pharma). Melphalan with or without TNF were added as boluses to the oxygenation reservoir. A roller pump (Watson Marlow type 505 U) recirculated the perfusate at a flow rate of 2.4 ml/min for 30 min. A washout with 5 ml oxygenated Haemaccel was performed at the end of the perfusion.

Assessment of tumor response. Tumor growth was daily recorded by caliper measurement. Tumor volume was calculated as 0.4 x (A^2 x B), where B represents the longest diameter and A the diameter perpendicular to B. The classification of tumor response was: progres-

sive disease (PD) = increase of tumor volume (>25%) within 8 days; no change (NC) = tumor volume equal to initial volume (in a range of -25% and + 25%); partial remission (PR) = decrease of tumor volume (-25% and -90%); complete remission (CR) = tumor volume less than 10% of initial volume. The animals with partial remission and complete remission were considered responders to the therapy.

Measurement of melphalan in tissue. At the end of the perfusion directly after the washout the tumor and part of the hind limb muscle were excised. The tissues were immediately frozen in liquid nitrogen to stop metabolism of melphalan and stored at -80(C. Tumor and muscle tissues were homogenized in 2 ml acetonitrile (Pro 200 homogenizer, Pro Scientific) and centrifuged at 2500 g. Melphalan was measured in the supernatant by gas chromatography-mass spectrometry. p-[Bis(2-chloroethyl)amino]-phenyl-acetic methyl ester was used as an internal standard. Samples were extracted over trifunctional C18 silica columns. After elution with methanol and evaporation, the compounds were derived with trifluoroacetic anhydride and diazomethane in ether. The stable derivates were separated on a methyl phenyl siloxane GC capillary column and measured selectively by single-ion monitoring GC-MS in the positive EI mode described earlier by Tjaden and de Bruijn [14].

Measurement of interstitial fluid pressure (IFP). IFP was measured in tumor and muscle during ILP with the Wick-in-Needle technique [15]. A 23-gauge needle (Venisystems) with a 2-3 mm side hole 5 mm from the tip was filled with five surgical sutures 6/0 (Braun Medical B.V.) and connected to a pressure transducer (DTXTM Plus Transducer, Becton Dickinson). Pressure was recorded on an analog-digital converter (AS/3 DATEX). After cannulating the femoral artery and vein, but before applying the tourniquet, the needle was inserted in the tumor and in the muscle of the same leg. The IFP was recorded until the end of the perfusion.

pH measurements. A calibrated pH electrode in a 20 Gauge Needle (Harvard Apparatus Inc) was inserted in the tumor just before the roller pomp was started. The pH of the perfusate was measured by inserting a portable pH meter (pH meter HI 8424, Hanna Instruments Inc) in the oxygenation reservoir.

Hematoxylin-eosin staining. Directly or 6 hours after perfusion tumors were excised and cut in two equal parts. Both parts were divided into a peripheral part and a central part. The tissues were stored in formalin and embedded in paraffin. 4 µm sections were stained with hematoxylin-eosin solution (Sigma) using standard procedures. Three or 4 different tumors in each experimental group were subjected to blind evaluation. At least 6 slides were examined from each tumor. All slides were examined on a Leica DM-RXA and photographed using a Sony 3CCD DXC 950 camera.

TUNEL/CD31PE double staining. Apoptotic cell death was detected using the technique of 3'hydroxy end labeling (In Situ Cell Death detection Kit, Fluorescein labeled, Roche Diagnostics). Tumor tissues were also stained for endothelial cells to differentiate between apoptosis of the endothelium and of tumor cells. After ILP the tumors were excised and immediately frozen in liquid nitrogen. Staining was performed on acetone-fixed 7 µm cryostat sections. The tumor sections were fixed in 4% paraformaldehyde for 30 min and incubated for 1 hour with mouse anti rat CD31PE (1:50; Becton Dickinson). After washing with PBS the sections were again fixed in 4% paraformaldehyde for 10 min and incubated in 0.1% Triton X-100 in 0.1% sodium citrate for 2 min on ice to allow permeabilization. The slides were incubated with the TUNEL mixture for 1 hour at 37°C and after that the slides were rinsed 3 times in PBS and mounted with mounting medium containing polyvinyl alcohol (Mowiol 4-88, Fluka). Endothelial cells were identified by red fluorescence and apoptosis by green fluorescence. Apoptotic endothelial cells were detected by co-localization of red and green (displayed as yellow) fluorescence.

Immunohistochemistry. Directly or 6 hours after ILP tumors were excised and frozen in liquid nitrogen. Immunohistochemical staining was performed on acetone-fixed 7 µm cryostat sections. The tumor sections were fixed for 30 min with 4% formaldehyde and after rinsing with PBS the endogenous peroxidase activity was blocked by incubation for 5 min in methanol/3% H_2O_2. The slides were incubated for 1 hour with mouse anti rat CD31, -CD4, -CD8, -granulocytes (1:50; Becton Dickinson) and -ED-1 for macrophages (1:50; Serotec). Thereafter, sections were washed with PBS and incubated for 1 hour with goat anti mouse peroxidase-labeled antibody (1:100; ITK Diagnostics BV). After rinsing with PBS, positive cells were revealed by immunoperoxidase reaction with DAB solution (ITK Diagnostics BV) and counterstained lightly with hematoxylin (Sigma). For quantification of infiltration and microvessel density two independent persons performed blinded analysis. Six representative fields (magnification 16x) in each section and 3 tumors per treatment were evaluated. The sections were examined on a Leica DM-RXA and photographed using a Sony DXC950 camera. For T cell, granulocyte and macrophage infiltration the total amount of positive cells were counted per field of interest. For the microvessel quantification, the number of tumor blood vessels (microvessel density, MVD) and the area of vessels per field of interest were measured in calibrated digital images (Research Assistant 3.0, RVC). The average size of a vessel was calculated by dividing the number of vessels with the area of vessels per field of interest.

Semi-quantitative RT-PCR. Total RNA was extracted from frozen tumor tissue using TRIzol reagent as suggested by the manufacturer (Invitrogen). cDNA synthesis was carried out by incubating 1.0 µg RNA with Omniscript Reverse Transcriptase (Qiagen) and oligo $d(T)_{16}$ (Invitrogen) for 1 hour at 42°C following heating for 5 min at 93°C to terminate the reaction. PCR reaction was performed with a Biometra T-gradient PCR machine on a reaction mix of 1.5 µl cDNA, 200 nM dNTP, 1,5 mM $MgCl_2$, 50 pM of the sense and antisense primers and 0.5 U Titanium Taq DNA polymerase (Becton Dickinson) in PCR buffer to 50 µl final volume. The primers were purchased from Invitrogen and primer sequences are shown in table 1. ß-actin was used as an internal standard. For PCR we used the following parameters: initial denaturation at 94˚C for 5 min followed by a maximum of 40 cycles of 94˚C for 45 sec, annealing for 45 sec (temperatures see **Table 1**) and extension 72˚C for 1 min. To obtain results from the exponential phase of the reaction every 2 cycles, 5 µl of PCR product was collected and the samples were separated on a 1.5% agarose gel, stained with ethidium bromide and photographed under ultraviolet light box. A 100-bp ladder was used as the standard. The threshold cycle was determined as the cycle where the visible band of a specific PCR product first appeared on the gel. The results were expressed as the cycle of first appearance of the band normalized with the cycle of first appearance of ß-actin.

Statistical analysis. Results were evaluated for statistical significance with the Mann Whitney U test. P-values below 0.05 were considered statistically significant. Calculations were performed on a personal computer using GraphPad Prism v3.0 and SPSS v11.0 for Windows 2000.

RESULTS

The combination TNF and melphalan results in increased antitumor response. Combination of TNF and melphalan resulted in an increased antitumor activity with a response rate (PR and CR) of 80% compared to perfusion with melphalan alone ($P < 0.001$). Progressive disease was found in all animals treated with sham or TNF alone. Perfusion with melphalan alone showed some inhibition of tumor growth compared to sham and TNF, resulting in 17% response. This tumor response increased to 80% when TNF was added (**Table 2**). Another important observation made was the softening of the tumor, during the 30 min of perfusion, when treated with TNF in combination with melphalan. A characteristic we did not observed in the other treatments.

Table 1. RT-PCR primers for the immune related genes.

Gene	Primers	Annealing temp.	Product size (bp)
ß-actin	f: 5'-ATGGATGACGATATCGCTG-3' r: 5'-ATGAGGTAGTCTGTCAGGT-3'	60°C	569
IL-6	f: 5'-GACTTCACAGAGGATACC-3' r: 5'-TAAGTTGTTCTTCACAAACTCC-3'	55°C	294
GRO/CINC-A	f: 5'-GAAGATAGATTGCACCGATG-3' r: 5'-CATAGCCTCTCACACATTTC-3'	57°C	367
IL-10	f: 5'-TGACAATAACTGCACCCACTT-3' r: 5'-TCATTCATGGCCTTGTAGACA-3'	60°C	402
IL-12	f: 5'-TCATCAGGGACATCATCAAACC-3' r: 5'-CGAGGAACGCACCTTTCTG-3'	65°C	210
TNF	f: 5'-TACTGAACTTCGGGGTGATCGGTCC-3' r: 5'-CAGCCTTGTCCCTTGAAGAGAACC-3'	60°C	295
IFN	f: 5'-GCCTCCTCTTGGATATCTGG-3' r: 5'-GTGCTGGATCTGTGGGTTG-3'	60°C	239
MCP-1	f: 5'-ATGCAGGTCTCTCTGTCACG-3' r: 5'-CTAGTTCTCTGTCATACT-3'	57°C	446
MIP-2	f: 5'-GGCACAATCGGTACGATCCAG-3' r: 5'-ACCCTGCCAAGGGTTGACTTC-3'	55°C	287
TGF-ß1	f: 5'-TGGAAGTGGATCCACGAGCCCAAG-3' r: 5'-GCAGGAGCGCACGATCATGTTGGAC-3'	55°C	240

Note: ß-actin, was used as a housekeeping gene. f, forward primer; r, reverse primer; IL, interleukin; GRO/CINC-A, growth regulated gene product/cytokine-induced neutrophil chemo attractant (rat analog for IL-8); TNF, tumor necrosis factor-alpha; IFN, interferon-gamma; MCP-1, monocyte chemoattractant protein-1; MIP-2, macrophage inflammatory protein-2; TGF-ß1, transforming growth factor-ß1.

Table 2. Tumor response and drug accumulation after TNF-based ILP with melphalan.

Treatment	Tumor volume (mm^3)[a]	Response rate (% of animals)[b]				Melphalan in tumor (ng/g tissue)[c]	Melphalan in skin/muscle (ng/g tissue)[c]
		PD	SD	PR	CR		
Sham	> 5000	100					
TNF	4570 ± 511	100					
Melphalan	1918 ± 293	33	42	25		136 ± 24	316 ± 91
TNF+melphalan	491 ± 245*	13	7	40	40	831 ± 293*	290 ± 125

Note: Animals were treated with ILP with sham, TNF, melphalan and melphalan plus TNF.

[a] Tumor volume was measured 8 days after ILP. Data represent tumor volume ± SD of at least 7 animals; *, $P < 0.01$ *versus* treatment with melphalan.

[b] Tumor response is classified as described in the experimental procedures. PD, progressive disease; SD, stable disease; PR, partial response; CR, complete response.

[c] Intratumoral and muscular melphalan concentration were measured at the end of perfusion as described in the experimental procedures. Data represents ng melphalan per gram tissue ± SD of at least 3 animals; *, $P < 0.01$ *versus* treatment with melphalan.

Addition of TNF increases intratumoral melphalan concentration. Immediately after perfusion with melphalan or melphalan in combination with TNF tumor and muscle were excised and melphalan concentration was measured. In tumor tissue perfused with melphalan and TNF, we measured a 6-fold increased melphalan uptake compared to tumor tissue treated with melphalan alone ($P < 0.01$). That an increased uptake of melphalan by TNF is specific for the tumor is demonstrated by the fact that in skin and muscle no effect of TNF was found on the uptake of melphalan (**Table 2**). The melphalan concentration increased from 136 ng/g tissue to 831 ng/g tissue when TNF was co-administered. The IC_{50} of melphalan on BN175 cells is 250 ng/ml [16], demonstrating that the addition of TNF to the ILP shift the intratumoral drug concentration in to an active range. Addition of TNF does not change the sensitivity of BN175 cells *in vitro*, indicating that only melphalan has a cytotoxic effect on the tumor cells. This indicates that the increased intratumoral melphalan concentration is responsible for the cytotoxic effect on the tumor cells leading to tumor regression. Important to mention is that the IC_{50} of melphalan on endothelial cells is must higher (40,000 ng/ml), which implies that endothelial cells are most likely not affected by melphalan in the ILP setting [17].

Addition of TNF results in destruction of the vasculature, extravasation of erythrocytes and increase apoptosis of endothelial cells. Previously, we demonstrated vascular damage, extravasation of erythrocytes and necrosis, causing drastic alterations in permeability and integrity of the vasculature 24 hours after ILP with melphalan in combination with TNF [7]. In HE stainings directly after perfusion with TNF plus melphalan, an increase in the number and size of necrotic areas was observed accompanied by scattered extravasation of erythrocytes (**Fig. 1**). In some areas we detected destruction of the vasculature and from these vessels infiltration of erythrocytes into the surrounding tumor tissue occurred. In tumors treated with TNF alone, we also observed destruction of the vasculature and erythrocyte infiltration from these vessels. After melphalan or sham treatment, no extravasation of erythrocytes, necrotic areas and loss in endothelial integrity was observed. Strikingly, no clear differences between central and peripheral part of the tumors were seen directly or 6 hours after ILP, with the exception that after 6 hours slightly more necrotic areas were detected (data not shown). For the de-

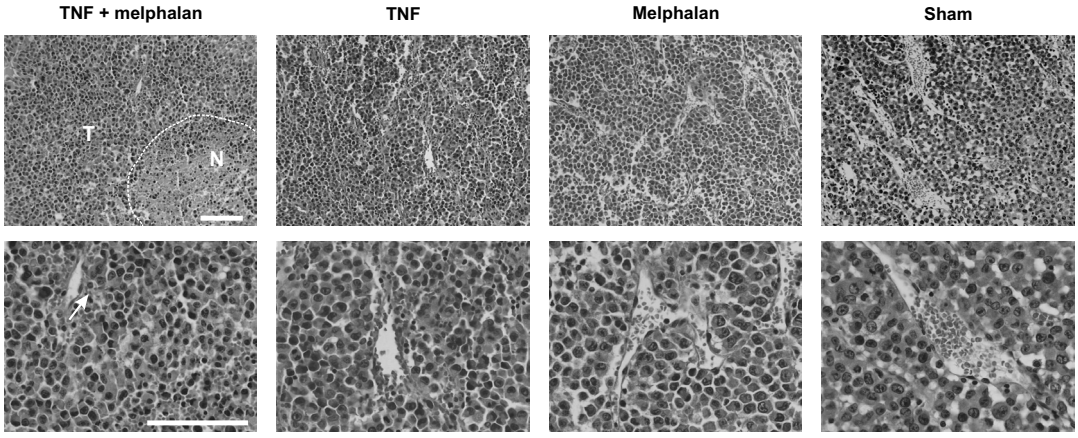

Figure 1. Effect of TNF on the histopathology of tumor tissue after ILP. HE staining directly after perfusion with melphalan in combination with TNF showed necrotic areas, destruction of the vascular lining and extravasation of erythrocytes (arrow). Perfusion with TNF alone also induced vascular damage and erythrocyte infiltration. In sham or melphalan-treated tumors the vessel lining was still intact. Dotted line denotes the boundary between normal tumor tissue (T) and necrotic tissue (N). Scale bar apply for all images, 100 µm. (See color section for a full-color version.)

tection of apoptotic endothelial cells we performed a tunnel/CD-31 double staining (**Fig. 2**). In all four treatments apoptotic tumor cells were observed sporadically. In the TNF and TNF plus melphalan treated tumors an increased number of apoptotic endothelial cells were detected directly after perfusion.

Addition of TNF has no effect on the interstitial fluid pressure. As TNF has been shown to reduce interstitial fluid pressure (IFP) in tumor tissue in a systemic treatment [18]. IFP measurements were performed in both tumor and muscle tissue during ILP to investigate if TNF-induced lowering of the IFP could be an explanation for the enhanced drug accumulation and softening of the tumor. Under normal

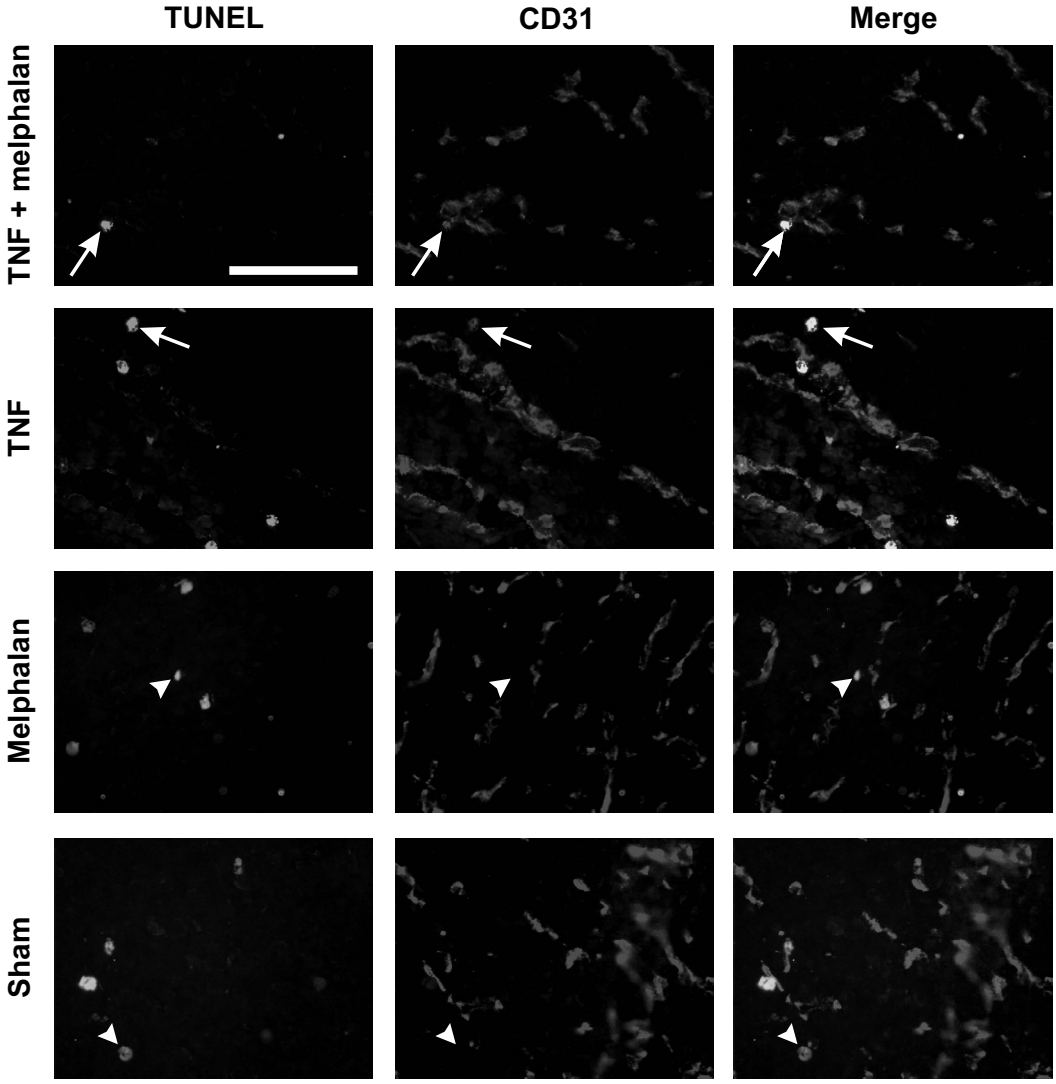

Figure 2. Effect of TNF on apoptosis of endothelial cells in tumor directly after ILP. Photographs demonstrating apoptotic tumor cells (green, arrowhead), endothelial cells (CD31, red) and apoptotic endothelial cells (yellow, arrow). Perfusion with melphalan in combination with TNF or with TNF alone induces apoptosis of endothelial cells whereas in the staining of tumor tissue after sham or melphalan perfusion no apoptotic endothelial cells were observed. Scale bar apply for all images, 100 µm. (See color section for a full-color version.)

conditions the IFP of tumor tissue is much higher than that of muscle tissue (**Fig. 3a**). Tightening of the tourniquet resulted in an increased IFP in both tissues and start of the perfusion pump did not further increase the IFP. None of the treatments had an effect on the IFP in the tumor and the only increase we could see was in the muscle of the melphalan treated group after 20 and 30 min ($P < 0.05$). We speculated that the pressure inflicted by the pump in the extracorporal circuit might have a major impact on the IFP. Indeed, when we increased the pump rate in our animal model, tumor IFP increased and decreased again when the pump rate was reduced (data not shown). Although only one test was performed clearly the effect of the pump rate on the IFP was confirmed in de clinical setting in which comparable results were obtained (**Fig. 3b**).

The pH in tumor and perfusate is not influenced by the treatments. Tumor acidity can increase the antitumor activities of weak acid chemotherapeutics like melphalan [19]. Although acidosis is already a known fact in the microenvironment of solid tumors and is found in hypoxic areas we tested the hypothesis whether treatment with TNF could cause a lowering of pH in tumor tissue. The pH of the tumor at the beginning of the perfusion was slightly acidic (6.9 ± 0.1) and lowered during perfusion until 6.6 ± 0.3. The pH of the perfusate was 6.9 ± 0.1. Adding the drugs had no effect whereas oxygenation lowered the pH to 6.2 ± 0.1. Directly after start of the perfusion the pH of the perfusate increased to 6.5 ± 0.3 and was 6.9 ± 0.1 at the end of perfusion. None of the treatments had an effect on the pH of the tumor or the perfusate indicating that TNF does not induce acidosis in this setting.

Addition of TNF has no effect on the number of vessels shortly after perfusion. The increased uptake of melphalan might be correlated with the functionality of the tumor-associated vasculature. Quantification of the microvessel density and functionality was performed by immunohistochemical staining of endothelial cells. The number of vessels as well as vessel area was measured. The area per vessel was computed by dividing the total area of vessels by the number of vessels. Although we

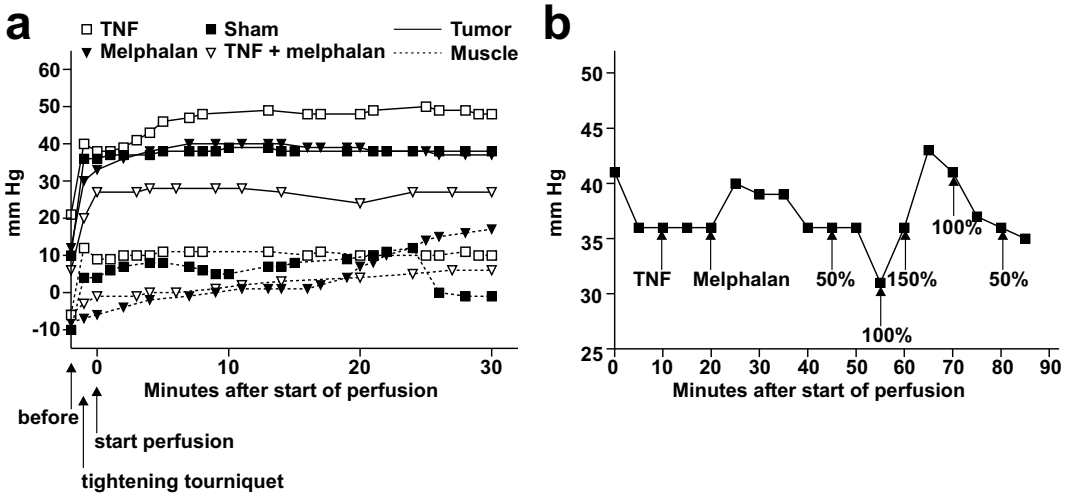

Figure 3. TNF has no effect on interstitial fluid pressure during ILP. (**a**) Representative graph of the IFP recorded during perfusion as described in the experimental procedure tumor (continuous line) and muscle (dotted line) and no effect of TNF was measured. (**b**) Representative graph of the IFP measured in a patient during ILP. Decreasing perfusion pump rate during ILP resulted in a lower IFP and *vice versa* indicating that in an ILP the IFP is dictated by the pump pressure.

observed endothelial damage in the HE staining, addition of TNF had no effect on the number and size of the vessels directly after perfusion (**Table 3**). The vessel area in the center or periphery part of the tumor was significantly decreased six hours after ILP compared to the area measured directly after perfusion with sham, TNF or melphalan ($P < 0.05$), however no change was observed after perfusion with TNF in combination with melphalan.

Tumor infiltration is not affected by the addition of TNF. In a previous study of ILP with IL-2 in combination with melphalan we observed an redistribution of macrophages which was not observed in a sham perfusion [20]. *In vitro* data showed that TNF has only an effect on endothelial cells when combined with IFN and pheripheral blood mononuclear cells [17]. Therefore we also examined the possible secondary effects of TNF in the ILP. Performing ILP with TNF, directly or 6 hours after perfusion, we found no evident alterations in number (**Table 4**) of localization (**Fig. 4**) of the examined tumor infiltrating cells in all 4 treatments groups.

Addition of TNF did not change the cytokine profile shortly after perfusion. As the number of tumor infiltrating cells was not affected by TNF, we hypothesized that TNF could probably activate macrophages and T lymphocytes resulting in the production of non-specific effector molecules. However, from the 9 cytokines examined we found no change in expression profile between the treatments groups (**Table 5**).

DISCUSSION

Clinical studies showed impressive improvement of the antitumor activity of melphalan in local treatment of different tumor types when TNF was co-administered [1,2]. In this paper and in previous studies, we demonstrate

Table 3. Microvessel density and area of the tumor vessels after ILP with sham, TNF, melphalan or TNF plus melphalan.

		Sham	TNF	Melphalan	TNF + melphalan
Number of vessels[a]					
center	0 hours	19 ± 6	21 ± 7	22 ± 2	34 ± 25
periphery	0 hours	43 ±12	32 ± 9	34 ± 6	19 ± 5
center	6 hours	46 ± 31	34 ± 13	32 ± 14	18 ± 7
periphery	6 hours	36 ± 15	29 ± 5	38 ± 26	25 ± 6
Total vessel area[b]					
center	0 hours	7.6 ± 0.7	10.7 ± 2.7	5.9 ± 0.9	5.7 ± 1.0
periphery	0 hours	7.6 ±0.3	7.2 ± 0.4	7.2 ± 0.1	5.0 ± 1.1
center	6 hours	4.0 ± 1.1*	4.0 ± 0.7*	6.1 ± 1.4	7.2 ± 2.4
periphery	6 hours	3.8 ± 0.5*	3.5 ± 0.4*	3.9 ± 1.5*	3.6 ± 0.5
Vessel size[c]					
center	0 hours	0.44 ± 0.09	0.59 ± 0.25	0.27 ± 0.03	0.41 ± 0.17
periphery	0 hours	0.22 ± 0.08	0.28 ± 0.10	0.23 ± 0.03	0.30 ± 0.08
center	6 hours	0.16 ± 0.05*	0.14 ± 0.0*	0.22 ± 0.03	0.48 ± 0.16
periphery	6 hours	0.14 ± 0.04	0.13 ± 0.02	0.18 ± 0.08	0.18 ± 0.07

Note: Animals were treated with ILP with sham, TNF, melphalan and melphalan plus TNF and directly or 6 hours after ILP the tumors were excised and sections of the center or periphery were stained for CD31 positive cells.

[a] Number of vessels per field of interest at magnification 16x. Data represent total number ± SEM of 6 sections of 3 individual tumors.

[b] Percentage of total vessel are per field of interest at magnification 16x. Data represent percentage of total area ± SEM of 6 sections of 3 individual tumors; *, $P < 0.05$ *versus* 0 hours of the same tumor region.

[c] Size of one vessel per field of interest at magnification 16x. Data represent percentage endothelium per vessel ± SEM of 6 sections of 3 individual tumors;*, $P < 0.05$ *versus* 0 hours of the same tumor region.

Table 4. Tumor infiltration after ILP with sham, TNF, melphalan or TNF plus melphalan.

		Sham	TNF	Melphalan	TNF + melphalan
CD4[a]					
center	0 hours	0.3 ±0.1	0.5 ± 0.3	0.2 ± 0.1	13.5 ± 13.0
periphery	0 hours	1.0 ± 0.5	1.4 ± 0.4	0.7 ± 0.5	0.5 ± 0.3
center	6 hours	1.0 ± 0.5	0.9 ± 0.4	1.2 ± 0.4	0.4 ± 0.1
periphery	6 hours	0.5 ± 0.3	0.6 ± 0.2	0.8 ± 0.3	1.6 ± 0.4
CD8[a]					
center	0 hours	34 ± 21	27 ± 21	67 ± 47	56 ± 55
periphery	0 hours	64 ± 26	35 ± 7	75 ± 27	139 ± 25
center	6 hours	22 ± 12	51 ± 16	41 ± 13	48 ± 29
periphery	6 hours	62 ± 20	33 ± 3[*]	51 ± 7	42 ± 8[#]
Granulocytes[a]					
center	0 hours	60 ± 4	89 ± 18	48 ± 3[*]	88 ± 12
periphery	0 hours	74 ± 19	81 ± 25	62 ± 10	37 ± 5
center	6 hours	69 ± 10	72 ± 18	79 ± 14	47 ± 6[*#]
periphery	6 hours	109 ± 39	71 ± 12	50 ± 13	81 ± 12[#]
Macrophages[a]					
center	0 hours	189 ± 5	192 ± 33	201 ± 20	172 ± 34
periphery	0 hours	221 ± 42	165 ± 11	207 ± 23	239 ± 11
center	6 hours	171 ± 34	174 ± 18	230 ± 29	147 ± 10
periphery	6 hours	246 ± 39	214 ± 34	180 ± 16	189 ± 2[#]

Note: Animals were treated with ILP with sham, TNF, melphalan and melphalan plus TNF and directly or 6 hours after ILP the tumors were excised and sections of the center or periphery were stained for CD4, CD8, granulocytes and macrophages.

[a] Number of positive cells per field of interest at magnification 16x. Data represent total number ± SEM of 6 sections of 3 individual tumors;*, $P < 0.05$ *versus* sham treatment of the same time point and region of the tumor; #, $P < 0.05$ *versus* 0 hours of the same tumor region.

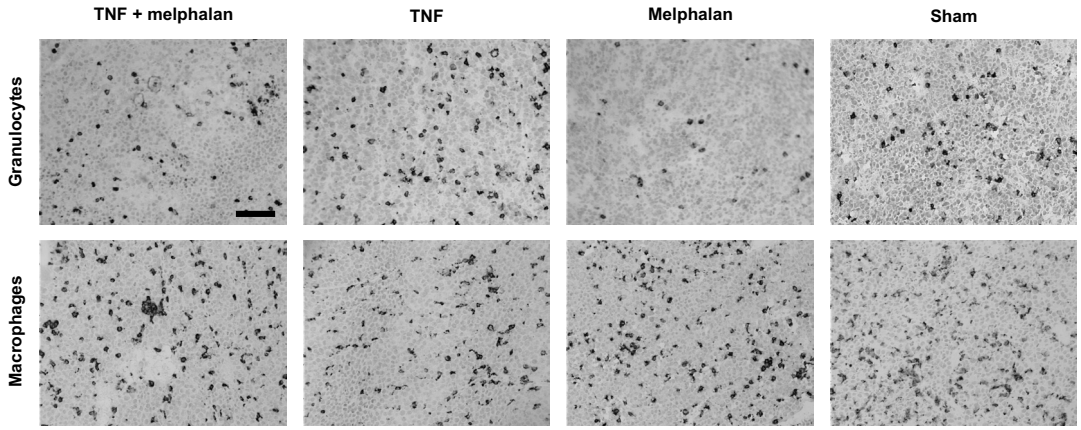

Figure 4. TNF has no effect on redistribution of granulocytes and macrophages. Directly after treatment tumors were excised and stained for granulocytes and macrophages. There was no change in the number or redistribution of the tumor infiltrating cells between the treatments. Scale bar apply for all images, 100 µm. (See color section for a full-color version.)

Table 5. Cytokine expression after ILP with sham, TNF, melphalan or TNF plus melphalan.

Gene	Sham[a]		TNF[a]		Melphalan[a]		TNF + melphalan[a]	
	0 hours	6 hours	0 hours	6 hours	0 hours	6 hours	0 hours	6 hours
IL-6	10 ± 1	8 ± 2	9 ± 0	6 ± 2	9 ± 0	9 ± 0	10 ± 1	7 ± 2
GRO/CINC-A	10 ± 1	5 ± 2*	7 ± 1	5 ± 3	10 ± 0	5 ± 1*	10 ± 2	4 ± 2*
IL-10	13 ± 1	13 ± 1	15 ± 4	13 ± 1	15 ± 1	13 ± 1	15 ± 1	12 ± 2
IL-12	15 ± 1	17 ± 3	14 ± 0	15 ± 3	13 ± 1	17 ± 1*	14 ± 0	16 ± 2
TNF	19 ± 1	13 ± 1*	17 ± 1	13 ± 2*	18 ± 2	14 ± 0*	17 ± 1	13 ± 1*
IFN	15 ± 1	11 ± 2	15 ± 1	13 ± 2	15 ± 1	13 ± 1	14 ± 0	13 ± 1
MCP-1	6 ± 1	5 ± 2	6 ± 1	6 ± 2	5 ± 0	6 ± 1	7 ± 0	6 ± 1
MIP-2	11 ± 1	8 ± 3	10 ± 3	7 ± 2	12 ± 1	9 ± 0*	12 ± 1	9 ± 2
TGF-ß1	3 ± 1	6 ± 2	4 ± 0	4 ± 2	3 ± 1	6 ± 0*	3 ± 1	5 ± 1

Note: Animals were treated with ILP with sham, TNF, melphalan and melphalan plus TNF and directly or 6 hours after ILP the tumors were excised and semiquantitative RT-PCR performed.

[a] Numbers are the cycles where the first band of each cytokine appeared corrected for the first band of ß-actin of the same sample. Data represent average ± SD of 3 individual tumors; *, $P < 0.05$ *versus* 0 hours

that isolated limb perfusion with melphalan in combination with TNF in soft tissue sarcoma-bearing rats results in high response rates. This combination therapy is also very effective for the rat osteosarcoma and with another chemotherapeutical agent, namely doxorubicin [21,22]. We demonstrated that the basis for the synergy is a significant enhancement of tumor drug accumulation. Subsequent events were selective destruction of the tumor-associated vasculature leaving the normal vessel of the targeted area intact. This impaired blood flow leads to edema and necrosis. Although we observed these features already in rodent tumor models with TNF alone, no significant tumor regression occurred in these animals. Also these effects were observed at least 24 hours after perfusion whereas the tumor specific uptake of the chemotherapeutic drug occurred within the 30 min of perfusion. Melphalan is an alkylating agent and has a cytotoxic effect on dividing tumor cells whereas TNF works selectively on tumor-associated vasculature. We therefore hypothesis that ILP with melphalan and TNF follows a two-way mechanism. First, TNF targets the tumor vasculature therefore facilitating access of melphalan in the tumor tissue followed by destruction of the tumor cells by melphalan.

Here we focus on the direct effects of TNF on the tumor microenvironment and secondary immunological effects during and shortly after perfusion. Already during perfusion with TNF and melphalan softening of the tumor was observed, a feature also observed in the clinical setting [23], which could be an indication of hemorrhage or inflammation. Histological analysis of these tumors revealed some areas with complete destruction of the vasculature. The size and number of tumor vessels were not affected by the treatments this shortly after perfusion. We hypothesize that the slightly increased apoptotic cell number found directly after ILP, only partly explain the vascular damage caused by TNF in combination with melphalan. Ruegg *et al*. showed that inhibition of the αVβ3-mediated endothelial cell adhesion results in apoptosis and finally disruption of the tumor vasculature induced by TNF and IFNγ, but in this study tumor biopsies were examined 24 hours after ILP [24], which might therefore be a secondary effect.

After perfusion with TNF in combination with melphalan or with TNF alone we observed scattered extravasation of erythrocytes in the surrounding tissue. This is not seen in sham or melphalan treated tumors. It is reported that erythrocytes can play an important role in the transport of certain drugs [25,26]. However, little is known about the contribution of erythrocytes in the transport of melphalan. Wildiers *et al.* showed that 1 hour after i.p. administration of melphalan 25% of the melphalan in the blood was transported via erythrocytes.

He also showed that although the transport of melphalan via erythrocytes was less than that in plasma it correlated well with melphalan availability in embryonic stem cell-derived tumors [27]. An increased extravasation of melphalan-encapsulated erythrocytes by TNF could be a plausible explanation for the augmented concentration of melphalan in the tumor environment and further experiments on the role of erythrocytes are currently performed in our laboratory.

Tumors are characterized by dilated hyperpermeable and irregular shaped blood vessels, a lack of functional lymphatics and an abnormal turnover of extracellulair matrix components. Fluid and serum proteins leak from the vessels and accumulate in the interstitium increasing the interstitial fluid pressure. This chaotic vascular structure and diminished buffering capacity of the interstitial fluid pressure contributes to an acidic microenvironment of the tumor. Poor uptake of drugs into tumor interstitium is thought to, at least in part, be responsible for the low efficiency in pharmacological treatment of solid malignancies [28,29]. Kristensen *et al*. showed that TNF caused a reduction in the IFP in human melanoma xenografts, what could lead to enhanced uptake of large molecules [18]. It has been demonstrated that lowering pH condition potentates the melphalan toxicity towards several tumor cell lines [19,30]. In our experiments we did not see an effect of TNF on the IFP during perfusion. Moreover, the pressure measured was solely ascribed to the design of this model. In our study we found that the pH in the BN175 tumor is slightly acidic and none of the treatments had an effect on the pH in the tumor during ILP.

TNF is able to up regulate expression of several cytokines (IL-1, IL-6, IL-8, IFNγ) in cancer and inflammatory responses. Up-regulation of these cytokines in the tumor microenvironment can account as a secondary effect of TNF. Tumor infiltrating lymphocytes that express these cytokine are equally important. *In vitro* studies showed that TNF alone has hardly a direct effect on endothelial cells, only in combination with IFNγ and peripheral blood mononuclear cells we observed morphological changes of the endothelial layer leading to increased permeability [17]. Mocellin *et al.* found 24 hours after ILP with TNF and doxorubicin an increase in CD4 mRNA expression in the tumor microenvironment compared with tumor tissue before treatment [31]. An increased TIA-1 gene expression in tumor biopsies 24 hours after TNF-based ILP compared to the patients treated with doxorubicin alone was found. They observed no change in tumor infiltrating lymphocytes as well as some other relevant cytokines, like IFNγ, IL-10 and TGF-ß. After *in vitro* stimulation with TNF of the different cell types that represent the tumor environment, TIA-1 expression is significantly increased in endothelial cells and NK cells. These experiments indicate that TNF-induced TIA-1 over-expression might sensitize endothelial cells to pro-apoptotic stimuli present in the tumor microenvironment and enhance NK cell cytotoxic activity against cancer cells [32]. Directly or 6 hours after ILP, we also found no effect on the expression profile of the panel of cytokines we tested and observed no variations in number or re-localization of tumor infiltrating lymphocytes between the treatments. A limitation of using the complete tumor for gene profiling is that we cannot link gene expression with a specific subset of cells. Further experiments are currently performed to investigate the gene expression in the different cell sources of the tumor and the importance of a local up- or down regulation of cytokines. The imbalance in the cytokine profile within the tumor microenvironment more than the absolute level of an individual cytokine may be responsible for an effective versus ineffective immune response and needs to be further exploited.

In conclusion, application of TNF in combination with melphalan in an isolated limb perfusion strongly improves response rates, which is due to an augmented melphalan accumulation in the tumor during ILP. We have recently reported a similar and crucial activity of histamine and interleukin-2 in this setting [16,20]. This increased drug accumulation by TNF is not explained by a lowering of the IFP. However, the tumor endothelial lining is damaged in TNF-based ILP, rendering the vessels lo-

cally more permeable to small molecules but also to erythrocytes that could function as carriers for melphalan. The exact mechanism of TNF-induced damage to the endothelial lining could not be explained by changes in cytokine expression or a redistribution of infiltrating lymphocytes around the vessels as we did observed after interleukin-2 based ILP although a local imbalance of cytokines around these vessels could be contribute to permeability changes and will be further investigated.

REFERENCE

1.Eggermont AM, de Wilt JH, and ten Hagen TL. Current uses of isolated limb perfusion in the clinic and a model system for new strategies. Lancet Oncol. 2003: 4(7), 429-437.

2.Grunhagen DJ, de Wilt JH, ten Hagen TL, and Eggermont AM. Technology insight: Utility of TNF-alpha-based isolated limb perfusion to avoid amputation of irresectable tumors of the extremities. Nat Clin Pract Oncol. 2006: 3(2), 94-103.

3.Nooijen PT, Eggermont AM, Schalkwijk L, Henzen-Logmans S, de Waal RM, and Ruiter DJ. Complete response of melanoma-in-transit metastasis after isolated limb perfusion with tumor necrosis factor alpha and melphalan without massive tumor necrosis: a clinical and histopathological study of the delayed-type reaction pattern. Cancer Res. 1998: 58(21), 4880-4887.

4.Renard N, Lienard D, Lespagnard L, Eggermont A, Heimann R, and Lejeune F. Early endothelium activation and polymorphonuclear cell invasion precede specific necrosis of human melanoma and sarcoma treated by intravascular high-dose tumour necrosis factor alpha (rTNF alpha). Int J Cancer. 1994: 57(5), 656-663.

5.Manusama ER, Nooijen PT, Stavast J, Durante NM, Marquet RL, and Eggermont AM. Synergistic antitumour effect of recombinant human tumour necrosis factor alpha with melphalan in isolated limb perfusion in the rat. Br J Surg. 1996: 83(4), 551-555.

6.de Wilt JH, Manusama ER, van Tiel ST, van Ijken MG, ten Hagen TL, and Eggermont AM. Prerequisites for effective isolated limb perfusion using tumour necrosis factor alpha and melphalan in rats. Br J Cancer. 1999: 80(1-2), 161-166.

7.Nooijen PT, Manusama ER, Eggermont AM, Schalkwijk L, Stavast J, Marquet RL et al. Synergistic effects of TNF-alpha and melphalan in an isolated limb perfusion model of rat sarcoma: a histopathological, immunohistochemical and electron microscopical study. Br J Cancer. 1996: 74(12), 1908-1915.

8.Manusama ER, Nooijen PT, Stavast J, de Wilt JH, Marquet RL, and Eggermont AM. Assessment of the role of neutrophils on the antitumor effect of TNFalpha in an in vivo isolated limb perfusion model in sarcoma-bearing brown Norway rats. J Surg Res. 1998: 78(2), 169-175.

9.Klimp AH, de Vries EG, Scherphof GL, and Daemen T. A potential role of macrophage activation in the treatment of cancer. Crit Rev Oncol Hematol. 2002: 44(2), 143-161.

10.Mocellin S, Wang E, and Marincola FM. Cytokines and immune response in the tumor microenvironment. J Immunother. 2001: 24(5), 392-407.

11.Cassatella MA. The production of cytokines by polymorphonuclear neutrophils. Immunol Today. 1995: 16(1), 21-26.

12.Kramer SM and Carver ME. Serum-free in vitro bioassay for the detection of tumor necrosis factor. J Immunol Methods. 1986: 93(2), 201-206.

13.UKCCCR. United Kingdom Co-ordinating Committee on Cancer Research (UKCCCR) Guidelines for the Welfare of Animals in Experimental Neoplasia (Second Edition). Br J Cancer. 1998: 77(1), 1-10.

14.Tjaden UR and de Bruijn EA. Chromatographic analysis of anticancer drugs. J Chromatogr. 1990: 531, 235-294.

15.Fadnes HO, Reed RK, and Aukland K. Interstitial fluid pressure in rats measured with a modified wick technique. Microvasc Res. 1977: 14(1), 27-36.

16.Brunstein F, Hoving S, Seynhaeve AL, van Tiel ST, Guetens G, de Bruijn EA et al. Synergistic antitumor activity of histamine plus melphalan in isolated limb perfusion: preclinical studies. J Natl Cancer Inst. 2004: 96(21), 1603-1610.

17.Seynhaeve AL, Vermeulen CE, Eggermont AM, and ten Hagen TL. Cytokines and vascular permeability: an in vitro study on human endothelial cells in relation to tumor necrosis factor-alpha-primed peripheral blood mononuclear cells. Cell Biochem Biophys. 2006: 44(1), 157-169.

18.Kristensen CA, Nozue M, Boucher Y, and Jain RK. Reduction of interstitial fluid pressure after TNF-alpha treatment of three human melanoma xenografts. Br J Cancer. 1996: 74(4), 533-536.

19.Skarsgard LD, Skwarchuk MW, Vinczan A, Kristl J, and Chaplin DJ. The cytotoxicity of melphalan and its relationship to pH, hypoxia and drug uptake. Anticancer Res. 1995: 15(1), 219-223.

20.Hoving S, Brunstein F, aan de Wiel-Ambagtsheer G, van Tiel ST, de Boeck G, de Bruijn EA et al. Synergistic antitu-

mor response of interleukin 2 with melphalan in isolated limb perfusion in soft tissue sarcoma-bearing rats. Cancer Res. 2005: 65(10), 4300-4308.
21.Manusama ER, Stavast J, Durante NM, Marquet RL, and Eggermont AM. Isolated limb perfusion with TNF alpha and melphalan in a rat osteosarcoma model: a new anti-tumour approach. Eur J Surg Oncol. 1996: 22(2), 152-157.
22.van der Veen AH, de Wilt JH, Eggermont AM, van Tiel ST, Seynhaeve AL, and ten Hagen TL. TNF-alpha augments intratumoural concentrations of doxorubicin in TNF-alpha-based isolated limb perfusion in rat sarcoma models and enhances anti-tumour effects. Br J Cancer. 2000: 82(4), 973-980.
23.Gutman M, Inbar M, Lev-Shlush D, Abu-Abid S, Mozes M, Chaitchik S et al. High dose tumor necrosis factor-alpha and melphalan administered via isolated limb perfusion for advanced limb soft tissue sarcoma results in a 90% response rate and limb preservation. Cancer. 1997: 79(6), 1129-1137.
24.Ruegg C, Yilmaz A, Bieler G, Bamat J, Chaubert P, and Lejeune FJ. Evidence for the involvement of endothelial cell integrin alphaVbeta3 in the disruption of the tumor vasculature induced by TNF and IFN-gamma. Nat Med. 1998: 4(4), 408-414.
25.Dumez H, Guetens G, de Boeck G, Highley MS, de Bruijn EA, van Oosterom AT et al. In vitro partition of docetaxel and gemcitabine in human volunteer blood: the influence of concentration and gender. Anticancer Drugs. 2005: 16(8), 885-891.
26.Millan CG, Marinero ML, Castaneda AZ, and Lanao JM. Drug, enzyme and peptide delivery using erythrocytes as carriers. J Control Release. 2004: 95(1), 27-49.
27.Wildiers H, Guetens G, de Boeck G, Landuyt W, Verbeken E, Highley M et al. Melphalan availability in hypoxia-inducible factor-1alpha+/+ and factor-1alpha-/- tumors is independent of tumor vessel density and correlates with melphalan erythrocyte transport. Int J Cancer. 2002: 99(4), 514-519.
28.Jain RK. Barriers to drug delivery in solid tumors. Sci Am. 1994: 271(1), 58-65.
29.Carmeliet P and Jain RK. Angiogenesis in cancer and other diseases. Nature. 2000: 407(6801), 249-257.
30.Siemann DW, Chapman M, and Beikirch A. Effects of oxygenation and pH on tumor cell response to alkylating chemot1.Eggermont AM, de Wilt JH, and ten Hagen TL. Current uses of isolated limb perfusion in the clinic and a model system for new strategies. Lancet Oncol. 2003: 4(7), 429-437.
31.Mocellin S, Provenzano M, Rossi CR, Pilati P, Nitti D, and Lise M. Use of quantitative real-time PCR to determine immune cell density and cytokine gene profile in the tumor microenvironment. J Immunol Methods. 2003: 280(1-2), 1-11.
32.Mocellin S, Provenzano M, Lise M, Nitti D, and Rossi CR. Increased TIA-1 gene expression in the tumor microenvironment after locoregional administration of tumor necrosis factor-alpha to patients with soft tissue limb sarcoma. Int J Cancer. 2003: 107(2), 317-322.

Chapter 8

TNFα mediates homogenous distribution of liposomes in murine melanoma that contributes to a better tumor response

Ann L.B. Seynhaeve
Saske Hoving
Debby Schipper
Cindy E. Vermeulen
Gisela aan de Wiel-Ambagtsheer
Sandra T. van Tiel
Alexander M.M. Eggermont
Timo L.M. ten Hagen

Cancer Research. 2007; 67(19), 9455-9462

Research article

TNF-α mediates homogenous distribution of liposomes in murine melanoma that contributes to a better tumor response

Ann L.B. Seynhaeve, Saske Hoving, Debby Schipper, Cindy E. Vermeulen, Gisela aan de Wiel-Ambagtsheer, Sandra T. van Tiel, Alexander M.M. Eggermont, and Timo L.M. ten Hagen

Department of Surgical Oncology, Erasmus MC, Rotterdam, The Netherlands

ARTICLE INFORMATION

Cancer Research. 2007; 67(19), 9455-9462

ACKNOWLEDGMENTS

We thank Dr. Gerben Koning for his insightful suggestions and thoughtful comments on the manuscript; Dr. Kirsten Kullak for the provision of TNF and Dr. Peter Working for the chemicals needed for the preparation of the liposomes; Joost Rens for his assistance in the dorsal skin-fold chamber model. This study was supported by grant DDHK 2000-2224 of the Dutch Cancer Society and a grant of the Foundation "Stichting Erasmus Heelkundig Kankeronderzoek".

ABSTRACT

Successful treatment of solid tumors with chemotherapeutics requires that adequate levels reach the tumor cells. Tumor vascular normalization has been proposed to enhance drug delivery and improve tumor response to chemotherapy. Differently, augmenting leakage of the tumor-associated vasculature, and as such enhance vascular abnormality, may improve tumor response as well. In the present study we show that addition of low-dose tumor necrosis factor-alpha (TNF) to systemic injections with pegylated long circulating liposomes, augmented the tumor accumulation of these liposomes 5 to 6-fold which strongly correlated with enhanced tumor response. Using intravital microscopy we could study the liposomal distribution inside the tumor in more detail. Especially 100 nm liposomes effectively extravasate in the surrounding tumor tissue in the presence of TNF and this occurred without any effect on tumor vascular density, branching and diameter. Next to that, we observed in living animals that tumor cells take up the liposomes intact, followed by intracellular degradation. To our knowledge this is an unprecedented observation. Taken together, TNF renders more tumor vessels permeable, leading to a more homogeneous distribution of the liposomes throughout the tumor, which is crucial for an optimal tumor response. We conclude that delivery of nano-particulate drug formulations to solid tumor benefits from augmenting the vascular leakage through vascular manipulation with vasoactive drugs like TNF.

INTRODUCTION

Delivery of drugs in solid tumors is still a major problem faced in chemotherapy and frequently responsible for failure of initially promising agents. It is well recognized that the pathophysiology of the tumor vasculature and stromal compartment presents a important obstacle [1]. This inadequate drug delivery leads to poor responses and regrowth of tumors. Several studies have shown that encapsulation of anticancer agents in pegylated long circulating liposomes can reduce systemic toxicity while retaining or even improving *in vivo* efficacy [2-4]. Because of their small size, long circulation time, and reduced interaction with serum proteins, these liposomes tend to accumulate in tumors, presumably due to leakage

through the often-compromised tumor vasculature [5,6].

Recently, a combination of tumor vascular therapy with chemotherapy gained interest. Administration of the anti-VEGF compound bevacizumab improved tumor response and survival in patients with metastatic colorectal cancer when used in combination with 5-fluorouracil/leucovorin [7,8]. While anti-VEGF therapy is thought to have its effect through inhibition of angiogenesis, the tumor vascular normalization inflicted by bevacizumab has been proposed as a major contribution to the observed clinical outcome [9,10]. Also, tumor vascular manipulation, next to destruction or inhibition, may be a useful approach in solid tumor chemotherapy. We propose that apposed to tumor vascular normalization, further abnormalization, in particular vascular leakage, as well may benefit chemotherapy [11]. Indeed, administration of TNF, histamine or interleukin-2 improved local drug delivery and tumor response [12-14]. An augmented vascular permeability and disruption of the vascular lining was the crucial observation in all these settings. With respect to TNF, we showed in previous studies that co-administration of liposomal doxorubicin (Doxil) and TNF resulted in a drug accumulation accompanied by pronounced tumor response in both rat and murine tumor models [15,16]. Also in the isolated limb perfusion (ILP), in which TNF is co-administered with a chemotherapeutic agent for the treatment of patients with limb threatening tumors, addition of TNF results in increased accumulation of drug inside the tumor accompanied by improved response rates [14,17]. TNF is likely to augment the leakiness of the vasculature by increasing the gaps in the endothelial lining, leading to improved extravasation of chemotherapeutic drugs into the tumor interstitium [18].

The goal of this present investigation was to dissect the effect of tumor vascular manipulation by TNF on intratumoral distribution of pegylated long circulating liposomes. For this we used labeled liposomes from different sizes and performed intravital microscopy in the mouse dorsal skin-fold chamber for a detailed insight in the intratumoral localization of the administered liposomes. Here we show that TNF not only increases the leakiness of some tumor vessels but also renders more vessels permeable to liposomes while leaving the vascular function (e.g. flow) intact. As a result a more homogeneous drug distribution in the tumor is reached explaining an improved tumor response.

EXPERIMENTAL PROCEDURES

Agents. Recombinant murine tumor necrosis factor-alpha (mTNF), with a specific activity of 3 x 10^7 U/mg and endotoxin levels below 1 units (EU) per mg protein [19] was kindly provide by Boehringer Ingelheim GmbH. Doxorubicin hydrochloride (Adriblastina) was purchased from Pharmachemie and pegylated long circulating liposomal doxorubicin (Doxil/Caleyx) was purchased from Schering-Plough.

Preparation of long circulating liposomes. For the preparation of liposomes following chemicals were used; partially hydrogenated egg phosphatidyl choline (PHEPC; lipoid GMbH), cholesterol (Sigma) and distearoyl phosphatidylethanolamine poly-(ethyleneglycol) (PEG-DSPE; ALZA Corporation) in a molar ratio of 1.85:1:0.15. Liposomes of 100 nm were prepared by sonication as described before [20]. Liposomes of 400 nm and 800 nm were obtained by multiple extrusions through polycabonate membranes (Nuclepore) with corresponding pore size. Liposomes were labeled with Gallium^{67} citrate (Nordian) according to Gabizon *et al.* [21]. Long circulating rhodamine liposomes (Rho-PEG-L) were composed of PHEPC, cholesterol and PEG-DSPE in a molar ratio of 1.85:1:0.15 and labeled with 0.1 mol% of the fluorescent bilayer marker lissamine-rhodamine-phosphatidyl-ethanolamine (Molecular Probes). The exact size was measured by dynamic light scattering (DLS, Malvern 4700 system, Malvern) and the amount of lipid was determined according to Bartlett [22]. Doxil-DiO liposomes were produced by incubating Doxil with 0.2 mol% of the lipophilic tracer dioctadecyloxacarbocyanine perchlorate (DiO-C_{18}(3)) (Molecular Probes) during 10 min at room temperature and sonicated for 20 sec.

Animals and tumor model. Specific pathogen-free female C57BL/6 mice were purchased from Harlan-CPB, weighing about 20 grams, and were fed a standard laboratory diet ad libitum (Hope Farms). The B16BL6 melanoma tumor model was used for this study. All animal studies were done in accordance with protocols approved by the committee on Animal Research of the Erasmus MC, Rotterdam, the Netherlands.

Treatment protocol. Experiments were started when the subcutaneous transplanted B16BL6 tumors reached a diameter of 8-10 mm. For tumor response, mice were randomized into the following 4 groups: saline, mTNF, Doxil and Doxil immediately followed by injection of mTNF. Mice were injected five times in the tail vein with an interval of 4 days between the injections; first dose of 4.5 mg/kg Doxil and 1.0 mg/kg for consecutive doses. Murine TNF in a dose of 1 µg/mouse, which is well tolerated in mice without any side effects, was given for all five treatments. Tumor growth was recorded by caliper measurement and volumes calculated using the formula 0.4 x (A^2 x B) where B represents the largest diameter and A the diameter perpendicular to B). The tumor size is expressed as tumor size index, i.e. the tumor volume in relation to initial tumor volume. For biodistribution studies and determination of doxorubicin levels in serum, mice were injected via the tail vein with 48 µmol/kg ^{67}Ga-labeled liposomes or 1 mg/kg Doxil in combination with saline or mTNF (1 µg/mouse). After sacrifice, tumor and tissues were collected, weighed, and counted in a Beckmann 8000 gamma counter and data are expressed as percentage of injected dose per gram tissue. Serum samples were collected by cardiac puncture before sacrifice. A Hitachi F4500 fluorescence spectrometer (excitation 472 nm and emission 590 nm) was used for measurement of the samples as previously described [16,23].

Biodistribution using the dorsal skin-fold chamber. Preparation of the dorsal skin-fold chamber is an adaptation from previously described procedures [24-26]. Briefly, mice were anesthetized (100 µl of a 2:1:1 (v:v:v) mixture of saline, ketamine and xylazine) and hair was removed from the back of the animal. After dissecting the skin, leaving the fascia and opposing skin, the skin-fold of the mouse was sandwiched between two frames, fixed with two light metal bolds and sutures. A small piece of tumor (0.1 mm^3) was transplanted in the fascia and on both sides the window was closed with a 12 mm diameter microscopic cover glass of 0.13-0.16 mm thick. The mice were housed in an incubation room with an ambient temperature of 32°C and a humidity of 70%. Experiments started 10 to 14 days after implantation of the dorsal skin-fold chamber. Mice were injected via the tail vein with 4.5 mg/kg doxorubicin, 4.5 mg/kg Doxil-DiO or 48 µmol/kg Rho-PEG-L immediately followed by injection with saline or mTNF (1 µg/mouse).

Fluorescent imaging. At given time points, mice were anesthetized and fixed to the heated microscope stage of a Zeiss LSM 510 META confocal microscope. Injection of 50 µl FITC-BSA (1 mg/ml, Sigma) allowed visualization of functional vessels. Randomly selected tumor regions were examined with 20x (NA 0.5) long working distance objective lens and detailed examination was performed using 40x water emersion objective lens (NA 0.8). Scans were made with a 488 argon laser for DiO and FITC-BSA (505-550 nm band pass filter) and a 543 nm Helium-Neon laser for doxorubicin/Doxil and rhodamine (560-615 nm band pass filter). Vessel morphology such as vessel density (the area of vessels as percentage of the total field of interest), vessel segments (the number of vessels connected to each other at the branching point) and diameters were analyzed using the Zeiss LSM Image Browser 4.0 software. Images were analyzed using Image Tool (Don Wilcox, University of Texas Health Science Center). The RGB color images of 512 x 512 pixels were converted to grayscale in Image Tool. The fluorescence intensity ranged form 0 to 255 and we distinguished specific staining from background using a threshold of 45. The proportion of pixels with fluorescence intensity above the threshold was calculated. To determine extrava-

sation of liposomes a gridline overlay was applied of 64x64 pixels using Adobe Photoshop 6.0. Extravasation of liposomes was scored by counting the number of times the gridlines intersected with intra- or extravascular presence of liposomes. Second, using a look-up table the fluorescence intensity of the representative grayscale images were converted to a pseudo color spectrum from 0 to 255 and transformed to a surface plot. The heights of the peaks correspond to the fluorescence intensity.

***In vitro* uptake.** B16BL6 melanoma cells were maintained in DMEM supplemented with 10% heat inactivated FCS. Tumor cells were cultured on a cover glass and grown till confluence. The cells were washed and Doxil or doxorubicin was added at a concentration of 5 µg/ml. The cells were placed under a Zeiss LSM 510 META confocal microscope equipped with an incubation chamber, which is maintained at 37°C with controlled CO_2-flow. Every 5 minutes scans were made using the 543 nm laser and 560-615 nm band pass filter.

Statistical analysis. Results were evaluated for statistical significance with the Kruskal Wallis and Mann Whitney U test. All statistical tests were two-sided and P-values below 0.05 were considered statistically significant. Calculations were performed on a personal computer using GraphPad Prism v3.0 and SPSS v11.0 for Windows 2000.

RESULTS

Addition of TNF improves response to Doxil. To evaluate the antitumor activity of Doxil in combination with low-dose mTNF, B16BL6-bearing mice were treated with saline, mTNF, Doxil and Doxil in combination with mTNF (**Table 1**). Combination of Doxil with mTNF resulted in a tumor growth arrest and all mice were still in the treatment at the end of the experiment. Control and mTNF treated mice showed progressive disease and had to be sacrificed between day 8 and 12. Treatment with Doxil alone showed some tumor response and at the end of treatment 33% of the mice had a tumor size index smaller than 4.

Addition of TNF increases accumulation of liposomes in the tumor. We speculated that the observed improved tumor response was not due to a direct effect of mTNF on the tumor cells. First, mTNF by itself has no effect on tumor progression. Second, the concentration of mTNF, which can theoretically be reached in the tumor, is too low to have a direct effect on these tumor cells (data not shown). Therefore we studied whether mTNF augmented liposomal delivery in the tumor. The results show a 6.3-fold increased accumulation of 100 nm liposomes in the tumor 12 hours after co-administration with mTNF compared to liposomes alone ($P < 0.05$), and a 5.5-fold increase after 24 hours ($P < 0.05$) (**Fig. 1a**). Co-administration of mTNF and 400 nm liposomes resulted in a 5.1-fold enhanced accumulation at 12 hours ($P < 0.05$) and 9.2-fold at 24 hours ($P < 0.01$) compared to liposomes alone. In case of 800 nm

Table 1. Tumor response after systemic treatment of B16BL6-bearing mice.

Treatment	Response of B16BL6 melanoma (tumor size index)				% mice with TSI < 4
	Day 4	Day 8	Day 12	Day 16	Day 16
Saline	2.4 ± 0.3	2.8 ± 0.8	-	-	0
mTNF	2.3 ± 0.8	3.2 ± 0.1	-	-	0
Doxil	2.1 ± 0.8	3.0 ± 1.0	4.0 ± 1.5	3.8 ± 0.4	33
Doxil + mTNF	1.3 ± 0.4$^{\#}$	1.4 ± 0.3*$^{\#}$	1.5 ± 0.3*	2.0 ± 0.8*	100

Note: Mice were injected 5 times via tail vein with an interval of 4 days with saline, mTNF, Doxil and Doxil in combination with mTNF and tumor size index (TSI, the tumor volume in relation to the tumor volume at the start of treatment) was calculated.

Data represent tumor size index ± SD of at least 4 individual animals; *, $P < 0.05$ *versus* injection with Doxil alone at the same time point; $^{\#}$, $P < 0.05$ *versus* injection with mTNF alone at the same time point.

liposomes, addition of mTNF did not cause an increased accumulation of these liposomes (4.1 ± 3.7% without mTNF, 3.8 ± 0.9% with mTNF, data not shown). Accumulation of 400 and 800 nm liposomes in tumor was significantly lower compared to 100 nm liposomes, even in the presence of mTNF, indicating the beneficial properties of small liposomes. Besides localization in tumor, liposomal distribution to other organs was investigated. In the spleen, mTNF did not increase uptake of all three liposome sizes. Only in hart and liver we observed a slight increase op liposomal uptake with the addition of mTNF with could potentially give an increase in cardiotoxicity (data not shown). Twelve hours after injection 51 ± 25% of the liposomes were still present in the blood circulation whereas free doxorubicin was hardly measurable (2.7 ± 0.9%, data not shown). Even after 72 hours still 15 ± 2% of the liposomes were measured in the circulation. With the addition of mTNF a lower liposomal percentage ($P < 0.05$) was found in the blood circulation (25 ± 18% for 12 hours and 6 ± 4% for 72 hours) (**Fig. 1b**). Liposome accumulation is selectively augmented in the tumor by the addition of mTNF and is the main cause of the increased clearance from the circulation.

Addition of TNF improves extravasation and homogenous distribution of 100 nm long circulating liposomes. Ten days after tumor implantation in the dorsal skin-fold chamber a tumor size of 4 to 5 mm was reached. Few supplying vessels could be observed. Unlike the normal blood vessels around the tumor, the newly formed vessels are not well organized. They display tortuous structure, frequent branching and irregular diameters (**Supplementary Fig. 1**). Clearly, addition of a tolerable dose of mTNF resulted in augmented liposome accumulation in tumor. However, it is still unclear how TNF affects the tumor vascular lining. Moreover, insight in the intratumoral localization of the liposomes is lacking. Therefore we studied the effect of mTNF on intra-

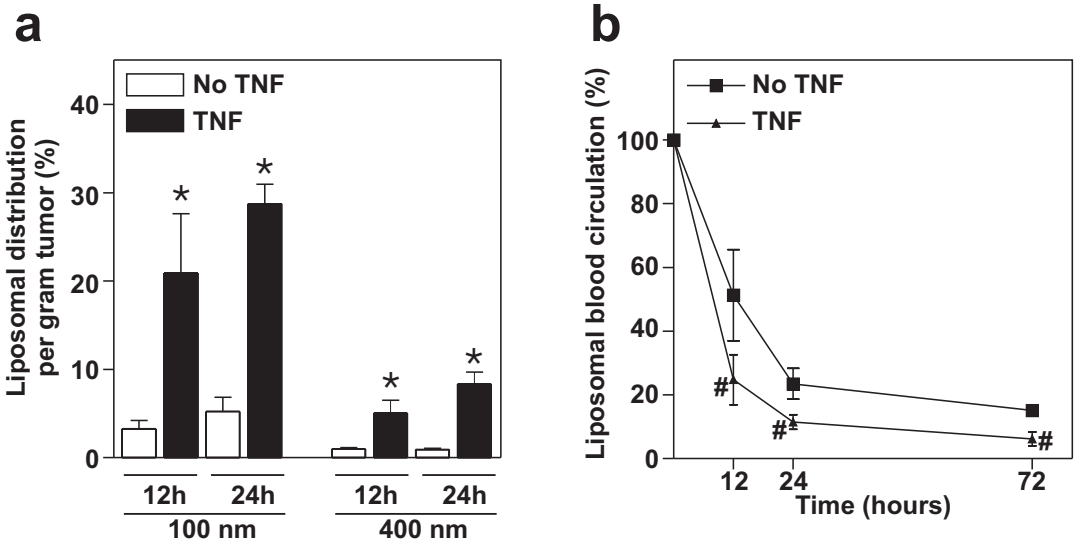

Figure 1. Addition of TNF increases uptake of long circulating liposomes in tumor tissue. (**a**) The effect of mTNF on ^{67}Ga-labeled liposome distribution of different sizes was analyzed 12 or 24 hours after systemic injection. Addition of mTNF increased tumor localization of liposomes significantly. Columns represent percentage liposomes per gram tumor tissue ± SEM of at least 3 individual animals; #, $P < 0.01$; *, $P < 0.05$ *versus* no mTNF of the same time point. (**b**) Analysis of Doxil in the blood circulation after systemic injection in combination with saline or mTNF. Twelve hours after injection significantly less liposomes were found in the blood circulation. Data points represents percentage liposomes in the blood circulation ± SD of at least 3 individual animals; *, $P < 0.05$ *versus* no TNF of the same time point.

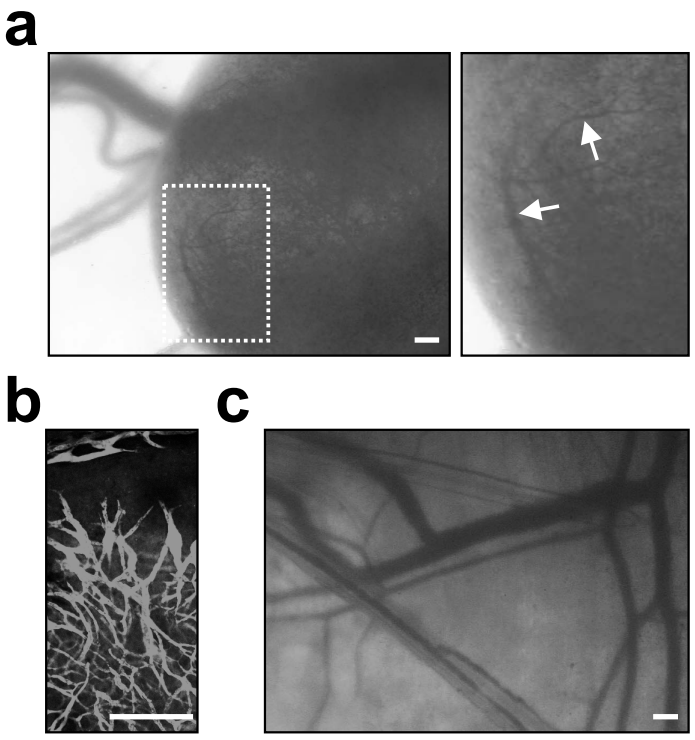

Supplementary Figure 1. Intravital microscopy reveals profound intratumoral vascularization in the B16BL6 model. Ten days after tumor implantation in the dorsal skin-fold chamber the tumor growth and vasculature were visualized. (**a**) While some newly formed blood vessels originating from the surrounding normal vasculature feed the B16BL6 tumor, abundant intratumoral branches were observed (magnification, arrow). (**b**) For a better visualization in the B16BL6 tumor, FITC-BSA was injected and a chaotic, branched tumor vasculature is observed in the tumor. (**c**) The pattern of the normal vasculature displayed minimal branching, even vessel diameter and a definable direction. Scale bar apply to all images, 250 µm. (See color section for a full-color version.)

tumoral distribution of liposomes with the use of intravital microscopy. We first investigated extravasation of Rho-PEG-L with a size of 100 nm. We observed hardly any extravasation when only Rho-PEG-L was administered. Interestingly, when liposomes were found, these appeared accumulated in tumor vessels. Addition of mTNF resulted in abundant extravasation of liposomes into the tumor interstitium (**Supplementary Fig. 2**). Only in a few areas liposomes were still present inside blood vessels. Twenty-four hours after injection of liposomes and mTNF, 50 µl FITC-BSA was administered intravenously to visualize functionality and permeability of blood vessels. With the addition of mTNF, FITC-BSA extravasated at the same spot as the liposomes indicating that these vessels were still leaky. At higher magnification we observed that FITC-BSA positive vessels were quite permeable for 100 nm liposomes. This indicates that liposomes extravasated from blood vessels that remained functional in spite of their increased leakiness (**Fig. 2a**). Surface plots of the liposomal fluorescence showed fluorescence peaks representing intravascular liposomes. Addition of mTNF resulted in broad areas with high fluorescence intensity representative of massive liposome extravasation (**Fig 2b**). Without mTNF the incidence that a liposome was found intravascular was 70 ± 16% and 74 ± 12% after 12 and 24 hours respectively. With the addition of mTNF hardly any liposomes could be found inside the vessels anymore (2 ± 2% after 12 hours and 1 ±

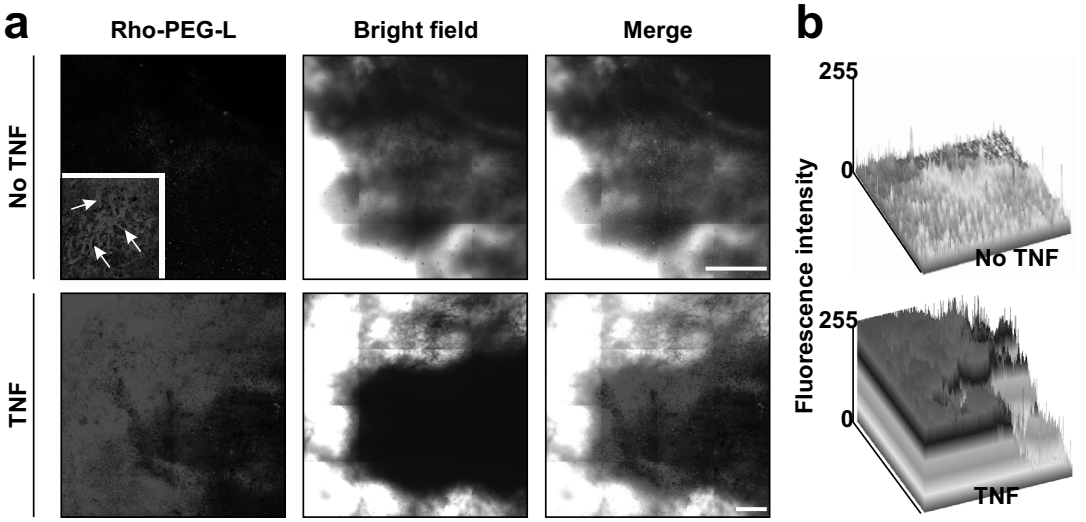

Supplementary Figure 2. Addition of TNF leads to an increased accumulation of long circulating liposomes (Rho-PEG-L) in the tumor tissue. Intravital microscopy scans of the B16BL6 melanoma were compared to illustrate the effect of mTNF on the liposomal uptake after systemic administration. (**a**) Hardly any liposomes were observed in the tumor tissue. Only in a few regions liposomes were seen intravascular (insert, arrow). Addition of mTNF clearly inflicted a homogenous intratumoral accumulation of liposomes. Scale bar apply to all images, 500 µm. (**b**) The increase in height of the fluorescence intensity peaks of the surface plots illustrates increased accumulation of liposomes when combined with mTNF. (See color section for a full-color version.)

1% after 24 hours) (**Fig. 2c**). Microvascular parameters were determined by intravital microscopy when the tumors were treated. Addition of mTNF had no effect on vessel density, number of segments and diameter, indicating that accumulation of liposomes was not the result of a change in vessel number or size (**Supplementary Table. 1**). Summarizing, the addition of mTNF caused an increased extravasation of 100 nm liposomes into the tumor interstitium in a more homogeneous way. Less liposomes were trapped inside blood vessels when mTNF was co-administered. These results indicate that administration of mTNF results in an increase in the number of leaky vessels.

Addition of TNF did not alter the intratumoral distribution of 400 nm long circulating liposomes. It has been shown previously that tumor vessel are permeable for transport of macromolecules with a maximum size of 400 nm, suggesting a cutoff size of the pores somewhere between 400 to 600 nm [27]. Strikingly, as shown above, most tumor vessels of the B16BL6 melanoma did not allow extravasation of the 100 nm liposomes, whereas addition of mTNF clearly affected the gap size. To investigate if mTNF has a comparable effect on intratumoral distribution of larger liposomes, Rho-PEG-L of 400 nm were injected. Without mTNF liposomes became mostly trapped inside blood vessels, rendering these vessels non-functional as no intravascular presence of FITC-BSA could be observed. Addition of mTNF enhanced the extravasation of liposomes only slightly, mostly at the periphery of the tumor (**Fig. 3a** and **Supplementary Fig. 3**). Analysis of the fluorescence intensity showed a 2-fold increase of intratumoral localization of liposomes due to the addition of mTNF (**Fig. 3b**). However, less then 10% of the liposomes were present in the surrounding tumor tissue even when co-administered with mTNF (**Fig. 3c** and **Fig.3d**). These results indicate a diminished usefulness of the 400 nm liposomes as compared to li-

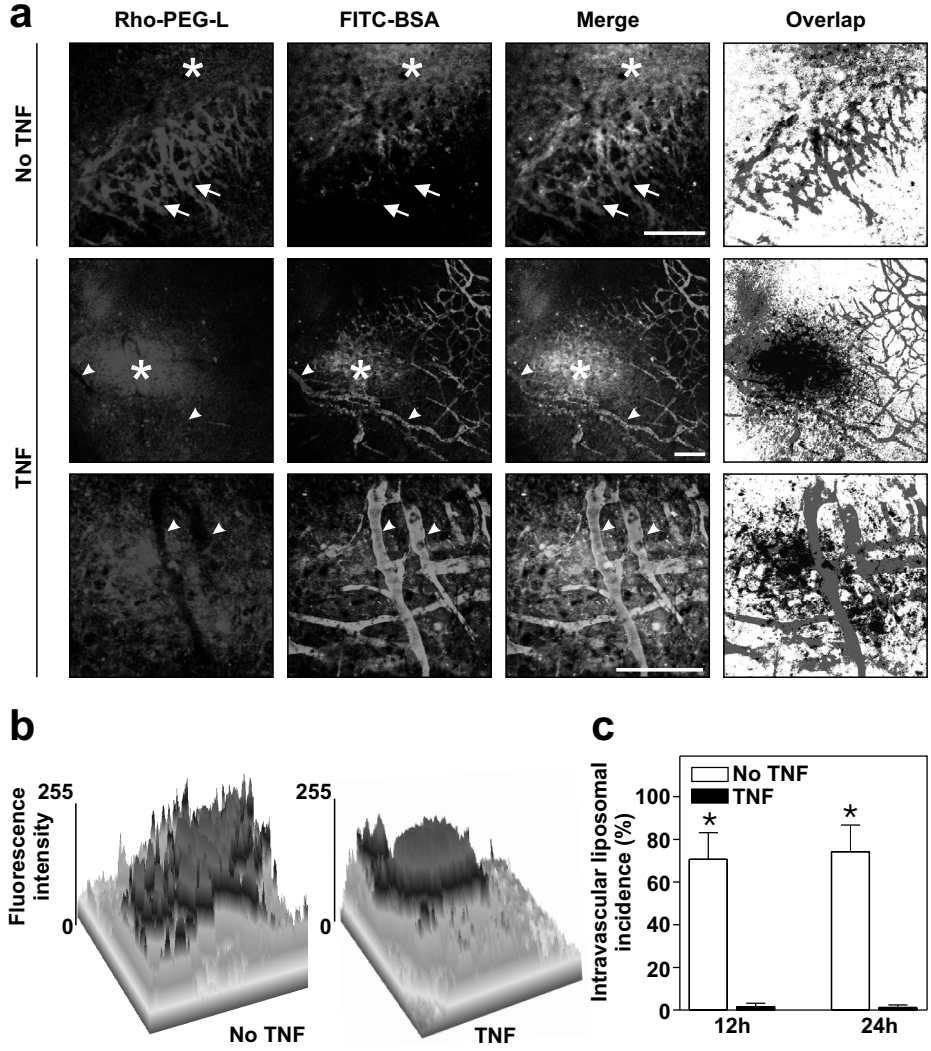

Figure 2. Addition of TNF promotes liposomal extravasation through hyperpermeable vessels. The effect of mTNF on tumor distribution of systemically injected long circulating liposomes (Rho-PEG-L) was studied by intravital microscopy. Twelve or 24 hours later mice were injected with FITC-BSA to visualize functional vessels. (**a**) In mice injected with Rho-PEG-L alone, some liposomes were seen in the surrounding tumor tissue (asterix), but predominantly in the blood vessels. In blood vessels filled with liposomes no green FITC-BSA fluorescence could be seen (arrow), indicating that these intravascular liposomes were obstructing the blood flow. When mTNF was added, liposomal extravasation was observed at sites were also FITC-BSA leaked out (asterix), indicating that mTNF rendered the vessels hyperpermeable for liposomes. FITC-BSA was seen in the tumor vessels (arrowhead) indicating intact functionality. These blood vessels seemed deprived of liposomes suggesting that all liposomes had extravasated into the surrounding tumor tissue. Scale bar apply to all images, 200 μm. (**b**) Surface plots show high intensity peaks in the tumor vessels when liposomes alone were given. Consistent with the confocal pictures, surface plot of images from mice injected with liposomes combined with mTNF show high fluorescence intensity at hyperpermeable sites in the tumor. (**c**) After calculation of the incidence that a liposome was found inside a vessel, a strong reduction in intravascular presence was found when mice were injected in combination with mTNF. Columns represent percentage liposomes found intravascular ± SEM of at least 6 scans of 5 individual animals; #, $P < 0.01$ *versus* no mTNF of the same time point. (See color section for a full-color version.)

Supplementary Table 1. Vessel morphology after treatment with saline or mTNF.

	12 hours		24 hours	
	Saline	mTNF	Saline	mTNF
Density [a]	13.0 ± 3.1	22.4 ± 5.0	22.0 ± 1.6	20.1 ± 2.0
Segments [b]	76 ± 9	96 ± 11	139 ± 20*	122 ± 26
Diameter [c]	16.8 ± 1.1	18.5 ± 0.6	17.8 ± 0.8	18.9 ± 1.0

Note: After the B16BL6 melanoma, implanted in the dorsal skin-fold chamber, established its own blood supply, mice were injected with saline or mTNF (1 µg/mouse). Twelve or 24 hours later vessel morphology was examined. Data represent the mean ± SEM of at least 6 scans in at least 3 individual animals; *, $P < 0.05$ *versus* 12 hours of the same treatment.

[a] Percentage of total vessel area per field of interest at magnification 20x.

[b] Number of vessels per mm^2.

[C] Vessel diameter (µm).

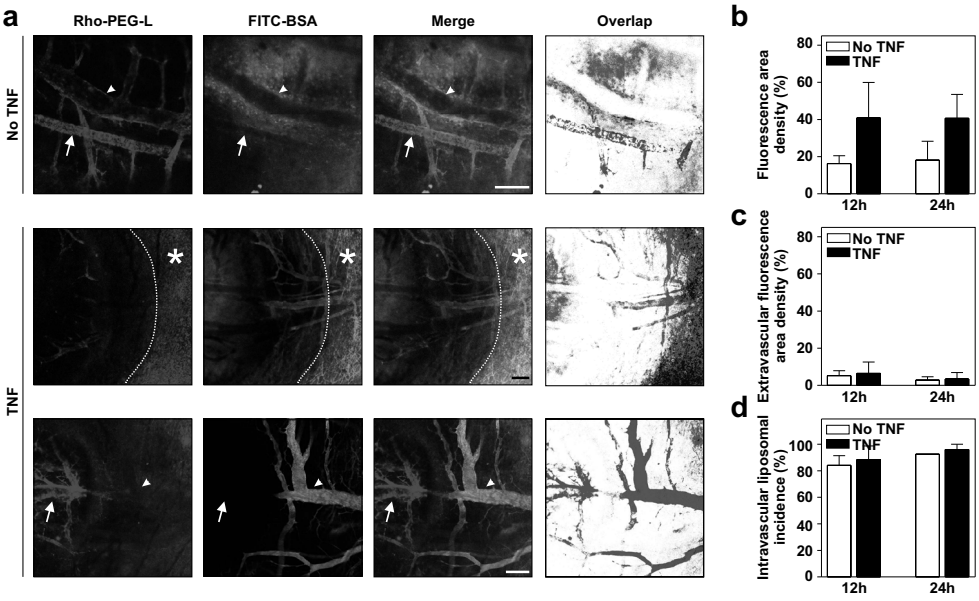

Figure 3. Addition of TNF does not render the tumor blood vessels permeable for 400 nm liposomes. Tumor distribution of systemic injection with long circulating liposomes (Rho-PEG-L) of 400 nm in combination with saline or mTNF using intravital microscopy was studied. Twelve or 24 hours later mice were injected with FITC-BSA to visualize functional vessels. (**a**) In mice injected with liposomes, even with the addition of mTNF, hardly any extravasation into the surrounding tumor tissue could be seen. Only at the rim of the tumor (dotted line) accumulation of liposomes could be observed (asterix). In some vessels liposomes were found to remain inside a FITC-BSA permeable tumor vessel (arrowhead). When vessels were filled with liposomes these vessel became non-functional (arrow). Scale bar apply to all images, 200 µm. (**b**) Although more 400 nm liposomes were found in the tumor with the addition of mTNF, levels were much lower compared to 100 nm liposomes. Columns represent percentage fluorescent area density ± SEM of at least 6 scans of 3 to 4 individual animals. (**c**) After calculation of the extravascular fluorescent intensity hardly any liposome could be measured outside the vessels, indicating that even with the addition of mTNF 400 nm liposomes remained trapped in the tumor vessels Columns represent percentage extravascular fluorescent area density ± SEM of at least 6 scans of 3 to 4 individual animals. (**d**) The incidence that a liposome was found inside the vessel no difference was found between the two treatment groups. Also when mTNF was co-administered liposomes were predominantly found inside the tumor vessels. Columns represent percentage liposomes found intravascular ± SEM of at least 6 scans of 3 individual animals. (See color section for a full-color version.)

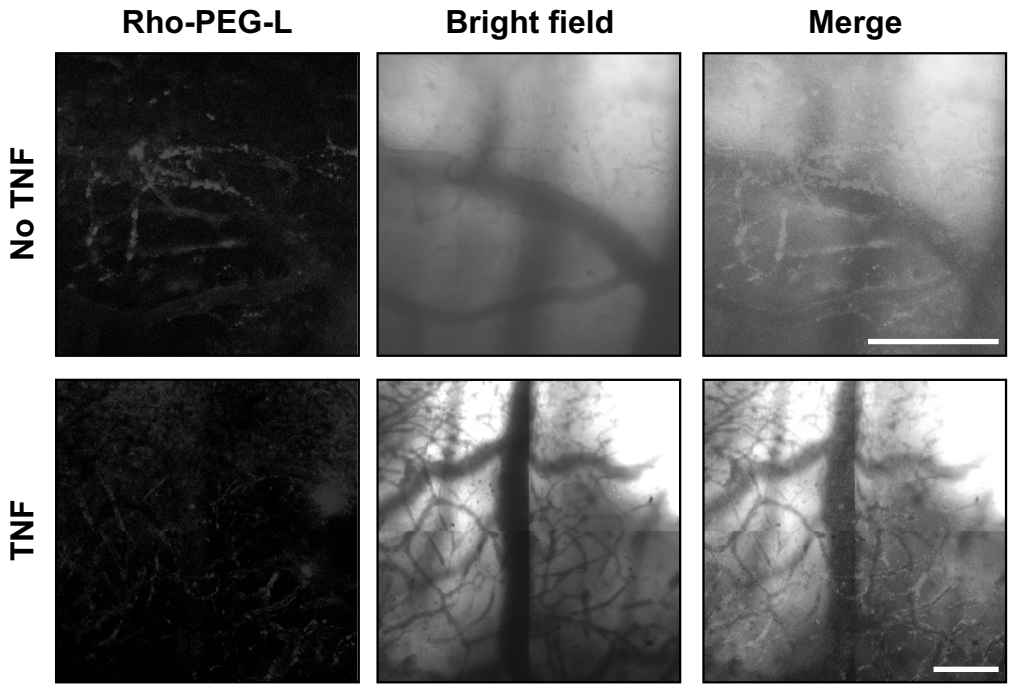

Supplementary Figure 3. Addition of TNF does not render the tumor blood vessels permeable for 400 nm liposomes. Tumor distribution of systemic injection with long circulating liposomes (Rho-PEG-L) of 400 nm in combination with saline or mTNF using intravital microscopy was studied. In mice injected with liposomes hardly any extravasation into the surrounding tumor tissue could be seen even with the addition of mTNF. The image overlay shows that obstruction of the 400 nm liposomes is found in the chaotic tumor related vessels. Scale bar apply to all images, 200 μm. (See color section for a full-color version.)

posomes of 100 nm for the treatment of solid tumors, also in combination with mTNF.

Addition of TNF improves uptake of liposomal doxorubicin but not of free doxorubicin. It is known from previous studies that total drug accumulation of free doxorubicin in tumor tissue is rather low compared to Doxil [15]. In the present study we examined the intratumoral distribution of free doxorubicin and Doxil. Doxil is labeled with DiO to distinguish between localization of the liposome and doxorubicin, which is red fluorescent. When free doxorubicin was administered, either with or without mTNF, hardly any drug was detectable in the tumor and if any extravasation could be observed it occurred at the highly vascularized rim of the tumor (**Fig. 4a**). Limited, focal and heterogeneous extravasation of Doxil was observed especially at the tumor periphery when injected alone. Addition of mTNF dramatically enhanced extravasation of Doxil (**Fig. 4b**). Significantly more liposomes (7.1-fold increase after 12 hours, $P < 0.01$ and 3.1-fold increase 24 hours after injection, $P < 0.05$) were present extravascular in the tumor tissue when mTNF was co-administered (**Fig. 4c**). Administration of mTNF augmented total liposomal accumulation 4.7-fold only at 12 hours after injection ($P < 0.01$) (**Supplementary Fig. 4**). Although liposomes did not penetrate far into the tumor tissue, abundant extravasation could be observed already at 12 and 24 hours after injection (**Fig. 4d**).

Doxil is taken up intact by the tumor cell and degraded intracellular. Insight in the intratumoral fate of liposomal doxorubicin is lim-

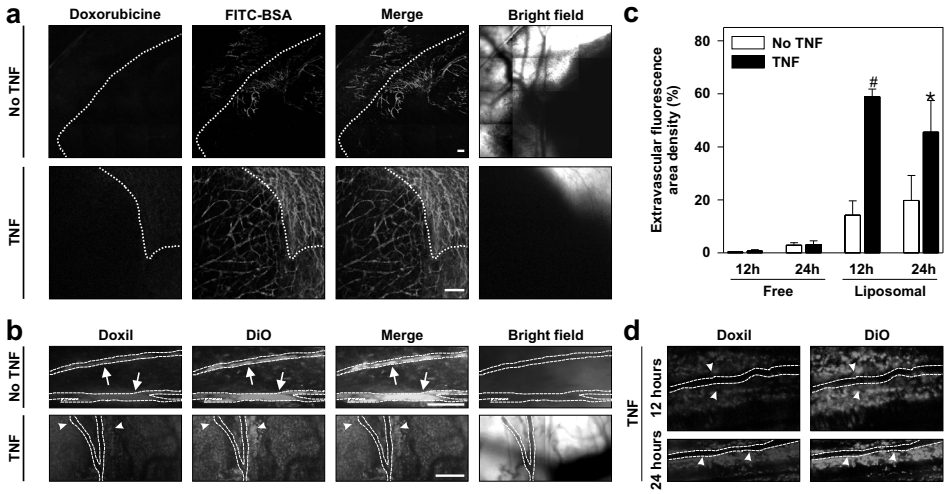

Figure 4. Addition of TNF provokes extravasation of long circulating liposomes. Tumor distribution of doxorubicin and Doxil was studied using intravital microscopy. Twelve hours after administration of doxorubicin, mice were injected with FITC-BSA to visualize functional vessels. In the case of Doxil, the liposomal component was labeled with a fluorescent marker DiO. B16BL6 melanoma-bearing mice were injected with doxorubicin or Doxil-DiO in combination with saline or mTNF. (**a**) In mice treated with doxorubicin, 12 hours later hardly any drug could be observed in the tumor tissue (dotted line = rim of the tumor) even in the presence of mTNF, although the vessels were functional. (**b**) When Doxil-DiO alone was administered, liposomes were observed in the vessels (arrows) and surrounding tissue. However, when Doxil-DiO was combined with mTNF massive extravasation of Doxil from the blood vessels (dotted line) into the tumor interstitium was observed (arrowheads). (**c**) After calculation of the extravascular fluorescent intensity a significant increase was found 12 hours and 24 hours after injection in combination with mTNF. Columns represent percentage extravascular fluorescent area density ± SEM of at least 6 scans of 5 individual animals; #, $P < 0.01$; *, $P < 0.05$ *versus* no mTNF at the same time point. (**d**) Twelve and 24 hours after administration of Doxil in combination with mTNF empty vessels (dotted line) were observed surrounded by extravasated liposomes (arrowheads). Scale bar apply to all images: 200 µm. (See color section for a full-color version.)

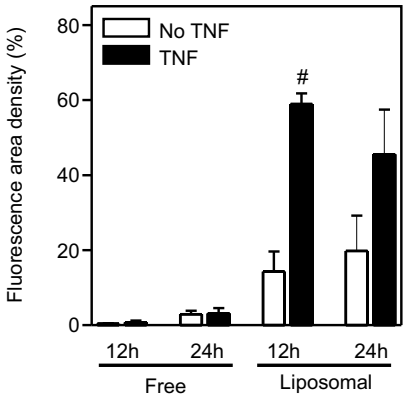

Supplementary Figure 4. Addition of TNF provokes extravasation of long circulating liposomes. Tumor distribution of doxorubicin and Doxil 12 hours after administration was studied using intravital microscopy. After calculation of the fluorescence area density of these pictures hardly any free doxorubicin in the tumor could be detected, even with the addition of mTNF. Murine TNF significantly increased Doxil accumulation 12 hours after injection. Columns represent percentage fluorescent area density ± SEM of at least 6 scans of 5 individual animals; #, $P < 0.01$ *versus* no mTNF of the same time point.

ited. Doxorubicin containing liposomes, such as Doxil, are relatively rigid and only slowly release their content resulting in a prolonged exposure of the tumor cells to the drug. However, this also means that low or moderate peak levels of free drug are reached. Elucidation of the liposomal fate and release of contents is useful for drug delivery strategies, certainly if controlled degradation of these carriers is applied [28]. Here, we observed *in vivo* that after extravasation of Doxil-DiO into the interstitial space, the liposomes were taken up as such by the tumor cells. Thirty-six hours after injection of Doxil-DiO in combination with mTNF a separation of the two dyes (DiO and doxorubicin) was observed and transport of doxorubicin to the nucleus of the tumor cells could be detected, while the lipid marker remained in the cytoplasm (**Fig. 5a**). These results indicate that presumably most liposomes are taken up intact by the cells and broken down in the cytoplasm. Also *in vitro* uptake of doxorubicin or Doxil by

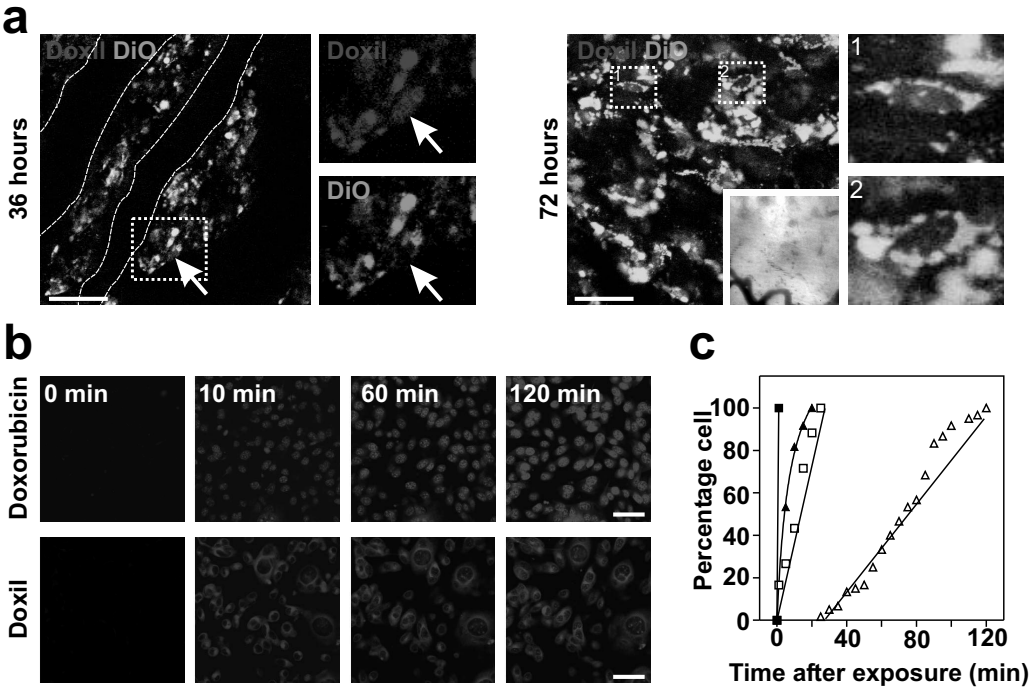

Figure 5. The complete liposome is taken up by the tumor cell and broken down in the cytoplasm. Using intravital microscopy the cellular uptake of Doxil was observed. (**a**) Thirty-six hours after systemic injection of Doxil-DiO, the liposomes (yellow) were seen in the cytoplasm of the tumor cell, whereas only doxorubicin (red) could be observed in the nucleus (arrow). At higher magnification, doxorubicin (red, arrow) was seen in the nucleus while the liposome (green, arrow) was only found in the cytoplasm. Also 72 hours after systemic injection the red fluorescent of doxorubicin in the nucleus of the tumor cell and the yellow fluorescent of the complete liposome inside the cytoplasm could still be observed. (**b**) For better understanding of the uptake of doxorubicin in the B16BL6 melanoma cell, cells were incubated with doxorubicin or Doxil and time-lapse microscopy was performed. Doxorubicin was immediately taken up by the cell and transported to the nucleus. On the other hand, Doxil took much longer to occur in the cytoplasm. Scale bar apply to all images; 200 µm. (**c**) The percentage B16BL6 cells positive for doxorubicin in the cytoplasm (■) and nucleus (▲) after incubation with free doxorubicin or in the cytoplasm (□) and nucleus (Δ) after incubation with Doxil were calculated. Very rapidly all cells had taken up the doxorubicin and stained positive for nuclear doxorubicin. In case of cells incubation with Doxil, doxorubicin was observed in the cytoplasm much later compared to the administration of free drug. Transport from the cytoplasm to the nucleus also took much longer. Data points represent the percentage cells that are positive for doxorubicin. (See color section for a full-color version.)

tumor cells was studied. Free doxorubicin was immediately taken up by the cells and directly transported to the nucleus. Twenty minutes after incubation all cell stained positive for nuclear doxorubicin. When B16BL6 cells were exposed to Doxil, accumulation of this drug in the cytoplasm was observed after 15 min. A marginal intracellular transport of doxorubicin to the nucleus was observed in a period of 2 hours (**Fig. 5b** and **Fig. 5c**). Uptake by cells as well as intracellular transport of doxorubicin was not affected by mTNF (data not shown). These results confirm our observations *in vivo* and indicate that Doxil is taken up intact by the tumor cells and remains predominantly in the cytoplasm, while intracellular breakdown is slow.

DISCUSSION

Here we demonstrate that addition of low-dose TNF to systemic administration of pegylated long circulating liposomes facilitates extravasation of these liposomes in solid tumor. Strikingly, this is in particular observed when liposomes of 100 nm are used, while larger liposomes, e.g. 400 and 800 nm, hardly extravasate, even in the presence of TNF. Our data shows that the permeability of the tumor vasculature is not only very heterogeneous but also does not allow passage of liposomes with a diameter of 400 nm or larger. Intratumoral distribution studies reveal that administration of TNF results in a strongly enhanced and more homogeneous distribution of the co-injected liposomes. These results indicate that more vessels become permeable with the administration of TNF. Next to this we show, and to our knowledge for the first time, by intravital microscopy that liposomes are taken up completely by tumor cells, followed by intracellular degradation of the liposomes upon which released doxorubicin enters the nucleus. These findings are confirmed by *in vitro* experiments. These results are in contradiction to the believe that the liposomes are degraded in the interstitial space followed by uptake of the released chemotherapeutic compound by the tumor cells [29].

In spite of promising results *in vitro* or even in animal studies chemotherapeutic agents appeared often disappointing in the treatment of patients. The major prerequisite for a good tumor response is an effective delivery of the systemically injected drug to its target, the tumor cell. However, when injected in the bloodstream many obstacles have to be overcome [30]. Some of these impediments can be obviated with the use of pegylated long circulating liposomes. Unlike free administered drug their liposomal encapsulated counterpart has limited toxicity and gives the drug prolonged circulation half-live, thereby enhancing the efficacy of targeted drug delivery [31,32]. Second, blood flow in a tumor is very heterogeneous due to the abnormal vascular organization. This irregular blood flow leads to well vascularized parts and necrotic/hypoxic parts obstructing the homogenous delivery of a drug [1]. Thirdly, the drug has to leave the circulation and cross the endothelial lining to reach its target, the tumor cell. In general, the endothelial lining of blood vessels forms a tight, uniform and continuous monolayer of cells. However, the endothelial cells in tumor blood vessels do not comply with this phenotype and can best be described as disorganized [33,34]. They appear to be permeable to macromolecules and particles, with a determined cut off of 400 nm [27,35]. The tumor-associated vasculature has become an important target for tumor treatment and several strategies have been reported. (I) The antiangiogenesis approach interferes with the formation of new tumor blood vessels and normalize the existing blood vessels to improve a more effective delivery [36,37]. (II) Vascular disrupting agents inflicts direct damage to the endothelial cells that will initially leads to vascular shutdown [38,39]. (III) Manipulation of the tumor vasculature with vasoactive drugs, like TNF or histamine, causes a better delivery of the co-administered chemotherapeutic drug that act on the tumor cells [14,40].

The main focus of our study is the use of tumor vascular manipulation as an effective way to improve solid tumor treatment. Previously, we demonstrated that addition of TNF to an isolated perfusion with melphalan or doxo-

rubicin dramatically improves tumor response [14,41]. Moreover, also in a systemic setting addition of TNF to liposomal chemotherapy improves tumor response [15,16]. This synergy is not, or at least not solely, due to a direct activity of TNF on the tumor cells and does not result from a direct destruction of the tumor-associated vasculature [17]. More importantly, addition of TNF, both in the perfusion setting as well as in the systemic setting, augmented the accumulation of the co-administered drug in the tumors. Other investigators showed that TNF also enhanced tumor accumulation of liposome-encapsulated adriamycin [42] and radio-labeled antibodies [43]. These findings led to our search for alternative agents with known vascular permeability increasing activity, such as histamine and interleukin-2. We have shown that these agents also enhance drug accumulation in the tumor resulting in synergistic antitumor activity in an isolated setting [13,44]. Apparently this dual approach consisting of a combination of tumor cell and tumor vasculature directed therapy is an important concept for a good tumor response. Although it is known that TNF is capable of increasing the permeability of an endothelial lining, the effect of TNF on tumor vessels in the tumor is largely unknown. Ruegg *et al.* showed that TNF in conjunction with interferon-gamma induced functional down-modulation of the αvβ3 integrin, resulting in detachment and anoikis of the endothelial cells [45]. This possibly explains why tumor vessels, in which αvβ3 exposure is increased, are more responsive to TNF than endothelial cells from healthy vessels, which are quiescent. It has also been shown that TNF in combination with interferon-gamma and peripheral blood mononuclear cells stimulates elongation and gap-formation between endothelial cells, increasing permeability of the endothelial lining [46].

In present study, we demonstrate that low-dose TNF does indeed augment extravasation of liposomes while the endothelial lining is not destroyed and the vessels remain functional. Further investigation is required to determine which type of tumor vessels are affected by TNF and if other components of the vasculature, like pericytes and basal membrane, play a role in this dual regimen. In conclusion, we show that systemically administered low-dose TNF improves drug accumulation in solid tumor by making more vessels permeable to 100 nm liposomes. This results in a more homogeneous drug distribution within the tumor exposing more tumor cells to the drug and causing increased antitumor efficacy. Additionally, we show that the liposomes are taken up intact by tumor cells and are degraded intracellular, releasing the cytotoxic drug. Our results indicate that the dual approach, tumor vascular manipulation, with TNF combined with chemotherapy, has strong potential for solid tumor therapy and necessitates the further development of clinical applicable formulations.

REFERENCES

1.Jain RK. Barriers to drug delivery in solid tumors. Sci Am. 1994: 271(1), 58-65.

2.Lasic DD. Doxorubicin in sterically stabilized liposomes. Nature. 1996: 380(6574), 561-562.

3.Papahadjopoulos D, Allen TM, Gabizon A, Mayhew E, Matthay K, Huang SK et al. Sterically stabilized liposomes: improvements in pharmacokinetics and antitumor therapeutic efficacy. Proc Natl Acad Sci U S A. 1991: 88(24), 11460-11464.

4.ten Hagen TL, Seynhaeve AL, van Tiel ST, Ruiter DJ, and Eggermont AM. Pegylated liposomal tumor necrosis factor-alpha results in reduced toxicity and synergistic antitumor activity after systemic administration in combination with liposomal doxorubicin (Doxil) in soft tissue sarcoma-bearing rats. Int J Cancer. 2002: 97(1), 115-120.

5.Gabizon AA. Selective tumor localization and improved therapeutic index of anthracyclines encapsulated in long-circulating liposomes. Cancer Res. 1992: 52(4), 891-896.

6.Wu NZ, Da D, Rudoll TL, Needham D, Whorton AR, and Dewhirst MW. Increased microvascular permeability contributes to preferential accumulation of Stealth liposomes in tumor tissue. Cancer Res. 1993: 53(16), 3765-3770.

7.Hurwitz H and Kabbinavar F. Bevacizumab combined with standard fluoropyrimidine-based chemotherapy regimens to treat colorectal cancer. Oncology. 2005: 69 Suppl 3, 17-24.

8.Kabbinavar F, Hurwitz HI, Fehrenbacher L, Meropol NJ, Novotny WF, Lieberman G et al. Phase II, randomized trial comparing bevacizumab plus fluorouracil (FU)/leucovorin

(LV) with FU/LV alone in patients with metastatic colorectal cancer. J Clin Oncol. 2003: 21(1), 60-65.
9.Tong RT, Boucher Y, Kozin SV, Winkler F, Hicklin DJ, and Jain RK. Vascular normalization by vascular endothelial growth factor receptor 2 blockade induces a pressure gradient across the vasculature and improves drug penetration in tumors. Cancer Res. 2004: 64(11), 3731-3736.
10.Jain RK. Normalization of tumor vasculature: an emerging concept in antiangiogenic therapy. Science. 2005: 307(5706), 58-62.
11.ten Hagen TL and Eggermont AM. Changing the pathophysiology of solid tumours: the potential of TNF and other vasoactive agents. Int J Hyperthermia. 2006: 22(3), 241-246.
12.Hoving S, Seynhaeve AL, van Tiel ST, Eggermont AM, and ten Hagen TL. Addition of low-dose tumor necrosis factor-alpha to systemic treatment with STEALTH liposomal doxorubicin (Doxil) improved anti-tumor activity in osteosarcoma-bearing rats. Anticancer Drugs. 2005: 16(6), 667-674.
13.Brunstein F, Rens J, van Tiel ST, Eggermont AM, and ten Hagen TL. Histamine, a vasoactive agent with vascular disrupting potential, improves tumour response by enhancing local drug delivery. Br J Cancer. 2006: 95(12), 1663-1669.
14.van der Veen AH, de Wilt JH, Eggermont AM, van Tiel ST, Seynhaeve AL, and ten Hagen TL. TNF-alpha augments intratumoural concentrations of doxorubicin in TNF-alpha-based isolated limb perfusion in rat sarcoma models and enhances anti-tumour effects. Br J Cancer. 2000: 82(4), 973-980.
15.ten Hagen TL, van der Veen AH, Nooijen PT, van Tiel ST, Seynhaeve AL, and Eggermont AM. Low-dose tumor necrosis factor-alpha augments antitumor activity of stealth liposomal doxorubicin (DOXIL) in soft tissue sarcoma-bearing rats. Int J Cancer. 2000: 87(6), 829-837.
16.Brouckaert P, Takahashi N, van Tiel ST, Hostens J, Eggermont AM, Seynhaeve AL et al. Tumor necrosis factor-alpha augmented tumor response in B16BL6 melanoma-bearing mice treated with stealth liposomal doxorubicin (Doxil) correlates with altered Doxil pharmacokinetics. Int J Cancer. 2004: 109(3), 442-448.
17.Hoving S, Seynhaeve AL, van Tiel ST, aan de Wiel-Ambagtsheer G, de Bruijn EA, Eggermont AM et al. Early destruction of tumor vasculature in tumor necrosis factor-alpha-based isolated limb perfusion is responsible for tumor response. Anticancer Drugs. 2006: 17(8), 949-959.
18.Nooijen PT, Manusama ER, Eggermont AM, Schalkwijk L, Stavast J, Marquet RL et al. Synergistic effects of TNF-alpha and melphalan in an isolated limb perfusion model of rat sarcoma: a histopathological, immunohistochemical and electron microscopical study. Br J Cancer. 1996: 74(12), 1908-1915.
19.Kramer SM and Carver ME. Serum-free in vitro bioassay for the detection of tumor necrosis factor. J Immunol Methods. 1986: 93(2), 201-206.
20.van der Veen AH, Eggermont AM, Seynhaeve AL, van Tiel ST, and ten Hagen TL. Biodistribution and tumor localization of stealth liposomal tumor necrosis factor-alpha in soft tissue sarcoma bearing rats. Int J Cancer. 1998: 77(6), 901-906.
21.Gabizon A and Papahadjopoulos D. Liposome formulations with prolonged circulation time in blood and enhanced uptake by tumors. Proc Natl Acad Sci U S A. 1988: 85(18), 6949-6953.
22.Bartlett GR. Phosphorus assay in column chromatography. J Biol Chem. 1959: 234(3), 466-468.
23.Mayer LD, Tai LC, Ko DS, Masin D, Ginsberg RS, Cullis PR et al. Influence of vesicle size, lipid composition, and drug-to-lipid ratio on the biological activity of liposomal doxorubicin in mice. Cancer Res. 1989: 49(21), 5922-5930.
24.Papenfuss HD, Gross JF, Intaglietta M, and Treese FA. A transparent access chamber for the rat dorsal skin fold. Microvasc Res. 1979: 18(3), 311-318.
25.Falkvoll KH, Rofstad EK, Brustad T, and Marton P. A transparent chamber for the dorsal skin fold of athymic mice. Exp Cell Biol. 1984: 52(4), 260-268.
26.Leunig M, Yuan F, Menger MD, Boucher Y, Goetz AE, Messmer K et al. Angiogenesis, microvascular architecture, microhemodynamics, and interstitial fluid pressure during early growth of human adenocarcinoma LS174T in SCID mice. Cancer Res. 1992: 52(23), 6553-6560.
27.Yuan F, Dellian M, Fukumura D, Leunig M, Berk DA, Torchilin VP et al. Vascular permeability in a human tumor xenograft: molecular size dependence and cutoff size. Cancer Res. 1995: 55(17), 3752-3756.
28.Ponce AM, Viglianti BL, Yu D, Yarmolenko PS, Michelich CR, Woo J et al. Magnetic resonance imaging of temperature-sensitive liposome release: drug dose painting and antitumor effects. J Natl Cancer Inst. 2007: 99(1), 53-63.
29.Storm G, Steerenberg PA, Emmen F, van Borssum WM, and Crommelin DJ. Release of doxorubicin from peritoneal macrophages exposed in vivo to doxorubicin-containing liposomes. Biochim Biophys Acta. 1988: 965(2-3), 136-145.
30.Jain RK. Delivery of molecular and cellular medicine to solid tumors. Adv Drug Deliv Rev. 2001: 46(1-3), 149-168.

31.Allen TM and Hansen C. Pharmacokinetics of stealth versus conventional liposomes: effect of dose. Biochim Biophys Acta. 1991: 1068(2), 133-141.
32.Gabizon A, Isacson R, Libson E, Kaufman B, Uziely B, Catane R et al. Clinical studies of liposome-encapsulated doxorubicin. Acta Oncol. 1994: 33(7), 779-786.
33.Feng D, Nagy JA, Hipp J, Pyne K, Dvorak HF, and Dvorak AM. Reinterpretation of endothelial cell gaps induced by vasoactive mediators in guinea-pig, mouse and rat: many are transcellular pores. J Physiol. 1997: 504 (Pt 3), 747-761.
34.Hashizume H, Baluk P, Morikawa S, McLean JW, Thurston G, Roberge S et al. Openings between defective endothelial cells explain tumor vessel leakiness. Am J Pathol. 2000: 156(4), 1363-1380.
35.Jain RK, Munn LL, and Fukumura D. Dissecting tumour pathophysiology using intravital microscopy. Nature Rev Cancer. 2002: 2(4), 266-276.
36.Dvorak HF. Angiogenesis: update 2005. J Thromb Haemost. 2005: 3(8), 1835-1842.
37.Jain RK, Duda DG, Clark JW, and Loeffler JS. Lessons from phase III clinical trials on anti-VEGF therapy for cancer. Nat Clin Pract Oncol. 2006: 3(1), 24-40.
38.Lippert JW, III. Vascular disrupting agents. Bioorg Med Chem. 2006.
39.Tozer GM, Kanthou C, and Baguley BC. Disrupting tumour blood vessels. Nat Rev Cancer. 2005: 5(6), 423-435.
40.Brunstein F, Hoving S, Seynhaeve AL, van Tiel ST, Guetens G, de Bruijn EA et al. Synergistic antitumor activity of histamine plus melphalan in isolated limb perfusion: preclinical studies. J Natl Cancer Inst. 2004: 96(21), 1603-1610.
41.de Wilt JH, ten Hagen TL, de Boeck G, van Tiel ST, de Bruijn EA, and Eggermont AM. Tumour necrosis factor alpha increases melphalan concentration in tumour tissue after isolated limb perfusion. Br J Cancer. 2000: 82(5), 1000-1003.
42.Suzuki S, Ohta S, Takashio K, Nitanai H, and Hashimoto Y. Augmentation for intratumoral accumulation and anti-tumor activity of liposome-encapsulated adriamycin by tumor necrosis factor-alpha in mice. Int J Cancer. 1990: 46(6), 1095-1100.
43.Folli S, Pelegrin A, Chalandon Y, Yao X, Buchegger F, Lienard D et al. Tumor-necrosis factor can enhance radioantibody uptake in human colon carcinoma xenografts by increasing vascular permeability. Int J Cancer. 1993: 53(5), 829-836.
44.Hoving S, Brunstein F, aan de Wiel-Ambagtsheer G, van Tiel ST, de Boeck G, de Bruijn EA et al. Synergistic antitumor response of interleukin 2 with melphalan in isolated limb perfusion in soft tissue sarcoma-bearing rats. Cancer Res. 2005: 65(10), 4300-4308.
45.Ruegg C, Yilmaz A, Bieler G, Bamat J, Chaubert P, and Lejeune FJ. Evidence for the involvement of endothelial cell integrin alphaVbeta3 in the disruption of the tumor vasculature induced by TNF and IFN-gamma. Nat Med. 1998: 4(4), 408-414.
46.Seynhaeve AL, Vermeulen CE, Eggermont AM, and ten Hagen TL. Cytokines and vascular permeability: an in vitro study on human endothelial cells in relation to tumor necrosis factor-alpha-primed peripheral blood mononuclear cells. Cell Biochem Biophys. 2006: 44(1), 157-169.

Chapter 9

TNFR1 expressing pericyte coverage of tumor-associated vasculature correlates with responsiveness to TNF in combination with chemotherapy

Ann L.B. Seynhaeve
Saske Hoving
Debby Schipper
Alexander M.M. Eggermont
Timo L.M. ten Hagen

Submitted for publication

Research article

TNFR1 expressing pericyte coverage of tumor-associated vasculature correlates with responsiveness to TNF in combination with chemotherapy

Ann L.B. Seynhaeve, Saske Hoving, Debby Schipper, Alexander M.M. Eggermont, and Timo L.M. ten Hagen

Department of Surgical Oncology, Erasmus MC-Daniel den Hoed Cancer Center, Rotterdam, the Netherlands

ARTICLE INFORMATION

Submitted for publication

ACKNOWLEDGMENTS

The authors thank Dr. Kirsten Kullak of Boehringer Ingelheim GmbH for the generous supply of TNF; Gisela aan de Wiel-Ambagtsheer, Dieuwertje Poel and Peter-Paul Wisman for their technical assistance. This study was supported by grant DDHK 2000-2224 of the Dutch Cancer Society.

ABSTRACT

Several strategies targeting the tumor-associated vasculature (TAV) have been developed to improve cancer therapy; the anti-angiogenesis and vascular destruction strategy. However combination therapy, in which induction of vascular hyperpermeability improves tumor response to chemotherapy, has become increasingly important in the treatment of solid tumors. Addition of the vasoactive cytokine tumor necrosis factor-alpha (TNF) to systemic treatment with liposomal encapsulated doxorubicin (Doxil) improves tumor response in mice bearing the B16BL6 melanoma or the human melanoma BLM correlating with an increased permeability of the TAV and extravasation of Doxil into the tumor intersitium. However, addition of TNF has no effect in the Lewis Lung Carcinoma (LLC) or the human melanoma 1F6. TNF-induced permeability acts predominantly through the stimulation of TNF-receptor 1 (TNFR1, p55) and we observe that TNFR1 in the TAV is primarily expressed by pericytes. Furthermore, we demonstrate a higher pericyte coverage in B16BL6 and BLM relatively to the LLC and 1F6, which suggests that the ubiquitous TNFR1-expressing pericytes are responsible for the TNF-induced vessel permeability leading to an augmented drug accumulation and ultimately to an improved tumor response. These results indicate pericytes as an alternative target for tumor vascular therapy.

INTRODUCTION

In contrast to the structured and organized blood vessels of basic organs, the tumor-associated vasculature (TAV) can best be described as "abnormal". The TAV displays a lack of hierarchical branching in which the recognizable features of arterioles, capillaries and venules are lost. Vessels are tortuous, leaky and unevenly dilated and this results in a chaotic blood flow [1]. Due to a better understanding of the involvement of the TAV in tumor progression, a prospective anticancer target is provided by inhibiting or destroying these tumor vessels [2-3]. Next to that, altered tumor physiology as a result of tumor vascular manipulation can be used to improve chemotherapy. Recently, anti-angiogenic therapy with Avestin was shown to improve clinical outcome that was suggested to result from tumor vascular normalization [4-6]. However, further manipulating the abnormality of the TAV, by vasoactive agents, can be used as well to improve the delivery of classical antitumor drugs, the cytotoxic agents that directly kill tumor cells. We showed that systemic

co-administration of such a vasoactive agent, tumor necrosis factor-alpha (TNF) in combination with liposomal encapsulated doxorubicin (Doxil), results in increased drug accumulation and improved tumor response [7,8] without a direct cytotoxic effect on the endothelial lining [9]. The majority of TNF biologic effects are mediated by TNF-receptor 1 (TNFR1, p55) and stimulation of TNFR1 is known to increase vascular permeability *in vitro* and *in vivo* [10] that could explain the intratumoral drug accumulation.

Blood vessels are composed of two major associating cell types. The endothelial cells that form the luminal layer of the vessel wall and the pericytes, also referred to as Rouget-cells or mural cells, surrounding and stabilizing the vascular tube. Until recently, pericytes were believed to be absent in the TAV but studies showed their significant contribution in tumor angiogenesis. As a result, pericytes gained new interest as a potential target in antiangiogenic therapies [11,12].

In the current study, using tumors with diverse tumor vasculature characteristics, we examined the efficacy of systemic treatment with low-dose TNF and Doxil and showed tumor dependent responsiveness to TNF-based combination treatment. In addition, we explored the initial status of endothelial cells and associated pericytes. We hypothesize that TNF-R1 positive pericytes play a determining role and likely explains the mechanism of TNF-induced permeability.

EXPERIMENTAL PROCEDURES

Agents. Recombinant murine tumor necrosis factor-alpha (mTNF) and recombinant human tumor necrosis factor-alpha (HuTNF) were kindly provided by Boehringer Ingelheim GmbH. Murine TNF had a specific activity of 3×10^7 U/mg and endotoxin levels were < 1 U/mg protein. HuTNF had a specific activity of 5.8×10^7 U/mg and endotoxin levels were < 1.25 U/mg protein. Pegylated long circulating liposomal doxorubicin (Doxil/Caleyx) was purchased from Schering-Plough.

Animals and tumor model. Specific pathogen-free male C57BL/6 mice (Harlan-CPB) and NMRI Nu/Nu mice (Charles River) were kept in a control environment with 12 hours light/dark cycles and fed a standard laboratory diet ad libitum (Hope Farms). Four tumors were used in these experiments: B16BL6 melanoma, Lewis Lung Carcinoma (LLC), the highly metastatic human melanoma cell line BLM and the non-metastatic human melanoma cell line 1F6 [13]. The mice were anesthetized by isoflurane (Pharmachemie) inhalation and a small tumor fragment of 3 mm^3 was implanted subcutaneously in the flank of the mice. When the tumor reached a diameter of 10 mm, tumor tissue was dissected under sterile conditions, cut in small identical pieces, and directly used for implantation in the dorsal skin-fold chamber (0.1 mm^3 tumor pieces) or subcutaneously (3 mm^3 tumor pieces) for the efficacy study, measurements of liposomal drug accumulation and immunohistochemistry as described below. All animal studies were done in accordance with protocols approved by the committee on Animal Research of the Erasmus MC, Rotterdam, the Netherlands.

Tumor treatment and monitoring. Treatment was started when tumors reached an average diameter of 8 to 10 mm. The mice were randomized into the following 4 groups: saline, mTNF, Doxil and Doxil plus mTNF. Mice were injected 5 times in the tail vein with an interval of 4 days between injections; first dose of 4.5 mg/kg Doxil and 1.0 mg/kg for consecutive doses. mTNF in a dose of 1 µg/mouse, which is well tolerated in the mice without any side effects, was given for all 5 treatments. When mice were treated with Doxil plus TNF, these agents were injected separately, Doxil directly followed by TNF. Tumor growth was recorded by caliper measurement and volumes calculated using the formula $0.4 \times (A^2 \times B)$ where B represents the largest diameter and A the diameter perpendicular to B. The tumor size was expressed as tumor size index i.e. the tumor volume in relation to initial tumor volume. Mice were sacrificed if the tumor weight exceeded 10% of

the body mass, the mice lost 10% body weight or at the end of the experiment.

Determination of doxorubicin levels in tumor tissue. Mice received a single dose of saline, 4.5 mg/kg Doxil or 4.5 mg/kg Doxil plus 1 µg/mouse mTNF via i.v. injection. Tumors were excised 12 hours after injection, immediately snap-frozen in liquid nitrogen and stored at –70°C until further analysis. Tissues were analyzed for doxorubicin and its fluorescent metabolites as previously described [14]. Briefly, tumors were weighted upon thawing, 5 ml of acidified isopropanol (0.075 N HCl in 90% isopropanol) was added and the tumors were homogenized. After incubation for 24 hours at 4°C the samples were centrifuged for 30 min at 2500 rpm and doxorubicin content in the supernatant was measured using a Hitachi F4500 fluorescence spectrometer (excitation 472 nm and emission 590 nm). A standard curve was prepared with known concentrations of doxorubicin diluted in acidified isopropanol. All measurements were repeated after addition of an internal doxorubicin standard. The amount of doxorubicin in the tumor was corrected for background and expressed as µg doxorubicin per gram tumor tissue.

Biodistribution using the dorsal skin-fold chamber. Preparation of the dorsal skin-fold chamber is an adaptation from previously described procedures [15-17]. Briefly, mice were anesthetized as described above and hair was removed from the back of the animal. After dissecting the skin, leaving the fascia and opposing skin intact, the skin-fold of the mouse was sandwiched between two frames, fixed with 2 light metal bolds and sutures. A small piece of tumor (0.1 mm^3) was transplanted between the fascia and on both sides the window was closed with a 12 mm diameter microscopic cover glass. The mice were housed in an incubation room with an ambient temperature of 29°C and a humidity of 70%. Experiments started when the tumor reached a size of 4 to 5 mm. Mice were injected i.v. with 4.5 mg/kg Doxil or 4.5 mg/kg Doxil plus 1 µg/mouse mTNF. The mice were anesthetized and fixed to the heated microscope stage of a Zeiss LSM 510 META confocal microscope. Randomly selected tumor regions were examined with 20x (NA 0.5) long working distance objective lens and detailed examination was performed using 40x (NA 0.8) water emersion objective lens. Scans were made with a 543 nm Helium-Neon laser with 560-615 band pass filter for Doxil and stored as digital files. For measurements of fluorescence intensity, images were analyzed using Image Toolv2 (Don Wilcox, University of Texas Health Science Center) and ImageJ 1.37v (Wayne Rasband, National Institute of Health). The RGB color images of 512 x 512 pixels were converted to grayscale. The fluorescence intensity ranged form 0 to 255 and we distinguished specific staining from background using a threshold of 45. The proportion of pixels with fluorescence intensity above the threshold was calculated. Using a look-up table the fluorescence intensity of the representative grayscale images were converted to a pseudo color spectrum from 0 to 255 and transformed to a surface plot. The heights of the peaks correspond to the fluorescence intensity.

Tissue samples and immunohistochemistry. For quantification of the vascular morphology, untreated tumors with a diameter of 8 to 10 mm were excised, immediately snap-frozen in liquid nitrogen and stored at –70°C until further analysis. Second, 10 min before tumor excision mice were intravenously injected with 50 µl *Griffonia simplicifolia* lectin I (1 mg/ml, Sigma) for visualization of functional vessels. Tumor material standardized taken pre-ILP from patients scheduled for TNF-based melphalan ILP at the Erasmus MC-Daniel de Hoed Cancer Centre was included in this study. Endothelial cells and vessel functionality were evaluated by immunohistochemistry using following primary antibodies: rat anti mouse monoclonal CD31 (1:100; BD Pharmingen), goat anti lectin I (1:400; Vector Laboratories), sheep anti human CD31 (1:100; R&D systems). Pericytes were stained with rabbit anti polyclonal NG2 Chondroitin Sulfate Proteoglycan (1:200; Chemicon). TNF receptor 1 was stained with goat anti mouse TNFR1 (1:10; R&D systems) and mouse

anti human TNFR1 (1:100; Alexis). Secondary antibodies used were green (488), red (555 or 594) and far red (645) Alexa Fluor (1:400; Molecular Probes). Cryostat sections of 5 or 30 µm were air dried and fixed with acetone for 10 or 30 min. Sections of 30 µm were permeabilized with PBS/0.5% TritonX-100 for 30 min. After the blocking step with PBS/1%BSA for 30 min sections were incubated overnight at 4°C with primary antibodies diluted in PBS/1%BSA. Sections were incubated for 1 hour at room temperature with corresponding secondary Alexa Fluor antibodies diluted in PBS/1%BSA. Thereafter the sections were mounted with mounting medium containing polyvinyl alcohol (MoWiol-488; Fluka).

Quantifications of the vascular morphology. Observations of the tumor vasculature in tumor sections were made with a Zeiss LSM 510 META confocal microscope. Randomly selected tumor regions were examined with Plan-Neofluar 40x or 63x oil lenses. Scans were made with a 488 nm Argon, 543 nm and 633 nm Helium-Neon laser. RGB color images of 512 x 512 pixels were made of at least 3 tumors. Six random fields of interest were taken of each tumor section and 3 sections per tumor. Vessel size and number were analyzed using the Zeiss LSM Image Browser 4.0 software. The microvessel size (MVS), microvessel density (MVD, the number of vessels per mm^2) and the percentage endothelial cells per vessel (the area of vessels per field of interest) were calculated. Vessels that stained positive for lectin were considered functional vessels. The microvessel pericytes coverage index (MPI) was analyzed with ImageJ. The RGB images of the endothelial cells and pericytes were both binarized. The area of the binarized endothelial cells was dilated with 4 µm from the original edges using an ImageJ macro, an overlap of the dilated endothelial cells with pericytes was made as described before [18]. The MPI was calculated using the formula: MPI = (pixel density of the endothelial cells/pixel density overlap) x 100 percent.

***In vitro* cytotoxicity assay.** B16BL6, LLC, BLM and 1F6 cells were maintained in DMEM (Lonza) supplemented with 10% heat inactivated fetal calf serum (Lonza). The tumor cells were added to 96 well-plate (Costar BV) at a final concentration of $6x10^3$ cells per well and allowed to grow for 24 hours at 37°C in 5% CO_2. Thereafter, tumor cells were incubated for 72 hours in the presence of various concentrations Doxil and mTNF for B16BL6 and LLC or HuTNF for BLM and 1F6. The range of final drug concentrations was 0.01 - 10 µg/ml TNF and 0.001 - 10 µg/ml Doxil. Cell viability was assessed using the MTT staining [19]. Briefly, 3 hours before the end of the incubation 50 µl MTT reagent (3 mg/ml, Sigma) was added to the medium. After incubation the medium was removed and the formazan crystals were dissolved in 100 µl DMSO (Sigma) and optical density (O.D.) was read at 540 nm in a microtiter plate reader. Tumor cell growth was calculated using the formula: cell growth = (O.D. test well/O.D. control) x 100 percent.

Human umbilical vein endothelial cells (HUVEC) were isolated by collagenase digestion using the method described by Jaffe *et al*. [20]. Each isolate was derived from an individual umbilical vein and used for experiments at passage 5. HUVEC were cultured in HUVEC medium containing human endothelial-serum free medium (Invitrogen), 20% newborn calf serum (Lonza) 10% human serum (Lonza), 20 ng/ml bFGF (Peprotech EC Ltd), 100 ng/ml EGF (Peprotech EC Ltd) in fibronectin (Roche) coated flasks. HUVEC had the characteristic cobblestone morphology and tested positive for CD31. Human umbilical vein smooth muscle cells (HUVSMC) were cultured in modified MCDB-107 medium supplemented with FCS, EGF and bFGF (CellMade). HUVSMCs were added to a 12 well-plate (Costar) at a final concentration of $9x10^4$ cells per well and allowed to grow for 24 hours at 37°C in 5% CO_2. Thereafter, the cells were incubated with 1 µg/ml TNF for 72 hours in HUVSMC-medium and supernatant was collected. As a control, HUVSMCs were incubated with medium alone. Also, as negative controls TNF and HUVSMC-medium was added to an empty well for the indicated time

period and collected. HUVEC were added to a 48 well-plate (Costar), coated with fitronectin, at a final concentration of $2x10^4$ cells per well and allowed to grow for 24 hours. HUVEC were incubated with the HUVSMC conditioned medium and control medium for 72 hours. Morphological changes of the HUVEC were examined with a 10x (NA 0.30) Plan-Neofluoar objective lens using an inverted Zeiss Axiovert 100M microscope equipped with an Axiocam digital camera (Carl Zeiss). Cell elongation was measured and expressed as the ratio of the length of the major cell axis to the width perpendicular to the length. Ten cells and at least four independent incubations were determined. Al measurements were done using the AxioVision 3.0 software. Growth of endothelial cells was measured using the sulphorhodamine B (SRB) protein stain assay, according to the method of Skehan [21]. Briefly, cells were washed with PBS, incubated with 10% trichloric acetic acid (1 hour, 4ºC) and washed in distilled water. Cells were then stained for 15 minutes with SRB, washed with 1% acetic acid and allowed to dry. Protein bound SRB was dissolved in 10 mM Tris buffer and optical density (O.D.) was measured at 545 nm in a microtiter plate reader. Cell growth was calculated using the formula: percentage cell growth = (O.D. test well/O.D control well) x 100 percent.

Statistical analysis. Results were evaluated for statistical significance with the Mann Whitney U test. The correlation between MVS and MPI was calculated with the two-tailed Pearson Correlation. P-values below 0.05 were considered statistically significant. Calculations were performed using GraphPad Prism v3.0 and SPSS v11.0 for Windows 2000.

RESULTS

Addition of low-dose mTNF increases antitumor activity and intratumoral distribution of Doxil in B16BL6 and BLM tumors. To evaluate the antitumor activity of Doxil in combination with low-dose mTNF, tumor-bearing mice were treated at 4 days intervals with a total of 5 injections of saline, mTNF, Doxil or Doxil in combination with mTNF. In B16BL6-bearing mice combination of low-dose mTNF and Doxil proved to be more effective than Doxil alone, with a prolonged tumor growth delay. However, in LLC-bearing mice the addition of low-dose mTNF to Doxil treatment did not improve tumor response and all animals showed progressive disease (**Fig. 1a**). Treatment of BLM melanoma with Doxil in combination with mTNF resulted in profound growth inhibition as compared to treatment with Doxil alone. No difference in tumor response was found between Doxil alone and Doxil in combination with mTNF in 1F6-bearing mice (**Fig. 1b**). Sham treatment or mTNF alone resulted in progressive disease in all 4 tumors and at the end of the treatment all tumors had a tumor size index more than 4 times the original size (**Table 1**). Summarizing, addition of low-dose mTNF to the Doxil regimen had a significant antitumor effect in the B16BL6 and BLM tumor. However, this synergistic effect was not found in the treatment of LLC and 1F6. *In vitro* experiments were performed to define whether direct cytotoxicity contributed to the improved tumor response of Doxil in combination with TNF. Exposure of B16BL6 or LLC cells showed a strong cytotoxic effect for Doxil and resulted in a response curve with an IC_{50} of 0.07 and 0.05 µg/ml respectively. Although both cell lines showed reduced cell viability after exposure to 10 µg/ml mTNF, addition of TNF did not significantly alter the IC_{50} of Doxil. Also when incubating the human melanomas BLM and 1F6 with Doxil and HuTNF we observed only a cytotoxic effect of Doxil with an IC_{50} of 0.1 µg/ml for both cell lines. Both cell lines were moderate sensitive for 10 µg/ml HuTNF but addition of HuTNF hardly changed the IC_{50} for Doxil. These data indicates that TNF *in vitro* did not influence the sensitivity of the tumor cells to Doxil (**Fig. 1c**). In previous experiments, using several animal models, we found that TNF in combination with a chemotherapeutic drug, like melphalan, doxorubicin or Doxil resulted in an improved antitumor response which most likely results from of the augmented intratumoral drug accumulation [7-9,22,23]. To investigate if intratumoral drug uptake corre-

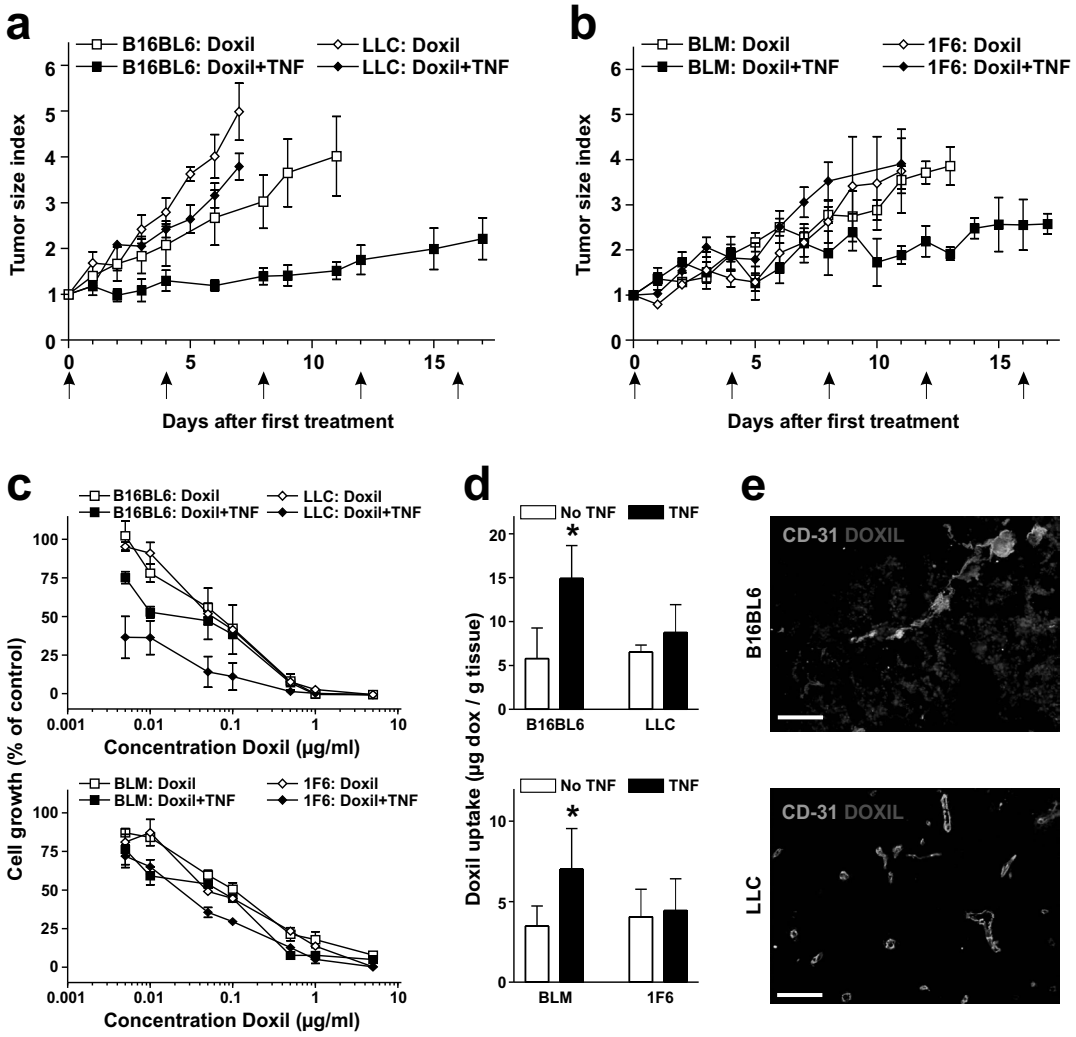

Figure 1. Addition of TNF improves tumor response and augments intratumoral drug uptake in B16BL6 and BLM. (**a**,**b**) Graphs show the tumor size index of subcutaneous implanted B16BL6 and LLC (**a**) and BLM and 1F6 (**b**) during systemic treatment with Doxil and low-dose mTNF. Mice were injected 5 times i.v. with an interval of 4 days (arrows). Addition of mTNF resulted in synergistic tumor response of the B16BL6 and BLM, but no effect of mTNF was observed in the LLC and 1F6. Data points represents tumor size index ± SD of 6 individual animals. (**c**) *In vitro* growth of tumor cells (B16BL6, LLC: upper graph; BLM, 1F6: lower graph) 72 hours following incubation with different concentration Doxil and 10 µg/ml TNF (mTNF for B16BL6, LLC and HuTNF for BLM and 1F6). Addition of TNF had no synergistic effect with Doxil on the tumor cells. Data points represent percentage cell growth of incubated cells compared to control treated cells at 0 hour ± SEM of 3 individual experiments in duplicate. (**d**) Doxil uptake in the tumors (B16BL6, LLC: upper graph; BLM, 1F6: lower graph) with or without addition of mTNF. Tumors were excised 24 hours following a single injection and the amount of doxorubicin was measured. Addition of mTNF to Doxil treatment enhanced drug accumulation in the B16BL6 and BLM tumors in contrast to LLC and 1F6. Columns represent µg doxorubicin per g tumor tissue ± SD of 3 to 5 individual animals; *, $P < 0.05$ TNF *versus* no TNF. (**e**) Representative immunofluorescent photographs of CD31 expression and Doxil accumulation in B16BL6 and LLC 12 hours following treatment with Doxil and TNF. In accordance with the Doxil uptake, accumulation of Doxil into the tumor intersititium was observed in the B16BL6 and hardly any Doxil was seen in the LLC. Scale bar apply to all images, 100 µm. (See color section for a full-color version.)

Table 1. Tumor response after systemic treatment with Doxil and TNF in tumor-bearing mice.

	B16BL6								LLC							
	Tumor size index				% mice with tumor size index < 4				Tumor size index				% mice with tumor size index < 4			
	Day 4	Day 8	Day 12	Day 16	Day 4	Day 8	Day 12	Day 16	Day 4	Day 8	Day 12	Day 16	Day 4	Day 8	Day 12	Day 16
Saline	2.4 ± 0.3	4.2 ± 0.1	-	-	100	0	0	0	1.7 ± 0.2	3.6 ± 1.0	-	-	100	66	0	0
TNF	2.3 ± 0.8	3.2 ± 0.1	-	-	100	33	0	0	1.3 ± 0.7	4.1 ± 1.6	7.7 ± 2.9	-	100	50	16	0
Doxil	2.1 ± 0.8	3.0 ± 1.0	4.0 ± 1.5	3.8 ± 0.4	100	66	66	33	2.8 ± 0.8	6.0 ± 1.9	7.1 ± 1.0	-	83	0	0	0
Doxil + TNF	1.3 ± 0.4	1.4 ± 0.3	1.5 ± 0.3*	2.0 ± 0.8*	100	100	100	100	2.4 ± 0.4	4.2 ± 0.9	6.5 ± 2.2	-	100	33	0	0

	BLM								1F6							
	Tumor size index				% mice with tumor size index < 4				Tumor size index				% mice with tumor size index < 4			
	Day 4	Day 8	Day 12	Day 16	Day 4	Day 8	Day 12	Day 16	Day 4	Day 8	Day 12	Day 16	Day 4	Day 8	Day 12	Day 16
Saline	2.2 ± 0.6	3.7 ± 0.9	5.2 ± 1.3	-	100	60	0	0	1.9 ± 0.6	3.8 ± 1.3	5.1 ± 2.2	-	88	33	11	0
TNF	2.4 ± 1.0	3.7 ± 1.0	6.0 ± 3.8	-	83	50	16	0	2.3 ± 1.0	4.7 ± 1.6	6.5 ± 3.1	-	100	16	16	0
Doxil	1.8 ± 0.4	2.6 ± 0.6	3.9 ± 0.7	4.3 ± 0.7	100	100	50	12	1.3 ± 0.4	2.6 ± 1.1	4.0 ± 1.5	5.3 ± 1.0	100	83	50	16
Doxil + TNF	1.9 ± 0.8	2.3 ± 1.2	2.1± 0.6*	2.5 ± 0.9*	100	100	60	60	1.8 ± 0.7	3.5 ± 0.9	5.7 ± 1.0	6.0 ± 0.8	100	50	16	0

Note: Tumor-bearing mice were injected 5 times via tail vein with an interval of 4 days with saline, mTNF, Doxil and Doxil in combination with mTNF and tumor size index (TSI, tumor volume in relation to tumor volume at start of treatment) was calculated. Data represent average ± SD of 4 to 6 individual animals; *, $P < 0.05$ *versus* Doxil alone at the same time point.

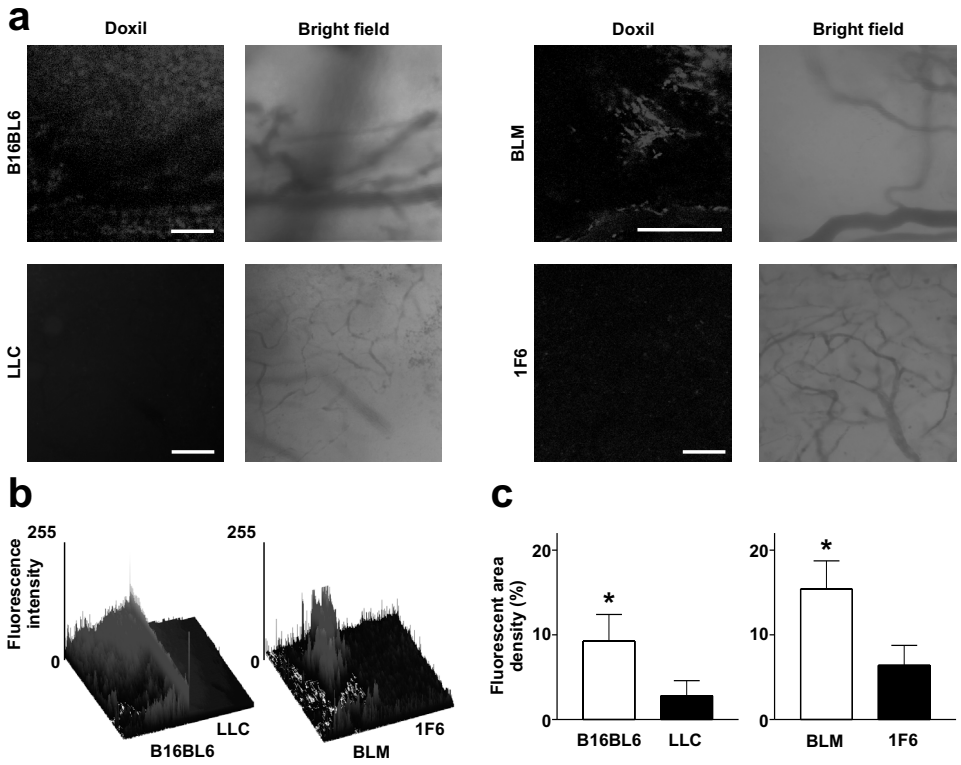

Figure 2. Addition of TNF strongly improves liposomal distribution in the tumor interstitium of the B16BL6 and BLM. (**a**) Representative intravital microscopy scans of the tumors were compared to illustrate the effect of mTNF on liposomal uptake following systemic administration. Addition of mTNF clearly inflicted an intratumoral accumulation of Doxil in the B16BL6 and BLM 24 hours after treatment. Scale bar apply to all images, 200 µm. (**b**) Increase in height of the fluorescence intensity peaks of the surface plots illustrates increased accumulation of liposomes when combined with mTNF in the B16BL6 and BLM. (**c**) After calculation of the extravascular fluorescent intensity a significant increase was found in the B16BL6 (left graph) and in BLM (right graph) 24 hours following injection of Doxil in combination with mTNF. Columns represent fluorescent area density ± SEM of at least 4 scans of 3 individual animals; *, $P < 0.05$ B16BL6 or BLM *versus* LLC or 1F6. (See color section for a full-color version.)

lates with tumor response, the concentration of doxorubicin in tumor tissue was measured. Doxorubicin levels in B16BL6 and BLM were higher with the addition of mTNF (2.5-fold in B16BL6, 2-fold in BLM). In contrast, mTNF did not increase doxorubicin concentrations in LLC and 1F6 (**Fig. 1d** and **Fig. 1e**). These data indicate a strong correlation between intratumoral drug uptake and tumor response.

Differential extravasation of Doxil induced by low-dose mTNF. Clearly, addition of a tolerable dose mTNF resulted in augmented liposome accumulation in B16BL6 and BLM tumors whereas no increase was observed in LLC and 1F6. Intravital microscopy was used to obtain a better insight in the effect of mTNF on the intratumoral localization of liposomes. When the tumor in the dorsal skin-fold chamber reached a size of approximately 4 to 5 mm it established its own blood supply and hardly any accumulation of liposomes was found when the tumors were treated with Doxil alone (data not shown). With the addition of mTNF abundant extravasation of liposomes into the tumor interstitium of B16BL6 and BLM was observed. This effect was not apparent in LLC and 1F6 (**Fig. 2a**). Surface plots show increased fluores-

cent peaks representing the intratumoral liposomes in the B16BL6 and BLM tumor (**Fig. 2b**). Analysis of the fluorescence intensity shows a 3.2-fold increase of intratumoral liposomes in B16BL6 compared to LLC and a 2.4-fold increase comparing BLM with 1F6 following addition with mTNF (**Fig. 2c**). These results indicate that administration of TNF causes an increased extravasation of Doxil into the tumor stroma, which is most likely caused by a difference in the vascular bed of the TNF-sensitive tumors, B16BL6 and BLM, versus the non-sensitive tumors LLC and 1F6.

B16BL6 and BLM tumors have fewer but larger vessels compared to LLC and 1F6. Immunohistochemical analysis revealed that B16BL6 contained predominantly large functional blood vessels with a mean vascular size (MVS) of 3097 ± 250 μm^2. In the LLC tumor the MVS was 572 ± 77 μm^2; 5.4-times smaller compared to the B16BL6 (**Fig. 3a** and **Fig. 3b**). The tumor vasculature of the BLM consists of a more heterogeneous vascular architecture. Around 34% of the vessels were small capillary size blood vessels (<300 μm^2), 35% had an intermediate size (between 300 and 1500 μm^2) and 31% were large vessels (>1500 μm^2) (**Fig. 3a** and **Supplementary Table 1**). The MVS in the BLM was 1150 ± 26 μm^2, significantly larger than the MVS of 448 ± 120 μm^2 in the 1F6 (**Fig. 3b**). Furthermore, the mean vascular density (MVD) of the LLC (123 ± 16) and the 1F6 (101 ± 32) yielded significant higher values than the MVD of the B16BL6 (26 ± 2) and BLM (64 ± 4) (**Fig. 3c**). Although a high

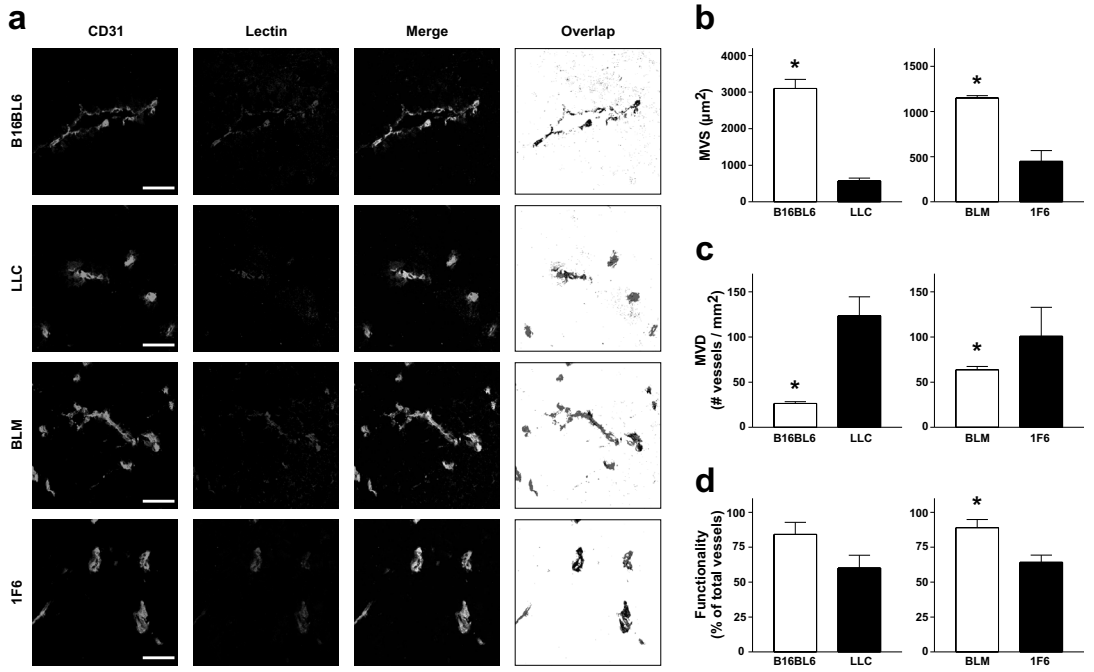

Figure 3. Structural differences in vasculature between TNF-sensitive and TNF-insensitive tumors. (**a**) Tumor-bearing mice were injected i.v. with lectin, 10 min later tumors were excised and histological sections were stained for endothelial cells (CD31, green) and functional blood vessels with an antibody against lectin (red). Scale bar apply to all images, 50 μm. (**b**) After measuring the microvessel size (MVS) significant larger blood vessels were found in the B16BL6 and BLM. (**c**) The microvessel density (MVD) was determined by counting the number of vessels per mm^2 and was found significant higher in the LLC and 1F6 (**d**) The percentage functional vessels was calculated and in spite of a significant difference in size and density, most of the tumor vessels were functional. Columns represent mean ± SEM of at least 6 scans from 3 sections of 3 individual tumors; *, $P < 0.05$ B16BL6 or BLM *versus* LLC or 1F6. (See color section for a full-color version.)

Supplementary table 1: Distribution of the microvessel size

Tumor	Microvessel size (% vessels)[a]		
	< 300 μm²	> 300 / <1500 μm²	> 1500 μm²
B16BL6	6.2 ± 3.4	22.0 ± 8.7	71.8 ± 9.2
LLC	54.5 ± 4.0	37.4 ± 3.0	8.1 ± 2.0
BLM	33.8 ± 1.9	35.0 ± 0.9	31.2 ± 1.9
1F6	49.2 ± 12.9	43.7 ± 9.0	7.1 ± 4.5

Note: Tumor sections stained for endothelial cells with an antibody against CD31 were analysed and the microvessel size (MVS) was measured.

[a] The vessels are subdivided into 3 categories: small (< 300 μm²), intermediate (between 300 and 1500 μm²) and large (> 1500 μm²) vessels. Data represent percentage vessels ± SEM of at least 6 scans from 3 sections of 3 individual tumors.

degree of vessels were functional in the 1F6 this was significant less than the amount of functional vessels found in the BLM. However, the majority of the vessels were functional in all tumors (**Fig. 3d**). Still, the variation in the vessel structure could not explain the difference in TNF-response between these two tumor types. The observed response and accompanied permeability change is more likely a result of an increase in the number of leaky vessels in the vascular bed of the B16BL6 and BLM.

Pericytes, but not endothelial cells, express TNFR1. TNF-induced vascular permeability is found to be regulated by stimulation of TNFR1 [24]. To identify TNFR1-expressing cells we co-stained tumor sections for endothelial cells or pericytes and TNFR1 in human melanoma biopsies and mice tumors before treatment. In previous experiments using human biopsies TNFR1 expression was found in cells in close proximity to the vessels but not on endothelial cells [25]. Here, in accordance to these experiments, endothelial cells hardly expressed TNFR1 (**Fig. 4a**). However, the TNFR1-expressing cells closely associated with the endothelial cells and were found to be pericytes (**Fig. 4b**). Therefore, pericytes rather then endothelial cells are likely involved in the TNF-induced permeability in this model.

Pericyte coverage correlates with induction of leakage in response to TNF. Pericytes were considered present in the tumor section if NG2 positive cells were observed surrounding the vessel as demonstrated in figure 5. Pericytes loosely associated with endothelial cells had a distinct morphology with multiple cytoplasmic extensions into the tumor parenchyma (**Fig. 5a** and **Fig. 5b**). It seemed that pericytes are moving away from the vessel wall occasionally connecting an adjacent blood vessel (**Fig. 5c**). Also CD31-positive endothelial sprouts migrating into the tumor tissue were associated with a pericyte sleeve (**Fig. 5d**). Secondly, LLC and 1F6 contained multiple cells that stained positive for NG2 without association with endothelial cells (**Fig. 5e**). These cells are usually defined as myofibroblasts and were rarely found in the B16BL6 and BLM. To explain the difference in TNF response, we examined the interaction between endothelial cells and TNFR1 expressing pericytes in the tumor-associated vasculature. The confocal images already showed a more extensive interaction of pericytes and endothelial cells in blood vessels of the B16BL6 and BLM (**Fig. 6a**). These images were analyzed using an ImageJ macro in which the endothelial lining is dilated (green) and the overlap with pericytes (red) is shown in black as illustrated (**Fig. 6b**) and calculated as microvessel pericytes coverage index (MPI). In accordance with the vessels size, significant more endothelial cells were found in the vasculature of B16BL6 and BLM compared to LLC and 1F6 (**Fig. 6c**). The MPI was significant higher in B16BL6 (70 ± 8%) and BLM (60 ± 1%) compared to LLC (46 ± 1%) and 1F6 (37 ± 4%) (**Fig. 6d**). This indicates that high TNFR1-expressing perciytes coverage is responsible for the TNF effects making the vessels more leaky for macromolecules. In addition, we found no correlation between MPI and MVS in all 4 tumors indicating that even small vessels in these tumors had a mature

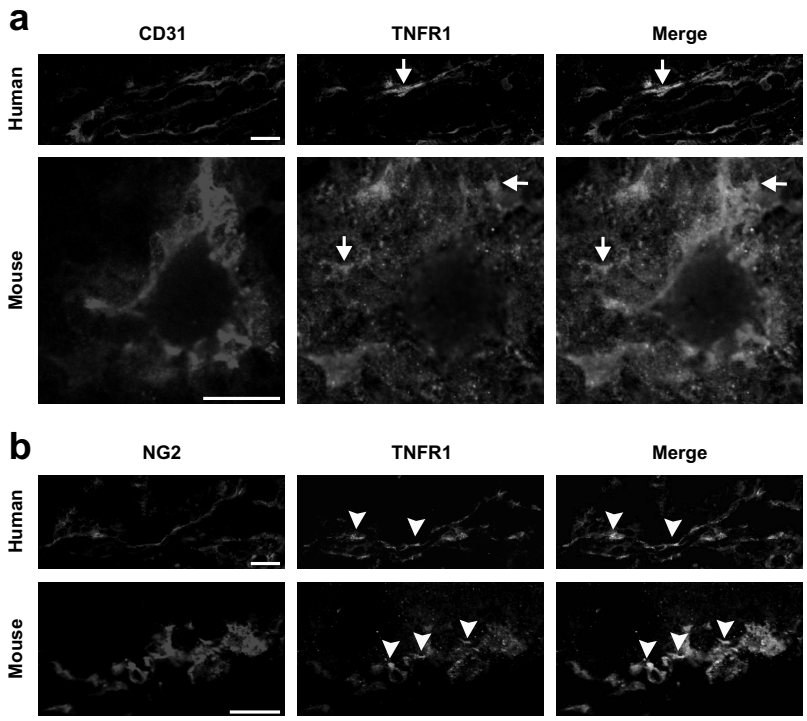

Figure 4. TNFR1 is expressed by pericytes of the tumor-associated vasculature. (**a**) Immunofluorescent staining for endothelial cells (CD31, red) and TNFR1 (green) in human (upper panels) and mouse (lower panels) tumor sections showed no co-localization (arrow). (**b**) Staining for pericytes (NG2, purple) and TNFR1 (green) showed TNFR1 expression by pericytes (arrowhead) of the tumor-associated vasculature of human (upper panels) and mouse (lower panels) tumor biopsies. Scale bar apply to all images, 20 µm. (See color section for a full-color version.)

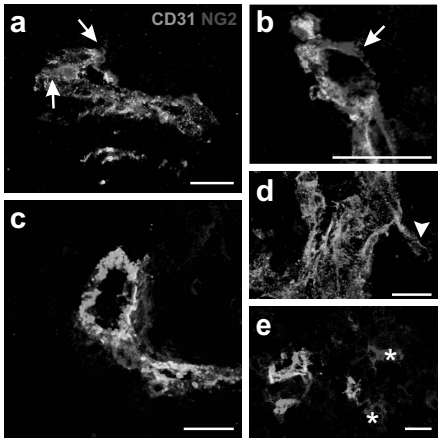

Figure 5. Morphology of the tumor-associated endothelial cells (CD31, green) and pericytes (NG2, red). (**a, b**) NG2 staining of pericytes show close association with endothelial cells, however multiple protrusions (arrows) into the tumor stroma were observed. (**c**) Some pericytes projected away from a vessel and connected neighboring vessels. (**d**) Endothelial cells migrating into the tumor parenchyma were found to be associated with pericytes at several occasions (arrowhead). (**e**) NG2 positive cells that were not associated with endothelial cells (asterix), designated as myofibroblasts, were found in the LLC. Scale bar applied to all images, 20 µm. (See color section for a full-color version.)

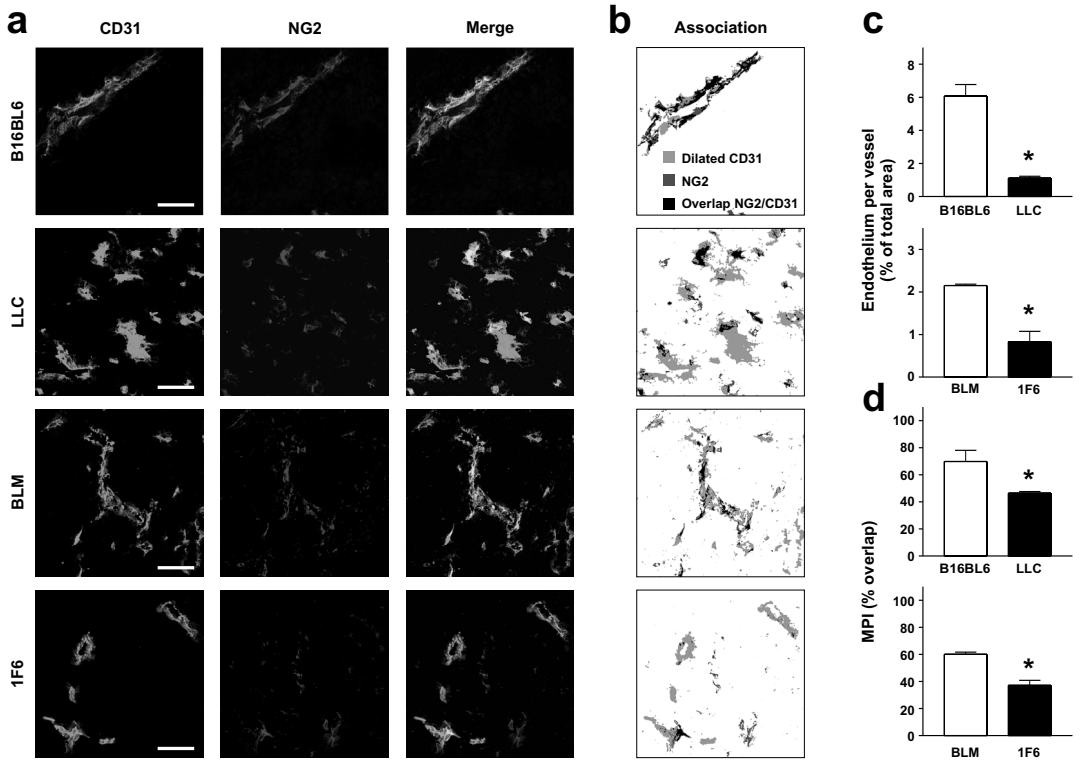

Figure 6. Difference in pericyte coverage is found between TNF-sensitive tumors and TNF-insensitive tumors. (**a**) Tumor sections were stained for endothelial cells (CD31, green) and pericytes (NG2, red). In the merge picture an intense association between endothelial cells and pericytes was seen in the B16BL6 and BLM. Scale bar apply to all images, 50 µm. (**b**) Analysis of the endothelial-pericyte association. Images of the endothelial cells (green) and pericytes (red) were binarized and the diameter of endothelial cells was dilated. The overlap of both cells is shown in black. (**c**) The percentage endothelial cells per vessel were calculated for B16BL6, LLC (left graph), BLM and 1F6 (right graph). In accordance with the MVS, B16BL6 and BLM contained significantly more endothelial cells per vessel then respectively the LLC and 1F6. Columns represent percentage area endothelium per vessel per field of interest ± SEM of at least 6 scans from 3 sections of 3 individual tumors; *, $P < 0.05$ B16BL6 or BLM *versus* LLC or 1F6. (**d**) Using the overlap images, microvessel pericyte coverage index (MPI) was measured in the B16BL6, LLC (left graph) and BLM, 1F6 (right graph). The MPI in tumor vessels of B16BL6 and BLM was significant higher compared to the MPI in LLC and 1F6. Columns represent percentage MPI of at least 6 scans from 3 sections of 3 individual tumors; *, $P < 0.05$ B16BL6 or BLM *versus* LLC or 1F6. (See color section for a full-color version.)

phenotype. However, there was a significant correlation between the MVS and functionality indicating that larger vessels are functional vessels (**Supplemental Fig.1**).

TNF-stimulated smooth muscle cells have an effect on endothelial cells *in vitro*. Furthermore we examined the interaction between endothelial cells and smooth muscle cells *in vitro*. TNF has hardly any effect on HUVSMC (data not shown). We observed that HUVEC incubated with TNF-conditioned HUVSMC medium became elongated and gaps between the cells were observed. HUVEC incubated with TNF showed also some cell elongation but not as severe as the incubation with TNF-conditioned HUVSMC medium. Incubating HUVEC with control-conditioned HUVSMC medium from had identical morphological features as the control (**Fig. 7a**). We also observed that en-

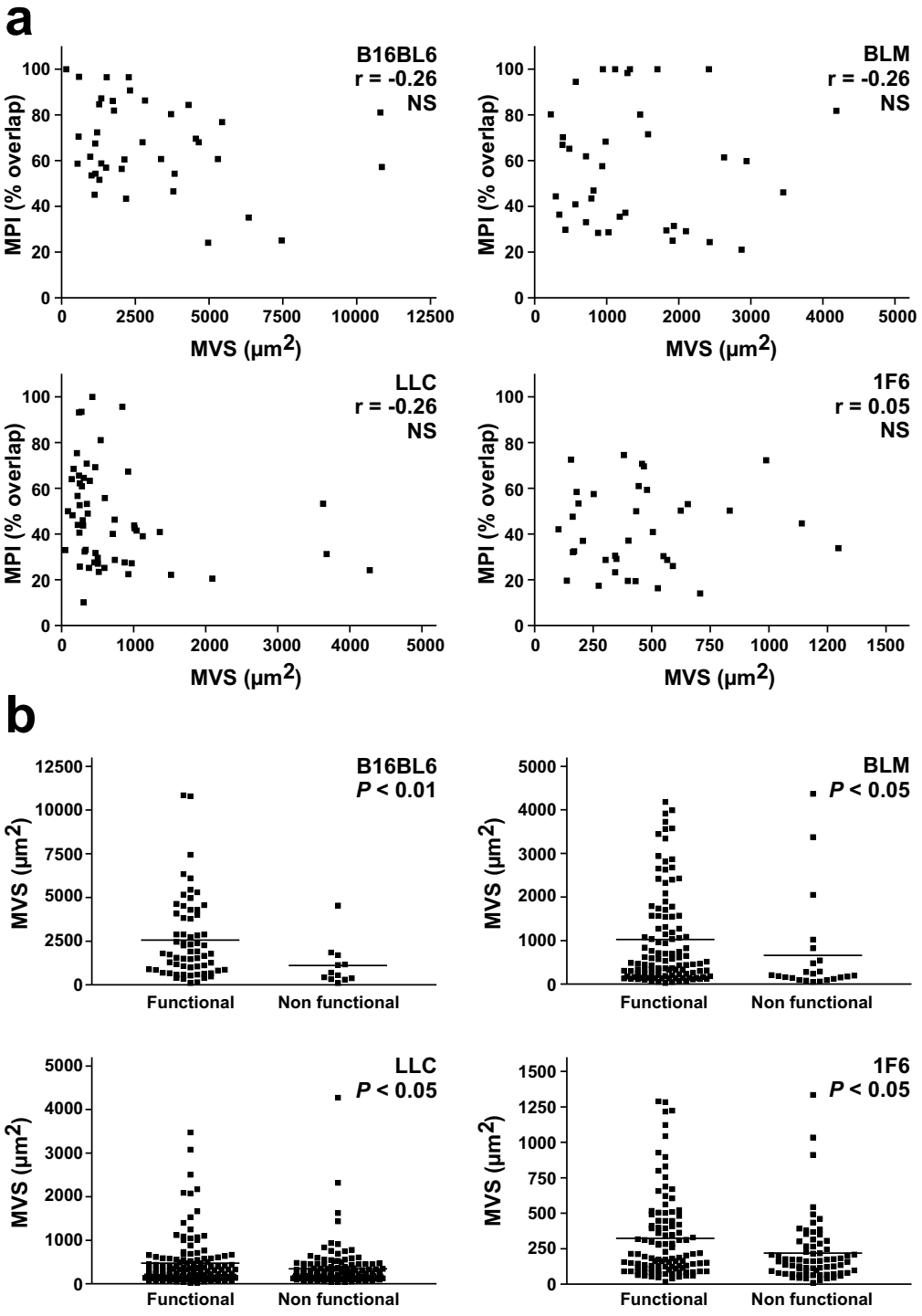

Supplementary Figure 1. (**a**) No correlation was found between the pericyte coverage and the size of a vessel. (**b**) There is a correlation found between the size of a vessel and its functionality.

dothelial cells incubated with TNF-conditioned HUVSMC medium went into growth arrest and induced stronger cell elongation compared to control-conditioned HUVSMC medium (**Fig. 7b**). This indicates that indeed mural cells are the target of TNF producing a factor that thereafter has an effect on the endothelial cells.

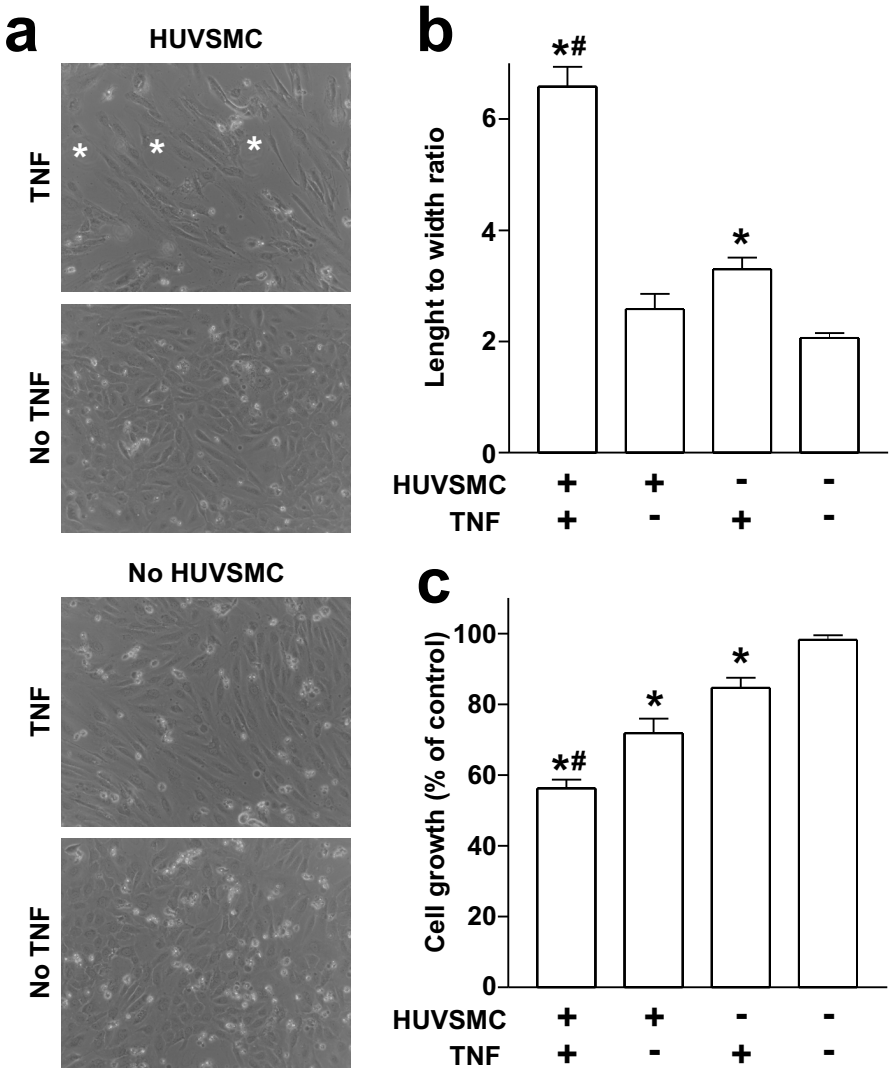

Figure 7. TNF-conditioned smooth muscle cell medium induces changes in endothelial cells. (a) HUVEC were incubated for 72 hours with TNF-conditioned HUVSMC medium, control-conditioned HUVSMC medium, TNF and medium and morphology was examined. Morphological analysis show cell elongation and gap formation (asterix) when incubate with TNF-conditioned HUVSMC medium. (**b, c**) Measurements of cell elongation (**b**) and cell growth (**c**) of HUVEC incubated with TNF-conditioned HUVSMC medium induced stretching of the endothelial cells and reduction in cell growth. Control-conditioned HUVSMC medium also induced a reduction in cell growth but not as severely as TNF-conditioned HUVSMC medium. Data represent mean ± SEM of at least 3 individual experiments in duplicate; *, $P < 0.05$ *versus* control; #, $P < 0.05$ TNF-conditioned HUVSMC medium *versus* control-conditioned HUVSMC medium.

DISCUSSION

In the present study we show that addition of low-dose mTNF to systemic Doxil treatment resulted in an enhanced antitumor response in B16BL6 and BLM, but not in LLC and 1F6-bearing mice. Tumor response correlates with an increased intratumoral Doxil concentration in B16BL6 and BLM, which was not found in LLC and 1F6. These results were confirmed in more detail by intravital microscopy, which showed that mTNF facilitates extravasation of liposomes into the tumor tissue in the B16BL6 and BLM tumor. Importantly, we show a correlation between augmented TNF-induced leakage and presence of TNFR1 expressing pericytes around tumor vessels in B16BL6 and BLM. These results indicate pericytes as primary target for TNF and likely responsible for the observed endothelial leakage.

Several studies report on the increased permeability of the tumor-associated vasculature due to their disorganized phenotype. Tumor endothelial cells are irregular shaped, sometimes even overlapping each other or display fenestrae [26]. These openings make the vessel highly permeable and allow passage of macromolecules, with an average cut off of 400 nm across the vasculature [27,28]. Commonly, endothelial cells form the inner lining of the vessel wall, while pericytes and other mural cells wrap around the vascular tube to form a stable blood vessel. The mature phenotype of the quiescent vasculature in organs is usually characterized by an extensive coverage with pericytes. Similarly to endothelial cells, pericytes have well-defined features in healthy blood vessels but exhibit bizarre properties in the TAV [29]. Also, the MPI varies greatly among tumor types. Eberhard *et al.* quantified maturation in glioblastoma and 5 different carcinoma's and found that MPI ranges from 10 to 20% in glioblastoma and renal cell carcinoma to approximately 65% in mammary and colon carcinomas [30]. Although, pericytes coverage is not a well-reliable parameter for tumor-angiogenesis and maturation, as pericytes can be associated well beyond the end of an endothelial sprout [29], these cells may present an useful target for therapy as we show here.

In 1971 Folkman proposed the hypothesis that prohibiting the development of newly formed tumor blood vessels would be an attractive new approach in cancer treatment [31] and several strategies for targeting the tumor-associated vasculature have been reported. First, antiangiogenic drugs prevent the formation of new blood vessels and normalize the existing blood vessels to improve a more efficient drug delivery [6,32]. Second, vascular disrupting agents directly kill the endothelial cells, leading to vascular shutdown [33,34] and, third the disorganized structure of the tumor vasculature can be further enhanced with vasoactive agents that increase intratumoral drug uptake [9,35-37]. In all these settings both endothelial cells but also other cells comprising the vasculature, such as pericytes, can be used as a target.

The main focus of our study is the use of the vasoactive agent TNF as an effective way to improve solid tumor treatment. TNF is a 17-kDa multicytokine involved in cell apoptosis as well as cell survival and signals via two distinct receptors, TNFR1 and TNFR2 from which TNFR1 initiates the majority of TNF's biological effects. TNFR1 has an intracellular Death Domain, which is absent in TNFR2, and signals to apoptosis via several caspases. Alternatively, binding of TNF to TNFR1 can also leads to the transcription of c-Jun and NF-kB that are important for cell proliferation and survival [38,39]. Previously, we demonstrate that low-dose TNF indeed enhances extravasation of liposomes in B16BL6 melanoma and BN-175 soft-tissue sarcoma while the endothelial lining is not destroyed and the vessels remain functional [7,9]. Ferrero *et al*. showed that stimulation of TNFR1 is sufficient to increase endothelial permeability *in vitro*. They found that neutralizing TNFR1 decreased TNF-induced permeability changes in the liver. However, detailed analysis to the TNF-sensitive cell type in the vasculature was lacking [24].

In this study, we show that the effectiveness of a dual targeting approach with the vasoactive agent TNF, in combination with Doxil, is dependent on the architecture of the tumor vessels. We have analyzed microvessel density,

microvessel size, functionality and pericyte coverage of the vascular bed and found distinctive differences correlating with the TNF-response. B16BL6 and BLM tumors contained large vessels with a low MVD. By comparison, a high degree of small vessels were present in the non-responding tumors LLC and 1F6. Despite the differences in vessel architecture the majority of the vessels in all four tumors were functional, but we observed only extravasation of liposomes in B16BL6 and BLM. Therefore, we concluded that direct endothelial targeting was not responsible for the TNF-induced permeability changes. Comparably, we observed *in vitro* hardly any passage of macromolecules through an endothelial cell layer when only exposed to TNF. Gap formation and permeability were increased when endothelial cells were co-incubated with TNF and IFN [40]. These results indicate that at least endothelial permeability is affected indirectly by TNF or that endothelial cells do not express TNFR1. Staining of human and mouse tumor tissue confirmed this as we observed that tumor-associated pericytes rather than endothelial cells expressed TNFR1. Correspondingly, B16BL6 and BLM showed a high pericyte coverage, which explains their responsiveness to TNF. In addition, LLC and 1F6 had a low pericyte coverage and this is consistent with the insensitivity to TNF and the absence of permeability changes.

From this study we conclude that high coverage of tumor vessels with TNFR1-expressing pericytes correlates with responsiveness to TNF. Based on these observations we hypothesize that pericytes rather then endothelial cells are the primary target for TNF, implying that beneficial activity of TNF in a combination treatment protocol could be predicted by the presence of pericytes in the tumor vasculature.

REFERENCES

1.Pasqualini R, Arap W, and McDonald DM. Probing the structural and molecular diversity of tumor vasculature. Trends Mol Med. 2002: 8(12), 563-571.

2.Balasubramanian L and Evens AM. Targeting angiogenesis for the treatment of sarcoma. Curr Opin Oncol. 2006: 18(4), 354-359.

3.Pilat MJ and Lorusso PM. Vascular disrupting agents. J Cell Biochem. 2006: 99(4), 1021-1039.

4.Jain RK. Molecular regulation of vessel maturation. Nat Med. 2003: 9(6), 685-693.

5.Collins TS and Hurwitz HI. Targeting vascular endothelial growth factor and angiogenesis for the treatment of colorectal cancer. Semin Oncol. 2005: 32(1), 61-68.

6.Jain RK. Normalization of tumor vasculature: an emerging concept in antiangiogenic therapy. Science. 2005: 307(5706), 58-62.

7.ten Hagen TL, van der Veen AH, Nooijen PT, van Tiel ST, Seynhaeve AL, and Eggermont AM. Low-dose tumor necrosis factor-alpha augments antitumor activity of stealth liposomal doxorubicin (DOXIL) in soft tissue sarcoma-bearing rats. Int J Cancer. 2000: 87(6), 829-837.

8.Brouckaert P, Takahashi N, van Tiel ST, Hostens J, Eggermont AM, Seynhaeve AL et al. Tumor necrosis factor-alpha augmented tumor response in B16BL6 melanoma-bearing mice treated with stealth liposomal doxorubicin (Doxil) correlates with altered Doxil pharmacokinetics. Int J Cancer. 2004: 109(3), 442-448.

9.Seynhaeve AL, Hoving S, Schipper D, Vermeulen CE, aan de Wiel-Ambagtsheer G, van Tiel ST et al. Tumor Necrosis Factor {alpha} Mediates Homogeneous Distribution of Liposomes in Murine Melanoma that Contributes to a Better Tumor Response. Cancer Res. 2007: 67(19), 9455-9462.

10.Kerkar S, Williams M, Blocksom JM, Wilson RF, Tyburski JG, and Steffes CP. TNF-alpha and IL-1beta increase pericyte/endothelial cell co-culture permeability. J Surg Res. 2006: 132(1), 40-45.

11.Lu C, Kamat AA, Lin YG, Merritt WM, Landen CN, Kim TJ et al. Dual targeting of endothelial cells and pericytes in antivascular therapy for ovarian carcinoma. Clin Cancer Res. 2007: 13(14), 4209-4217.

12.Bagley RG, Rouleau C, Morgenbesser SD, Weber W, Cook BP, Shankara S et al. Pericytes from human non-small cell lung carcinomas: an attractive target for anti-angiogenic therapy. Microvasc Res. 2006: 71(3), 163-174.

13.van Muijen GN, Cornelissen LM, Jansen CF, Figdor CG, Johnson JP, Brocker EB et al. Antigen expression of metastasizing and non-metastasizing human melanoma cells xenografted into nude mice. Clin Exp Metastasis. 1991: 9(3), 259-272.

14.Mayer LD, Tai LC, Ko DS, Masin D, Ginsberg RS, Cullis PR et al. Influence of vesicle size, lipid composition, and drug-to-lipid ratio on the biological activity of liposomal doxorubicin in mice. Cancer Res. 1989: 49(21), 5922-5930.

15.Papenfuss HD, Gross JF, Intaglietta M, and Treese FA. A transparent access chamber for the rat dorsal skin fold. Microvasc Res. 1979: 18(3), 311-318.
16.Falkvoll KH, Rofstad EK, Brustad T, and Marton P. A transparent chamber for the dorsal skin fold of athymic mice. Exp Cell Biol. 1984: 52(4), 260-268.
17.Leunig M, Yuan F, Menger MD, Boucher Y, Goetz AE, Messmer K et al. Angiogenesis, microvascular architecture, microhemodynamics, and interstitial fluid pressure during early growth of human adenocarcinoma LS174T in SCID mice. Cancer Res. 1992: 52(23), 6553-6560.
18.Kashiwagi S, Izumi Y, Gohongi T, Demou ZN, Xu L, Huang PL et al. NO mediates mural cell recruitment and vessel morphogenesis in murine melanomas and tissue-engineered blood vessels. J Clin Invest. 2005: 115(7), 1816-1827.
19.Carmichael J, DeGraff WG, Gazdar AF, Minna JD, and Mitchell JB. Evaluation of a tetrazolium-based semiautomated colorimetric assay: assessment of chemosensitivity testing. Cancer Res. 1987: 47(4), 936-942.
20.Jaffe EA, Nachman RL, Becker CG, and Minick CR. Culture of human endothelial cells derived from umbilical veins. Identification by morphologic and immunologic criteria. J Clin Invest. 1973: 52(11), 2745-2756.
21.Skehan P, Storeng R, Scudiero D, Monks A, McMahon J, Vistica D et al. New colorimetric cytotoxicity assay for anticancer-drug screening. J Natl Cancer Inst. 1990: 82(13), 1107-1112.
22.van der Veen AH, de Wilt JH, Eggermont AM, van Tiel ST, Seynhaeve AL, and ten Hagen TL. TNF-alpha augments intratumoural concentrations of doxorubicin in TNF-alpha-based isolated limb perfusion in rat sarcoma models and enhances anti-tumour effects. Br J Cancer. 2000: 82(4), 973-980.
23.de Wilt JH, ten Hagen TL, de Boeck G, van Tiel ST, de Bruijn EA, and Eggermont AM. Tumour necrosis factor alpha increases melphalan concentration in tumour tissue after isolated limb perfusion. Br J Cancer. 2000: 82(5), 1000-1003.
24.Ferrero E, Zocchi MR, Magni E, Panzeri MC, Curnis F, Rugarli C et al. Roles of tumor necrosis factor p55 and p75 receptors in TNF-alpha-induced vascular permeability. Am J Physiol Cell Physiol. 2001: 281(4), C1173-C1179.
25.van Horssen R, Rens JA, Brunstein F, Guns V, van Gils M, ten Hagen TL et al. Intratumoural expression of TNF-R1 and EMAP-II in relation to response of patients treated with TNF-based isolated limb perfusion. Int J Cancer. 2006: 119(6), 1481-1490.
26.Hashizume H, Baluk P, Morikawa S, McLean JW, Thurston G, Roberge S et al. Openings between defective endothelial cells explain tumor vessel leakiness. Am J Pathol. 2000: 156(4), 1363-1380.
27.Jain RK, Munn LL, and Fukumura D. Dissecting tumour pathophysiology using intravital microscopy. Nature Rev Cancer. 2002: 2(4), 266-276.
28.Yuan F, Dellian M, Fukumura D, Leunig M, Berk DA, Torchilin VP et al. Vascular permeability in a human tumor xenograft: molecular size dependence and cutoff size. Cancer Res. 1995: 55(17), 3752-3756.
29.Morikawa S, Baluk P, Kaidoh T, Haskell A, Jain RK, and McDonald DM. Abnormalities in pericytes on blood vessels and endothelial sprouts in tumors. Am J Pathol. 2002: 160(3), 985-1000.
30.Eberhard A, Kahlert S, Goede V, Hemmerlein B, Plate KH, and Augustin HG. Heterogeneity of angiogenesis and blood vessel maturation in human tumors: implications for antiangiogenic tumor therapies. Cancer Res. 2000: 60(5), 1388-1393.
31.Folkman J. Tumor angiogenesis: therapeutic implications. N Engl J Med. 1971: 285(21), 1182-1186.
32.Quesada AR, Munoz-Chapuli R, and Medina MA. Anti-angiogenic drugs: from bench to clinical trials. Med Res Rev. 2006: 26(4), 483-530.
33.Cooney MM, van Heeckeren W, Bhakta S, Ortiz J, and Remick SC. Drug insight: vascular disrupting agents and angiogenesis--novel approaches for drug delivery. Nat Clin Pract Oncol. 2006: 3(12), 682-692.
34.Tozer GM, Kanthou C, and Baguley BC. Disrupting tumour blood vessels. Nat Rev Cancer. 2005: 5(6), 423-435.
35.Brunstein F, Hoving S, Seynhaeve AL, van Tiel ST, Guetens G, de Bruijn EA et al. Synergistic antitumor activity of histamine plus melphalan in isolated limb perfusion: preclinical studies. J Natl Cancer Inst. 2004: 96(21), 1603-1610.
36.Hoving S, Brunstein F, aan de Wiel-Ambagtsheer G, van Tiel ST, de Boeck G, de Bruijn EA et al. Synergistic antitumor response of interleukin 2 with melphalan in isolated limb perfusion in soft tissue sarcoma-bearing rats. Cancer Res. 2005: 65(10), 4300-4308.
37.ten Hagen TL and Eggermont AM. Manipulation of the tumour-associated vasculature to improve tumour therapy. J Liposome Res. 2002: 12(1-2), 149-154.
38.Chen G and Goeddel DV. TNF-R1 signaling: a beautiful pathway. Science. 2002: 296(5573), 1634-1635.
39.van Horssen R, ten Hagen TL, and Eggermont AM. TNF-alpha in cancer treatment: molecular insights, antitumor

effects, and clinical utility. Oncologist. 2006: 11(4), 397-408.
40.Seynhaeve AL, Vermeulen CE, Eggermont AM, and ten Hagen TL. Cytokines and vascular permeability: an in vitro study on human endothelial cells in relation to tumor necrosis factor-alpha-primed peripheral blood mononuclear cells. Cell Biochem Biophys. 2006: 44(1), 157-169.

Part 4 - General discussion

About the authors (in alphabetical order)
Alexander M.M. Eggermont; Department of Surgical Oncology, Erasmus MC-Daniel den Hoed Cancer Center, Rotterdam, The Netherlands - **Timo L.M. ten Hagen**; Department of Surgical Oncology, Erasmus MC-Daniel den Hoed Cancer Center, Rotterdam, The Netherlands – **Ann Seynhaeve**; Department of Surgical Oncology, Erasmus MC-Daniel den Hoed Cancer Center, Rotterdam, The Netherlands

Chapter 10

TNF and manipulation of the tumor cell – stromal Interface: "Ways to make chemotherapy effective"

Ann L.B. Seynhaeve
Alexander M.M. Eggermont
Timo L.M. ten Hagen

Frontiers in Bioscience 2006: 13(1), 3034-3045

Review article

TNF and manipulation of the tumor cell – stromal Interface: "Ways to make chemotherapy effective"

Ann L.B. Seynhaeve, Alexander M.M. Eggermont, and Timo L.M. ten Hagen

Department of Surgical Oncology, Erasmus MC-Daniel den Hoed Cancer Center, Rotterdam, the Netherlands

ARTICLE INFORMATION

Frontiers in Bioscience 2006: 13(1), 3034-3045

ACKNOWLEDGMENTS

We like to thank the members of our group for critical discussions and technical support. We also thank Dr. Kirsten Kullak for the provision of TNF and Dr. Peter Working for the chemicals needed for the preparation of the liposomes.

ABSTRACT

Growth of solid tumors depends largely on the development of a functional vasculature, which has been the focus in antitumor therapy since Folkman in 1971 proposed that prohibiting the formation of new vessels could inhibit tumor growth. The recognition of the tumor vascular bed as an important target led to the development of 3 vascular-targeted strategies. I) The antiangiogenesis strategy that prevents the formation of new blood vessels and normalizes the remaining vessels. II) Applying vasculodestructive agents to induce apoptosis in the endothelium of the tumor-associated vasculature that results in vascular collapse and tumor necrosis. III) Promoting further abnormalization of the already abnormal features of the tumor-associated vasculature with vasoactive agents to enhance vessel permeability. Tumor necrosis factor-alpha (TNF) is a very promising vasoactive agent because of its antitumor effects but its severe systemic toxicity is a major drawback. Therefore a new setting, in which the optimal therapeutic benefit of TNF could be exploited, needed to be found. Through an isolated perfusion high dose of TNF can be administered in the blood circulation of the tumor-bearing extremity or organ. Alternatively, systemically low doses can be safely administered for several times. Importantly, TNF has no antitumor effect by itself and the combination with a conventional chemotherapeutic drug that targets the tumor cell is a prerequisite for a good tumor response. In this dual approach, TNF enhances intratumoral accumulation of the chemotherapeutic drug resulting in an impressive tumor response.

INTRODUCTION

At the end of the 19th century Dr. William Coley, a surgeon from New York, observed spontaneous tumor regression in patients suffering from a bacterial infection. Later, he developed a vaccine from two dead bacteria stains Streptococcus pyogenes and Serratia marcescens, the so-called Coley's Toxin, to successfully treat sarcoma patients. This toxin was also used for carcinomas, melanomas, lymphomas and myelomas and inducing a fever seemed the essential requirement for a good tumor response [1]. It was not until 1975 that Dr. Carswell isolated tumor necrosis factor (TNF) in serum form mice treated with bacterial endotoxin and found it to induce identical haemorrhagic necrosis of methylcholanthrene A fibrosarcoma (Meth A) tumors as the endotoxin itself [2]. With the development of new recombinant DNA techniques, human TNF became available for pre-clinical and clinical application [3,4]. However, TNF appeared to exert cytotoxic activ-

ity only towards some animal and human tumor cell lines [5] while the majority of malignant cells and most normal cells, including fibroblasts and endothelial cells are relative insensitive to TNF *in vitro* [6-9]. Also, systemic and intramuscular TNF therapy proved less successful than originally anticipated with ineffective tumor response and severe toxic effects including fever, fatigue, hypotension, shock and cachexia [10,11].

The development of chemotherapeutic agents, that would kill cancer cells, has long been the focus for the treatment of solid tumors. Agents may seem promising in a culture disk but when administered as a single agent in patients the results are often disappointing. Insufficient delivery at the target site, the tumor cell, results often in failure of the therapy and development of alternative strategies to increase chemotherapeutic agents at the tumor site proved to be a major success in treatment of solid tumors. TNF induces a better delivery of these agents at the tumor site by manipulating the tumor-associated vasculature. The models used and the mechanism behind this effect will be further discussed.

THE FORMATION OF NEW VESSELS

Vessel development. Angiogenesis, the process in which new blood vessels are formed form pre-existing blood vessels, is required for further growth and development of most tissues. Once the vasculature has been established, it remains mostly quiescent except in the ovary, uterus and the placenta during pregnancy. All other activation of the endothelium is found in processes during wound healing and inflammation and several other pathological conditions, like cancer, artherosclerosis, diabetic retinopathy and arthritis. There is a delicate balance between pro-angiogenic and antiangiogenic molecules and in many pathological conditions the balance changes in favor of angiogenesis, the so-called angiogenic switch [12]. Vascular endothelial growth factor (VEGF) and fibroblast growth factor (FGF) are among the initial factors involved in the angiogenic vessel growth. Mature blood vessels consist of endothelial cells (ECs), that form the luminal lining of the vessel wall, and perivascular cells (pericytes in capillaries and smooth muscle cells in larger vessels), which remain in close association with the ECs. These perivascular cells are responsible for vasoconstriction and dilation and prevent rupture due to blood flow pressure [13]. Blood vessels are embedded in the extracellular matrix (ECM), existing of several proteins including fibronectin, vitronectine, collagen and laminin [14].

One of the initial steps in the formation of a new blood vessel is weakening of contact between neighboring ECs, between ECs and underlying basal membrane (BM), detachment of pericytes and production of proteases that degrade the components of the ECM. The molecular mechanism involved in capillary sprouting has been extensively studied [15,16]. Pericytes have been shown to restrict the proliferation and migration of ECs so loss of pericytes from the vessels is required in the initiation of ECs sprouting [17-20]. In the presence of VEGF, angiopoietin-2 (Ang2) binds to the Tie receptor tyrosine kinase, Tie-2, which is upregulated in angiogenic vessels and results in the loss of interaction between endothelial cells, pericytes and ECM [21]. Next, for an EC to migrate and subsequently form a new blood vessel, the BM and the ECM have to be demodulated. Additionally, the ECM is a reservoir of several growth factors like VEGF, bFGF and transforming growth factor (TGF), which are released during angiogenesis contributing to further migration, proliferation and survival of the cells. The rearrangement of the ECM is facilitated by matrix metalloproteinases (MMPs), zinc-dependent endopeptidases capable of degrading and reorganizing the matrix proteins to suit better migration [22,23].

The leading EC in the angiogenic sprout is a non-proliferating cell with long protrusions scanning the microenvironment and migrating towards the angiogenic stimulus. Second, the VEGF-A gradient also stimulates proliferation of the stalk cells forming a bipolar (basal-luminal) cord [24]. After an endothelial sprout is formed, perivascular cells are needed to stabilize the tubular struc-

ture. Platelet-derived growth factor B (PDGFB) is secreted by endothelial cells in the presence of VEGF and signals though the PDGF-β receptor, which is expressed on perivascular cells. Also, angiopoetin-1 (Ang1) is produced by perivascular cells and binds to the Tie-2 receptor at the EC membrane. The Ang1/Tie-2 association promotes interaction between ECs and perivascular cells and is therefore important in stabilization of newly formed vessels [25,26]. Maturation of the sprout is initiated by transforming growth factor-beta (TGF-ß), secreted by ECs and perivascular cells. In a dose-dependent manner, TGF-ß can promote proliferation in ECs but also maintains EC quiescence to induce maturation of the vessel by stimulating the migration and recruitment of perivascular cells to the endothelial tube [19,27]. Furthermore, TGF-ß stimulates synthesis and deposition of ECM proteins and prevents their degradation by inducing plasminogen activator inhibitor 1 in ECs [28,29].

The tumor-associated vasculature. The presence of blood vessels is essential for growth and survival of a tumor. Tumors start as avascular masses that depend on diffusion of oxygen from pre-existing nearby vessels. When tumor cells starts to proliferate further growth will rely on the formation of blood vessels. In areas localized beyond the diffusion distance of 200 µm hypoxia will arise and will stimulate tumor cells to produce several pro-angiogenic factors, like VEGF-A and bFGF shifting the angiogenic balance in favor of angiogenesis [30]. In contrast to the structurally precise organization of the vascular bed of the basic organs, the tumor-associated vasculature (TAV) is "abnormal". They display a lack of hierarchical branching organization in which the recognizable features of arterioles, capillaries and venules is lost. They are tortuous and unevenly dilated. As a result, tumor blood flow is chaotic, might be stationary and can even change direction. This leads to hypoxia and acidosis in solid tumors [31].

Tumor ECs are disorganized with irregular shape, sometime even overlapping each other or displaying fenestrae [32]. These intracellular openings make the vessel highly permeable and allow passage of molecules across the vasculature. Dvorak *et al*. demonstrated that the leaky vessels are predominantly mature veins and venules lined by a continuous endothelium and that immature interface vessels and tumor penetrating vessels do not leak macromolecules [33]. This leakage subsequently results in an increased interstitial pressure that is maintained by the absence of functional lymphatics. Tumor-associated pericytes also display phenotypic differences not found in normal conditions. They are loosely associated with the ECs, display long extensions into the tumor stroma and are irregularly scattered [34]. Also, ECs and pericytes are loosely associated with the basal membrane which is irregular in thickness, matrix composition, assembly and structure [35]. The TAV varies greatly among tumor types. Eberhard *et al*. quantified maturation in glioblastoma and 5 different carcinoma's and found that microvessel pericyte coverage ranges form 10 to 20 % in glioblastoma and renal cell carcinoma to approximately 65 % in mammary and colon carcinomas [36]. Therefore, it seems logically that tumors that are less dependable on their vessel structure are less likely to react to tumor vessel therapy. In the K1735 murine melanoma tumors angiogenic sprouts lacking pericytes are evolving into functional endothelial tubes. Coverage of pericytes comes later and these vessels are larger in size and lack proliferating ECs [37]. In contradiction, in Lewis lung carcinoma and MCa-IV pericytes are present in practically all vessels undependably of size. Moreover, the endothelial sprouts were closely associated with pericytes and these even extended the endothelial tip cell [34].

TREATMENT OF SOLID TUMORS BY USING THE TUMOR-ASSOCIATED VASCULATURE

In 1971 Folkman proposed the hypothesis that prohibiting the development of newly formed

tumor blood vessels would be an attractive new approach in cancer treatment [38]. Starving the tumor to death through withdrawal of the inflow of nutrients using vascular targeting agents was in theory a strait forward approach. However, putting the theory in practice proved not so simple, but this idea led to several strategies focusing on the TAV. First, the antiangiogenesis strategy interferes with the formation of new tumor blood vessel and deprives the tumor of oxygen and nutrients required for tumor development. Several growth factors are important in this process and VEGF is believed to be the most important. VEGF is an important mitogen for vascular endothelial cells, mediates secretion and activation of MMPs and increases vascular permeability [38-42]. All these actions promote tumor vessel formation and it is not surprising that development of VEGF antagonists became the major focus in antiangiogenic therapy. Besides preventing the development of new blood vessels, the antiangiogenic therapy also normalizes the existing TAV. These normalized tumor vessels are believed to be more susceptible to conventional chemotherapy [43,44].

A second approach is the direct damage of the established tumor vasculature by vascular disrupting agents (VDAs) that will initiate vascular collapse, shutdown of tumor blood flow depriving the tumor of oxygen and nutrients leading to tumor necrosis [45]. VDAs exploit the difference in tumor ECs, because these cells have a the higher proliferating status and dependence on a tubulin cytoskeleton to maintain their shape then ECs in normal vessel [46,47].

A third approach consists of further enhancing the abnormal features of the TAV to improve a more homogenous drug delivery. A chemotherapeutic agent may show promising antitumor effects *in vitro*, but *in vivo* the antitumor effect will be limited if insufficient amounts of the agents reach its target, the tumor cell. This inadequate drug delivery has always been a major problem in the treatment of solid tumors. After systemic injection the drug dilutes massively in the blood stream and is rapidly cleared by liver and kidney. Because of the severe side effects of most chemotherapeutic drugs simply increasing the injected dose is not an option. When reaching the tumor site, a homogeneous drug distribution is difficult to accomplice due to the irregular blood flow and inhomogeneous perfusion of tumors. Also, the drug has to leave the blood circulation across the endothelial lining into the tumor interstitial space. Although ECs in tumor vessels display fenestrae and mature veins appear to be permeable for macromolecules with a cut off around 400 nm [32,33,48,49], extravasation of drug is often limited to the rim of the tumor. The dense tumor microenvironment, rich in a variety of matrix components (i.e. collagen, laminins, trombospondin, fibronectin, hyaluronate) and multiple types of stromal cells (fibroblasts, myofibroblasts, inflammatory cells) accompanied with a high interstitial fluid pressure, provide a solid barrier. Therefore, a dual approach is required combining an agent with vasoactive properties with a conventional chemotherapeutic agent that target the tumor cell.

MANIPULATION OF THE TUMOR-ASSOCIATED VASCULATURE

The isolated limb perfusion. The technique of the isolated limb perfusion (ILP) was first described in 1958 by Creech *et al*. and was used for the treatment of a patient with multiple in transit melanoma who refused amputation. With this technique, isolation of the blood circulation is achieved by clamping the major vein and artery, ligating the collateral vessels and application of a tourniquet around the basis of the limb to compress the remaining minor vessels. The main artery and vein is cannulated and connected to an oxygenated extracorporeal circuit. After isolation, chemotherapeutic agents can be injected into the circuit and regional concentrations 15 to 25 times higher can be reached compared to systemic administration [50]. After the procedure a washout is performed to ensure minimal systemic exposure to the drug. Also, ILP can be performed with mild hyperthermia (38.5 – 40°C) that improves local drug uptake whereas true hyperthermia (>41°C) is associated with increased toxicity. The main advantage of this method

is that locally very high concentrations of cytotoxic drugs can be accomplished with minimal systemic leakage and side effects. To use the antitumor properties of TNF, while limiting the side effects, Lejeune introduced TNF in the ILP [51,52]. The combination of TNF with the chemotherapeutic drug melphalan is now primarily used for the treatment of soft tissue sarcoma (STS) and melanoma in transit metastasis (IT-mets) of the extremities. STS are fast growing tumors and IT-mets exist of several large ulcerating lesions providing much painful discomfort for the patients and amputation was often the only option available. However, with the development of the ILP limb salvage and tumor control has replaced amputation in managing STS and IT-mets [53-55]. The excellent response rates and limb salvage of the TNF-based ILP with melphalan led to the approval of TNF by the European Medicine Evaluation Agency [56,57]. Angiograms taken from patients before perfusion show a well-developed tumor vasculature, which is selectively destroyed after TNF-based ILP while leaving the normal vessels intact [58-60].

For pre-clinical studies a rat ILP is developed that resembles the clinical setting to further investigate the role of TNF in this model [61]. Two different sarcomas are used: the rapidly growing and metastasizing high grade soft tissue sarcoma BN175 and the rapidly growing and metastasizing intermediated grade osteosarcoma ROS-1. A perfusion of BN175-bearing rats with TNF alone has no effect on the tumor growth and treatment with only melphalan resulted in a stable disease. However, complete remission in 75% of the animals is found with the combination of TNF and melphalan [62]. Also, in the ROS-1 tumor, the combination TNF and melphalan results in an significant increased tumor response [63]. *In vitro*, TNF has no direct cytotoxic effects in these cell lines and, more importantly, no synergistic effects between TNF and melphalan could be observed [63,64]. These observations indicate that the activity of TNF is most likely not directed towards the tumor cells but to the stromal compartment of the tumor. Histopathology of the tumors revealed that TNF induces edema, extravasation of erythrocytes and haemorrhagic necrosis suggestive of radical alteration in permeability and integrity of the tumor vasculature [65]. Indeed, directly after perfusion with TNF plus melphalan, taking 30 minutes, vascular destruction was detected and erythrocyte extravasated into the surrounding tumor tissue from these damaged vessels [66]. This endothelial damage, however, is not directly responsible for the tumor response since these effects are also observed with TNF alone and the combination with melphalan is necessary to obtain an efficient tumor response. Further studies revealed that immediately after TNF-based perfusion a six-fold increase of intratumoral melphalan concentration has been demonstrated compared to a perfusion with melphalan alone. This event is specific for the tumor environment as no increase was found in the skin and muscle [66,67]. Bauer *et al*. performed ILP on nude rats bearing a human melanoma xenograph and also reported high response rates with TNF and melphalan. Although they found no TNF-induced increase in intratumoral melphalan concentration, they observed extensive erythrostasis in the tumor vasculature [68].

After the success with the TNF-based ILP other chemotherapeutic drugs, like actinomycin D and doxorubicin were investigated. Actinomycin D is an anticancer antibiotic that has been used in patients with osteogenic sarcoma in combination with bleomycin and cyclophosphamide but this treatment is associated with severe nausea and anorexia [69]. Martijn *et al*. showed that melphalan-based ILP with actinomycin D in patients with IT-mets offer no improved response rates compared to melphalan alone [70]. However, actinomycin D increase the TNF sensitivity of tumor cells *in vitro* [71] and local administration of TNF in combination with actinomycin D in mice delays the growth of several tumors [72,73]. In the rat ILP model synergy between TNF and actinomycin D is observed but is accompanied with severe idiosyncratic locoregional toxicity to the normal tissue and therefore abandoned for further studies in this setting [74]. However, the TNF-based ILP with doxorubicin is more promising. Doxorubicin is the agent of choice for the treatment of sarcoma but is also accompanied with rigorous toxicity [75-77] and could therefore be a suitable agent for ILP. TNF-based ILP with doxorubicin results in an impressive tumor response

compared to ILP with doxorubicin alone in both tumor models (54 % versus 0% for the BN175 and 100% versus 0% in the ROS-1) without any side effects. In accordance with the melphalan treatment this tumor effect was also accompanied with enhanced intratumoral doxorubicin concentrations [78].

Systemic liposomal treatment. Another strategy to increase the amount of chemotherapy at the site of the tumor is the systemic use of liposomal-encapsulated drug. Liposomes are vesicular structures that exist of one or more phospholipid bilayers and have been developed to improve drug delivery at the tumor site and decrease toxicity normally associated with the conventional drug. However, development of liposomal chemotherapeutic agents has been hindered primarily by their rapid uptake by the mononuclear phagocyte system. Coating the liposomes with polyethylene glycol (PEG) increases the hydrophilic properties of the liposomal surface, thereby avoiding phagocytosis and prolonging blood circulation with a reserved or even improved tumor response [79-83]. As a result several of these sterically stabilized liposomes are developed for clinical use and two pegylated liposomal antracyclines are commercially available: pegylated liposomal doxorubicin (Doxil in the US, Caelyx in Europe) and liposomal daunorubicin (DaunoXome). Doxil, encapsulated doxorubicin in small (100 nm) unilamellar liposomes, shows a decrease in toxic effect, as alopecia, nausea, vomiting and cardiotoxicity, associated with the use of free doxorubicin [84-86]. Systemic treatment with low-dose TNF in combination with Doxil of BN175-bearing rats and B16BL6 or Meth A-bearing mice results in improved tumor response compared to treatment with Doxil alone [87-89]. In agreement with the ILP, TNF-induced enhanced accumulation of the liposomes in the tumor appears to be crucial for the observed response. Also *in vitro*, no direct cytotoxic effect of TNF, or synergism with Doxil was observed indicating a TNF host-mediated effect.

The use of intravital microscopy allows a better insight in the intratumoral location of the liposomes and enables longitudinal studies on the kinetics of intratumoral events. We used this technique to understand the effect of low-dose TNF on intratumoral fate of liposomes. Mice, implanted with the B16BL6 melanoma tumor in a dorsal skin-fold chamber were injected i.v. with liposomes together with a low well-tolerated dose of TNF. Liposomes, without the addition of TNF, remain predominantly in the vessels and hardly any accumulation in the tumor tissue could be observed. In contradiction, co-administration of TNF and liposomes resulted in abundant extravasation of liposomes from the blood stream into the surrounding tissue. Even 24 hours later, a fluorescent marker extravasated at the same spot indicating that these tumor vessels remain leaky and functional. Additionally, we observed no effect of this low-dose TNF on several microvessel parameters, like branching, density and diameter, indicating that the observed effect is not the result of vascular destruction but rather results from further enhancement of the already leaky properties if the tumor vasculature to allow passage of molecules with a certain size [90]. Apparently to achieve vascular destruction higher levels of TNF, like those administered in the ILP, are needed. Further investigation into the exact mechanism of this TNF effect is ongoing.

Also, encapsulating TNF into long circulating liposomes reduce the TNF associated side effects, shows similar biological activity and results in an increased localization of the cytokine in the tumor [91-93]. Systemic injection with long circulating liposomal TNF in combination with Doxil resulted in an improved tumor response in soft tissue sarcoma-bearing rats [94] and enhanced the effects of radiation against human colon cancer xenographs due to increased lymphocyte infiltration [95,96].

Sensitizers for TNF. Intravenous administration of a low dose TNF (3 – 5 µg) in Meth A-bearing mice results in thrombosis, increased vessel permeability, leukostasis, and hemorrhage in the tumor vessels leading to necrosis and regression of the tumor. *In vitro*, Meth A cells are relative

insensitive to TNF, further indicating a host-mediated effect [2]. From the supernatant of Meth A culture medium several factors were isolated that modulate the endothelial properties; vascular permeability factor, nowadays known as VEGF, and endothelial monocyte activating polypeptides I and II (EMAP) [97-99]. EMAP has the ability to induce tissue factor procoagulant activity in ECs and it was speculated that over-expression of EMAP-II might predispose the tumor vasculature to the procoagulant effects of TNF and increase sensitivity to the cytokine. B16BL6 melanoma and HT-1080 human fibrosarcoma-bearing mice underwent hemorrhage after intratumoral EMAP-II administration followed by systemic injection of TNF [100]. Also upregulation of EMAP-II using retroviral gene transfer shows that initially TNF-resistant tumors become sensitive to systemic TNF therapy [101] and therefore EMAP-II could be of additional benefit in the ILP. To investigate the role of EMAP-II in the ILP retroviral gene transfer was used to generate EMAP-II expressing BN175 and secondly wild-type tumor-bearing rats were pre-treated intravenously with recombinant EMAP-II. The results form these studies showed that EMAP II renders the otherwise resistant tumor responsive to TNF [102,103].

Tumor biopsies taken from patients with IT-mets revealed that the upregulation of EMAP-II strongly correlates with complete response. No correlation was found in the STS patients due to an overall low expression of proEMAP and EMAP-II in this type of tumor [104]. Therefore EMAP-II could potentially be a prognostic factor for TNF-treatment of patients with IT-mets. *In vitro* experiments show that EMAP-II facilitates TNFR1 apoptotic signaling in the ECs [105,106]. However, little is known about the TNFR1 expression profile within tumor tissue before and after ILP but co-staining for ECs and TNFR1 shows that TNFR1 is mainly expressed by cells closely associated with ECs but not by ECs themselves. In contradiction to EMAP-II that co-localizes with ECs [104]. This is very surprising and suggests that another cell type beside the ECs in the tumor vasculature is responsible for the TNF-induced antitumor effects. This might be a first indication that ECs are indirectly involved in the TNF-induced effect and could explain why ECs *in vitro* are resistant to TNF alone and need other cytokines like interferon-gamma (IFN), EMAP-II, interleukine-1beta (IL-1ß) or blood cells to induce changes in macromolecule permeability, morphological changes and apoptosis [6,107]. Apparently, the underlying mechanism of TNF-based therapy is more complicated then a simple binding of TNF to TNFR1 expressing ECs and is currently under investigation.

Transformation of TNF. Besides local treatment or drug encapsulation to reduce the toxicity or improve delivery, the chemical structure of the compound can be altered. Corti *et al*. coupled TNF with a cyclic CNGRC peptide, a CD13 ligand, to better target the tumor vasculature (NGR-TNF). Mice bearing B16F3 melanoma or RMA-T lymphoma were pretreated with NGR-TNF intraperitoneal followed 2 hours later by interperitoneal injection of doxorubicin or melphalan. Although the LD_{50} values of mTNF and NGR-mTNF are similar, mTNF was inactive at doses lower than 100 to 1,000 ng while NGR-mTNF inflicted antitumor effects with doses as low as 0.001 – 0.1 ng without any toxic side effects [108]. This low dose is sufficient to improve the antitumor effects of doxorubicin or melphalan in lymphoma and B16F1-bearing mice as a result of a better penetration of the chemotherapeutic drug in the tumor tissue [108,109]. Second, coupling TNF with RGD, also induced a delay in tumor growth without toxic effects [110].

Mayumi and colleagues chemically modified TNF with water-soluble polymers like PEG or polyvinylpyrollidone (PVP). This increase of the steric hindrance and protection from proteolytic degradation resulted in an increased drug stability and circulation time. However, the increase in size limits the distribution from blood to target tissue and steric hindrance can inhibit binding to the receptor. Therefore an optimal modification was designed to find the balance between clearance, toxicity and antitumoral activity [111-113], which proved to be effective in treatment of S-180 tumor-bearing mice [114]. Shibata *et al*. designed a pegylated lysine-deficient mutant TNF (sp-

PEG-mTNF-K90R) with higher affinity for both TNF-receptors with an antitumor activity 60-fold higher than native TNF in the Meth A mouse model [115]. Also binding of TNF at the surface of gold nanoparticles (cAu-TNF) improved the safety of TNF while retaining the antitumor efficacy by selectively altering the permeability of the tumor vasculature [116].

Another mutant, TNF-SAM2, with increased N-terminal basicity has a higher biological activity and milder toxicity than conventional TNF [117,118] and has similar antitumor activity in the melphalan- or doxorubicin-based ILP in BN175-rats [119] . It is being tested in the clinical ILP because of its potential decreased toxicity and is potentially applicable in regional perfusions that are not leakage free.

Alternatives for TNF. As mentioned, TNF targets the tumor-associated vasculature and improves intratumoral drug delivery. So agents with identical vasoactive properties could potentially be an alternative for TNF-based therapy. Histamine is found to be a excellent candidate. It is an inflammatory modulator that is predominantly formed and stored in the granules of mast cells and basophils and causes edema by promoting gaps between ECs and in so doing increases the permeability in venules [120-122]. Replacing TNF with histamine in the ILP in combination with either melphalan or doxorubicin results in a tumor response comparable to TNF-based ILP. Histopathology of the tumor showed vasodilatation of the tumor vasculature, damage to the ECs and extravasation of erythrocytes into the tumor interstitium. As a consequence edema and massive hemorrhage occurred. Similar to TNF-based ILP, the major antitumor effect could be explained by an indirect effect through a histamine-mediated accumulation of chemotherapeutic drug in the tumor tissue [64,123]. Although, histamine is only slight cytotoxic to ECs *in vitro*, within 15 minutes after histamine exposure gap-formation between the cells resulted in increased permeability [64]. These histamine-induced changes are also found by others and are believed to act through changes in VE-cadherin expression [124-126].

Second, interleukine-2 (IL-2) is a cytokine produced by activated T-cells to maintain their growth and cytotoxic response [127] and has been widely used in the treatment of solid tumors [128-130]. High doses of IL-2 causes serious side effects, like hypotension and vascular leakage syndrome causing intravascular liquid entering the organ interstitial space [131]. Because of its ability to induce vascular permeability this cytokine was speculated to be a good candidate for ILP. Indeed, we found a synergistic antitumor response in BN175-bearing rats after perfusion with IL-2 and melphalan correlating with an increased melphalan concentration in the tumor [132]. However, in contradiction to TNF and histamine no apparent vascular damage is seen after ILP although scattered erythrocytes are observed between the tumor cells indicating an increased vascular leakage. Interestingly, no increased extravasation of macrophages was found in the tumor tissue after ILP but there was a clear difference in distribution of these cells. In control and melphalan-treated animals an even distribution of macrophages throughout the tumor tissue was observed, while a clear clustering of these cells was found in the IL-2 plus melphalan group [132].

As histamine and IL-2 are tested in combination for the treatment of melanoma [133], we further investigated the triple combination histamine, IL-2 and melphalan. Histamine or IL-2-based melphalan perfusion resulted in an overall response of respectively 66% and 67%. Surprisingly, histamine and IL-2 together with melphalan led to on overall response of only 29%. Immunohistology revealed that the histamine-induced hemorrhage and vascular destruction was abolished by the addition of IL-2. Because of these poor results investigation on the triple combination therapy was discontinued [134].

Interaction and adhesion of sprouting endothelial cells with the ECM is mediated by endothelial transmembrane receptors or integrins like αVß3 and αVß5. Quiescent cells shown no luminal expression of these receptors while enhanced exposure of these integrins is found on tumor ECs making these integrins an potential target for antitumor therapy [135,136]. In preventing interac-

tion between the integrins αVβ3 and αVβ5 and their ECM ligands apoptosis of ECs take place. Cilengitide (EMD 121974) is a cyclic RGD containing peptide with high affinity for αV-integrins. Intraperitoneal injection with Cilengitide resulted in tumor growth arrest of glioblastoma, a highly vascularized invasive tumor, in mice [137] and improved, in combination with radioimmunotherapy, the treatment of breast cancer xenographs [138]. The potential contribution of Cilengitide in the melphalan-based ILP to improve solid tumor response is currently under investigation in our laboratory.

GENERAL CONCLUSION

Although antiangiogenic or vascular disrupting strategies are more generally known, manipulation of existing tumor vasculature, strategies to enhance vascular leakage and fluid flow into the tumor, also have been demonstrated to be useful. So, next to vascular normalization, as is shown with for instance anti-VEGF-based therapy, we would like to propose vascular abnormalization as a powerful alternative in solid tumor combination chemotherapy. We and other demonstrated that vasoactive agents like TNF or histamine further enhance these abnormal features in the tumor-associated vessels and as such augments the accumulating of conventional chemotherapy into the tumor tissue, ultimately resulting in an enhanced tumor response.

REFERENCES

1.Hoption Cann SA, van Netten JP, and van Netten C. Dr William Coley and tumour regression: a place in history or in the future. Postgrad Med J. 2003: 79(938), 672-680.

2.Carswell EA, Old LJ, Kassel RL, Green S, Fiore N, and Williamson B. An endotoxin-induced serum factor that causes necrosis of tumors. Proc Natl Acad Sci U S A. 1975: 72(9), 3666-3670.

3.Shirai T, Yamaguchi H, Ito H, Todd CW, and Wallace RB. Cloning and expression in Escherichia coli of the gene for human tumour necrosis factor. Nature. 1985: 313(6005), 803-806.

4.Wang AM, Creasey AA, Ladner MB, Lin LS, Strickler J, van Arsdell JN et al. Molecular cloning of the complementary DNA for human tumor necrosis factor. Science. 1985: 228(4696), 149-154.

5.Sgagias MK, Kasid A, and Danforth DN, Jr. Interleukin-1 alpha and tumor necrosis factor-alpha (TNF alpha) inhibit growth and induce TNF messenger RNA in MCF-7 human breast cancer cells. Mol Endocrinol. 1991: 5(11), 1740-1747.

6.Seynhaeve AL, Vermeulen CE, Eggermont AM, and ten Hagen TL. Cytokines and vascular permeability: an in vitro study on human endothelial cells in relation to tumor necrosis factor-alpha-primed peripheral blood mononuclear cells. Cell Biochem Biophys. 2006: 44(1), 157-169.

7.Morikawa K and Fidler IJ. Heterogeneous response of human colon cancer cells to the cytostatic and cytotoxic effects of recombinant human cytokines: interferon-alpha, interferon-gamma, tumor necrosis factor, and interleukin-1. J Biol Response Mod. 1989: 8(2), 206-218.

8.Sugarman BJ, Aggarwal BB, Hass PE, Figari IS, Palladino MA, Jr., and Shepard HM. Recombinant human tumor necrosis factor-alpha: effects on proliferation of normal and transformed cells in vitro. Science. 1985: 230(4728), 943-945.

9.Schiller JH, Bittner G, Storer B, and Willson JK. Synergistic antitumor effects of tumor necrosis factor and gamma-interferon on human colon carcinoma cell lines. Cancer Res. 1987: 47(11), 2809-2813.

10.Smith JW, Urba WJ, Clark JW, Longo DL, Farrell M, Creekmore SP et al. Phase I evaluation of recombinant tumor necrosis factor given in combination with recombinant interferon-gamma. J Immunother. 1991: 10(5), 355-362.

11.Schiller JH, Morgan-Ihrig C, and Levitt ML. Concomitant administration of interleukin-2 plus tumor necrosis factor in advanced non-small cell lung cancer. Am J Clin Oncol. 1995: 18(1), 47-51.

12.Folkman J. Angiogenesis and apoptosis. Semin Cancer Biol. 2003: 13(2), 159-167.

13.Allt G and Lawrenson JG. Pericytes: cell biology and pathology. Cells Tissues Organs. 2001: 169(1), 1-11.

14.Kalluri R. Basement membranes: structure, assembly and role in tumour angiogenesis. Nat Rev Cancer. 2003: 3(6), 422-433.

15.Carmeliet P and Collen D. Molecular basis of angiogenesis. Role of VEGF and VE-cadherin. Ann N Y Acad Sci. 2000: 902, 249-262.
16.Conway EM, Collen D, and Carmeliet P. Molecular mechanisms of blood vessel growth. Cardiovasc Res. 2001: 49(3), 507-521.
17.Orlidge A and D'Amore PA. Inhibition of capillary endothelial cell growth by pericytes and smooth muscle cells. J Cell Biol. 1987: 105(3), 1455-1462.
18.Fillinger MF, Sampson LN, Cronenwett JL, Powell RJ, and Wagner RJ. Coculture of endothelial cells and smooth muscle cells in bilayer and conditioned media models. J Surg Res. 1997: 67(2), 169-178.
19.Sato Y and Rifkin DB. Inhibition of endothelial cell movement by pericytes and smooth muscle cells: activation of a latent transforming growth factor-beta 1-like molecule by plasmin during co-culture. J Cell Biol. 1989: 109(1), 309-315.
20.Nehls V, Schuchardt E, and Drenckhahn D. The effect of fibroblasts, vascular smooth muscle cells, and pericytes on sprout formation of endothelial cells in a fibrin gel angiogenesis system. Microvasc Res. 1994: 48(3), 349-363.
21.Zhang L, Yang N, Park JW, Katsaros D, Fracchioli S, Cao G et al. Tumor-derived vascular endothelial growth factor up-regulates angiopoietin-2 in host endothelium and destabilizes host vasculature, supporting angiogenesis in ovarian cancer. Cancer Res. 2003: 63(12), 3403-3412.
22.Foda HD and Zucker S. Matrix metalloproteinases in cancer invasion, metastasis and angiogenesis. Drug Discov Today. 2001: 6(9), 478-482.
23.Rundhaug JE. Matrix metalloproteinases and angiogenesis. J Cell Mol Med. 2005: 9(2), 267-285.
24.Gerhardt H, Golding M, Fruttiger M, Ruhrberg C, Lundkvist A, Abramsson A et al. VEGF guides angiogenic sprouting utilizing endothelial tip cell filopodia. J Cell Biol. 2003: 161(6), 1163-1177.
25.Nishishita T and Lin PC. Angiopoietin 1, PDGF-B, and TGF-beta gene regulation in endothelial cell and smooth muscle cell interaction. J Cell Biochem. 2004: 91(3), 584-593.
26.Guo P, Hu B, Gu W, Xu L, Wang D, Huang HJ et al. Platelet-derived growth factor-B enhances glioma angiogenesis by stimulating vascular endothelial growth factor expression in tumor endothelia and by promoting pericyte recruitment. Am J Pathol. 2003: 162(4), 1083-1093.
27.Ma J, Wang Q, Fei T, Han JD, and Chen YG. MCP-1 mediates TGF-beta-induced angiogenesis by stimulating vascular smooth muscle cell migration. Blood. 2007: 109(3), 987-994.
28.Sankar S, Mahooti-Brooks N, Bensen L, McCarthy TL, Centrella M, and Madri JA. Modulation of transforming growth factor beta receptor levels on microvascular endothelial cells during in vitro angiogenesis. J Clin Invest. 1996: 97(6), 1436-1446.
29.Iruela-Arispe ML and Sage EH. Endothelial cells exhibiting angiogenesis in vitro proliferate in response to TGF-beta 1. J Cell Biochem. 1993: 52(4), 414-430.
30.Kelly BD, Hackett SF, Hirota K, Oshima Y, Cai Z, Berg-Dixon S et al. Cell type-specific regulation of angiogenic growth factor gene expression and induction of angiogenesis in nonischemic tissue by a constitutively active form of hypoxia-inducible factor 1. Circ Res. 2003: 93(11), 1074-1081.
31.Jain RK. Barriers to drug delivery in solid tumors. Sci Am. 1994: 271(1), 58-65.
32.Hashizume H, Baluk P, Morikawa S, McLean JW, Thurston G, Roberge S et al. Openings between defective endothelial cells explain tumor vessel leakiness. Am J Pathol. 2000: 156(4), 1363-1380.
33.Dvorak HF, Nagy JA, Dvorak JT, and Dvorak AM. Identification and characterization of the blood vessels of solid tumors that are leaky to circulating macromolecules. Am J Pathol. 1988: 133(1), 95-109.
34.Morikawa S, Baluk P, Kaidoh T, Haskell A, Jain RK, and McDonald DM. Abnormalities in pericytes on blood vessels and endothelial sprouts in tumors. Am J Pathol. 2002: 160(3), 985-1000.
35.Baluk P, Morikawa S, Haskell A, Mancuso M, and McDonald DM. Abnormalities of basement membrane on blood vessels and endothelial sprouts in tumors. Am J Pathol. 2003: 163(5), 1801-1815.
36.Eberhard A, Kahlert S, Goede V, Hemmerlein B, Plate KH, and Augustin HG. Heterogeneity of angiogenesis and blood vessel maturation in human tumors: implications for antiangiogenic tumor therapies. Cancer Res. 2000: 60(5), 1388-1393.
37.Gee MS, Procopio WN, Makonnen S, Feldman MD, Yeilding NM, and Lee WM. Tumor vessel development and maturation impose limits on the effectiveness of anti-vascular therapy. Am J Pathol. 2003: 162(1), 183-193.

38.Folkman J. Tumor angiogenesis: therapeutic implications. N Engl J Med. 1971: 285(21), 1182-1186.
39.Ferrara N. Role of vascular endothelial growth factor in physiologic and pathologic angiogenesis: therapeutic implications. Semin Oncol. 2002: 29(6 Suppl 16), 10-14.
40.Yuan F, Chen Y, Dellian M, Safabakhsh N, Ferrara N, and Jain RK. Time-dependent vascular regression and permeability changes in established human tumor xenografts induced by an anti-vascular endothelial growth factor/vascular permeability factor antibody. Proc Natl Acad Sci U S A. 1996: 93(25), 14765-14770.
41.Zucker S, Mirza H, Conner CE, Lorenz AF, Drews MH, Bahou WF et al. Vascular endothelial growth factor induces tissue factor and matrix metalloproteinase production in endothelial cells: conversion of prothrombin to thrombin results in progelatinase A activation and cell proliferation. Int J Cancer. 1998: 75(5), 780-786.
42.Dvorak HF, Brown LF, Detmar M, and Dvorak AM. Vascular permeability factor/vascular endothelial growth factor, microvascular hyperpermeability, and angiogenesis. Am J Pathol. 1995: 146(5), 1029-1039.
43.Batchelor TT, Sorensen AG, di Tomaso E, Zhang WT, Duda DG, Cohen KS et al. AZD2171, a pan-VEGF receptor tyrosine kinase inhibitor, normalizes tumor vasculature and alleviates edema in glioblastoma patients. Cancer Cell. 2007: 11(1), 83-95.
44.Tong RT, Boucher Y, Kozin SV, Winkler F, Hicklin DJ, and Jain RK. Vascular normalization by vascular endothelial growth factor receptor 2 blockade induces a pressure gradient across the vasculature and improves drug penetration in tumors. Cancer Res. 2004: 64(11), 3731-3736.
45.Hill S, Williams KB, and Denekamp J. Vascular collapse after flavone acetic acid: a possible mechanism of its antitumour action. Eur J Cancer Clin Oncol. 1989: 25(10), 1419-1424.
46.Denekamp J and Hobson B. Endothelial-cell proliferation in experimental tumours. Br J Cancer. 1982: 46(5), 711-720.
47.Hobson B and Denekamp J. Endothelial proliferation in tumours and normal tissues: continuous labelling studies. Br J Cancer. 1984: 49(4), 405-413.
48.Jain RK, Munn LL, and Fukumura D. Dissecting tumour pathophysiology using intravital microscopy. Nature Rev Cancer. 2002: 2(4), 266-276.
49.Yuan F, Dellian M, Fukumura D, Leunig M, Berk DA, Torchilin VP et al. Vascular permeability in a human tumor xenograft: molecular size dependence and cutoff size. Cancer Res. 1995: 55(17), 3752-3756.
50.Benckhuijsen C, Kroon BB, van Geel AN, and Wieberdink J. Regional perfusion treatment with melphalan for melanoma in a limb: an evaluation of drug kinetics. Eur J Surg Oncol. 1988: 14(2), 157-163.
51.Lienard D, Ewalenko P, Delmotte JJ, Renard N, and Lejeune FJ. High-dose recombinant tumor necrosis factor alpha in combination with interferon gamma and melphalan in isolation perfusion of the limbs for melanoma and sarcoma. J Clin Oncol. 1992: 10(1), 52-60.
52.Lienard D, Lejeune FJ, and Ewalenko P. In transit metastases of malignant melanoma treated by high dose rTNF alpha in combination with interferon-gamma and melphalan in isolation perfusion. World J Surg. 1992: 16(2), 234-240.
53.Eroglu A, Kocaoglu H, Demirci S, and Akgul H. Isolated limb perfusion with cisplatin and doxorubicin for locally advanced soft tissue sarcoma of an extremity. Eur J Surg Oncol. 2000: 26(3), 213-221.
54.Grunhagen DJ, de Wilt JH, ten Hagen TL, and Eggermont AM. Technology insight: Utility of TNF-alpha-based isolated limb perfusion to avoid amputation of irresectable tumors of the extremities. Nat Clin Pract Oncol. 2006: 3(2), 94-103.
55.Grunhagen DJ, de Wilt JH, van Geel AN, and Eggermont AM. Isolated limb perfusion for melanoma patients-a review of its indications and the role of tumour necrosis factor-alpha. Eur J Surg Oncol. 2006.
56.Eggermont AM, Schraffordt KH, Lienard D, Kroon BB, van Geel AN, Hoekstra HJ et al. Isolated limb perfusion with high-dose tumor necrosis factor-alpha in combination with interferon-gamma and melphalan for nonresectable extremity soft tissue sarcomas: a multicenter trial. J Clin Oncol. 1996: 14(10), 2653-2665.
57.Eggermont AM, Schraffordt KH, Klausner JM, Lienard D, Kroon BB, Schlag PM et al. Isolation limb perfusion with tumor necrosis factor alpha and chemotherapy for advanced extremity soft tissue sarcomas. Semin Oncol. 1997: 24(5), 547-555.
58.Renard N, Lienard D, Lespagnard L, Eggermont A, Heimann R, and Lejeune F. Early endothelium activation and polymorphonuclear cell invasion precede specific necrosis of human melanoma and sarcoma treated by intravascular high-dose tumour necrosis factor alpha (rTNF alpha). Int J Cancer. 1994: 57(5), 656-663.

59.Eggermont AM, de Wilt JH, and ten Hagen TL. Current uses of isolated limb perfusion in the clinic and a model system for new strategies. Lancet Oncol. 2003: 4(7), 429-437.
60.Lejeune FJ, Lienard D, Matter M, and Ruegg C. Efficiency of recombinant human TNF in human cancer therapy. Cancer Immun. 2006: 6, 6.
61.Manusama ER, Durante NM, Marquet RL, and Eggermont A. Ischemia promotes the antitumor effect of tumor necrosis factor alpha (TNF-alpha) in isolated limp perfusion in the rat. Reg Cancer Treat. 1994: 7, 155-159.
62.Manusama ER, Nooijen PT, Stavast J, Durante NM, Marquet RL, and Eggermont AM. Synergistic antitumour effect of recombinant human tumour necrosis factor alpha with melphalan in isolated limb perfusion in the rat. Br J Surg. 1996: 83(4), 551-555.
63.Manusama ER, Stavast J, Durante NM, Marquet RL, and Eggermont AM. Isolated limb perfusion with TNF alpha and melphalan in a rat osteosarcoma model: a new anti-tumour approach. Eur J Surg Oncol. 1996: 22(2), 152-157.
64.Brunstein F, Hoving S, Seynhaeve AL, van Tiel ST, Guetens G, de Bruijn EA et al. Synergistic antitumor activity of histamine plus melphalan in isolated limb perfusion: preclinical studies. J Natl Cancer Inst. 2004: 96(21), 1603-1610.
65.Nooijen PT, Manusama ER, Eggermont AM, Schalkwijk L, Stavast J, Marquet RL et al. Synergistic effects of TNF-alpha and melphalan in an isolated limb perfusion model of rat sarcoma: a histopathological, immunohistochemical and electron microscopical study. Br J Cancer. 1996: 74(12), 1908-1915.
66.Hoving S, Seynhaeve AL, van Tiel ST, aan de Wiel-Ambagtsheer G, de Bruijn EA, Eggermont AM et al. Early destruction of tumor vasculature in tumor necrosis factor-alpha-based isolated limb perfusion is responsible for tumor response. Anticancer Drugs. 2006: 17(8), 949-959.
67.de Wilt JH, ten Hagen TL, de Boeck G, van Tiel ST, de Bruijn EA, and Eggermont AM. Tumour necrosis factor alpha increases melphalan concentration in tumour tissue after isolated limb perfusion. Br J Cancer. 2000: 82(5), 1000-1003.
68.Bauer TW, Gutierrez M, Dudrick DJ, Li J, Blair IA, Menon C et al. A human melanoma xenograft in a nude rat responds to isolated limb perfusion with TNF plus melphalan. Surgery. 2003: 133(4), 420-428.
69.Mosende C, Gutierrez M, Caparros B, and Rosen G. Combination chemotherapy with bleomycin, cyclophosphamide and dactinomycin for the treatment of osteogenic sarcoma. Cancer. 1977: 40(6), 2779-2786.
70.Martijn H, Oldhoff J, and Koops HS. Hyperthermic regional perfusion with melphalan and a combination of melphalan and actinomycin D in the treatment of locally metastasized malignant melanomas of the extremities. J Surg Oncol. 1982: 20(1), 9-13.
71.Alexander RB, Nelson WG, and Coffey DS. Synergistic enhancement by tumor necrosis factor of in vitro cytotoxicity from chemotherapeutic drugs targeted at DNA topoisomerase II. Cancer Res. 1987: 47(9), 2403-2406.
72.Lasek W, Giermasz A, Kuc K, Wankowicz A, Feleszko W, Golab J et al. Potentiation of the anti-tumor effect of actinomycin D by tumor necrosis factor alpha in mice: correlation between in vitro and in vivo results. Int J Cancer. 1996: 66(3), 374-379.
73.Lasek W, Wankowicz A, Kuc K, Feleszko W, Giermasz A, and Jakobisiak M. Augmentation of antitumor efficacy by the combination of actinomycin D with tumor necrosis factor-alpha and interferon-gamma on a melanoma model in mice. Oncology. 1996: 53(1), 31-37.
74.Seynhaeve AL, de Wilt JH, van Tiel ST, Eggermont AM, and ten Hagen TL. Isolated limb perfusion with actinomycin D and TNF-alpha results in improved tumour response in soft-tissue sarcoma-bearing rats but is accompanied by severe local toxicity. Br J Cancer. 2002: 86(7), 1174-1179.
75.Bielack SS, Erttmann R, Kempf-Bielack B, and Winkler K. Impact of scheduling on toxicity and clinical efficacy of doxorubicin: what do we know in the mid-nineties? Eur J Cancer. 1996: 32A(10), 1652-1660.
76.Borden EC, Amato DA, Edmonson JH, Ritch PS, and Shiraki M. Randomized comparison of doxorubicin and vindesine to doxorubicin for patients with metastatic soft-tissue sarcomas. Cancer. 1990: 66(5), 862-867.
77.Budd GT. Palliative chemotherapy of adult soft tissue sarcomas. Semin Oncol. 1995: 22(2 Suppl 3), 30-34.
78.van der Veen AH, de Wilt JH, Eggermont AM, van Tiel ST, Seynhaeve AL, and ten Hagen TL. TNF-alpha augments intratumoural concentrations of doxorubicin in TNF-alpha-based isolated limb perfusion in rat sarcoma models and enhances anti-tumour effects. Br J Cancer. 2000: 82(4), 973-980.
79.Allen TM. Long-circulating (sterically stabilized) liposomes for targeted drug delivery. Trends Pharmacol Sci. 1994: 15(7), 215-220.

80.Gabizon A, Shiota R, and Papahadjopoulos D. Pharmacokinetics and tissue distribution of doxorubicin encapsulated in stable liposomes with long circulation times. J Natl Cancer Inst. 1989: 81(19), 1484-1488.
81.Uziely B, Jeffers S, Isacson R, Kutsch K, Wei-Tsao D, Yehoshua Z et al. Liposomal doxorubicin: antitumor activity and unique toxicities during two complementary phase I studies. J Clin Oncol. 1995: 13(7), 1777-1785.
82.Allen TM and Hansen C. Pharmacokinetics of stealth versus conventional liposomes: effect of dose. Biochim Biophys Acta. 1991: 1068(2), 133-141.
83.Gabizon A and Papahadjopoulos D. Liposome formulations with prolonged circulation time in blood and enhanced uptake by tumors. Proc Natl Acad Sci U S A. 1988: 85(18), 6949-6953.
84.Safra T, Muggia F, Jeffers S, Tsao-Wei DD, Groshen S, Lyass O et al. Pegylated liposomal doxorubicin (doxil): reduced clinical cardiotoxicity in patients reaching or exceeding cumulative doses of 500 mg/m2. Ann Oncol. 2000: 11(8), 1029-1033.
85.Alberts DS and Garcia DJ. Safety aspects of pegylated liposomal doxorubicin in patients with cancer. Drugs. 1997: 54 Suppl 4, 30-35.
86.Gabizon A and Martin F. Polyethylene glycol-coated (pegylated) liposomal doxorubicin. Rationale for use in solid tumours. Drugs. 1997: 54 Suppl 4, 15-21.
87.Brouckaert P, Takahashi N, van Tiel ST, Hostens J, Eggermont AM, Seynhaeve AL et al. Tumor necrosis factor-alpha augmented tumor response in B16BL6 melanoma-bearing mice treated with stealth liposomal doxorubicin (Doxil) correlates with altered Doxil pharmacokinetics. Int J Cancer. 2004: 109(3), 442-448.
88.ten Hagen TL, van der Veen AH, Nooijen PT, van Tiel ST, Seynhaeve AL, and Eggermont AM. Low-dose tumor necrosis factor-alpha augments antitumor activity of stealth liposomal doxorubicin (DOXIL) in soft tissue sarcoma-bearing rats. Int J Cancer. 2000: 87(6), 829-837.
89.Suzuki S, Ohta S, Takashio K, Nitanai H, and Hashimoto Y. Augmentation for intratumoral accumulation and antitumor activity of liposome-encapsulated adriamycin by tumor necrosis factor-alpha in mice. Int J Cancer. 1990: 46(6), 1095-1100.
90.Seynhaeve AL, Hoving S, Schipper D, Vermeulen CE, aan de Wiel-Ambagtsheer G, van Tiel ST et al. Tumor Necrosis Factor A Mediates Homogeneous Distribution of Liposomes in Murine Melanoma that Contributes to a Better Tumor Response. Cancer Res. 2007: In press.
91.van der Veen AH, Eggermont AM, Seynhaeve AL, van Tiel ST, and ten Hagen TL. Biodistribution and tumor localization of stealth liposomal tumor necrosis factor-alpha in soft tissue sarcoma bearing rats. Int J Cancer. 1998: 77(6), 901-906.
92.Debs RJ, Fuchs HJ, Philip R, Brunette EN, Duzgunes N, Shellito JE et al. Immunomodulatory and toxic effects of free and liposome-encapsulated tumor necrosis factor alpha in rats. Cancer Res. 1990: 50(2), 375-380.
93.Nii A, Fan D, and Fidler IJ. Cytotoxic potential of liposomes containing tumor necrosis factor-alpha against sensitive and resistant target cells. J Immunother. 1991: 10(1), 13-19.
94.ten Hagen TL, Seynhaeve AL, van Tiel ST, Ruiter DJ, and Eggermont AM. Pegylated liposomal tumor necrosis factor-alpha results in reduced toxicity and synergistic antitumor activity after systemic administration in combination with liposomal doxorubicin (Doxil) in soft tissue sarcoma-bearing rats. Int J Cancer. 2002: 97(1), 115-120.
95.Kim DW, Andres ML, Li J, Kajioka EH, Miller GM, Seynhaeve AL et al. Liposome-encapsulated tumor necrosis factor-alpha enhances the effects of radiation against human colon tumor xenografts. J Interferon Cytokine Res. 2001: 21(11), 885-897.
96.Kim DW, Andres ML, Miller GM, Cao JD, Green LM, Seynhaeve AL et al. Immunohistological analysis of immune cell infiltration of a human colon tumor xenograft after treatment with Stealth(R) liposome-encapsulated tumor necrosis factor-alpha and radiation. Int J Oncol. 2002: 21(5), 973-979.
97.Kao J, Houck K, Fan Y, Haehnel I, Libutti SK, Kayton ML et al. Characterization of a novel tumor-derived cytokine. Endothelial-monocyte activating polypeptide II. J Biol Chem. 1994: 269(40), 25106-25119.
98.Clauss M, Gerlach M, Gerlach H, Brett J, Wang F, Familletti PC et al. Vascular permeability factor: a tumor-derived polypeptide that induces endothelial cell and monocyte procoagulant activity, and promotes monocyte migration. J Exp Med. 1990: 172(6), 1535-1545.

99.Clauss M, Murray JC, Vianna M, de Waal R, Thurston G, Nawroth P et al. A polypeptide factor produced by fibrosarcoma cells that induces endothelial tissue factor and enhances the procoagulant response to tumor necrosis factor/cachectin. J Biol Chem. 1990: 265(12), 7078-7083.
100.Marvin MR, Libutti SK, Kayton M, Kao J, Hayward J, Grikscheit T et al. A novel tumor-derived mediator that sensitizes cytokine-resistant tumors to tumor necrosis factor. J Surg Res. 1996: 63(1), 248-255.
101.Wu PC, Alexander HR, Huang J, Hwu P, Gnant M, Berger AC et al. In vivo sensitivity of human melanoma to tumor necrosis factor (TNF)-alpha is determined by tumor production of the novel cytokine endothelial-monocyte activating polypeptide II (EMAPII). Cancer Res. 1999: 59(1), 205-212.
102.Lans TE, ten Hagen TL, van Horssen R, Wu PC, van Tiel ST, Libutti SK et al. Improved antitumor response to isolated limb perfusion with tumor necrosis factor after upregulation of endothelial monocyte-activating polypeptide II in soft tissue sarcoma. Ann Surg Oncol. 2002: 9(8), 812-819.
103.Lans TE, van Horssen R, Eggermont AM, and ten Hagen TL. Involvement of endothelial monocyte activating polypeptide II in tumor necrosis factor-alpha-based anti-cancer therapy. Anticancer Res. 2004: 24(4), 2243-2248.
104.van Horssen R, Rens JA, Brunstein F, Guns V, van Gils M, ten Hagen TL et al. Intratumoural expression of TNF-R1 and EMAP-II in relation to response of patients treated with TNF-based isolated limb perfusion. Int J Cancer. 2006: 119(6), 1481-1490.
105.van Horssen R, Rens JA, Schipper D, Eggermont AM, and ten Hagen TL. EMAP-II facilitates TNF-R1 apoptotic signalling in endothelial cells and induces TRADD mobilization. Apoptosis. 2006: 11(12), 2137-2145.
106.Berger AC, Alexander HR, Wu PC, Tang G, Gnant MF, Mixon A et al. Tumour necrosis factor receptor I (p55) is upregulated on endothelial cells by exposure to the tumour-derived cytokine endothelial monocyte- activating polypeptide II (EMAP-II). Cytokine. 2000: 12(7), 992-1000.
107.Yilmaz A, Bieler G, Spertini O, Lejeune FJ, and Ruegg C. Pulse treatment of human vascular endothelial cells with high doses of tumor necrosis factor and interferon-gamma results in simultaneous synergistic and reversible effects on proliferation and morphology. Int J Cancer. 1998: 77(4), 592-599.
108.Curnis F, Sacchi A, and Corti A. Improving chemotherapeutic drug penetration in tumors by vascular targeting and barrier alteration. J Clin Invest. 2002: 110(4), 475-482.
109.Curnis F, Sacchi A, Borgna L, Magni F, Gasparri A, and Corti A. Enhancement of tumor necrosis factor alpha antitumor immunotherapeutic properties by targeted delivery to aminopeptidase N (CD13). Nat Biotechnol. 2000: 18(11), 1185-1190.
110.Zarovni N, Monaco L, and Corti A. Inhibition of tumor growth by intramuscular injection of cDNA encoding tumor necrosis factor alpha coupled to NGR and RGD tumor-homing peptides. Hum Gene Ther. 2004: 15(4), 373-382.
111.Tsunoda S, Ishikawa T, Yamamoto Y, Kamada H, Koizumi K, Matsui J et al. Enhanced antitumor potency of polyethylene glycolylated tumor necrosis factor-alpha: a novel polymer-conjugation technique with a reversible amino-protective reagent. J Pharmacol Exp Ther. 1999: 290(1), 368-372.
112.Tsutsumi Y, Tsunoda S, Kamada H, Kihira T, Nakagawa S, Kaneda Y et al. Molecular design of hybrid tumour necrosis factor-alpha. II: The molecular size of polyethylene glycol-modified tumour necrosis factor-alpha affects its anti-tumour potency. Br J Cancer. 1996: 74(7), 1090-1095.
113.Kamada H, Tsutsumi Y, Tsunoda S, Kihira T, Kaneda Y, Yamamoto Y et al. Molecular design of conjugated tumor necrosis factor-alpha: synthesis and characteristics of polyvinyl pyrrolidone modified tumor necrosis factor-alpha. Biochem Biophys Res Commun. 1999: 257(2), 448-453.
114.Kamada H, Tsutsumi Y, Yamamoto Y, Kihira T, Kaneda Y, Mu Y et al. Antitumor activity of tumor necrosis factor-alpha conjugated with polyvinylpyrrolidone on solid tumors in mice. Cancer Res. 2000: 60(22), 6416-6420.
115.Shibata H, Yoshioka Y, Ikemizu S, Kobayashi K, Yamamoto Y, Mukai Y et al. Functionalization of tumor necrosis factor-alpha using phage display technique and PEGylation improves its antitumor therapeutic window. Clin Cancer Res. 2004: 10(24), 8293-8300.
116.Farma JM, Puhlmann M, Soriano PA, Cox D, Paciotti GF, Tamarkin L et al. Direct evidence for rapid and selective induction of tumor neovascular permeability by tumor necrosis factor and a novel derivative, colloidal gold bound tumor necrosis factor. Int J Cancer. 2007: 120(11), 2474-2480.

117.Gatanaga T, Noguchi K, Tanabe Y, Inagawa H, Soma G, and Mizuno D. Antitumor effect of systemic administration of novel recombinant tumor necrosis factor (rTNF-S) with less toxicity than conventional rTNF-alpha in vivo. J Biol Response Mod. 1989: 8(3), 278-286.
118.Soma G, Tsuji Y, Tanabe Y, Noguchi K, Kitahara-Tanabe N, Gatanaga T et al. Biological activities of novel recombinant tumor necrosis factor having N-terminal amino acid sequences derived from cytotoxic factors produced by THP-1 cells. J Biol Response Mod. 1988: 7(6), 587-595.
119.de Wilt JH, Soma G, ten Hagen TL, Kanou J, Takagi K, Nooijen PT et al. Synergistic antitumour effect of TNF-SAM2 with melphalan and doxorubicin in isolated limb perfusion in rats. Anticancer Res. 2000: 20(5B), 3491-3496.
120.Wu NZ and Baldwin AL. Transient venular permeability increase and endothelial gap formation induced by histamine. Am J Physiol. 1992: 262(4 Pt 2), H1238-H1247.
121.Horan KL, Adamski SW, Ayele W, Langone JJ, and Grega GJ. Evidence that prolonged histamine suffusions produce transient increases in vascular permeability subsequent to the formation of venular macromolecular leakage sites. Proof of the Majno-Palade hypothesis. Am J Pathol. 1986: 123(3), 570-576.
122.Majno G and Palade GE. Studies on inflammation. 1. The effect of histamine and serotonin on vascular permeability: an electron microscopic study. J Biophys Biochem Cytol. 1961: 11, 571-605.
123.Brunstein F, Rens J, van Tiel ST, Eggermont AM, and ten Hagen TL. Histamine, a vasoactive agent with vascular disrupting potential, improves tumour response by enhancing local drug delivery. Br J Cancer. 2006: 95(12), 1663-1669.
124.Andriopoulou P, Navarro P, Zanetti A, Lampugnani MG, and Dejana E. Histamine induces tyrosine phosphorylation of endothelial cell-to-cell adherens junctions. Arterioscler Thromb Vasc Biol. 1999: 19(10), 2286-2297.
125.Leach L, Eaton BM, Westcott ED, and Firth JA. Effect of histamine on endothelial permeability and structure and adhesion molecules of the paracellular junctions of perfused human placental microvessels. Microvasc Res. 1995: 50(3), 323-337.
126.Shasby DM, Ries DR, Shasby SS, and Winter MC. Histamine stimulates phosphorylation of adherens junction proteins and alters their link to vimentin. Am J Physiol Lung Cell Mol Physiol. 2002: 282(6), L1330-L1338.
127.Morgan DA, Ruscetti FW, and Gallo R. Selective in vitro growth of T lymphocytes from normal human bone marrows. Science. 1976: 193(4257), 1007-1008.
128.Dutcher J. Current status of interleukin-2 therapy for metastatic renal cell carcinoma and metastatic melanoma. Oncology (Williston Park). 2002: 16(11 Suppl 13), 4-10.
129.Tarhini AA and Agarwala SS. Interleukin-2 for the treatment of melanoma. Curr Opin Investig Drugs. 2005: 6(12), 1234-1239.
130.Grande C, Firvida JL, Navas V, and Casal J. Interleukin-2 for the treatment of solid tumors other than melanoma and renal cell carcinoma. Anticancer Drugs. 2006: 17(1), 1-12.
131.Siegel JP and Puri RK. Interleukin-2 toxicity. J Clin Oncol. 1991: 9(4), 694-704.
132.Hoving S, Brunstein F, aan de Wiel-Ambagtsheer G, van Tiel ST, de Boeck G, de Bruijn EA et al. Synergistic antitumor response of interleukin 2 with melphalan in isolated limb perfusion in soft tissue sarcoma-bearing rats. Cancer Res. 2005: 65(10), 4300-4308.
133.Middleton M, Hauschild A, Thomson D, Anderson R, Burdette-Radoux S, Gehlsen K et al. Results of a multicenter randomized study to evaluate the safety and efficacy of combined immunotherapy with interleukin-2, interferon-{alpha}2b and histamine dihydrochloride versus dacarbazine in patients with stage IV melanoma. Ann Oncol. 2007.
134.Brunstein F, Hoving S, aan de Wiel-Ambagtsheer G, de Bruijn EA, Guetens G, Eggermont AM et al. Decreased response rates by the combination of histamine and IL-2 in melphalan-based isolated limb perfusion. Cancer Immunol Immunother. 2007: 56(4), 573-580.
135.Ruegg C, Dormond O, and Mariotti A. Endothelial cell integrins and COX-2: mediators and therapeutic targets of tumor angiogenesis. Biochim Biophys Acta. 2004: 1654(1), 51-67.
136.Hynes RO. A reevaluation of integrins as regulators of angiogenesis. Nat Med. 2002: 8(9), 918-921.
137.Yamada S, Bu XY, Khankaldyyan V, Gonzales-Gomez I, McComb JG, and Laug WE. Effect of the angiogenesis inhibitor Cilengitide (EMD 121974) on glioblastoma growth in nude mice. Neurosurgery. 2006: 59(6), 1304-1312.

138.Burke PA, DeNardo SJ, Miers LA, Lamborn KR, Matzku S, and DeNardo GL. Cilengitide targeting of alpha(v)beta(3) integrin receptor synergizes with radioimmunotherapy to increase efficacy and apoptosis in breast cancer xenografts. Cancer Res. 2002: 62(15), 4263-4272.

Chapter 11

TNF-mediated interactions between inflammatory response and tumor vascular bed

Timo L.M. ten Hagen
Ann L.B. Seynhaeve
Alexander M.M. Eggermont

Immunological Reviews. 2008: 222, 299-315

Review article

TNF-mediated interactions between inflammatory response and tumor vascular bed

Timo L.M. ten Hagen, Ann L.B. Seynhaeve, and Alexander M.M. Eggermont

Department of Surgical Oncology, Erasmus MC – Daniel den Hoed Cancer Center, Rotterdam, the Netherlands

ARTICLE INFORMATION

Immunological Reviews. 2008: 222, 299-315

ABSTRACT

Solid tumor therapy with chemotherapeutics greatly depends on the efficiency with which drugs are delivered to tumor cells. The typical characteristics of the tumor physiology both promote but also appose accumulation of blood borne agents. The leaky tumor vasculature allows easy passage of drugs. However, the disorganized vasculature causes heterogeneous blood flow and together with the often elevated interstitial fluid pressure this results in poor intratumoral drug levels and failure of treatment. Manipulation of the tumor vasculature could overcome these barriers and promote drug delivery. Targeting the vasculature has several advantages. The endothelial lining is readily accessible and the first to be encountered after systemic injection. Second, endothelial cells tend to be more stable than tumor cells and thus less likely to develop resistance to therapy. Third, targeting the tumor vasculature can have dual effects: 1) Manipulation of the vasculature can enhance concomitant chemotherapy, and 2) subsequent destruction of the vasculature will add to kill the tumor. In particular tumor necrosis factor-alpha is studied. Its action on solid tumors, both directly through tumor cell kill and destruction of the tumor vasculature, and indirectly through manipulation of the tumor physiology, appears complex. Understanding the mechanism of TNF and agents with comparable action on solid tumors is an important focus to further develop combination immunotherapy strategies.

INTRODUCTION

One of the main problems of chemotherapy is getting the active drug to the tumor site. There are a number of factors related to characteristics of the drug, such as binding to blood components, circulation time, toxicity, stability and solubility, which determine efficacy of the chemotherapy and therefore simply increasing the dose is not the answer. Also typical features of the tumor affect intratumoral accumulation of agents. Solid tumors tend to exhibit a leaky vasculature with gaps between endothelial cells of around 400 nm but ranging as far as more than a micrometer [1-4]. This feature enables passive accumulation of blood borne elements such as antibodies or liposomes in the tumor interstitial space. On the other hand a number of factors are identified which negatively influence drug delivery to solid tumors. The rapid angiogenesis typically associated with solid tumor growth results in an immature and disorganized vasculature, which is tortuous and curved, and chaotic in its hierarchy [5-7]. The presence of shunts and uncontrolled branching results in irregular or even absent blood flow that results in an inadequate heterogeneous delivery

of drugs. In addition, tumors tend to exhibit an elevated interstitial fluid pressure [8-10], which works against the drug accumulation. Moreover, lymphatic vessels may be compressed impairing the flow of lymph [11-13] and thus the inflow of antitumor agents. Lastly, the blood volume of a tumor is generally quite low compared to the total body volume. So, massive dilution occurs after systemic administration while only a limited fraction distributes to the tumor.

It is our believe that if enough of a chemotherapeutic agent could be delivered, i.e. the concentration reached in the tumor cell is above the level needed to kill the cell, the desired tumor response is achieved. In other words, we do not need to improve the killing capacity of the drug *per se*, but we need to improve the delivery of the administered agent to the tumor. There are a number of techniques that can be used to augment intratumor drug concentrations. For instance loco-regional treatment strategies are used such as intratumoral injection, infusion or perfusion, which impairs the volume of distribution and raises local drug levels. Delivery may be improved by targeting or encapsulation in liposomes. Here we will discus the use of vasoactive agents, in particular TNF and agents with comparable activity, to manipulate the tumor physiology to enhance drug accumulation.

The use of vasoactive drugs and especially understanding their mechanism of action is crucial in further development of better or new combination therapies. Although ample knowledge on TNF exists detailed insight in its precise actions is missing. It appears that rather complex and multifactorial immunological pathways are involved. While direct triggering of apoptosis in tumor cells has long been thought to be a main route of action it became clear that indirect pathways through cells of the immune system and their cytokines are probably more likely to be of importance. To unravel the pathways and key factors involved in TNF-based combination immunotherapy is key in our research and key to the success of combination immunotherapy with tumor manipulating agents.

TUMOR MANIPULATION – COMBINATION CHEMOTHERAPY

The use of vascular manipulating agents. A major step forward in the treatment of solid tumors is the recognition of the tumor-associated vasculature as an important target for therapy. There are several ways at which the tumor-associated vasculature can be approached in solid tumor therapy (**Fig. 1**). First, as advocated by Folkman in 1971, inhibition of the tumor vascular development, also known as antiangiogenic therapy, has a direct effect on growth and progression of the tumor [14,15]. As typically further growth of the tumor is inhibited this type of approach is particularly of value in early disease stages. However, O'Reilly *et al*. as well as others demonstrated tumor regression with the single use of antiangiogenic agents in mouse tumor models [16-18]. Second, already established tumors can be treated with so-called vascular disrupting agents (VDAs) by destruction of the existing tumor-associated vasculature [19-21]. The lack of oxygen and nutrient supply results in serious damage to the tumor cells and consequently tumor regression. Last, the tumor vascular bed can be manipulated to improve intratumoral drug delivery by facilitating enhanced permissiveness of the tumor for co-administered chemotherapeutics. Here two approaches can be identified: vascular normalization [5,22] and vascular abnormalization [23,24].

The use of VEGFR-antibodies, results in inhibition of tumor growth or tumor regression, through inhibition of angiogenesis [25-28]. VEGF, initially also referred to as vascular permeability factor (VPF), is considered the central factor both in physiological angiogenesis as well as in angiogenesis involved in pathological processes [29,30]. VEGF is a mitogen and survival factor for endothelial cells but has also vasoactive properties, as the name VPF indicates. Together with the angiopoietins (Ang1 and 2) VEGF regulates interaction of endothelial cells with other endothelial cells, pericytes and basal membrane, in which VEGF triggers dissociation of the endothelial cells

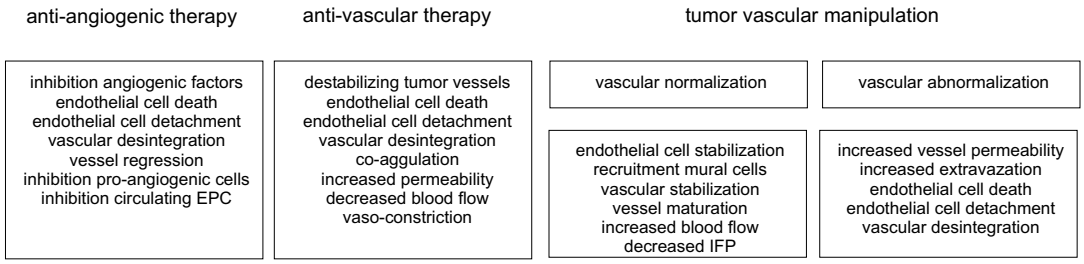

Figure 1. Different approaches can be used to utilize the tumor vascular bed as target in solid tumor therapy. Firstly, antiangiogenic therapy, initially intended to have a direct antitumor activity, may possibly facilitate improved tumor response to concomitant chemo- or radiotherapy. Secondly, direct disruption of the tumor vasculature may induce a tumor response. But more importantly, this type of approach appears to render favorable response particularly when used in combination with chemotherapy. Thirdly, manipulation for the tumor physiology may facilitate better accumulation of concomitant chemotherapy. Here, two opposing concepts apply. The possibility of tumor vascular normalization has been advocated recently as an important facilitator of chemotherapeutic drug accumulation. Normalization results in a more clear-cut structure of the vasculature with improved blood flow and lower interstitial fluid pressure in the tumor. Contrary to this principal, we coined the concept of tumor vascular abnormalisation. It has been shown that the tumor vascular properties, in particular the elevated permeability, allow preferential accumulation of blood borne elements. As not all vessels in tumors are leaky, further abnormalisation results in higher and more homogeneous extravasation of drugs into the tumor.

resulting in leakage and formation of edema [31-33]. It was observed that inhibition of VEGF decreased vascular leakage, but also normalized the tumor-associated vasculature [5,22,25]. The highly irregular and abundant branching, immature vascular status and chaotic structure was reversed to a more normal, healthy and mature looking vascular bed. As a result of this normalization the interstitial fluid pressure drops and a better and more homogeneous blood flow is observed which potentially brings more chemotherapeutic to the tumor and thus inflicts a better tumor response.

An alternative approach, and quite the opposite of the mechanism described above, is the induction of further abnormalization of the tumor vasculature by vasoactive agents. The already leaky vasculature of solid tumor permits preferential accumulation of blood borne elements, which is also referred to as natural fate. Whenever material in the blood circulates long enough it will eventually accumulate in leaky tissue, such as exists in the tumor [34-36]. However, not all tumor-associated vessels of solid tumors exhibit an increased permeability. Dvorak *et al*. demonstrated that the leaky vessels are predominantly mature veins and venules lined by a continuous endothelium and immature interface vessels while tumor-penetrating vessels do not leak macromolecules [4]. By certain vasoactive agents, known for their capacity to induce edema, the permeability of the tumor-associated vasculature can be (further) enhanced. As discussed below the augmented permeability, which is inflicted by these agents, results firstly from a further widening of the already existing gaps [37]. For instance high dose TNF or histamine treatment in an isolated perfusion setting inflicts massive extravasation of erythrocytes [38,39]. Moreover, vascular abnormalization may also affect tumor-associated vessel previously impermeable and showing characteristics of mature vessels, relatively straight with a continuous endothelial lining, enabling leakage of particulate matter up to a size of 100 nm as we showed for low dose TNF [40]. Especially this latter effect of TNF results in a more homogeneous distribution of the concomitant administered chemotherapeutic drug in the tumor.

The capacity of vasoactive drugs to change the tumor pathophysiology, and by doing so facilitate a better chemotherapeutic delivery, is our main focus. Here the use of vasoactive agents,

such as tumor necrosis factor-alpha (TNF), IL-2 and Histamine in local and systemic therapy in conjunction with chemotherapy for the treatment of solid tumors, will be discussed. In these settings these vasoactive drugs demonstrate potent and selective activity on the tumor vascular bed, which strongly improves tumor response.

Biochemotherapy with vasoactive agents. Biochemotherapy is based on a dual approach: first a chemotherapeutic drug is needed to target to tumor cells. Second, a vasoactive agent is administered. For successful treatment with a combination therapy of solid tumors a chemotherapeutic drug is indeed crucial as the tumor vascular manipulation is not principally intended to have an effect by itself but initially serves as a facilitator for the co-administered chemotherapeutic drug. Next to that, we believe and it is our observation that in order to obtain a beneficial and especially lasting tumor response, solely targeting the tumor-associated vasculature is not enough. The choice of the cytotoxic drug may largely depend on the type of tumor under treatment but is also determined by the treatment approach. Irrespective of its action the chemotherapeutic drug should have pharmacological properties that are compatible with combination immunotherapy with vasoactive agents.

To achieve an effective concentration of a chemotherapeutic drug in tumor it is desirable to minimize distribution of the active compound and to increase local exposure. One such method is regional application of the therapeutic agent. Depending on the type of local therapy, for instance isolated perfusion or single pass infusion, augmented drug concentrations can be prolonged or respectively initially reached. Secondly, inhibition of distribution of the chemotherapeutic agent throughout the body not only impairs clearance and dilution of the applied agent but also minimalizes systemic toxicity, allowing therefore higher dosages to be applied [41]. Another method is to formulate the chemotherapeutic agent in such way that its circulation time is prolonged. Typically this can be achieved by inhibiting binding to elements in the blood, preventing clearance and diminishing extravasation at unwanted sites. In our systemic treatment setting we use for this purpose liposomal encapsulation, providing completely different pharmacokinetics and toxicity profile to the chemotherapeutic drug [34,42]. For instance the circulation half time of doxorubicin is prolonged from minutes to three days in humans when encapsulated in long circulating pegylated liposomes such as Doxil. At the same time the potential cardiotoxicity is reduced while a new dose limiting toxicity is observed to hands and feet.

The prolonged and elevated concentration in blood is of crucial importance in biochemotherapy with vasoactive drugs. In order to enable the chemotherapeutic drug to reach the tumor and benefit from the induced leakage the agent has to pass preferably the vascular bed of the solid tumor indefinitely. In that setting all drug will eventually end up in the tumor because of its leaky vasculature. It has been shown that increased circulation time of liposomes directly correlates with better accumulation in the solid tumor [43,44]. To optimally utilize the permeabilizing properties of the vasoactive agents the enhanced leakiness should be maintained at long as possible while at the same time this change in property of the vessel should not negatively influence functionality of these vessels. Therefore it is imperative that the blood flow through the vessels is maintained, or even better increased, as shutdown of course only impairs intratumoral drug accumulation and distribution. An excellent example of a vasoactive agent with these properties is the cytokine tumor necrosis factor-alpha.

VASCULAR MANIPULATION AGENTS

The history of TNF started at the end of the 19th century when Dr. William Coley, a surgeon from New York, observed that cancer patients with a bacterial infection sometime showed spontaneous tumor regression [45]. He developed a vaccine from two dead bacteria strains *Streptococcus*

pyogenes and *Serratia marcescens*, the so-called Coley's Toxin, that could mimicked the tumor regression. It was also found that inducing fever was a prerequisite for a good tumor response [46]. This led to the further investigation to identify the active compound in the toxin and the host factors produced after toxin challenge. However, this appeared not an easy task, as the immune response induced by the toxin is a successive cascade stimulating other cascades and cellular responses, so the single cytokine that initiated this cascade was difficult to identify. Bacterial lipopolysaccharide (LPS) was found to induce hemorrhagic necrosis in mouse tumors and a serum factor, induced by LPS appeared responsible for this effect [47]. In 1975 Dr. Carswell isolated a factor, that he named tumor necrosis factor, from the serum of bacillus *Calmette-Guerin* (BCG)-infected mouse treated with LPS and TNF induced identical hemorrhagic necrosis of methylcholantherene A fibrosarcoma (Meth A) tumors as the LPS itself [48]. With the development of new recombinant DNA techniques, human TNF became available for pre-clinical and clinical application [49,50].

Phase I trails designed to determine the maximal tolerated doses and toxicity demonstrated severe side effects as vasoplegia, multiorgan failure, shock and cachexia. Moreover, in phase II trial the maximal tolerated dose of 200-400 μg/m^2 proved insufficient to cause an antitumor effect [51-55]. Given the poor responses and severe toxicities, clinical application of TNF was largely abandoned. Until, in 1998 Lejeune *et al*. introduced TNF in the isolated limb perfusion, taking advantage of this system to achieve loco-regional doses up to 30 times higher than the maximal tolerated dose [56,57] and is further discussed in this paper.

Monocytes and macrophages are the main source of TNF, but many other cells of the immune system, smooth muscle cells, endothelial cells and tumor cells also produce TNF [58]. TNF binds as a trimer of 17 kDa subunits and exerts its effects by binding to high-affinity receptors, which are present on the plasma membrane. Thus far two receptors, a TNF receptor of 55 kDa (TNFR1), which is expressed on a majority of cell types and a TNF receptor of 75 kDa (TNFR2), which is predominantly expressed by immune cells have been identified. Although the affinity for TNFR2 is 5 times higher compared to TNFR1, the latter initiates the majority of biological activities of TNF. Binding of TNF to TNFR1 can initiates two opposite pathways; cell survival or apoptosis. TNF binding to TNFR1 leads to the binding of TNFR-associated death domain (TRADD) to the death domain of the receptor and recruits receptor interacting protein (RIP), FAS-associated death domain (FADD) and TNFR-associated factor 2 (TRAF-2). These proteins are responsible for further signaling. FADD binds to pro-caspase 8 leading to the activation of caspase 8. This activation initiates a protease cascade leading to apoptosis also involving the release of cytochrome C from mitochondria. Alternatively, the complex can recruit TRAF-2 leading to the nuclear factor kappa B transcription factor (NF-kB) activation. This results in the phosphorylation of the inhibitor of kB (IkB) that is normally bound to NF-kB retaining the transcription factor in the cytoplasm. Upon release the NF-kB is translocated to the nucleus activating several proliferating genes [59,60].

Selective sensitivity of the tumor-associated vasculature to TNF. A large number of studies focused on the ability of TNF to kill cancer cells. However, soon after the identification of TNF as a major mediator of tumor necrosis, the attention has been shifted to an indirect TNF-induced antitumor effect rather than a TNF-cytotoxic effect. This was based on experiments with the same Meth A, as these cells were resistant to TNF *in vitro*. Also, systemic administration of TNF cause necrosis in well established subcutenous tumors whereas small early tumors and intraperitoneal tumors did not respond to TNF therapy [61]. Furthermore, TNF only affected tumor-associated vasculature as the vascularization of normal tissue implants remained intact [62]. Stoeckler claim that TNF-R1 expression on the tumor vasculature and presumably on the surface of tumor endothelial cells is likely to be the most important target of TNF antitumor activity. They observed that TNF antitumor effect remained in TNFR2-/- mice and was absent in TNFR1-/- mice. TNF induced tumor

necrosis in TNFR1-/- tumors in WT mice still occurred, indicating a host mediated effect [63]. Ferrero *et al*. showed that stimulation of TNFR1 is sufficient to increase endothelial permeability *in vitro*. She found that neutralizing TNFR1 decreased TNF-induced permeability changes in the liver. However, detailed analysis to the TNF-sensitive cell type in the vasculature was lacking [64]. When we stained for TNFR1 in human melanoma biopsies we found that endothelial cells express hardily any TNFR1, but TNFR1 expressing cells were found in close proximity with the endothelial cells, suggesting another cell-member of the TAV as possible target for TNF [65].

ISOLATED LIMB PEFUSION; GATEWAY TO UNDERSTANDING ACTIONS AND SUCCESFUL APPLICATION OF TNF

Probably one of the most favorable examples of regional cancer therapy is the isolated limb perfusion. Both ease of the technique and superior control over drug distribution contributes to the success of this method in the treatment of locally advanced sarcoma and multiple or bulky melanoma of the extremity. The isolated limb perfusion (ILP) procedure was first described by Creech *et al*. in 1958 and further improved in the following years [66,67]. Basically it consists of temporary isolating the circulation of the limb from the rest of the body, by cannulating the main limb vessels, connecting them to a heart-lung machine via a pumping role and a primer perfusate. The collateral vessels are ligated and a tourniquet placed in the root of the limb assuring a safe isolation to allow local administration of high doses of chemotherapeutic agents, up to 15 to 30 times higher than the maximal tolerated dose, without systemic side effects as exposure of the rest of the body is kept to a minimum. This procedure is typically combined with mild hyperthermia (39-40°C).

ILP with the alkylating cytotoxic agent melphalan (L-phenyl-alanine-mustard) has been used for the treatment of patients with advanced extremity melanoma while achieving complete responses of about 50%. Other chemotherapeutic agents have been tried as alternatives to, or combined with melphalan, such as doxorubicin, cisplatin, fotemustine, but none provided better tumor responses as compared to melphalan alone [68]. In spite of the good results seen for melanoma, mainly for small lesions, the responses for of bulky tumors and sarcomas were as poor as 20% overall response rates [67,69,70]. The combination of TNF to this treatment positively changed this scenario, increasing the overall response rate to the range of 80% and a limb salvage index of 70%. Based on these data TNF-melphalan ILP was recognized as the best treatment option for limb threatening soft tissue sarcomas and licensed for this use in 1998 by the European Agency for the Evaluation of Medical Products (EMEA) [71]. Currently we and others demonstrated that application of melphalan together with TNF in ILP renders inoperable tumors resectable (sarcoma or bulky melanoma) with an 70-100% limb salvage rate [56,72-74].

Improvement and understanding TNF-based ILP. Acknowledging the possible importance of understanding underlying mechanisms involved in TNF-based ILP in combination with melphalan or doxorubicin we developed several animal models. Especially the rat models, and to lesser extent mouse models, are instrumental in elucidating mechanisms and to study these combinations. Larger animals, such as pigs, have been used to practice new technique and gain insight in pharmacokinetics.

Initially the rat sarcoma ILP model was utilized to improve the established TNF-based ILP and further fine-tune certain aspects that cannot be tested in humans. This model closely mimics the clinical setting, not only qua technique but also with respect to response rate [75,76]. We tested a number of requisites such as optimal temperature and duration of perfusion, impact of local oxygenation and minimally needed TNF concentration in the perfusate. Normally the ILP is

conducted under mild hyperthermia (around 38-39°C), which appeared the optimal temperature as the response rate dropped severely with lower temperature. At a temperature above 40°C, in spite of slightly increased response rate, local toxicity appeared uncontrollable. In the rat model a perfusion-duration of 30 minutes seems adequate as longer duration did not improve response, and most importantly, no melphalan could be detected anymore in the perfusate. If ILP duration is shortened the response rate rapidly drops. Strikingly we observed that during the ILP the concentration of TNF in the perfusate hardly declines over time, indicating that only a fraction of the TNF binds to the available receptors and is consumed [77]. From this one would conclude that a much lower concentration of TNF would be sufficient. Indeed the concentration of TNF can be lowered 5-fold, which is however much less than anticipated. It is well established that the sensitivity of tumor cells and endothelial cells to certain cytotoxic agents is affected by hypoxic conditions [78]. The ILP currently conducted on patients is oxygenated. We observed that hypoxia did not improve response in ILP, but also performing the ILP under anoxic conditions did not affect local toxicity [77]. Skipping the oxygenation during ILP makes it more practical and less expensive to perform.

Like hypoxia, also certain agents are known to enhance the cytotoxicity of TNF. Therefore next to TNF also IFNγ (IFN) was used in the clinical ILP [56,73,79-82]. It is believed and shown *in vitro* that IFN and TNF synergistically induce apoptosis in certain tumor cell lines [83,84]. Importantly, we showed that addition of IFN by pre-ILP injections only marginally adds to the tumor response and can be omitted [85]. Comparable to IFN, actinomycin D is well known for its capacity to dramatically increase TNF-induced cell death *in vitro*. However, addition of actinomycin D also drastically enhances local toxicity of TNF to such an extent that its use is not to be considered in patients [86]. We speculated that inhibition of NO production could possibly promote tumor response in a TNF-based ILP. During the TNF-based ILP triggering of the NO production may occur which could both have a negative effect on the tumor through direct cytotoxicity. However, elevated levels of NO may also affect angiogenesis and thus potential regrowth of the tumor. Indeed, addition of L-NAME, a known NO inhibitor, further improved tumor response in a TNF-based ILP with melphalan [87].

With the aid of our ILP models we could not only optimize the clinical protocol but also investigate the working mechanism of TNF. It was generally believed that while the chemotherapeutic drug, melphalan mostly but also doxorubicin is used in ILP, targets the tumor cells, both tumor cells and endothelial cells are killed by TNF. Angiograms made before and after ILP in patients demonstrate specific disappearance of the tumor vascular bed while healthy vessels remain visible [88,89]. Importantly, we and others demonstrated that ILP with TNF alone has no or marginal effect on tumor progression [77,90], indicating that irrespective of the nature of the tumor vascular effects TNF is not able to inflict serious damage to the tumor. More so, if a tumor response is observed with TNF alone this could be directly related to a sensitivity of the tumor cell itself [76,91]. From this we concluded that ILP with TNF alone is not useful. Next to that, based on these observations we formulated the hypothesis that TNF rather influenced the effectiveness of the co-administered chemotherapeutic drug. In particular we found that addition of TNF augmented intratumoral drug accumulation irrespective of the chemotherapeutic drug used. We showed that TNF changes the pathophysiology of the tumor in an ILP setting resulting in an augmented accumulation of the co-administered drug melphalan or doxorubicin [91,92]. This was also observed in isolated hepatic perfusion (IHP) model, and systemic setting in which lower local levels of TNF are reached as discussed below [40,93-97].

TOXICITY REDUCTION OF TNF TO BROADEN ITS USEFULNESS

As TNF has high intrinsic toxicity several attempts were made to lower toxicity while at the same time maintain or increase bioactivity [94,98-105]. We tested in our ILP model the TNF mutant

SAM2. TNF-SAM2, developed by Soma *et al*., has increased N-terminal basicity and has been shown to have both a two-fold higher cytotoxic activity *in vitro* and up to 20-fold lower acute toxicity in a murine model, compared to conventional TNF [98,103,106]. Reduced systemic toxicity was demonstrated in a canine model [107]. Moreover, an increase in tumor cytotoxicity on several different tumors *in vitro* was demonstrated when compared to conventional TNF [108]. In spite of these favorable results ILP with TNF-SAM2 combined with melphalan resulted in comparable synergistic tumor response [109]. Increased antitumor activity and lowered toxicity has been reported for other TNF mutants, in which specific amino acids has been altered. Besides affecting the toxicity of the molecule directly, attempts to modify the usefulness of TNF has been made by improving delivery. Corti *et al*. coupled TNF with a cyclic CNGRC peptide, an aminopeptidase N (CD13) ligand, to better target the tumor vasculature (NGR-TNF) [110]. This fusion product showed 12-15 times more antitumor activity than TNF. The binding appears quite specific for tumor vessels as it binds to CD13 isoforms expressed by the tumor blood vessels and not to CD13 expressed on kidney tissue of myeloid cells. Mice bearing B16F3 melanoma or RMA-T lymphoma were pretreated with NGR-TNF intraperitoneally followed 2 hours later by interperitoneal injection of doxorubicin or melphalan. Although the LD_{50} values of mTNF and NGR-mTNF are similar, mTNF was inactive at doses lower than 100 to 1,000 ng but NGR-mTNF has an antitumor effects with doses as low as 0.001 – 0.1 ng without any toxic side effects. This low dose is sufficient to improve the antitumor effects in lymphoma and B16F1 bearing mice with doxorubicin or melphalan as a result of a better penetration of the chemotherapeutic drug in the tumor tissue [110,111]. Modification of the NGR peptide demonstrated that both the cyclic CNGRC and the linear GNGRG target tumor vessels, but the cyclic form has 10-fold more antitumor activity [112]. These results direct also attention to targeting of chemotherapeutics to tumor vessels by coupling of NGR ligands [113]. Moreover, as TNF increases drug delivery to solid tumors combination of NGR-TNF with chemotherapy seems obvious. Indeed, pretreatment of tumor-bearing mice with NGR-TNF enhanced response to a number of chemotherapeutics (doxorubicin, melphalan, cisplatin, paclitaxel and gemcitabine) [114]. As was shown with TNF by us [37] also NGR-TNF has no direct effect on cytotoxicity of the used chemotherapeutics *in vitro*. So, NGR-TNF most likely works indirectly through an action of the stroma. An indication is the observation that NGR-TNF lacks activity in the absence of IFNγ [115]. No synergy was observed when NGR-TNF was used in combination with doxorubicin in IFN knockout mice or mice treated with anti-IFN antibodies. Moreover, administration of IFN to the knockout mice restored the NGR-TNF activity. Typically it was observed that NGR-TNF in the presence of IFN doubled the accumulation of doxorubicin in the tumor. These observations are in correlation with MRI studies showing increased leakage of contrast agent into the tumor in mice treated with NGR-TNF [116]. Targeting of TNF can also be improved by coupling antibodies directed towards tumor vessel specific ligands. A possible target found is the extra-domain B (ED-B) of fibronectin, which is found around neovasculature of growing tumors. The antibody L19 has a high affinity for ED-B and localizes to tumor vessels after injection in tumor-bearing mice [117,118], and its pharmaceutical properties can be adjusted by tailoring the antibody moiety [119]. When coupled to IL-2 L19 strongly enhances the antitumor activity of IL-2 [120]. Moreover, L19-12 and L19-TNF both showed good antitumor activity and when combined led to eradication of tumors in mice [121,122]. Treatment with L19-TNF in combination with melphalan induced strong tumor response [123]. This treatment resulted in rejection of challenges with tumors from syngeneic and different origin, indicating profound immune activation. Mayumi *et al*. chemically modified TNF with water-soluble polymers like polyethyleneglycol or polyvinylpyrollidone. This increase of the steric hindrance and protection from proteolytic degradation results in an increased drug stability and circulation time. However, the increase in size limits the distribution from blood to target tissue and steric hindrance can inhibit binding to the receptor. Therefore an optimal modification was designed to find the balance between clearance, toxicity and antitumoral activ-

ity [124-126] and proved to be effective in treatment of S-180 tumor-bearing mice [127]. Shibata *et al.* designed a pegylated lysine-deficient mutant TNF (sp-PEG-mTNF-K90R) with higher affinity for both TNF-receptors with an antitumor activity 60-fold higher than native TNF in the meth A mouse model [128]. Also binding of TNF at the surface of gold nanoparticles (cAu-TNF) improved the safety of TNF while retaining the antitumor efficacy by selectively altering the permeability of the tumor vasculature [129].

SYSTEMIC APPLICATION OF TNF

The success of TNF in the ILP setting reinitiated interest in systemic application. Initially TNF was used as a single drug and failed as such. However, recognition of the activity of TNF towards the tumor-associated vasculature presented new possibilities for this drug. We hypothesized that like in the ILP setting TNF could possibly improve tumor response to chemotherapy in a systemic treatment protocol. However, it is far from easy to establish a local TNF concentration, when systemically injected, in the tumor as can be reached in the ILP. To improve tumor delivery we encapsulated TNF in stealth liposomes and showed improved tumor localization [130]. More so, addition of liposomal TNF to chemotherapy with Doxil (liposomal doxorubicin) resulted in strongly improved tumor response in a rat soft tissue sarcoma model [131]. We observed in this setting that a small fraction of the TNF was released from the liposomes shortly after injection, while the main fraction remained liposome associated. The fraction released appeared to be responsible for the improved outcome. Addition of low dose free TNF (15 μg/kg) to treatment with Doxil inflicted dramatic tumor response (partial or complete remission) in 75% of the rats, while all other treatments at the best resulted in a delay of tumor outgrowth [94,132]. Comparable to observations in the ILP, repeated systemic injection with a non-toxic low dose TNF augmented the accumulation of doxorubicin in the tumor. This could be confirmed in a mouse B16BL6 melanoma model showing strong responses in the TNF plus Doxil treatment groups accompanied by augmented intratumoral drug accumulation [97]. Addition of TNF also improved treatment with cisplatin containing liposomes indicating that the interaction was not drug dependent [133]. Using intravital microscopy we demonstrated that TNF induced permeability of the tumor vasculature and rendered more vessel leaky [40]. Strikingly, increased vascular permeability did not affect tumor vascular function, as we demonstrated that vessels remained functional even when turned leaky to the liposomes for at least 2 days. We proposed that the beneficial effect of TNF in the systemic treatment protocol with Doxil is due to a higher accumulation of the drug in the tumor but especially results from a more homogeneous distribution. It is possible that a vasoactive agent like TNF could be used in a plethora of chemotherapies to improved local delivery and thus tumor response. It is important to note that in this setting TNF is used to facilitate a better functionality of the used chemotherapeutic drug while TNF itself has no or hardly a direct effect on the tumor.

ALTERNATIVE VASOACTIVE AGENTS IL-2 AND HISTAMINE

Interleukin-2. Since its identification by Morgan *et al*. in 1976, T cell growth factor or interleukin-2 (IL-2) remains the major cytokine used in long-term culture of T lymphocytes [134]. IL-2 is a 15 kDa glycoprotein and primarily expressed by activated CD4+ T lymphocytes, although production by naïve CD8+ T lymphocytes, dendritic cells and thymic cells has been reported. It activates immune cells by binding to the IL-2 receptor, which is found on all classes of lymphocytes. IL-2R consists of three subunits: the α- (CD25), β- (CD122) and the common γ-chain (CD132) and all three subunits are required for high affinity binding.

In different animal models interleukin-2 (IL-2), as a single agent, has been shown to have antitumor activity [135,136]. Clinical studies have been carried out mainly in patients with renal

cell cancer and melanomas [137,138]. High doses and multiple dosing are needed, which is associated with serious systemic toxicity with hypotension, massive vascular leakage syndrome and multiple organ failure leading to death [139-141].

IL-2 as a vasoactive agent. We hypothesized that IL-2 could be a good candidate to be used in an isolated limb perfusion. IL-2 is known not to have direct antitumor activity, but we speculated that IL-2 could well impact on the tumor pathophysiology in a similar way as TNF. Indeed, we found a synergistic antitumor response in our rat ILP model after perfusion with IL-2 and melphalan correlating with an increased melphalan uptake in the tumor tissue [142]. However, although an influx of erythrocytes into the tumor tissue and obstruction in the blood vessels was observed, the damage to the vasculature and the hemorrhagic necrosis was not so dramatic as compared to TNF-perfusion. Directly after ILP no clear difference was seen in the number of infiltrating T lymphocytes, granulocytes and macrophages. Macrophages were present in larger number than the other cells, without difference between the treatments. Yet, there was a profound distinction in the cell distribution, showing an even distribution in the control treated animals and a clustering of these cells after IL-2 plus melphalan ILP. IL-2 is known to activate macrophages to produce several cytokines, like TNF and free radicals that could contribute to the further cytotoxic effect on the tumor cells. Endogenous produced TNF was found to be upregulated in tumors after ILP with IL-2. From this study we concluded that IL-2 could be a good candidate for improved tumor response, as an alternative for TNF.

Histamine. Histamine was first isolated in early 1900 but at that time point there was no knowledge of its physiological activity or potential interest. In 1910 Barger and Dale isolated it from a particular ergot extract, the *Ergotinum dialysatum* [143,144]. Although Ackermann and Kutscher also succeeded in isolating of histamine independently, particularly the almost complete description of its pharmacological actions by Dale receives credits. Dale was particularly interested in the capillary dilator effect of histamine and considered the possibility that, either its release or the release of a histamine-like substance might contribute to the regulation of capillary blood flow. According to him, this liberation would be the result of metabolic activity, and could provide fine adjustment of the capillary circulation to the needs of the tissues. He also described its role in the anaphylactic shock and showed that histamine could be extracted from tissues [145].

Histamine is a primary amine synthesized and stored within secretory granules of human mast cells and basophils; but also in cells of the epidermis, gastric mucosa, neurons of the central nervous system, as well as in cells in regenerating or rapidly growing tissues. It is one of the most important mediators involved in various physiological and pathological conditions, including neurotransmission, numerous brain functions, secretion of pituitary hormones, regulation of gastrointestinal and circulatory functions and inflammatory reactions [146,147]. Histamine has also been shown to potently influence the immune response, being the principal mediator of the immediate hypersensitivity reaction that follows interaction of antigen with specific IgE molecules on the surface of mast cells and/or basophiles, and vascular endothelial cells are major targets for the biological actions of histamine. Interestingly, pending on the timing of exposure, histamine limits TNF responses through a direct effect on TNF receptor shedding, characterizing its regulatory effect [148].

Histamine as vasoactive agent. Histamine's classical effect on fine vessels is the formation of edema by an increase in the flow of lymph and its protein content to the extracellular space and also the formation of gaps between endothelial cells, increasing transcapillary vesicular transport [149]. Inflammatory edema facilitates the transfer of immunologically active molecules and cells from the vascular space to the tissues. In spite of the beneficial effects, excessive loss of molecules

and water from the vascular space can also impair organ physiology; therefore, the importance of rapidly restoring normal barrier properties. Histamine is accredited as meeting these properties, rapidly and transiently increasing endothelial permeability in post capillary venules [150,151]. The exact mechanism responsible for the formation of endothelial gaps and recovery in these vessels has been explored in the past decades, revealing a multiple step process. Histamine binds to H1 receptors, activating the inositol phosphate second messenger system and consequently increasing the intracellular calcium concentration [152,153]. These events may in the end lead to endothelial contraction, the mechanism claimed responsible for gap formation [151,154,155].

There is a consensus that histamine-induced increased permeability is a transient event and that recovery happens, even in the presence of histamine. This permeability recovery phenomenon, mediated by increased intracellular cAMP level, also involves negative feedback inhibition, resulting in reversible modulation of the dimension of junctional gaps [156]. This pathway is shared by a number of so-called "endothelial stabilizers" preventing permeability increase by inflammatory mediators. Prostaglandin (PGI2), a member of postanoid family, acts as one of these "endothelial stabilizers" to prevent the histamine induced permeability increase in venules and to decrease permeability of endothelial monolayers by activating the cAMP second messenger system. The increase in intracellular cAMP concentration in endothelial cells, linked to the gap reclosure phenomenon, is associated with an increase in the amount of F-actin in these cells. Probably the stabilization of the machinery involved in endothelial contraction occurs by increased polymerisation of actin filaments and prevention of the actin-myosin contraction [157]. PGI2 is mainly produced by endothelial cells and histamine stimulates its production after very short time incubation periods of 1 to 2 minutes [158]. In agreement with this, Wu and Baldwin used the PGI2 synthetase inhibitor tranylcypromine and showed that permeability recovery was totally abolished in some vessels, but still existed in others. Nevertheless, the extent of recovery for the latter ones was decreased [150].

Examining the temporal changes in the permeability coefficient over a 2 hour period Ehringer *et al.* showed that there are dynamic alterations in the time course of changes in HUVEC permeability, which are different for different vasoactive mediators of inflammation, namely thrombin, histamine and bradykinin [159]. For histamine, permeability coefficients *in vitro* reached a maximum at 0-30 minutes and remained at this peak value for the entire 120 minutes studied. Since HUVEC cells were constantly exposed to histamine during the whole duration of the experiment, the authors speculated that it could have led to a deleterious effect on vascular integrity. Contrary to his observation we showed by a FACS apoptosis/necrosis assay that HUVEC were still viable, even when histamine remained present, while permeability continued to rise for the whole 60 minutes evaluated. Although our evaluation period ran for half the time, the concentrations of histamine used by us were 200-times higher (circa $2x10^{-3}$ M against 10^{-5} M) [38].

In line with the endothelium heterogeneity, barrier integrity differs not only between organs but also between different vascular segments of the same organ. Moreover, endothelial cells derived from conduit vessels and microvessels are phenotypically distinct and thus, present site specific vascular responses to inflammation [160]. Discriminating between key events that regulate these responses and the signaling events activated to coordinate these processes shall provide a better understanding of the microvascular biology process and open new possibilities of treatment in sepsis, but also in oncology for a better drug delivery to tumor cells.

Based on the properties of histamine, we hypothesized that histamine could be a good alternative to TNF in the isolated perfusion setting. Indeed, histamine dramatically improved tumor response when co-administered with melphalan in an ILP [38]. Like TNF addition of histamine caused severe hemorrhage and even more dramatic disruption of the endothelial lining of the tumor vascular bed. Also we showed that histamine augmented intratumor melphalan or doxorubicin concentration and established a more homogeneous distribution [161] and could be a

excellent alternative to TNF in an isolated hepatic perfusion due to absence of noticeable toxicity in this setting [162].

INFLAMMATORY ASPECTS OF TNF THERAPY IN CANCER

Vascular leakage and destruction. Infection or tissue injury induces an inflammatory response, a cascade of molecular and cellular events that provides protection by containing the tissue damage at the site of infection or injury. The acute inflammatory reaction is initiated after activation of tissue macrophages and the release of several cytokines, such as TNFα, IL-1 and IL-6. The cytokines act on fibroblast and endothelial cells inducing coagulation and permeability increase by loss of intracellular adhesion. TNF and IL-1 stimulate the upregulation of specific cell surface receptors, like selectins, intercellular adhesion molecules (ICAM) and vascular adhesion molecules (VCAM) [163-166]. Cells in the blood circulation recognize these specific adhesion molecules and adhere to the endothelium followed by transmigration into the tissue space. This results in a massive influx of immune cells into the damage tissue participating in eradication of the pathogen and stimulation of the healing process. In turn, TNF affects the function of macrophages and endothelial cells that leads to the secretion of other cytokines like IL-1, IL-8 and IFN further promoting the phagocytic activity [167]. Also several colony-stimulating factors are secreted that increase the production of leukocytes. Triggered by TNF, IL-1 and IL-6, the local inflammatory response is accompanied by the acute-phase response that induces several acute-phase proteins [168]. Each of these cytokines has an effect on the hypothalamus to induce fever. Increase in body temperature inhibits the growth of pathogens and enhance the immune response.

TNF was first identified as the most potent anticancer cytokine in serum from cancer patients, treated with bacterial extract or endotoxins [48]. The induction of a fever after the bacterial infection was crucial for a good antitumor response. In Meth A tumor-bearing mice, TNF was found to induce hemorrhagic necrosis as a result of massive extravasation of erythrocytes into the tissue. Already during TNF-based melphalan ILP softening of the tumor was observed, a feature also observed in the clinical setting [169], which could be an indication of hemorrhage or inflammation. Indeed, histological analysis of these tumors showed destruction of the vasculature, extravasation of erythrocytes in parts of the tumor and hemorrhagic necrosis [170]. However, also TNF alone induced edema, vascular congestion, extravasation of erythrocytes and hemorrhagic necrosis but this hardly influences tumor response, as a combination with melphalan is necessary to obtain good tumor activity. Reports have been made about the important role of erythrocytes in the transport of certain drug [171,172]. Wildiers *et al*. showed that 1 hour after i.p. administration of melphalan 25% of the melphalan in the blood was transported via the erythrocytes [173].

Vascular bed activation. Factors expressed at the luminal side of endothelial cells play a central role in the clotting system by regulating the expression of binding sites for anticoagulant or procoagulant factors. Blood flow, in a normal functional vasculature is maintained in the quiescent endothelial cells by the expression of several anticoagulant pathways. TNF shift the haemostatic properties of the endothelium to favor clot formation by increasing the expression of the procoagulant tissue factor and plasminogen activator inhibitor-1 and suppressing of the cofactor activity of procoagulant protein C and the anticoagulant cofactor thrombomodulin [174-176]. Adhesion of leukocytes to the endothelium also induce procoagulant tissue factor by endothelial cells [177]. When tissue factor is inhibited, the TNF-induced fibrin deposition is decreased and blood flow restored [178]. TNF also mediates the release of von Willebrand factor (vWF) from endothelial cells. vWF supports thrombus formation by maintaining platelet adhesion (platelet-endothelium) but also by forming platelet aggregates (platelet-platelet) [179]. vWF which is restricted to the

endothelial layer prior to perfusion was redistribute to the perivascular and subepidermal pattern in patients biopsies 3 hours after TNF-based melphalan perfusion. Within a period of 24 hours, intravascular thrombocyte aggregation and erythrostasis was observed without tissue factor and fibrin deposits, indicating that the thrombocyte aggregation was no a result of local procoagulant activity, but rather a result of endothelium damage. This could indicate that TNF induced endothelial damage leads to expression of vWF and adhesion of thrombocytes that eventually impairs the blood flow leading to obstruction and edema [180]. During the first hours after perfusion the endothelial cells appeared swollen and the vessels were progressively destroyed [181]. These observations were also made in the TNF-based melphalan ILP in the rat model. Blood vessels were loaded with erythrocytes, showed platelet aggregation and the endothelial cells were round with swollen mitochondria [39].

Delayed-type reaction. We also studied the delayed-type reaction in slowly regressing melanoma biopsies because tumor remission without massive hemorrhagic necrosis frequently requires a period of weeks or even months following ILP. Around 60% of the lesions in the melanoma patients with a delayed-time response were less that 0.5 cm in diameter at the time of ILP and the immediate effect of TNF is known to relate with tumor size, because of the prerequisite of an established vasculature. In these delayed-type lesions, degenerated tumor cells were in close associated with melanin-loaded macrophages and an increased amount of eosinophils were found in the dermis near the tumor but not in the tumor itself. Melphalan synergizes with TNF to yield better response rates then melphalan alone. However histopathology findings in the delayed-time response with TNF-based melphalan showed an identical pattern suggesting the long term effect of melphalan [182].

Involvement of leukocytes. Recruitment of polymorphonuclear cells (PMN) was observed 3 hours after perfusion followed by intratumoral localization within 3 days. T lymphocytes and macrophages were detected during the first 7 days and B lymphocytes during the second week. Tumors that were treated with melphalan alone did not show significant necrosis and PMN infiltration [181]. The angiograms taken from patients after 7 to 10 days after TNF-based melphalan ILP showed a complete destruction of the tumor-associated vasculature while normal tissue vessels were spared [72,183]. However, these were long-term effects whereas the increased accumulation of chemotherapeutic drug was observed directly after perfusion. When we investigated the presence of tumor-infiltrating immune cells we observed no evident change between the treatments in the infiltration or tumor localization of CD4 and CD8-positive cells, granulocytes and macrophages in rat tumors taken immediately or 6 hours after perfusion [170]. In that time period also no effect on the expression profile of several important cytokines (IL-6, IL-8, IL-10, IL-12 and IFN) was observed. A limitation of using the complete tumor for gene profiling is that we cannot link gene expression with the specific subset of cells. This indicates that the tumor-infiltrating immune cells are not a prerequisite for the induction for the permeability changes of the endothelial cells during perfusion. However, they are required for the further eradication of the tumor. A schematic overview of the different tumor-associated cells is depicted in figure 2 (**Fig. 2**).

Although there is no difference in distribution of leukocytes directly after perfusion, the TNF-induced effects as hemorrhage were lost in leukopenic rats after TNF-based melphalan ILP, resulting in impaired tumor response, indicating an important role of leucocytes in the outcome [184]. *In vitro* studies revealed that TNF had negligible effect on tumor cells and even endothelial cells. However TNF in combination with IFN induced morphological changes of endothelial cells; the cells became elongated and gap formation between the cells occurred [37,185]. Importantly, these morphologic changes were much more pronounced when peripheral blood mononuclear cells (PBMC) were added. Cells became further elongated, therefore intensifying gap formation

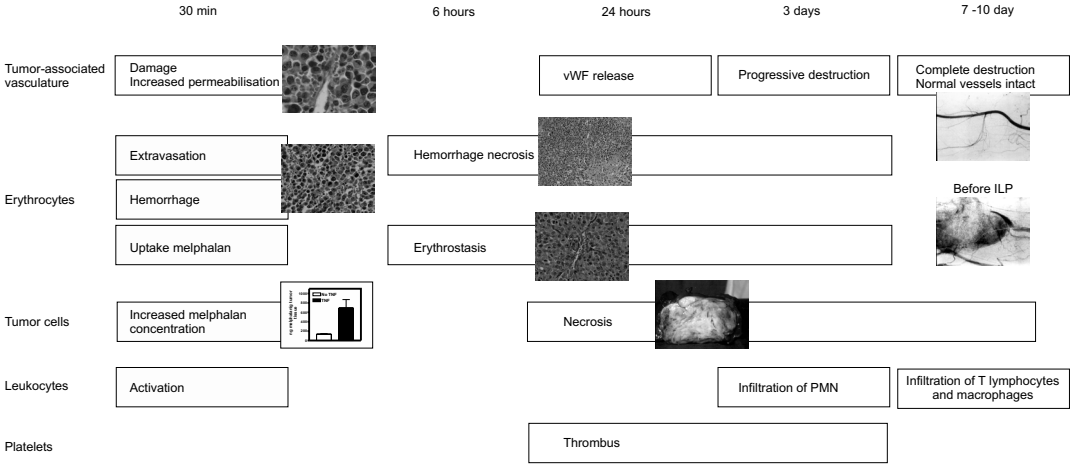

Figure 2. Schematic overview. Involvement of the different tumor compartments after TNF- based melphalan perfusion. (See color section for a full-color version.)

that contributed to an increased permeability. PBMC-derived interleukin-1beta (IL-1ß) was responsible for this effect [37]. IL-1ß mediated the production of several matrix metalloproteinases participating in degradation of the extracellular matrix leading to detachment of the endothelial cells. Furthermore, IL-1ß is also known to decrease the endothelial integrity by affecting adherens junctions proteins, like VE-cadherin and ß-catenin. These effects were observed in a long term *in vitro* experiments. On the other hand TNF-activated PMN are able to increase the permeability of this monolayer for small molecules, with minimal damage to the endothelial monolayer, within 30 minutes. These observations led us to the conclusion that TNF-induced vascular damage partially mediated by the activated PMN already localized in the tumor increased the extravasation of the chemotherapeutic drug and erythrocytes into the tumor tissue. A simplified scheme is depicted in

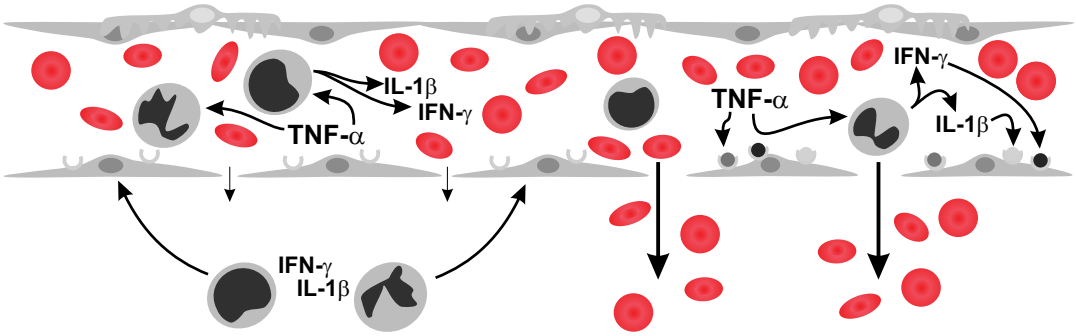

Figure 3. Action of TNF on the vascuar bed. The action of TNF on the tumor vascular bed involves at least two key leukocyte members: PMN and cells present in the PBMC pool. In particular cells producing IL-1ß and IFN are involved. TNF triggers the release of these cytokines and affects the endothelial cells directly. When interacting together TNF, IL-1ß and IFN resort endothelial gap formation, which is absent or less apparent when one of these cytokines is missing. We speculate that activated immune cells already present in the tumor contribute to the cytokine production as well. (See color section for a full-color version.)

figure 3 (**Fig. 3**). Once located in the tumor tissue the chemotherapeutic drug kills the tumor cells. Infiltration of other leucocytes contributes in the further eradication of the tumor tissue.

LESSONS TO BE LEARNED FROM TNF-BASED COMBINATION THERAPY

The results obtained with TNF are exemplary for the current increasing interest in combination therapy. The use of antiangiogenic agents in combination with chemotherapy already indicated that tumor cell-targeted therapy benefits also directly from this antiangiogenic approach through alterations in the tumor physiology. The application of TNF shows excellently that manipulation of the tumor physiology in such way that additional chemotherapy is improved is a powerful tool in solid tumor therapy. Moreover, the central lesson to be learned here is that such a vasoactive agent not necessarily has to have a direct antitumoral activity. It changes the way we should look at combination therapy. Next to that, recognition of the essential effect of TNF allowed us to identify new and potentially better drugs, such as histamine, which could be of particular usefulness in settings that do not permit the use of TNF. We have now a better understanding of the pathways triggered by the vasoactive agents leading to the alterations in the tumor vascular bed and how these alterations affect intratumoral drug distribution. We anticipate that eventually tumor-manipulating agents will earn a central role in chemotherapy solid tumor therapy.

REFERENCES

1.Baxter LT and Jain RK. Vascular permeability and interstitial diffusion in superfused tissues: a two-dimensional model. Microvasc Res. 1988: 36(1), 108-115.

2.Yuan F, Dellian M, Fukumura D, Leunig M, Berk DA, Torchilin VP et al. Vascular permeability in a human tumor xenograft: molecular size dependence and cutoff size. Cancer Res. 1995: 55(17), 3752-3756.

3.Yuan F, Leunig M, Huang SK, Berk DA, Papahadjopoulos D, and Jain RK. Microvascular permeability and interstitial penetration of sterically stabilized (stealth) liposomes in a human tumor xenograft. Cancer Res. 1994: 54(13), 3352-3356.

4.Dvorak HF, Nagy JA, Dvorak JT, and Dvorak AM. Identification and characterization of the blood vessels of solid tumors that are leaky to circulating macromolecules. Am J Pathol. 1988: 133(1), 95-109.

5.Jain RK. Normalization of tumor vasculature: an emerging concept in antiangiogenic therapy. Science. 2005: 307(5706), 58-62.

6.Jain RK. Delivery of novel therapeutic agents in tumors: physiological barriers and strategies. J Natl Cancer Inst. 1989: 81(8), 570-576.

7.Leunig M, Yuan F, Menger MD, Boucher Y, Goetz AE, Messmer K et al. Angiogenesis, microvascular architecture, microhemodynamics, and interstitial fluid pressure during early growth of human adenocarcinoma LS174T in SCID mice. Cancer Res. 1992: 52(23), 6553-6560.

8.Kristensen CA, Nozue M, Boucher Y, and Jain RK. Reduction of interstitial fluid pressure after TNF-alpha treatment of three human melanoma xenografts. Br J Cancer. 1996: 74(4), 533-536.

9.Netti PA, Baxter LT, Boucher Y, Skalak R, and Jain RK. Time-dependent behavior of interstitial fluid pressure in solid tumors: implications for drug delivery. Cancer Res. 1995: 55(22), 5451-5458.

10.Salnikov AV, Iversen VV, Koisti M, Sundberg C, Johansson L, Stuhr LB et al. Lowering of tumor interstitial fluid pressure specifically augments efficacy of chemotherapy. FASEB J. 2003: 17(12), 1756-1758.

11.Jain RK and Fenton BT. Intratumoral lymphatic vessels: a case of mistaken identity or malfunction? J Natl Cancer Inst. 2002: %20;94(6), 417-421.

12.Baxter LT and Jain RK. Transport of fluid and macromolecules in tumors. II. Role of heterogeneous perfusion and lymphatics. Microvasc Res. 1990: 40(2), 246-263.

13.Padera TP, Stoll BR, So PT, and Jain RK. Conventional and high-speed intravital multiphoton laser scanning microscopy of microvasculature, lymphatics, and leukocyte-endothelial interactions. Mol Imaging. 2002: 1(1), 9-15.

14Folkman J. Tumor angiogenesis: therapeutic implications. N Engl J Med. 1971: 285(21), 1182-1186.

15.Folkman J. Angiogenesis in cancer, vascular, rheumatoid and other disease. Nat Med. 1995: 1(1), 27-31.
16.O'Reilly MS, Boehm T, Shing Y, Fukai N, Vasios G, Lane WS et al. Endostatin: an endogenous inhibitor of angiogenesis and tumor growth. Cell. 1997: 88(2), 277-285.
17.Griffioen AW and Molema G. Angiogenesis: potentials for pharmacologic intervention in the treatment of cancer, cardiovascular diseases, and chronic inflammation. Pharmacol Rev. 2000: 52(2), 237-268.
18.O'Reilly MS, Holmgren L, Shing Y, Chen C, Rosenthal RA, Moses MXLW et al. Angiostatin: a novel angiogenesis inhibitor that mediates the suppression of metastases by a Lewis lung carcinoma. Cell. 1994: 79(2), 315-328.
19.Davis PD, Dougherty GJ, Blakey DC, Galbraith SM, Tozer GM, Holder AL et al. ZD6126: a novel vascular-targeting agent that causes selective destruction of tumor vasculature. Cancer Res. 2002: 62(24), 7247-7253.
20.Tozer GM, Kanthou C, and Baguley BC. Disrupting tumour blood vessels. Nat Rev Cancer. 2005: 5(6), 423-435.
21.Chaplin DJ, Horsman MR, and Siemann DW. Current development status of small-molecule vascular disrupting agents. Curr Opin Investig Drugs. 2006: 7(6), 522-528.
22.Tong RT, Boucher Y, Kozin SV, Winkler F, Hicklin DJ, and Jain RK. Vascular normalization by vascular endothelial growth factor receptor 2 blockade induces a pressure gradient across the vasculature and improves drug penetration in tumors. Cancer Res. 2004: 64(11), 3731-3736.
23.ten Hagen TL and Eggermont AM. Solid tumor therapy: manipulation of the vasculature with TNF. Technol Cancer Res Treat. 2003: 2(3), 195-203.
24.ten Hagen TL and Eggermont AM. Manipulation of the tumour-associated vasculature to improve tumour therapy. J Liposome Res. 2002: 12(1-2), 149-154.
25.Willett CG, Boucher Y, di Tomaso E, Duda DG, Munn LL, Tong RT et al. Direct evidence that the VEGF-specific antibody bevacizumab has antivascular effects in human rectal cancer. Nat Med. 2004: 10(2), 145-147.
26.Azizi AA, Haberler C, Czech T, Gupper A, Prayer D, Breitschopf H et al. Vascular-endothelial-growth-factor (VEGF) expression and possible response to angiogenesis inhibitor bevacizumab in metastatic alveolar soft part sarcoma. Lancet Oncol. 2006: 7(6), 521-523.
27.de Gramont A and van Cutsem E. Investigating the potential of bevacizumab in other indications: metastatic renal cell, non-small cell lung, pancreatic and breast cancer. Oncology. 2005: 69 Suppl 3:46-56. Epub;%2005 Nov 21., 46-56.
28.Hurwitz H, Fehrenbacher L, Novotny W, Cartwright T, Hainsworth J, Heim W et al. Bevacizumab plus irinotecan, fluorouracil, and leucovorin for metastatic colorectal cancer. N Engl J Med. 2004: 350(23), 2335-2342.
29.Carmeliet P. VEGF as a key mediator of angiogenesis in cancer. Oncology. 2005: 69 Suppl 3:4-10.
30.Ferrara N, Gerber HP, and LeCouter J. The biology of VEGF and its receptors. Nat Med. 2003: 9(6), 669-676.
31.Pal S, Iruela-Arispe ML, Harvey VS, Zeng H, Nagy JA, Dvorak HF et al. Retinoic Acid Selectively Inhibits the Vascular Permeabilizing Effect of VPF/VEGF, an Early Step in the Angiogenic Cascade. Microvasc Res 2000 Sep;60 (2):112 -120. 60(2), 112-120.
32.Dvorak HF, Brown LF, Detmar M, and Dvorak AM. Vascular permeability factor/vascular endothelial growth factor, microvascular hyperpermeability, and angiogenesis. Am J Pathol. 1995: 146(5), 1029-1039.
33.Nagy JA, Vasile E, Feng D, Sundberg C, Brown LF, Detmar MJ et al. Vascular permeability factor/vascular endothelial growth factor induces lymphangiogenesis as well as angiogenesis. J Exp Med. 2002: 196(11), 1497-1506.
34.Gabizon A, Shmeeda H, and Barenholz Y. Pharmacokinetics of pegylated liposomal Doxorubicin: review of animal and human studies. Clin Pharmacokinet. 2003: 42(5), 419-436.
35.Gabizon A and Papahadjopoulos D. Liposome formulations with prolonged circulation time in blood and enhanced uptake by tumors. Proc Natl Acad Sci U S A. 1988: 85(18), 6949-6953.
36.Allen TM, Hansen C, and Rutledge J. Liposomes with prolonged circulation times: factors affecting uptake by reticuloendothelial and other tissues. Biochim Biophys Acta. 1989: 981(1), 27-35.
37.Seynhaeve AL, Vermeulen CE, Eggermont AM, and ten Hagen TL. Cytokines and vascular permeability: an in vitro study on human endothelial cells in relation to tumor necrosis factor-alpha-primed peripheral blood mononuclear cells. Cell Biochem Biophys. 2006: 44(1), 157-169.
38.Brunstein F, Hoving S, Seynhaeve AL, van Tiel ST, Guetens G, de Bruijn EA et al. Synergistic antitumor activity of histamine plus melphalan in isolated limb perfusion: preclinical studies. J Natl Cancer Inst. 2004: 96(21), 1603-1610.

39.Nooijen PTGA, Manusama ER, Eggermont AMM, Schalkwijk L, Stavast J, Marquet RL et al. Synergistic effects of TNF-alpha and melphalan in an isolated limb perfusion model of rat sarcoma: a histopathological, immunohistochemical and electron microscopical study. Br J Cancer. 1996: 74(12), 1908-1915.
40.Seynhaeve AL, Hoving S, Schipper D, Vermeulen CE, aan dW-A, van Tiel ST et al. Tumor Necrosis Factor {alpha} Mediates Homogeneous Distribution of Liposomes in Murine Melanoma that Contributes to a Better Tumor Response. Cancer Res. 2007: 67(19), 9455-9462.
41.Benckhuijsen C, Varossieau FJ, Hart AA, Wieberdink J, and Noordhoek J. Pharmacokinetics of melphalan in isolated perfusion of the limbs. J Pharmacol Exp Ther. 1986: 237(2), 583-588.
42Allen TM. Liposomes. Opportunities in drug delivery. Drugs. 1997: 54 Suppl 4, 8-14.
43.Gabizon A and Martin F. Polyethylene glycol-coated (pegylated) liposomal doxorubicin. Rationale for use in solid tumours. Drugs. 1997: 54 Suppl 4, 15-21.
44.Gabizon A, Catane R, Uziely B, Kaufman B, Safra T, Cohen R et al. Prolonged circulation time and enhanced accumulation in malignant exudates of doxorubicin encapsulated in polyethylene- glycol coated liposomes. Cancer Res. 1994: 54(4), 987-992.
45.Coley WB. The therapeutic value of the mixed toxins of the streptococcus of erysipelas and bacillus prodigious in the treatment of inoperable malignant tumors. Am J Med Sci. 1896: 112, 251-281.
46Hoption Cann SA, van Netten JP, and van Netten C. Dr William Coley and tumour regression: a place in history or in the future. Postgrad Med J. 2003: 79(938), 672-680.
47.O'Malley WE, Achinstein B, and Shear MJ. Action of Bacterial polysaccharide on tumors. III. Repeated response of sarcoma 37, in tolerant mice, to Serratia Marcescens endotoxin. Cancer Res. 1963: 23, 890-895.
48.Carswell EA, Old LJ, Kassel RL, Green S, Fiore N, and Williamson B. An endotoxin-induced serum factor that causes necrosis of tumors. Proc Natl Acad Sci U S A. 1975: 72(9), 3666-3670.
49.Shirai T, Yamaguchi H, Ito H, Todd CW, and Wallace RB. Cloning and expression in Escherichia coli of the gene for human tumour necrosis factor. Nature. 1985: 313(6005), 803-806.
50.Wang AM, Creasey AA, Ladner MB, Lin LS, Strickler J, van Arsdell JN et al. Molecular cloning of the complementary DNA for human tumor necrosis factor. Science. 1985: 228(4696), 149-154.
51.Lenk H, Tanneberger S, Muller U, Ebert J, and Shiga T. Phase II clinical trial of high-dose recombinant human tumor necrosis factor. Cancer Chemother Pharmacol. 1989: 24(6), 391-392.
52.Aulitzky WE, Tilg H, Gastl G, Mull R, Flener R, Vogel W et al. Recombinant tumour necrosis factor alpha administered subcutaneously or intramuscularly for treatment of advanced malignant disease: a phase I trial. Eur J Cancer. 1991: 27(4), 462-467.
53.Kimura K, Taguchi T, Urushizaki I, Ohno R, Abe O, Furue H et al. Phase I study of recombinant human tumor necrosis factor. Cancer Chemother Pharmacol. 1987: 20(3), 223-229.
54.Spriggs DR, Sherman ML, Michie H, Arthur KA, Imamura K, Wilmore D et al. Recombinant human tumor necrosis factor administered as a 24-hour intravenous infusion. A phase I and pharmacologic study. J Natl Cancer Inst. 1988: 80(13), 1039-1044.
55.Wiedenmann B, Reichardt P, Rath U, Theilmann L, Schule B, Ho AD et al. Phase-I trial of intravenous continuous infusion of tumor necrosis factor in advanced metastatic carcinomas. J Cancer Res Clin Oncol. 1989: 115(2), 189-192.
56.Lienard D, Ewalenko P, Delmotte JJ, Renard N, and Lejeune FJ. High-dose recombinant tumor necrosis factor alpha in combination with interferon gamma and melphalan in isolation perfusion of the limbs for melanoma and sarcoma. J Clin Oncol. 1992: 10(1), 52-60.
57.Lienard D, Lejeune FJ, and Ewalenko P. In transit metastases of malignant melanoma treated by high dose rTNF alpha in combination with interferon-gamma and melphalan in isolation perfusion. World J Surg. 1992: 16(2), 234-240.
58.Bemelmans MH, van Tits LJ, and Buurman WA. Tumor necrosis factor: function, release and clearance. Crit Rev Immunol. 1996: 16(1), 1-11.
59.van Horssen R, ten Hagen TL, and Eggermont AM. TNF-alpha in cancer treatment: molecular insights, antitumor effects, and clinical utility. Oncologist. 2006: 11(4), 397-408.
60.Wullaert A, Heyninck K, and Beyaert R. Mechanisms of crosstalk between TNF-induced NF-kappaB and JNK activation in hepatocytes. Biochem Pharmacol. 2006: 72(9), 1090-1101.

61.Manda T, Shimomura K, Mukumoto S, Kobayashi K, Mizota T, Hirai O et al. Recombinant human tumor necrosis factor-alpha: evidence of an indirect mode of antitumor activity. Cancer Res. 1987: 47(14), 3707-3711.
62.McIntosh JK, Mule JJ, Travis WD, and Rosenberg SA. Studies of effects of recombinant human tumor necrosis factor on autochthonous tumor and transplanted normal tissue in mice. Cancer Res. 1990: 50(8), 2463-2469.
63.Stoelcker B, Ruhland B, Hehlgans T, Bluethmann H, Luther T, and Mannel DN. Tumor necrosis factor induces tumor necrosis via tumor necrosis factor receptor type 1-expressing endothelial cells of the tumor vasculature. Am J Pathol. 2000: 156(4), 1171-1176.
64.Ferrero E, Zocchi MR, Magni E, Panzeri MC, Curnis F, Rugarli C et al. Roles of tumor necrosis factor p55 and p75 receptors in TNF-alpha-induced vascular permeability. Am J Physiol Cell Physiol. 2001: 281(4), C1173-C1179.
65.van Horssen R, Rens JA, Brunstein F, Guns V, van Gils M, Hagen TL et al. Intratumoural expression of TNF-R1 and EMAP-II in relation to response of patients treated with TNF-based isolated limb perfusion. Int J Cancer. 2006: 119(6), 1481-1490.
66.Creech OJ, Krementz ET, Ryan RF, and Winblad JN. Chemotherapy of cancer: regional perfusion utilizing an extracorporeal circuit. Ann Surg. 1958: 148, 616-632.
67.Krementz ET, Carter RD, Sutherland CM, Muchmore JH, Ryan RF, Creech O et al. Regional chemotherapy for melanoma. A 35-year experience. Ann Surg. 1994: 220(4), 520-34; discussion 534-5.
68.Grunhagen DJ, de Wilt JH, ten Hagen TL, and Eggermont AM. Technology Insight: utility of TNF-alpha-based isolated limb perfusion to avoid amputation of irresectable tumors of the extremities. Nat Clin Pract Oncol. 2006: 3(2), 94-103.
69.Krementz ET, Carter RD, Sutherland CM, and Hutton I. Chemotherapy of sarcomas of the limbs by regional perfusion. Ann Surg. 1977: 185(5), 555-564.
70.Hoekstra HJ, Schraffordt Koops H, Molenaar WM, and Oldhoff J. Results of isolated regional perfusion in the treatment of malignant soft tissue tumors of the extremities. Cancer. 1987: 60(8), 1703-1707.
71.Grunhagen DJ, de Wilt JH, Graveland WJ, Verhoef C, van Geel AN, and Eggermont AM. Outcome and prognostic factor analysis of 217 consecutive isolated limb perfusions with tumor necrosis factor-alpha and melphalan for limb-threatening soft tissue sarcoma. Cancer. 2006: 106(8), 1776-1784.
72.Eggermont AM, de Wilt JH, and ten Hagen TL. Current uses of isolated limb perfusion in the clinic and a model system for new strategies. Lancet Oncol. 2003: 4(7), 429-437.
73.Eggermont AMM, Schraffordt Koops H, Lienard D, Kroon BBR, van Geel AN, Hoekstra HJ et al. Isolated limb perfusion with high-dose tumor necrosis factor- alpha in combination with interferon-gamma and melphalan for nonresectable extremity soft tissue sarcomas: a multicenter trial. J Clin Oncol. 1996: 14(10), 2653-2665.
74.Eggermont AMM, Schraffordt Koops H, Klausner JM, Kroon BBR, Schlag PM, Lienard D et al. Isolated limb perfusion with tumor necrosis factor and melphalan for limb salvage in 186 patients with locally advanced soft tissue extremity sarcomas. The cumulative multicenter European experience. Ann Surg. 1996: 224(6), 756-64; discussion 764-5.
75.Manusama ER, Nooijen PTGA, Stavast J, Durante NMC, Marquet RL, and Eggermont AMM. Synergistic antitumour effect of recombinant human tumour necrosis factor alpha with melphalan in isolated limb perfusion in the rat. Br J Surg. 1996: 83(4), 551-555.
76.Manusama ER, Stavast J, Durante NMC, Marquet RL, and Eggermont AMM. Isolated limb perfusion with TNF alpha and melphalan in a rat osteosarcoma model: a new anti-tumour approach. Eur J Surg Oncol. 1996: 22(2), 152-157.
77.de Wilt JHW, Manusama ER, van Tiel ST, van Ijken MGA, ten Hagen TLM, and Eggermont AMM. Prerequisites for effective isolated limb perfusion using tumour necrosis factor alpha and melphalan in rats. Br J Cancer. 1999: 80(1-2), 161-166.
78.Tredan O, Galmarini CM, Patel K, and Tannock IF. Drug resistance and the solid tumor microenvironment. J Natl Cancer Inst. 2007: 99(19), 1441-1454.
79.Lienard D, Eggermont AMM, Schraffordt Koops H, Kroon BBR, Rosenkaimer F, Autier P et al. Isolated perfusion of the limb with high-dose tumour necrosis factor-alpha (TNF-alpha), interferon-gamma (IFN-gamma) and melphalan for melanoma stage III. Results of a multi-centre pilot study. Melanoma Res. 1994: 4 Suppl 1, 21-26.
80.Olieman AF, Lienard D, Eggermont AM, Kroon BB, Lejeune FJ, Hoekstra HJ et al. Hyperthermic isolated limb perfusion with tumor necrosis factor alpha, interferon gamma, and melphalan for locally advanced nonmelanoma skin tumors of the extremities: a multicenter study. Arch Surg. 1999: 134(3), 303-307.

81.Vaglini M, Santinami M, Manzi R, Inglese MG, Santoro N, Persiani L et al. Treatment of in-transit metastases from cutaneous melanoma by isolation perfusion with tumour necrosis factor-alpha (TNF-alpha), melphalan and interferon-gamma (IFN-gamma). Dose-finding experience at the National Cancer Institute of Milan. Melanoma Res. 1994: 4 Suppl 1, 35-38.
82.Fraker DL, Alexander HR, Andrich M, and Rosenberg SA. Treatment of patients with melanoma of the extremity using hyperthermic isolated limb perfusion with melphalan, tumor necrosis factor, and interferon gamma: results of a tumor necrosis factor dose-escalation study. J Clin Oncol. 1996: 14(2), 479-489.
83.Salmon SE, Young L, Scuderi P, and Clark B. Antineoplastic effects of tumor necrosis factor alone and in combination with gamma-interferon on tumor biopsies in clonogenic assay. J Clin Oncol. 1987: 5(11), 1816-1821.
84.Schiller JH, Bittner G, Storer B, and Willson JK. Synergistic antitumor effects of tumor necrosis factor and gamma- interferon on human colon carcinoma cell lines. Cancer Res. 1987: 47(11), 2809-2813.
85.Manusama ER, de Wilt JH, ten Hagen TL, Marquet RL, and Eggermont AM. Toxicity and antitumor activity of interferon gamma alone and in combinations with TNFalpha and melphalan in isolated limb perfusion in the BN175 sarcoma tumor model in rats. Oncol Rep. 1999: 6(1), 173-177.
86.Seynhaeve AL, de Wilt JH, van Tiel ST, Eggermont AM, and ten Hagen TL. Isolated limb perfusion with actinomycin D and TNF-alpha results in improved tumour response in soft-tissue sarcoma-bearing rats but is accompanied by severe local toxicity. Br J Cancer. 2002: 86(7), 1174-1179.
87.de Wilt JH, Manusama ER, van Etten B, van Tiel ST, Jorna AS, Seynhaeve AL et al. Nitric oxide synthase inhibition results in synergistic anti-tumour activity with melphalan and tumour necrosis factor alpha-based isolated limb perfusions. Br J Cancer. 2000: 83(9), 1176-1182.
88.Eggermont AMM, Schraffordt Koops H, Lienard D, Lejeune FJ, and Oudkerk M. Angiographic observations before and after high dose TNF isolated limb perfusion in patients with extremity soft tissue sarcomas. Eur J Surg Oncol. 1994: 20, 323.
89.Olieman AFT, van Ginkel RJ, Hoekstra HJ, Mooyaart EL, Molenaar WM, and Koops HS. Angiographic response of locally advanced soft-tissue sarcoma following hyperthermic isolated limb perfusion with tumor necrosis factor. Ann Surg Oncol. 1997: 4(1), 64-69.
90.Weksler B, Blumberg D, Lenert JT, Ng B, Fong Y, and Burt ME. Isolated single-lung perfusion with TNF-alpha in a rat sarcoma lung metastases model. Ann Thorac Surg. 1994: 58(2), 328-31; discussion 332.
91.van der Veen AH, de Wilt JHW, Eggermont AMM, van Tiel ST, Seynhaeve ALB, and ten Hagen TLM. TNF-alpha augments intratumoural concentrations of doxorubicin in TNF-alpha-based isolated limb perfusion in rat sarcoma models and enhances anti-tumour effects. Br J Cancer. 2000: 82(4), 973-980.
92de Wilt JH, ten Hagen TL, de Boeck G, van Tiel ST, de Bruijn EA, and Eggermont AM. Tumour necrosis factor alpha increases melphalan concentration in tumour tissue after isolated limb perfusion. Br J Cancer. 2000: 82(5), 1000-1003.
93.van Etten B, de Vries MR, van Ijken MGA, Lans TE, Guetens G, Ambagtsheer G et al. Degree of tumour vascularity correlates with drug accumulation and tumour response upon TNF-alpha-based isolated hepatic perfusion. Br J Cancer. 2003: 88(2), 314-319.
94.ten Hagen TLM, van der Veen AH, Nooijen PTGA, van Tiel ST, Seynhaeve ALB, and Eggermont AMM. Low-dose tumor necrosis factor-alpha augments antitumor activity of stealth liposomal doxorubicin (DOXIL) in soft tissue sarcoma-bearing rats. Int J Cancer. 2000: 87(6), 829-837.
95.van Ijken MG, van Etten B, de Wilt JH, van Tiel ST, ten Hagen TL, and Eggermont AM. Tumor necrosis factor-alpha augments tumor effects in isolated hepatic perfusion with melphalan in a rat sarcoma model. J Immunother. 2000: 23(4), 449-455.
96.ten Hagen TLM, Eggermont AMM, and Lejeune FJ. TNF is here to stay--revisited. Trends Immunol. 2001: 22(3), 127-129.
97.Brouckaert P, Takahashi N, van Tiel ST, Hostens J, Eggermont AM, Seynhaeve AL et al. Tumor necrosis factor-alpha augmented tumor response in B16BL6 melanoma-bearing mice treated with stealth liposomal doxorubicin (Doxil) correlates with altered Doxil pharmacokinetics. Int J Cancer. 2004: 109(3), 442-448.
98Soma G, Kitahara N, Tsuji Y, Kato M, Oshima H, Gatanaga T et al. Improvement of cytotoxicity of tumor necrosis factor (TNF) by increase in basicity of its N-terminal region. Biochem Biophys Res Commun. 1987: 148(2), 629-635.

99.van Ostade X, Vandenabeele P, Everaerdt B, Loetscher H, Gentz RXBM, Lesslauer W et al. Human TNF mutants with selective activity on the p55 receptor. Nature. 1993: 361(6409), 266-269.
100.Kuroda K, Miyata K, Shikama H, Kawagoe T, Nishimura K, Takeda K et al. Novel muteins of human tumor necrosis factor with potent antitumor activity and less lethal toxicity in mice. Int J Cancer. 1995: 63(1), 152-157.
101.Tsutsumi Y, Kihira T, Tsunoda S, Kanamori T, Nakagawa S, and Mayumi T. Molecular design of hybrid tumour necrosis factor alpha with polyethylene glycol increases its anti-tumour potency. Br J Cancer. 1995: 71(5), 963-968.
102.Lucas R, Echtenacher B, Sablon E, Juillard P, Magez S, Lou J et al. Generation of a mouse tumor necrosis factor mutant with antiperitonitis and desensitization activities comparable to those of the wild type but with reduced systemic toxicity. Infect Immun. 1997: 65(6), 2006-2010.
103.Gatanaga T, Noguchi K, Tanabe Y, Inagawa H, Soma G, and Mizuno D. Antitumor effect of systemic administration of novel recombinant tumor necrosis factor (rTNF-S) with less toxicity than conventional rTNF-alpha in vivo. J Biol Response Mod. 1989: 8(3), 278-286.
104.Kaneda Y, Yamamoto Y, Kamada H, Tsunoda S, Tsutsumi Y, Hirano T et al. Antitumor activity of tumor necrosis factor alpha conjugated with divinyl ether and maleic anhydride copolymer on solid tumors in mice. Cancer Res. 1998: 58(2), 290-295.
105.Loetscher H, Stueber D, Banner D, Mackay F, and Lesslauer W. Human tumor necrosis factor alpha (TNF alpha) mutants with exclusive specificity for the 55-kDa or 75-kDa TNF receptors. J Biol Chem. 1993: 268(35), 26350-26357.
106.Soma GI, Tsuji Y, Tanabe Y, Noguchi K, Kitahara-Tanabe N, Gatanaga T et al. Biological activities of novel recombinant tumor necrosis factor having N-terminal amino acid sequences derived from cytotoxic factors produced by THP-1 cells. J Biol Response Mod. 1988: 7, 587-595.
107.Lodato RF, Feig B, Akimaru K, Soma G, and Klostergaard J. Hemodynamic evaluation of recombinant human tumor necrosis factor (TNF)-alpha, TNF-SAM2 and liposomal TNF-SAM2 in an anesthetized dog model. J Immunother Emphasis Tumor Immunol. 1995: 17(1), 19-29.
108.Akimaru K, Auzenne E, Akimaru Y, Leroux ME, Hayman AC, Utsumi T et al. Formulation and antitumor efficacy of liposomal-caprylated-TNF-SAM2. Cytokines Mol Ther. 1995: 1(3), 197-210.
109.de Wilt JH, Soma G, ten Hagen TL, Kanou J, Takagi K, Nooijen PT et al. Synergistic antitumour effect of TNF-SAM2 with melphalan and doxorubicin in isolated limb perfusion in rats. Anticancer Res. 2000: 20(5B), 3491-3496.
110.Curnis F, Sacchi A, Borgna L, Magni F, Gasparri A, and Corti A. Enhancement of tumor necrosis factor alpha antitumor immunotherapeutic properties by targeted delivery to aminopeptidase N (CD13). Nat Biotechnol. 2000: 18(11), 1185-1190.
111.Curnis F, Sacchi A, and Corti A. Improving chemotherapeutic drug penetration in tumors by vascular targeting and barrier alteration. J Clin Invest. 2002: 110(4), 475-482.
112.Colombo G, Curnis F, De Mori GM, Gasparri A, Longoni C, Sacchi A et al. Structure-activity relationships of linear and cyclic peptides containing the NGR tumor-homing motif. J Biol Chem. 2002: 277(49), 47891-47897.
113.Corti A and Ponzoni M. Tumor vascular targeting with tumor necrosis factor alpha and chemotherapeutic drugs. Ann N Y Acad Sci. 2004: 1028:104-12., 104-112.
114.Sacchi A, Gasparri A, Gallo-Stampino C, Toma S, Curnis F, and Corti A. Synergistic antitumor activity of cisplatin, paclitaxel, and gemcitabine with tumor vasculature-targeted tumor necrosis factor-alpha. Clin Cancer Res. 2006: 12(1), 175-182.
115.Sacchi A, Gasparri A, Curnis F, Bellone M, and Corti A. Crucial role for interferon gamma in the synergism between tumor vasculature-targeted tumor necrosis factor alpha (NGR-TNF) and doxorubicin. Cancer Res. 2004: 64(19), 7150-7155.
116.van Laarhoven HW, Gambarota G, Heerschap A, Lok J, Verhagen I, Corti A et al. Effects of the tumor vasculature targeting agent NGR-TNF on the tumor microenvironment in murine lymphomas. Invest New Drugs. 2006: 24(1), 27-36.
117.Tarli L, Balza E, Viti F, Borsi L, Castellani P, Berndorff D et al. A high-affinity human antibody that targets tumoral blood vessels. Blood. 1999: 94(1), 192-198.
118.Demartis S, Tarli L, Borsi L, Zardi L, and Neri D. Selective targeting of tumour neovasculature by a radiohalogenated human antibody fragment specific for the ED-B domain of fibronectin. Eur J Nucl Med. 2001: 28(4), 534-539.

119.Borsi L, Balza E, Bestagno M, Castellani P, Carnemolla B, Biro A et al. Selective targeting of tumoral vasculature: comparison of different formats of an antibody (L19) to the ED-B domain of fibronectin. Int J Cancer. 2002: 102(1), 75-85.
120.Carnemolla B, Borsi L, Balza E, Castellani P, Meazza R, Berndt A et al. Enhancement of the antitumor properties of interleukin-2 by its targeted delivery to the tumor blood vessel extracellular matrix. Blood. 2002: 99(5), 1659-1665.
121.Borsi L, Balza E, Carnemolla B, Sassi F, Castellani P, Berndt A et al. Selective targeted delivery of TNFalpha to tumor blood vessels. Blood. 2003: 102(13), 4384-4392.
122.Halin C, Gafner V, Villani ME, Borsi L, Berndt A, Kosmehl H et al. Synergistic therapeutic effects of a tumor targeting antibody fragment, fused to interleukin 12 and to tumor necrosis factor alpha. Cancer Res. 2003: 63(12), 3202-3210.
123.Balza E, Mortara L, Sassi F, Monteghirfo S, Carnemolla B, Castellani P et al. Targeted delivery of tumor necrosis factor-alpha to tumor vessels induces a therapeutic T cell-mediated immune response that protects the host against syngeneic tumors of different histologic origin. Clin Cancer Res. 2006: 12(8), 2575-2582.
124.Tsunoda S, Ishikawa T, Yamamoto Y, Kamada H, Koizumi K, Matsui J et al. Enhanced antitumor potency of polyethylene glycolylated tumor necrosis factor-alpha: a novel polymer-conjugation technique with a reversible amino-protective reagent. J Pharmacol Exp Ther. 1999: 290(1), 368-372.
125.Kamada H, Tsutsumi Y, Tsunoda S, Kihira T, Kaneda Y, Yamamoto Y et al. Molecular design of conjugated tumor necrosis factor-alpha: synthesis and characteristics of polyvinyl pyrrolidone modified tumor necrosis factor-alpha. Biochem Biophys Res Commun. 1999: 257(2), 448-453.
126.Tsutsumi Y, Tsunoda S, Kamada H, Kihira T, Nakagawa S, Kaneda YXKT et al. Molecular design of hybrid tumour necrosis factor-alpha. II: The molecular size of polyethylene glycol-modified tumour necrosis factor-alpha affects its antitumour potency. Br J Cancer. 1996: 74(7), 1090-1095.
127.Kamada H, Tsutsumi Y, Yamamoto Y, Kihira T, Kaneda Y, Mu Y et al. Antitumor activity of tumor necrosis factor-alpha conjugated with polyvinylpyrrolidone on solid tumors in mice. Cancer Res. 2000: 60(22), 6416-6420.
128.Shibata H, Yoshioka Y, Ikemizu S, Kobayashi K, Yamamoto Y, Mukai Y et al. Functionalization of tumor necrosis factor-alpha using phage display technique and PEGylation improves its antitumor therapeutic window. Clin Cancer Res. 2004: 10(24), 8293-8300.
129.Farma JM, Puhlmann M, Soriano PA, Cox D, Paciotti GF, Tamarkin L et al. Direct evidence for rapid and selective induction of tumor neovascular permeability by tumor necrosis factor and a novel derivative, colloidal gold bound tumor necrosis factor. Int J Cancer. 2007: 120(11), 2474-2480.
130.van der Veen AH, Eggermont AM, Seynhaeve AL, van Tiel ST, and ten Hagen TL. Biodistribution and tumor localization of stealth liposomal tumor necrosis factor-alpha in soft tissue sarcoma bearing rats. Int J Cancer. 1998: 77(6), 901-906.
131.ten Hagen TL, Seynhaeve AL, van Tiel ST, Ruiter DJ, and Eggermont AM. Pegylated liposomal tumor necrosis factor-alpha results in reduced toxicity and synergistic antitumor activity after systemic administration in combination with liposomal doxorubicin (Doxil) in soft tissue sarcoma-bearing rats. Int J Cancer. 2002: 97(1), 115-120.
132.Hoving S, Seynhaeve AL, van Tiel ST, Eggermont AM, and ten Hagen TL. Addition of low-dose tumor necrosis factor-alpha to systemic treatment with STEALTH liposomal doxorubicin (Doxil) improved anti-tumor activity in osteosarcoma-bearing rats. Anticancer Drugs. 2005: 16(6), 667-674.
133.Hoving S, van Tiel ST, Eggermont AM, and ten Hagen TL. Effect of low-dose tumor necrosis factor-alpha in combination with STEALTH liposomal cisplatin (SPI-077) on soft-tissue- and osteosarcoma-bearing rats. Anticancer Res. 2005: 25(2A), 743-750.
134.Morgan DA, Ruscetti FW, and Gallo R. Selective in vitro growth of T lymphocytes from normal human bone marrows. Science. 1976: 193(4257), 1007-1008.
135.Baselmans AH, Koten JW, Battermann JJ, Van Dijk JE, and Den Otter W. The mechanism of regression of solid SL2 lymphosarcoma after local IL-2 therapy. Cancer Immunol Immunother. 2002: 51(9), 492-498.
136.Atkins MB. Interleukin-2: clinical applications. Semin Oncol. 2002: 29(3 Suppl 7), 12-17.
137.Rosenberg SA. Interleukin 2 for patients with renal cancer. Nat Clin Pract Oncol. 2007: 4(9), 497.
138.Fisher RI, Rosenberg SA, and Fyfe G. Long-term survival update for high-dose recombinant interleukin-2 in patients with renal cell carcinoma. Cancer J Sci Am. 2000: 6 Suppl 1, S55-S57.
139.Epstein AL, Mizokami MM, Li J, Hu P, and Khawli LA. Identification of a protein fragment of interleukin 2 responsible for vasopermeability. J Natl Cancer Inst. 2003: 95(10), 741-749.

140.Siegel JP and Puri RK. Interleukin-2 toxicity. J Clin Oncol. 1991: 9(4), 694-704.
141.Winkelhake JL and Gauny SS. Human recombinant interleukin-2 as an experimental therapeutic. Pharmacol Rev. 1990: 42(1), 1-28.
142.Hoving S, Brunstein F, aan de Wiel-Ambagtsheer G, van Tiel ST, de Boeck G, de Bruijn EA et al. Synergistic antitumor response of interleukin 2 with melphalan in isolated limb perfusion in soft tissue sarcoma-bearing rats. Cancer Res. 2005: 65(10), 4300-4308.
143.Barger G and Dale HH. Chemical structure and sympathomimetic action of amines. J Physiol. 1910: 41(1-2), 19-59.
144.Dale HH and Laidlaw PP. The physiological action of beta-iminazolylethylamine. J Physiol. 1910: 41(5), 318-344.
145.Schild HO. The multiple facets of histamine research. Agents Actions. 1981: 11(1-2), 12-19.
146.Jutel M, Blaser K, and Akdis CA. The role of histamine in regulation of immune responses. Chem Immunol Allergy. 2006: 91:174-87., 174-187.
147.Jutel M, Watanabe T, Akdis M, Blaser K, and Akdis CA. Immune regulation by histamine. Curr Opin Immunol. 2002: 14(6), 735-740.
148.Wang J, Al Lamki RS, Zhang H, Kirkiles-Smith N, Gaeta ML, Thiru S et al. Histamine antagonizes tumor necrosis factor (TNF) signaling by stimulating TNF receptor shedding from the cell surface and Golgi storage pool. J Biol Chem. 2003: 278(24), 21751-21760.
149.Garrison JC. Histamine, Bradykinin, 5-Hydroxytryptamine and their antagonists. 8th ed Elmsford - New York: Pergamon Press. 1990: 575-599.
150.Wu NZ and Baldwin AL. Possible mechanism(s) for permeability recovery of venules during histamine application. Microvasc Res. 1992: 44(3), 334-352.
151.Wu NZ and Baldwin AL. Transient venular permeability increase and endothelial gap formation induced by histamine. Am J Physiol. 1992: 262(4 Pt 2), H1238-H1247.
152.Carson MR, Shasby SS, and Shasby DM. Histamine and inositol phosphate accumulation in endothelium: cAMP and a G protein. Am J Physiol. 1989: 257(4 Pt 1), L259-L264.
153.Rotrosen D and Gallin JI. Histamine type I receptor occupancy increases endothelial cytosolic calcium, reduces F-actin, and promotes albumin diffusion across cultured endothelial monolayers. J Cell Biol. 1986: 103(6 Pt 1), 2379-2387.
154.Joris I, Majno G, and Ryan GB. Endothelial contraction in vivo: a study of the rat mesentery. Virchows Arch B Cell Pathol. 1972: 12(1), 73-83.
155.Majno G and PALADE GE. Studies on inflammation. 1. The effect of histamine and serotonin on vascular permeability: an electron microscopic study. J Biophys Biochem Cytol. 1961: 11:571-605., 571-605.
156.Horan KL, Adamski SW, Ayele W, Langone JJ, and Grega GJ. Evidence that prolonged histamine suffusions produce transient increases in vascular permeability subsequent to the formation of venular macromolecular leakage sites. Proof of the Majno-Palade hypothesis. Am J Pathol. 1986: 123(3), 570-576.
157.Stelzner TJ, Weil JV, and O'Brien RF. Role of cyclic adenosine monophosphate in the induction of endothelial barrier properties. J Cell Physiol. 1989: 139(1), 157-166.
158.Resink TJ, Grigorian GY, Moldabaeva AK, Danilov SM, and Buhler FR. Histamine-induced phosphoinositide metabolism in cultured human umbilical vein endothelial cells. Association with thromboxane and prostacyclin release. Biochem Biophys Res Commun. 1987: 144(1), 438-446.
159.Ehringer WD, Edwards MJ, and Miller FN. Mechanisms of alpha-thrombin, histamine, and bradykinin induced endothelial permeability. J Cell Physiol. 1996: 167(3), 562-569.
160.Stevens T, Garcia JG, Shasby DM, Bhattacharya J, and Malik AB. Mechanisms regulating endothelial cell barrier function. Am J Physiol Lung Cell Mol Physiol. 2000: 279(3), L419-L422.
161.Brunstein F, Rens J, van Tiel ST, Eggermont AM, and ten Hagen TL. Histamine, a vasoactive agent with vascular disrupting potential, improves tumour response by enhancing local drug delivery. Br J Cancer. 2006: 95(12), 1663-1669.
162.Brunstein F, Eggermont AM, Wiel-Ambagtsheer G, van Tiel ST, Rens J, and ten Hagen TL. Synergistic antitumor effects of histamine plus melphalan in isolated hepatic perfusion for liver metastases. Ann Surg Oncol. 2007: 14(2), 795-801.
163.Nooijen PTGA, Eggermont AMM, Verbeek MM, Schalkwijk L, Buurman WA, De Waal RM et al. Transient induction of E-selectin expression following TNF alpha- based isolated limb perfusion in melanoma and sarcoma patients is not tumor specific. J Immunother Emphasis Tumor Immunol. 1996: 19(1), 33-44.

164.Yang L, Froio RM, Sciuto TE, Dvorak AM, Alon R, and Luscinskas FW. ICAM-1 regulates neutrophil adhesion and transcellular migration of TNF-alpha-activated vascular endothelium under flow. Blood. 2005: 106(2), 584-592.
165.Vanhee D, Delneste Y, Lassalle P, Gosset P, Joseph M, and Tonnel AB. Modulation of endothelial cell adhesion molecule expression in a situation of chronic inflammatory stimulation. Cell Immunol. 1994: 155(2), 446-456.
166.VandenBerg E, Reid MD, Edwards JD, and Davis HW. The role of the cytoskeleton in cellular adhesion molecule expression in tumor necrosis factor-stimulated endothelial cells. J Cell Biochem. 2004: 91(5), 926-937.
167.Imaizumi T, Itaya H, Fujita K, Kudoh D, Kudoh S, Mori K et al. Expression of tumor necrosis factor-alpha in cultured human endothelial cells stimulated with lipopolysaccharide or interleukin-1alpha. Arterioscler Thromb Vasc Biol. 2000: 20(2), 410-415.
168.Streetz KL, Wustefeld T, Klein C, Manns MP, and Trautwein C. Mediators of inflammation and acute phase response in the liver. Cell Mol Biol (Noisy -le-grand). 2001: 47(4), 661-673.
169.Gutman M, Inbar M, Lev-Shlush D, Abu-Abid S, Mozes M, Chaitchik SXMI et al. High dose tumor necrosis factor-alpha and melphalan administered via isolated limb perfusion for advanced limb soft tissue sarcoma results in a >90% response rate and limb preservation. Cancer. 1997: 79(6), 1129-1137.
170.Hoving S, Seynhaeve AL, van Tiel ST, aan de Wiel-Ambagtsheer G, de Bruijn EA, Eggermont AM et al. Early destruction of tumor vasculature in tumor necrosis factor-alpha-based isolated limb perfusion is responsible for tumor response. Anticancer Drugs. 2006: 17(8), 949-959.
171.Millan CG, Marinero ML, Castaneda AZ, and Lanao JM. Drug, enzyme and peptide delivery using erythrocytes as carriers. J Control Release. 2004: 95(1), 27-49.
172.Dumez H, Guetens G, de Boeck G, Highley MS, de Bruijn EA, van Oosterom AT et al. In vitro partition of irinotecan (CPT-11) in human volunteer blood: the influence of concentration, gender and smoking. Anticancer Drugs. 2005: 16(8), 893-895.
173.Wildiers H, Guetens G, de Boeck G, Landuyt W, Verbeken E, Highley M et al. Melphalan availability in hypoxia-inducible factor-1alpha+/+ and factor-1alpha-/- tumors is independent of tumor vessel density and correlates with melphalan erythrocyte transport. Int J Cancer. 2002: 99(4), 514-519.
174.Grignani G and Maiolo A. Cytokines and hemostasis. Haematologica. 2000: 85(9), 967-972.
175.Beretz A, Klein-Soyer C, Archipoff G, Camilla C, Brisson C, Freyssinet JM et al. Modulation by cytokines of leukocyte-endothelial cell interactions. Implications for thrombosis. Biorheology. 1990: 27(3-4), 455-460.
176.Magueresse-Battistoni B, Pernod G, Kolodie L, Morera AM, and Benahmed M. Tumor necrosis factor-alpha regulates plasminogen activator inhibitor-1 in rat testicular peritubular cells. Endocrinology. 1997: 138(3), 1097-1105.
177.Napoleone E, Di Santo A, and Lorenzet R. Monocytes upregulate endothelial cell expression of tissue factor: a role for cell-cell contact and cross-talk. Blood. 1997: 89(2), 541-549.
178.Clauss M, Gerlach M, Gerlach H, Brett J, Wang F, Familletti PC et al. Vascular permeability factor: a tumor-derived polypeptide that induces endothelial cell and monocyte procoagulant activity, and promotes monocyte migration. J Exp Med. 1990: 172(6), 1535-1545.
179.van der Poll T., van Deventer SJ, Pasterkamp G, van Mourik JA, Buller HR, and ten Cate JW. Tumor necrosis factor induces von Willebrand factor release in healthy humans. Thromb Haemost. 1992: 67(6), 623-626.
180.Renard N, Nooijen PT, Schalkwijk L, De Waal RM, Eggermont AM, Lienard et al. VWF release and platelet aggregation in human melanoma after perfusion with TNF alpha. J Pathol. 1995: 176(3), 279-287.
181.Renard N, Lienard D, Lespagnard L, Eggermont A, Heimann R, and Lejeune F. Early endothelium activation and polymorphonuclear cell invasion precede specific necrosis of human melanoma and sarcoma treated by intravascular high-dose tumour necrosis factor alpha (rTNF alpha). Int J Cancer. 1994: 57(5), 656-663.
182.Nooijen PTGA, Eggermont AMM, Schalkwijk L, Henzen-Logmans S, de Waal RMW, and Ruiter DJ. Complete response of melanoma-in-transit metastasis after isolated limb perfusion with tumor necrosis factor alpha and melphalan without massive tumor necrosis: a clinical and histopathological study of the delayed-type reaction pattern. Cancer Res. 1998: 58(21), 4880-4887.
183.Lejeune FJ, Lienard D, Matter M, and Ruegg C. Efficiency of recombinant human TNF in human cancer therapy. Cancer Immun. 2006: 6, 6.

184.Manusama ER, Nooijen PT, Stavast J, de Wilt JH, Marquet RL, Eggermont et al. Assessment of the role of neutrophils on the antitumor effect of TNFalpha in an in vivo isolated limb perfusion model in sarcoma- bearing brown Norway rats. J Surg Res. 1998: 78(2), 169-175.
185.Ruegg C, Yilmaz A, Bieler G, Bamat J, Chaubert P, and Lejeune FJ. Evidence for the involvement of endothelial cell integrin alphaVbeta3 in the disruption of the tumor vasculature induced by TNF and IFN-gamma. Nat Med. 1998: 4(4), 408-414.

Chapter 12

General discussion: “Aiming for both tumor cells and stroma.”

Additional information

General discussion: "Aiming for both tumor cells and stroma"

GENERAL DISCUSSION OF THIS THESIS

The primary aim of the research, described in this thesis was to improve the efficacy of conventional chemotherapy by increasing accessibility of the agent to the tumor cell. Achieving adequate drug concentrations at the site of its target, the tumor cell, remains a major challenge in systemic therapy. Pathophysiologic conditions at the tumor site hamper drug uptake because of heterogenous and chaotic blood flow patterns with hypoperfusion in multiple areas of the tumor, non-functional vessels and shunting of blood, high interstitial pressure zones due to a lack of lymphatic vessels, stasis and reversed blood flow (**Fig. 1**). In addition, the abnormal features and composition of the endothelial cells, pericytes, basal membrane and extracellular matrix hinders passage of the drug.

Improving drug uptake at the tumor site. Achieving better intratumoral drug levels by manipulating the TAV with vasoactive agents or using drug formulations that will utilize the physiologic particularities, are important approaches to improve antitumor efficacy. Liposomal formulations,

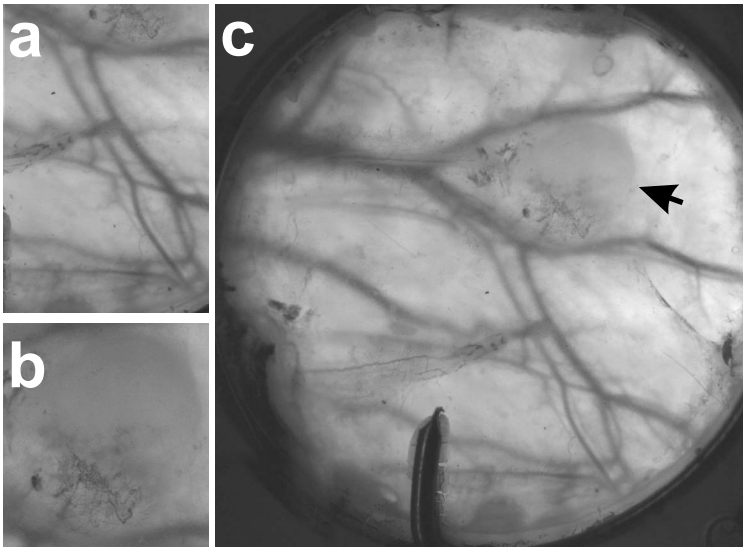

Figure 1. The difference in tumor-associated vasculature and normal vasculature. (**a**) Blood vessels deliver nutrients, oxygen and other molecules in the tissues it passes and removes toxins. This system is arranged in arteries, veins and capillaries with their own specific characteristics and phenotype. (**b**) In contrast to the structural organized blood vessels of the basic organs, the tumor-associated vasculature is "abnormal". It display a lack of hierarchical branching and organization in which the recognizable features of arterioles, capillaries and venules is lost. The vessels are tortuous and unevenly dilated. As a result, tumor blood flow is chaotic, might be stationary and can even change direction. This leads to hypoxia and acidosis in solid tumors. Due to these properties of the tumor-associated vasculature the intratumoral drug accumulation is very heterogeneous. (**c**) The complete overview of the dorsal skin-fold window with a lewis lung carcinoma (arrow) 6 days after tumor implantation. (See color section for a full-color version.)

especially long circulating liposomes, lead to improved intratumoral drug levels because of capitalization on the leakiness of the TAV in comparison to normal vessels. Encapsulated doxorubicin (Doxil/Caelyx) is such an example and is used for AIDS-related Kaposi's sarcoma, recurrent ovarian cancer and has recently also been approved by the FDA for multiple myeloma [1]. Alternatively, the chemical structure of a drug can be altered to reduce its toxicity. This has been done for TNF. TNF-SAM2, developed by Soma *et al*. has an increased N-terminal basicity with milder side effects compared to conventional TNF [2]. TNF coupled to cyclic CNGRC peptide (a CD13 ligand, expressed specifically on tumor vasculature) or to the antibody L19 (against the extra-domain B of fibronectin) has the tendency to home and bind more specifically to the tumor-associated vasculature making these TNF-mutants more active in significant lower dose [3,4]. Also binding of TNF at the surface of gold nanoparticles (cAu-TNF) improved the safety of TNF while retaining the antitumor efficacy by selectively altering the permeability of the tumor vasculature [5]. Locoregional administration of drugs is another strategy to increase intratumoral drug levels. One of such methods is utilized in our experiments; the isolated limb perfusion (ILP). This method allows the administration of very high doses of chemotherapeutic drugs and other agents (e.g. cytokines) and achieves drug levels 15 to 50 times higher than can be achieved using the systemic administration that is limited by the maximal tolerated dose. This leads to very high response rates and tumor control [6].

Targeting both the stromal compartment and the tumor cells. A tumor does not solely exist of tumor cells and the stromal compartment is equally important in tumor development and growth. The TAV provides thereafter an interesting target in anticancer therapy. Endothelial cells are easily targeted and are believed to have more genetic stability then tumor cells, hence drug resistance is not likely to appear [7]. In 1971 Folkman proposed the hypothesis that prohibiting the development of newly formed tumor blood vessels would be an attractive new approach in cancer treatment [8]. The antiangiogenesis strategy inhibits the function of growth factors that are needed for the development and growth of new vessels. A second approach is the direct damage of the established tumor vasculature by vascular disrupting agents (VDAs) that will initiate vascular collapse, shutdown of tumor blood flow, depriving the tumor of oxygen and nutrients, leading to tumor necrosis [9]. It was demonstrated that these antiangiogenic and vascular disruptive strategies are not sufficiently effective and that the combination with chemotherapy is required for optimal antitumor responses.

Improving tumor response by dual targeting. Besides the antiangiogenic and vascular destructive approaches we propose a third strategy, "tumor vessel abnormalization" in which the tumor-associated vasculature is manipulated with vasoactive agents like TNF or Cilengitide to improve the delivery of the chemotherapeutic compound at the site of the tumor cells. As the other strategies both attack the vasculature this is a counter intuitive approach in which an adequate vasculature is a prerequisite for a good antitumor response.

Two animal models were used to better investigate the underlying mechanisms. First, the isolated limb perfusion with high-dose TNF or Cilengitide in combination with the chemotherapeutic drug melphalan in a short exposure setting. Second, the systemic treatment with multiple injections of low-dose TNF and Doxil. The choice of a chemotherapeutic agent depends on its efficacy in killing the tumor cells. However, for successful treatment the bioavailability of the chemotherapeutic drug has to be facilitated by an agent with vasoactive/modulating properties. Low-levels of TNF in the systemic setting and short exposure to Cilengitide in the ILP are sufficient to give a significant tumor response. In the ILP with high-dose TNF damage of the endothelial cells is already observed immediately after perfusion [10]. De Wilt *et al.* found that the TNF concentration could be reduced 5-fold while retaining synergy, but that below a certain threshold synergy between

TNF and melphalan or doxorubicin was completely lost [11]. Observations made in the dorsal skin-fold chamber show that a single injection of low-dose TNF suffices to increase the permeability of the vessels without affecting the functionality of the vessel [12]. Systemic low-dose TNF therapy synergizes with Doxil in the treatment of both the soft tissue sarcoma BN175 [13] and the less vascularized osteosarcoma ROS-1 [14]. Drug accumulation was measured 24 hours after the third injection. A significant increase in intratumoral drug concentration was observed (1 µg/g for Doxil versus 2.3 µg/g for Doxil + TNF) in the BN175 soft tissue sarcoma model. In contrast, TNF had no effect on drug accumulation in the ROS-1 osteosarcoma model. We speculate that the vessels of this tumor are already quite leaky, which is supported by the higher drug concentration (4 µg/g) in this tumor without the presence of TNF. *In vitro* we observed that TNF had no direct effect BN175 cells while a 40% reduction in cell growth was observed when TNF was added to ROS-1 cells. These results indicate that TNF can have a direct effect on tumor cells (if sensitive) or an effect on the intratumoral drug delivery through manipulation of the vasculature.

About the liposomal fate we gained more insight using the dorsal skin-fold chamber. We observed that after leaving the vasculature a perivascular rim of cells take up the complete liposome. The liposome is intracellularly degraded and releases its content (doxorubicin) which then enters the nucleus. Also *in vitro* we observed that free doxorubicin almost immediately transports into the nucleus. In contrast, when we incubated cells with liposomal doxorubicin (Doxil) this remains for days inside the cytoplasm and the doxorubicin content is released very slowly after which it can be observed in the nucleus (**Fig. 2**) [12]. This is in contradiction to previous publications that believe that doxorubicin is released in the interstitial space.

Also in the ILP, an increased uptake of the chemotherapeutic melphalan is found with the addition of TNF within the time frame of the perfusion and already during perfusion softening of the tumor occurs [10,15]. Histological analysis reveals that directly after perfusion some areas with destruction of the endothelial lining and erythrocytes infiltration can be seen. Because erythrocytes are know to be the main carrier for melphalan this is most likely the route by which

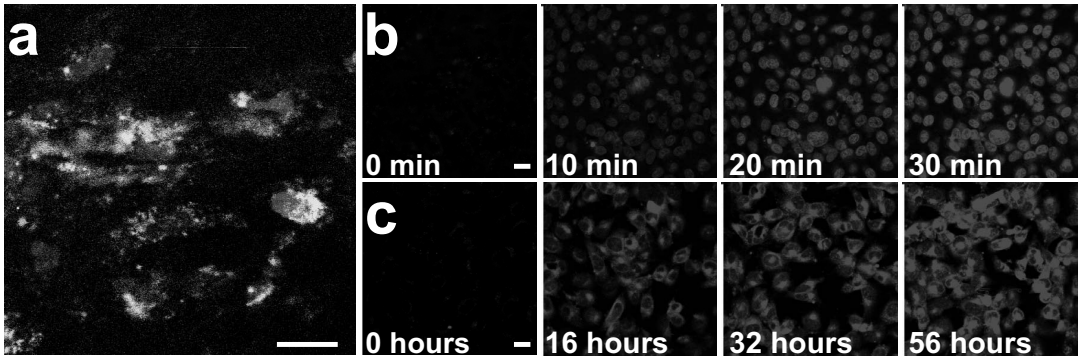

Figure 2. Intratumoral and intracellular fate of Doxil. Using the dorsal skin-fold chamber we observed that, with the addition of TNF, Doxil labeled with a green fluorescent marker extravasates from the tumor blood vessels into the tumor intersitium between 12 to 24 hours. (**a**) Seventy-two hours after systemic injection, the liposomes (green fluorescent) remained in the cytoplasm of the cell, while doxorubicin (red fluorescent) was found in the nucleus. No indications of Doxil or liposomes outside the cells in the interstitial space were found. This suggest that the liposome is taken up completely by the cells and is thereafter broken down. (**b**) Tumor cells were incubated with doxorubicin in a migration ring and the fate of the free drug was followed for several hours. Almost immediately after adding the drug, doxorubicin was taken up by the cells and transported to the nucleus. (**c**) In contrary to the free drug, when cells were incubated with Doxil hardly any drug was observed in the nucleus and most remained in the cytoplasm. Scale bar apply for all images, 20 µm. (See color section for a full-color version.)

melphalan enters the tumor tissue [16]. In previous studies, we already noted the infiltration of immune cells several days after perfusion [17,18]. However, within a time-frame of 6 hours we did not observe significant differences in infiltration of these cells and cytokines, indicating that they are not required for the initiation of vessel changes but play rather a role in the eradication of the tumor [10]. Besides TNF, we investigated other vasoactive compounds like histamine, IL-2 and Cilengitide [19,20]. Cilengitide is an integrin inhibitor capable of disrupting the endothelial layer of angiogenic vessels. As for TNF, Cilengitide alone is not sufficient to trigger an antitumor response and needs to be accompanied by a chemotherapeutic agent.

The exact target of TNF: endothelial cells or pericytes? The prevailing hypothesis until recently has been that the chemotherapeutic drug targets the tumor cells whereas the tumor-associated endothelial cells are targeted by TNF. Immediately after TNF-based perfusion we observed in histological analysis some areas with complete destruction of the vasculature, but this is not enough to cause significant regression of the tumor [10]. Using the dorsal skin-fold chamber we observed that a combination with a chemotherapeutic compound is a prerequisite because TNF augment the intratumoral concentration of the co-administered chemotherapy [12]. TNF induces permeability of the tumor vasculature and increases the leakiness of vessels for macromolecules resulting in a better and more homogenous drug distribution. This increased permeability did not affect the functionality and size of the vessels for at least 2 days after treatment. However, we also found that TNF-induced vascular permeability is not a general phenomenon, as there is no increased accumulation of Doxil in the lewis lung carcinoma (LLC) and the 1F6 human melanoma resulting in a poor antitumor response. Obviously the properties of the tumor-associated vasculature are very important in TNF-response. The TNF-responding tumor, the B16BL6 mouse melanoma and the highly aggressive human melanoma BLM, contain large vessels in low-density whereas the non-responding tumors, LLC and 1F6, have a high degree of small vessels. Despite the difference in vessel architecture, the majority of the vessels are functional. This observation suggests that endothelial cells may not be the primary target of TNF. The lack of TNF-effect was already observed *in vitro* as hardly any passage of macromolecules through the endothelial layer was observed. Gap formation and permeability changes were only eminent when TNF was co-incubated with IFN [21]. Also, in an earlier study we reported that when human biopsies were stained for TNFR1, the receptor was located at cells that were not endothelial cells but cells closely associated with the endothelial cells [22]. Further histological survey of human and mouse tumor biopsies revealed that, rather than endothelial cells, the tumor-associated pericytes are the TNFR1 expressing cells. This discovery substantiates the observations regarding the tumor response. B16BL6 and BLM have a higher pericyte coverage compared to LLC and 1F6, making the latter less responsive to the addition of TNF. Based on these observations we hypothesize that pericytes rather then endothelial cells are the primary target for TNF, implying that beneficial activity of TNF in a combination treatment protocol could be predicted by the presence of pericytes in the tumor vasculature. Most likely in the presence of TNF the pericytes produce a factor that in turn stimulated permeability increase of the endothelial cells. Further investigation is required to uncover the factor responsible for these changes.

GENERAL CONCLUSION

In the past multiple studies have demonstrated spectacular antitumor effects obtained with high-dose TNF and chemotherapy in the ILP model. Here we show that also a low doses of TNF can be effective. Further research has shown that the TNF-effect depends on the cellular make-up of the vascular bed and that not the endothelial cells but the pericytes are the primary target for TNF (**Fig. 3**). Aiming at multiple targets improves efficacy of therapeutic approaches. Manipulat-

ing the tumor-associated vasculature with vasoactive agents increases the bioavailability of the chemotherapeutic compound in the tumor and is a prerequisite for a good tumor response. Manipulating and exploiting the pathophysiologic properties of the tumor vasculature, a process that we have called "tumor vessel abnormalization", is different from the regular antiangiogenic and vascular destruction strategies. Results in this thesis show that this strategy improves the efficacy of chemotherapeutics. Isolated limb perfusion using TNF is already an approved treatment and other vasoactive agents have become available to be used in this system. We have demonstrated that low-dose TNF can mediate a good antitumor response in combination with liposomal che-

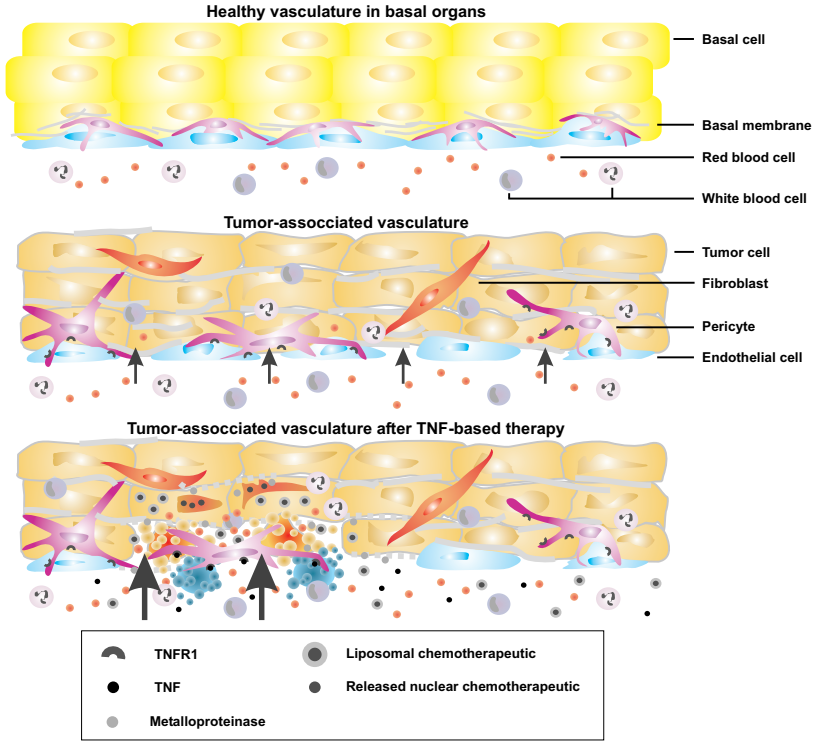

Figure 3. Abnormalization of the tumor-associated vasculature. In the vasculature of basic organs the endothelial cells forms a quiescent and tightly packed lining separating the blood and blood-born elements from the rest of the body. Mural cells (smooth muscle cells and pericytes) form the muscle of the blood vessel and have specific properties according to the type of blood vessel they can be found at. The tumor-associated vasculature has endothelial cells that are morphological different from these in the normal vessels. Because of the fast growing properties of most tumors they are highly active and have irregular shapes with openings between the cells making the vessel highly permeable. Also the pericytes are different, forming a loose association with the endothelial cells and displaying extensions into the intersitium. The basal membrane is irregular in size with a different protein composition and structure. After TNF-based therapy, TNF binds to the TNFR1 located on the pericytes. These cells produce to further elucidate endogenous factors that has its effect on endothelial cells. The permeability of the endothelial lining is further increased for the co-administered drug, melphalan (in free form this will have micromolecular properties however absorbed in erythrocytes melphalan will act as a macromolecule) or long-circulating liposomes Doxil. MMPs produced by the endothelial cells will degrade the underlying matrix providing a better entrance for the chemotherapeutic compound. The liposomal drug enters as a whole the tumor cell were it is slowly degraded releasing the active drug intracellulary that eventually kills the tumor cell. (See color section for a full-color version.)

motherapeutic drug formulations. Partially based on these results a clinical trial will start using nano(gold)particle TNF with enhanced tumor uptake kinetics and in the near future in melanoma patients.

REFERENCES

1.Haley B and Frenkel E. Nanoparticles for Drug Delivery in Cancer Treatment. Urol Oncol 2008: 26(1), 57-64
2.Soma G, Kitahara N, Tsuji Y, Kato M, Oshima H, Gatanaga T et al. Improvement of Cytotoxicity of Tumor Necrosis Factor (TNF) by Increase in Basicity of Its N-Terminal Region. Biochem Biophys Res Commun 1987: 148(2), 629-635
3.Demartis S, Tarli L, Borsi L, Zardi L, and Neri D. Selective Targeting of Tumour Neovasculature by a Radiohalogenated Human Antibody Fragment Specific for the ED-B Domain of Fibronectin. Eur J Nucl Med 2001: 28(4), 534-539
4.Zarovni N, Monaco L, and Corti A. Inhibition of Tumor Growth by Intramuscular Injection of CDNA Encoding Tumor Necrosis Factor Alpha Coupled to NGR and RGD Tumor-Homing Peptides. Hum Gene Ther 2004: 15(4), 373-382
5.Farma JM, Puhlmann M, Soriano PA, Cox D, Paciotti GF, Tamarkin L et al. Direct Evidence for Rapid and Selective Induction of Tumor Neovascular Permeability by Tumor Necrosis Factor and a Novel Derivative, Colloidal Gold Bound Tumor Necrosis Factor. Int J Cancer 2007: 120(11), 2474-2480
6.Benckhuijsen C, Kroon BB, van Geel AN, and Wieberdink J. Regional Perfusion Treatment With Melphalan for Melanoma in a Limb: an Evaluation of Drug Kinetics. Eur J Surg Oncol 1988: 14(2), 157-163
7.Kerbel R and Folkman J. Clinical Translation of Angiogenesis Inhibitors. Nat Rev Cancer 2002: 2(10), 727-739
8.Folkman J. Tumor Angiogenesis: Therapeutic Implications. N Engl J Med 1971: 285(21), 1182-1186
9.Tozer GM, Kanthou C, and Baguley BC. Disrupting Tumour Blood Vessels. Nat Rev Cancer 2005: 5(6), 423-435
10.Hoving S, Seynhaeve AL, van Tiel ST, aan de Wiel-Ambagtsheer G, de Bruijn EA, Eggermont AM et al. Early Destruction of Tumor Vasculature in Tumor Necrosis Factor-Alpha-Based Isolated Limb Perfusion Is Responsible for Tumor Response. Anticancer Drugs 2006: 17(8), 949-959
11.de Wilt JH, Manusama ER, van Tiel ST, van Ijken MG, ten Hagen TL, and Eggermont AM. Prerequisites for Effective Isolated Limb Perfusion Using Tumour Necrosis Factor Alpha and Melphalan in Rats. Br J Cancer 1999: 80(1-2), 161-166
12.Seynhaeve AL, Hoving S, Schipper D, Vermeulen CE, aan de Wiel-Ambagtsheer G, van Tiel ST et al. Tumor Necrosis Factor {Alpha} Mediates Homogeneous Distribution of Liposomes in Murine Melanoma That Contributes to a Better Tumor Response. Cancer Res 2007: 67(19), 9455-9462
13.ten Hagen TL, van der Veen AH, Nooijen PT, van Tiel ST, Seynhaeve AL, and Eggermont AM. Low-Dose Tumor Necrosis Factor-Alpha Augments Antitumor Activity of Stealth Liposomal Doxorubicin (DOXIL) in Soft Tissue Sarcoma-Bearing Rats. Int J Cancer 2000: 87(6), 829-837
14.Hoving S, Seynhaeve AL, van Tiel ST, Eggermont AM, and ten Hagen TL. Addition of Low-Dose Tumor Necrosis Factor-Alpha to Systemic Treatment With STEALTH Liposomal Doxorubicin (Doxil) Improved Anti-Tumor Activity in Osteosarcoma-Bearing Rats. Anticancer Drugs 2005: 16(6), 667-674
15.de Wilt JH, ten Hagen TL, de Boeck G, van Tiel ST, de Bruijn EA, and Eggermont AM. Tumour Necrosis Factor Alpha Increases Melphalan Concentration in Tumour Tissue After Isolated Limb Perfusion. Br J Cancer 2000: 82(5), 1000-1003
16.Wildiers H, Guetens G, de Boeck G, Landuyt W, Verbeken E, Highley M et al. Melphalan Availability in Hypoxia-Inducible Factor-1alpha+/+ and Factor-1alpha-/- Tumors Is Independent of Tumor Vessel Density and Correlates With Melphalan Erythrocyte Transport. Int J Cancer 2002: 99(4), 514-519
17.Nooijen PT, Manusama ER, Eggermont AM, Schalkwijk L, Stavast J, Marquet RL et al. Synergistic Effects of TNF-Alpha and Melphalan in an Isolated Limb Perfusion Model of Rat Sarcoma: a Histopathological, Immunohistochemical and Electron Microscopical Study. Br J Cancer 1996: 74(12), 1908-1915
18.Renard N, Lienard D, Lespagnard L, Eggermont A, Heimann R, and Lejeune F. Early Endothelium Activation and Polymorphonuclear Cell Invasion Precede Specific Necrosis of Human Melanoma and Sarcoma Treated by Intravascular High-Dose Tumour Necrosis Factor Alpha (RTNF Alpha). Int J Cancer 1994: 57(5), 656-663
19.Brunstein F, Hoving S, Seynhaeve AL, van Tiel ST, Guetens G, de Bruijn EA et al. Synergistic Antitumor Activity of Histamine Plus Melphalan in Isolated Limb Perfusion: Preclinical Studies. J Natl Cancer Inst 2004: 96(21), 1603-1610

20.Hoving S, Brunstein F, aan de Wiel-Ambagtsheer G, van Tiel ST, de Boeck G, de Bruijn EA et al. Synergistic Antitumor Response of Interleukin 2 With Melphalan in Isolated Limb Perfusion in Soft Tissue Sarcoma-Bearing Rats. Cancer Res 2005: 65(10), 4300-4308

21.Seynhaeve AL, Vermeulen CE, Eggermont AM, and ten Hagen TL. Cytokines and Vascular Permeability: an in Vitro Study on Human Endothelial Cells in Relation to Tumor Necrosis Factor-Alpha-Primed Peripheral Blood Mononuclear Cells. Cell Biochem Biophys 2006: 44(1), 157-169

22.van Horssen R, Rens JA, Brunstein F, Guns V, van Gils M, ten Hagen TL et al. Intratumoural Expression of TNF-R1 and EMAP-II in Relation to Response of Patients Treated With TNF-Based Isolated Limb Perfusion. Int J Cancer 2006: 119(6), 1481-1490Additional information

Chapter 13

Summary/Samenvatting

Additional information

Summary / Samenvatting

SUMMARY

In this thesis a third strategy in tumor vessel targeted anticancer therapy is investigated. This provascular approach, which we have called "tumor vessel abnormalization", enhances the already abnormal features of the tumor-associated vasculature and further improves the permeability of these vessels. This results in an increased extravasation of cytotoxic agents from the blood circulation into the tumor tissue ultimately leading to improved tumor response. This is rather a counterintuitive approach as the other two concepts; antiangiogenesis and vascular destruction are antivascular strategies in which tumor vessel formation is respectively prohibited or destroyed.

In **chapter 1** an introduction on the tumor-associated vasculature and previous results is given.

In **chapter 2** we investigate the efficacy of the systemic treatment with free doxorubicin or liposomal encapsulated doxorubicin (Doxil) in osteosarcoma-bearing rats, and the effect of tumor necrosis factor-alpha (TNF) on this approach. We observed an improved antitumor effect when using Doxil compared to doxorubicin, correlating with a higher intratumoral drug concentration. Addition of TNF further increased the tumor response to Doxil although no further increase in intratumoral concentration was measured. We also observed that this osteosarcoom was less vascularized compared to the previous investigated soft tissue sarcoma (BN175) in which TNF does increase intratumoral drug concentration. However, the intratumoral concentration of Doxil, without the addition of TNF, was 4-times higher in the ROS-1 osteosarcoma compared to BN175 indicating that these vessels are already quite permeable or become permeable earlier in the treatment. Compared to the BN175, ROS-1 is 10-times less sensitive to Doxil. However, in contradiction to BN175, TNF has a direct toxic effect on the ROS-1. From this we conclude that TNF affects the tumor cells directly and due to presence of already permeable vessels massive extravazation of Doxil occurs.

Chapter 3 describes the efficacy of the integrin inhibitor Cilengitide in the melphalan-based isolated limb perfusion (ILP) in soft tissue sarcoma-bearing rats. The results show that addition of Cilengitide improved the antitumoral activity of melphalan accompanied with an augmented intratumoral concentration. These results also corroborate a critical role of the integrins αVβ3 and αVβ5 for the integrity and survival of angiogenic tumor vessels. *In vitro* we observed that Cilengitide prevents cell adhesion and promotes detachment of endothelial cells. *In vivo* no damage of the endothelial cells was observed after treatment with Cilengitide alone, most likely due to the short exposure time. However, in contradiction to TNF, Cilengitide renders the tumor cells, as well as the endothelial cells, more sensitive to melphalan, which may very well explain the observed antitumor response. From this data we conclude that when using the integrin inhibitor Cilengitide, endothelial cells become more sensitive to melphalan leading to apoptosis of the endothelial cells. This results in an increased melphalan accumulation and erythrocytes extravasation in the tumor microenvironment, leading to tumor necrosis and hemorrhage.

As becomes clear from the data presented in **chapter 4,** TNF as a single agent has little effect on endothelial cells *in vitro*. Only when TNF is combined with interferon-gamma we observed significant structural changes in the endothelial layer, which were further enhanced by the addition of peripheral blood mononuclear cells (PBMC). Additionally, we found that TNF-primed PBMC produce endogenous interleukin-1beta (IL-1ß), which is at least partly responsible for the observed effect. These changes in monolayer morphology, such as cell elongation and gap forma-

tion, changed the dense cobblestone-like endothelial monolayer into a more fibroblast-like phenotype accountable for the observed permeability increase of the endothelial layer. Translating this to the *in vivo* situation, we speculate that although there is a rapid damage to the endothelial cells when using TNF in the ILP, these damages are not a result of a direct cytotoxic effect of TNF on the endothelial cells and a interaction with other, locally produced factors is required.

Chapter 5 addresses the role of matrix metalloproteinases (MMPs) in cell detachment and gap formation of endothelial cells. We investigated the production of MMPs after TNF-stimulation of PBMC and endothelial cells. It seemed that the production of MMP-9 is in part responsible for the induced morphological changes and increased permeability. Also in these experiments we observed that endogenously produced IL-1ß is accountable for these changes in cell to matrix contact. Again a rather counterintuitive approach as elevated levels of MMPs are often correlated with tumor aggressiveness and bad prognosis. From these experiments we conclude that the production of MMPs is required to induce changes in the endothelial lining that lead to increased permeability and extravasation of the chemotherapeutic drug.

Besides the effect on cell to matrix degradation, the effect of TNF-primed PBMC on endothelial cells was also investigated on the cell to cell adhesion in **chapter 6**. We looked primarily at VE-cadherin, the transmembrane protein of the adherens junctions. Using immunohistology staining, western blotting and PCR we found that increased permeability and morphological changes in the endothelial cells are rather accompanied with degradation of VE-cadherin at the cell membrane, while the overall expression is not changed.

In **chapter 7** we demonstrate the TNF effect on the tumor microenvironment directly after ILP and conclude that TNF rapidly damages the tumor endothelial lining. This damage turns the vessels more permeable for small molecules like melphalan but also for erythrocytes, inducing hemorrhage. Erythrocytes have been reported as carriers for melphalan and may account for the increased drug delivery in the tumor. No tumor response was observed in animals treated with TNF alone, indicating that a chemotherapeutic drug is mandatory to obtain a tumor response. We also measured no change in interstitial fluid pressure during the procedure. In addition, early in the treatment we observed no change in gene profile in the set of cytokines we have tested. However, as the immune profile was measured in the complete tumor, this is still open for debate. Most likely the expression profiles of the individual cells in the tumor microenvironment rather than the overall levels may be responsible for the immune response. Nevertheless, based on the results mentioned in this chapter we conclude that TNF in the ILP-setting has no effect on the interstitial fluid pressure and the augmented melphalan accumulation is most likely the result of an increased permeability of the tumor vasculature.

More detailed information about the TNF effect on the vasculature is given in **chapter 8** using the systemic approach instead of the locoregional treatment. In accordance with previous experiments, we found increased intratumoral drug concentration in tumors treated systemically with low-dose TNF in combination with a conventional chemotherapy, in this case liposomal encapsulated doxorubicin (Doxil). Using the dorsal skin-fold chamber we observed that liposomes present in the tumors were primarily located in the vessels. However, in combination with TNF a more homogenous intratumoral distribution was accomplished and Doxil extravasated out of the vessels into the tumor tissue. With this technique, we studied the intracellular location of Doxil. To our knowledge for the first time, it was observed *in vivo* that liposomes are completely taken up by a cell and are broken down in the cytoplasm. These results indicate that TNF, in a non-toxic dose, renders the tumor vessels more permeable contributing to a better extravasation of Doxil resulting in an improved tumor response.

The efficiency of TNF in this setting is further elucidated in **chapter 9.** Four tumors types, with different vessel characteristics, were investigated regarding their sensitivity towards TNF in combination with Doxil. We found that in tumors with large vessels the addition of TNF increased the

tumor response compared to the treatment with Doxil alone. However, in tumors with small vessels addition of TNF to Doxil had no effect on tumor growth. More detailed investigation revealed that the receptor for TNF (TNFR1) was not located on the tumor-associated endothelial cells but on the pericytes and these TNFR1 expressing pericytes were present in a higher degree in the TNF-responding tumors. From this study we conclude that high coverage of tumor vessels with TNFR1-expressing pericytes correlates with responsiveness to TNF. This is a first indication that pericytes and not endothelial cells may be the primary target of TNF. Our results imply that benefit of TNF could be predicted by the presence of pericytes in the tumor vasculature.

SAMENVATTING

In deze thesis wordt een derde strategie onderzocht op het gebied van kankertherapie, die zich richt op de tumorvasculatuur. In een tumor hebben de bloedvaten reeds abnormale eigenschappen die zich over het algemeen niet bevinden in bloedvaten van andere organen. Door de "abnormalisatie"-methode toe te passen worden deze kenmerken versterkt. Bij deze methode neemt voornamelijk de doorlaatbaarheid van de vaten toe. Dit resulteert in een verhoogde uittreding van een chemotherapeuticum vanuit de bloedstroom in het tumorweefsel en resulteert uiteindelijk in een verbeterde tumorrespons.

Deze provasculaire benadering is controversieel vergeleken met de twee andere vasculaire strategieën. Deze behandelwijzen; de antiangiogene en vasculair destructieve strategieën zijn antivasculaire methodes waarbij de vorming van nieuwe tumorbloedvaten wordt voorkomen of waarbij de reeds bestaande bloedvaten worden vernietigd.

In **hoofdstuk 1** wordt een introductie gegeven over het tumorvaatbed en de resultaten voorafgaande aan deze thesis.

In **hoofdstuk 2** wordt onderzoek beschreven naar de werkzaamheid van een systemische behandeling met vrij doxorubicine of liposomaal doxorubicine (Doxil) in combinatie met tumor necrosis factor-alpha (TNF) in ratten met een osteosarcoom, de ROS-1 tumor. We zien een beter antitumor effect met Doxil dan met doxorubicine en dit correleert met de mate van aanwezigheid van het chemotherapeuticum in het tumorweefsel. Er wordt meer Doxil in de tumor gevonden dan doxorubicine. Door het chemotherapeuticum te combineren met TNF wordt een nog betere tumorrespons verkregen. We merkten echter ook op dat TNF niet bijdraagt aan een verhoogde concentratie van Doxil of doxorubicine in de tumor. De ROS-1 heeft minder vaten vergeleken met een andere tumor, het weke delen sarcoom BN175, die we in eerdere experimenten uitvoerig hebben bestudeerd. In de BN175 zorgt TNF namelijk wel voor een verhoogde concentratie van Doxil in de tumor. De tumorconcentratie van Doxil is echter in de ROS-1 viermaal hoger dan in de BN175. Dit impliceert mogelijk dat de bloedvaten in de ROS-1 reeds een verhoogde doorlaatbaarheid hebben. Het is ook denkbaar dat de verhoogde doorlaatbaarheid bij de ROS-1 vroeger in de behandeling ontstaat. Vergeleken met BN175 zijn ROS-1 tumorcellen tienmaal minder gevoelig voor Doxil maar zijn wel gevoelig voor TNF, terwijl de BN175 tumorcellen dat niet zijn. Uit de resultaten concluderen wij dat TNF een direct toxisch effect op deze tumor heeft. Daarnaast komt, door de reeds aanwezige doorlaatbaarheid van de bloedvaten, een grote concentratie van het Doxil in de tumor terecht. Deze factoren dragen daardoor bij aan de goede tumorrespons wanneer Doxil in combinatie met TNF wordt toegediend.

Hoofdstuk 3 beschrijft de werking van de integrine inhibitor Cilengitide in een geïsoleerde ledemaat perfusie (ILP) in ratten met een weke delen sarcoom. De resultaten laten zien dat Cilengitide de werking van het chemotherapeuticum melphalan versterkt. Ook in deze setting is een verhoogde concentratie van melphalan in de tumor waar te nemen. Deze resultaten bevestigen eveneens de belangrijke rol van de integrines, $\alpha V\beta 3$ en $\alpha V\beta 5$, in de integriteit en overleving van

tumorvaten. *In vitro* observaties toonden aan dat Cilengitide de aanhechting van cellen verhindert en daarnaast het loslaten van cellen bevordert. *In vivo* werd geen beschadiging van endotheelcellen waargenomen wat hoogst waarschijnlijk te wijten is aan de korte blootstelling van de cellen aan Cilengitide. Echter, in tegenstelling tot TNF worden tumor- en endotheelcellen die zijn blootgesteld aan Cilengitide gevoeliger voor melphalan. Vermoedelijk is dit een belangrijke verklaring voor de waargenomen verbeterde tumorrespons. Uit deze data kunnen we concluderen dat door het gebruik van de inhibitor Cilengitide endotheelcellen gevoeliger worden voor melphalan, wat leidt tot apoptose van deze cellen. Vervolgens resulteert dit in een verhoogde melphalan accumulatie en extravasatie van rode bloedcellen in het tumorweefsel. Deze uittreding is verantwoordelijk voor tumornecrose en bloedingen en levert uiteindelijk een goede tumorrespons op.

De data verkregen in **hoofdstuk 4** maakt duidelijk dat TNF als een alleenstaande behandeling weinig effect heeft op endotheelcellen *in vitro*. Significante structurele veranderingen in de endotheellaag werden waargenomen wanneer de cellen aan TNF in combinatie met interferon- gamma (IFN) worden blootgesteld. Deze veranderingen werden nog sterker door verdere toevoeging van mononucleaire bloedcellen (PBMC). Eveneens vonden we dat TNF-behandelde PBMC endogeen interleukine-1beta (IL-1ß) produceren, dat gedeeltelijk verantwoordelijk is voor de veranderingen in de endotheellaag. Deze morfologische veranderingen, zoals celverlenging en het ontstaan van gaten, geven de hechte kobbelsteenachtige laag cellen een meer fibroblastachtig uiterlijk en zijn verantwoordelijk voor de verhoogde doorlaatbaarheid van de cellaag. Aan de hand van deze resultaten speculeren we dat de schade aan de endotheelcellen, die wordt waargenomen in de ILP, niet rechtstreeks door TNF worden veroorzaakt, maar met name door IFN en IL-1ß en dat de interactie met andere endogeen geproduceerde elementen een belangrijke rol spelen.

Hoofdstuk 5 behandelt de rol van matrix metalloproteinases (MMP's) bij de aanhechting van endotheelcellen en het ontstaan van gaten in de endotheellaag. We onderzochten de aanmaak van MMP's na TNF stimulatie van PBMC en endotheelcellen. Het lijkt erop dat de productie van MMP-9 gedeeltelijk verantwoordelijk is voor de morfologische veranderingen en de toegenomen doorlaatbaarheid van de endotheelcellen. In deze experimenten werd ook waargenomen dat endogeen IL-1ß belangrijk is voor de veranderingen in de aanhechting van cellen aan de onderliggende matrix. Dit is opnieuw een controversiële bevinding aangezien verhoogde MMP waarden worden gecorreleerd met agressiviteit van de tumor en een slechte prognose. Uit deze experimenten concluderen wij dat de MMP productie verantwoordelijk is voor de veranderingen in de endotheellaag, wat vervolgens voor een betere doorlaatbaarheid en extravasatie van het chemotherapeuticum zorgt

Naast cel-matrix contact wordt in **hoofdstuk 6** ook gekeken naar het effect van TNF-gestimuleerde PBMC op de aanhechting van endotheelcellen onderling. Dit onderzoek focust zich voornamelijk op VE-cadherine, het transmembraan eiwit van de adherens junctions. Door gebruik te maken van technieken als immunohistologie, western blot en PCR vonden we dat de toegenomen doorlaatbaarheid en morfologische veranderingen in de endotheellaag samengaan met de afbraak van VE-cadherine aan het celmembraan en niet te wijten is aan een verminderde aanmaak.

In **hoofdstuk 7** wordt het effect van TNF in de tumor na het uitvoeren van de ILP besproken. Na de perfusie is al meteen een flinke schade aan de tumor vasculatuur waar te nemen. Door deze beschadigingen wordt de doorlaatbaarheid van de bloedvaten verhoogd voor zowel kleine moleculen als melphalan. We zagen ook een toename in extravasatie van rode bloedcellen die bloedingen in het tumorweefsel veroorzaken. Uit eerder onderzoek is gebleken dat rode bloedcellen melphalan kunnen opnemen en dit fenomeen zal zeker bijdragen aan de verhoogde melphalan concentratie in de tumor. Bij dieren die enkel met TNF behandeld zijn werd geen betere tumorrespons waargenomen wat impliceert dat een chemotherapeuticum noodzakelijk is voor een goede respons. Er werd ook geen verandering in de intersitiële drug gemeten tijdens de ILP.

Bovendien zagen we geen veranderingen in het genetische profiel van een aantal geteste cytokinen in de tumor, alhoewel dit nog steeds ter discussie staat aangezien dit werd gemeten in de volledige tumor. Hoogstwaarschijnlijk is het expressiepatroon van de individuele cel en niet die van de volledige tumor belangrijker in een immuunreactie. Desondanks kunnen we concluderen dan TNF in de ILP geen effect heeft op de interstitiële druk en dat de verhoogde melphalan accumulatie in de tumor een resultaat is van een toegenomen doorlaatbaarheid van de tumorvasculatuur.

Meer gedetailleerde informatie over het TNF-effect op de bloedvaten wordt gegeven in **hoofdstuk 8** waar we gebruik maken van een systemische behandeling. In samenspraak met de voorgaande resultaten vonden we hier ook toegenomen concentraties van het chemotherapeuticum in tumoren van dieren die systemisch behandeld zijn met een lage dosis TNF in combinatie met Doxil. Door gebruik te maken van het huidflapmodel kunnen we zien dat de liposomen hoofdzakelijk in de bloedvaten te vinden zijn wanneer geen TNF werd gegeven. Door Doxil echter te combineren met TNF ontstaat een homogenere verspreiding van de liposomen in de tumor en treedt ook meer Doxil uit de bloedvaten in het omliggende tumorweefsel. Met deze techniek kunnen we ook de intracellulaire aanwezigheid van Doxil bestuderen in een *in vivo* situatie. Naar onze mening werd hier voor het eerst aangetoond dat liposomen volledig door een tumorcel worden opgenomen en in het cytoplasma worden afgebroken. De resultaten in dit hoofdstuk wijzen er op dat een lage niet-toxische dosis TNF zorgt voor een verhoogde doorlaatbaarheid van de bloedvaten dat bijdraagt aan een betere uittreding van Doxil naar het omliggende weefsel en uiteindelijk resulteert in een verbeterde tumorrespons.

De efficiëntie van TNF is verder bestudeerd in **hoofdstuk 9**. Vier tumortypes met verschillende vasculaire eigenschappen werden onderzocht op hun gevoeligheid voor TNF in combinatie met Doxil. We vonden dat in tumoren met grote vaten de toevoeging van TNF bijdraagt aan een verhoogde tumorrespons vergeleken met de respons op enkel Doxil. Dit in tegenstelling tot de tumoren met kleine vaten waar TNF geen effect op de repons heeft. Uit meer gedetailleerd onderzoek blijkt dat de receptor voor TNF (TNFR1) niet op de tumor endotheelcellen zit maar op de pericyten. Ook blijkt dat deze TNFR1 tot expressie brengende pericyten in grotere aantallen aanwezig zijn in de tumoren die reageren op TNF. Uit deze studie concluderen we dat de aanwezigheid van deze pericyten correleert met de gevoeligheid van de tumor voor TNF. Voor het eerst werd waargenomen dat TNF werkt op de tumor geassocieerde pericyten en niet per se op de endotheelcellen. Deze resultaten houden in dat de TNF-respons kan worden voorspeld aan de hand van de aanwezigheid van pericyten in de tumor vasculatuur.

Addendum

List of publications/award

About the author

Statement of appreciation

Addendum

List of publications/Award

LIST OF PUBLCATIONS

1.Verseijden F, Jahr H, Posthumus-van Sluijs SJ, ten Hagen TL, Hovius SE, Seynhaeve AL, van Neck JW, van Osch GJ, and Hofer SO. Angiogenic Capacity of Human Adipose-Derived Stromal Cells during Adipogenic Differentiation: An In Vitro Study.Tissue Eng Part A 2008: Jul 24 Epub ahead of print

2.ten Hagen TL, Seynhaeve AL, and Eggermont AM. TNF-mediated interactions between inflammatory response and tumor vascular bed. Immunol. Reviews 2008: 222, 299-315

3.Seynhaeve AL, Eggermont AM, and ten Hagen TL. TNF and Manipulation of the Tumor Cell-Stromal Interface: "Ways to Make Chemotherapy Effective". Front Biosci 2008: 13(1), 3034-3045

4.Seynhaeve AL, Hoving S, Schipper D, Vermeulen CE, aan de Wiel-Ambagtsheer G, van Tiel ST, Eggermont AM, and ten Hagen TL. Tumor Necrosis Factor {Alpha} Mediates Homogeneous Distribution of Liposomes in Murine Melanoma That Contributes to a Better Tumor Response. Cancer Res 2007: 67(19), 9455-9462

5.Alagappan VK, Willems-Widyastuti A, Seynhaeve AL, Garrelds IM, ten Hagen TL, Saxena PR, and Sharma HS. Vasoactive Peptides Upregulate MRNA Expression and Secretion of Vascular Endothelial Growth Factor in Human Airway Smooth Muscle Cells. Cell Biochem Biophys 2007: 47(1), 109-118

6.Hoving S, Seynhaeve AL, van Tiel ST, aan de Wiel-Ambagtsheer G, de Bruijn EA, Eggermont AM, and ten Hagen TL. Early Destruction of Tumor Vasculature in Tumor Necrosis Factor-Alpha-Based Isolated Limb Perfusion Is Responsible for Tumor Response. Anticancer Drugs 2006: 17(8), 949-959

7.Seynhaeve AL, Vermeulen CE, Eggermont AM, and ten Hagen TL. Cytokines and Vascular Permeability: an *in Vitro* Study on Human Endothelial Cells in Relation to Tumor Necrosis Factor-Alpha-Primed Peripheral Blood Mononuclear Cells. Cell Biochem Biophys 2006: 44(1), 157-169

8.Hoving S, Seynhaeve AL, van Tiel ST, Eggermont AM, and ten Hagen TL. Addition of Low-Dose Tumor Necrosis Factor-Alpha to Systemic Treatment With STEALTH Liposomal Doxorubicin (Doxil) Improved Anti-Tumor Activity in Osteosarcoma-Bearing Rats. Anticancer Drugs 2005: 16(6), 667-674

9.Brunstein F, Hoving S, Seynhaeve AL, van Tiel ST, Guetens G, de Bruijn EA, Eggermont AM, and ten Hagen TL. Synergistic Antitumor Activity of Histamine Plus Melphalan in Isolated Limb Perfusion: Preclinical Studies. J Natl Cancer Inst 2004: 96(21), 1603-1610

10.Brouckaert P, Takahashi N, van Tiel ST, Hostens J, Eggermont AM, Seynhaeve AL, Fiers W, and ten Hagen TL. Tumor Necrosis Factor-Alpha Augmented Tumor Response in B16BL6 Melanoma-Bearing Mice Treated With Stealth Liposomal Doxorubicin (Doxil) Correlates With Altered Doxil Pharmacokinetics. Int J Cancer 2004: 109(3), 442-448

11.Kim DW, Andres ML, Miller GM, Cao JD, Green LM, Seynhaeve AL, ten Hagen TL, and Gridley DS. Immunohistological Analysis of Immune Cell Infiltration of a Human Colon Tumor Xenograft After Treatment With Stealth(R) Liposome-Encapsulated Tumor Necrosis Factor-Alpha and Radiation. Int J Oncol 2002: 21(5), 973-979

12.van der Veen AH, ten Hagen TL, Seynhaeve AL, and Eggermont AM. Lack of Cell-Cycle Specific Effects of Tumor Necrosis Factor-Alpha on Tumor Cells *in Vitro*: Implications for Combination Tumor Therapy With Doxorubicin. Cancer invest 2002: 20(4), 499-508

13.Kim DW, Andres ML, Kajioka EH, Dutta-Roy R, Miller GM, Seynhaeve AL, ten Hagen TL, and Gridley DS. Modulation of Innate Immunological Factors by STEALTH Liposome-Encapsulated Tumor Necrosis Factor-Alpha in a Colon Tumor Xenograft Model. Anticancer Res 2002: 22(2A), 777-788

14.Seynhaeve AL, de Wilt JH, van Tiel ST, Eggermont AM, and ten Hagen TL. Isolated Limb Perfusion With ActinomycinD and TNF-Alpha Results in Improved Tumour Response in Soft-Tissue Sarcoma-Bearing Rats but Is Accompanied by Severe Local Toxicity. Br J Cancer 2002: 86(7), 1174-1179

15.ten Hagen TL, Seynhaeve AL, van Tiel ST, Ruiter DJ, and Eggermont AM. Pegylated Liposomal Tumor Necrosis Factor-Alpha Results in Reduced Toxicity and Synergistic Antitumor Activity After Systemic Administration in Combination With Liposomal Doxorubicin (Doxil) in Soft Tissue Sarcoma-Bearing Rats. Int J Cancer 2002: 97(1), 115-120

16.Kim DW, Andres ML, Li J, Kajioka EH, Miller GM, Seynhaeve AL, ten Hagen TL, and Gridley DS. Liposome-Encapsulated Tumor Necrosis Factor-Alpha Enhances the Effects of Radiation Against Human Colon Tumor Xenografts. J Interferon Cytokine Res 2001: 21(11), 885-897
17.de Wilt JH, Manusama ER, van Etten B, van Tiel ST, Jorna AS, Seynhaeve AL, ten Hagen TL, and Eggermont AM. Nitric Oxide Synthase Inhibition Results in Synergistic Anti-Tumour Activity With Melphalan and Tumour Necrosis Factor Alpha-Based Isolated Limb Perfusions. Br J Cancer 2000: 83(9), 1176-1182
18.ten Hagen TL, van der Veen AH, Nooijen PT, van Tiel ST, Seynhaeve AL, and Eggermont AM. Low-Dose Tumor Necrosis Factor-Alpha Augments Antitumor Activity of Stealth Liposomal Doxorubicin (DOXIL) in Soft Tissue Sarcoma-Bearing Rats. Int J Cancer 2000: 87(6), 829-837
19.de Wilt JH, Soma G, ten Hagen TL, Kanou J, Takagi K, Nooijen PT, Seynhaeve AL, and Eggermont AM. Synergistic Antitumour Effect of TNF-SAM2 With Melphalan and Doxorubicin in Isolated Limb Perfusion in Rats. Anticancer Res 2000: 20(5B), 3491-3496
20.van der Veen AH, de Wilt JH, Eggermont AM, van Tiel ST, Seynhaeve AL, and ten Hagen TL. TNF-Alpha Augments Intratumoural Concentrations of Doxorubicin in TNF-Alpha-Based Isolated Limb Perfusion in Rat Sarcoma Models and Enhances Anti-Tumour Effects. Br J Cancer 2000: 82(4), 973-980
21.van der Veen AH, Seynhaeve AL, Bruers J, Nooijen PT, Marquet RL, and Eggermont AM. In Vivo Isolated Kidney Perfusion With Tumour Necrosis Factor Alpha (TNF-Alpha) in Tumour-Bearing Rats. Br J Cancer 1999: 79(3-4), 433-439
22.van der Veen AH, Eggermont AM, Seynhaeve AL, van Tiel ST, and ten Hagen TL. Biodistribution and Tumor Localization of Stealth Liposomal Tumor Necrosis Factor-Alpha in Soft Tissue Sarcoma Bearing Rats. Int J Cancer 1998: 77(6), 901-906

SCIENTIFIC AWARD

"The Young Investigator Award Gold Prize" at the 11th Liposomal Research Days Conference, Japan 2008.

Addendum

About the author

Born on: January 15, 1973

1979 Childhood

At a young age, Ann was interested in science and was always keen to discover and explore new things. When she was seven years old, she received her first scientific book, "Sterren en planeten" (Stars and Planets). After moving from the city of Kortrijk to the countryside, she had plenty of space to discover new things

1986 Junior high school, Saint Theresia Institute

At high school Ann met her nemesis; "mathematics". Even though she was an excellent student in biology, chemistry and physics, educators forced her to lower her standards which prevented her from realizing her potential as a university graduate.

At the age of eighteen she received her high school diploma in industrial chemistry. Because she felt she was too young to start the rest of her life in this line of work, which provided her with no intellectual challenge, she searched for something new. Encouraged by her parents and some devoted teachers, Ann packed her bags and went to college in Brugge, in September of 1991.

1991 Institute for Higher Education, Simon Stevin

In college, Ann developed into a reliable and hard working student. She loved the educational program that was provided by the dedicated teachers. However, during her internship at the Hospital in Brugge, she discovered two interesting things: First, her difficulties with math proved to be a general problem in the recognition of numbers. Second, the mundane act of putting blood tubes into a machine and arranging tissues left her less than enthusiastic. Ann was excited to hear from a former student who informed her about additional training that was being offered in The Netherlands. After obtaining her degree in clinical chemistry, she packed her bags for The Netherlands.

1995 Polytechnical Institute, West Brabant

The training consisted of four and a half months at College West-Brabant which was located in Etten-leur and a four and a half month internship. Accustomed to living in the lively Brugge, the calm village of Etten-Leur and the Dutch mentality proved to be an interesting change in mindset.

1996 Eramus MC, Internship

After passing the exams, she moved to the second biggest town of The Netherlands. In Rotterdam she began her internship at the surgery department. In those days the lab was located in the parking lot of the Erasmus building and despite the deprivation of sunlight, she loved the challenge that this kind of work had to offer.

1996 Technician

After her graduation and receiving a Dutch diploma in biochemistry, she was offered a technician position at the department were she helped several medical doctors getting their PhD degrees. During that time, the lab became the LECO and relocated to the first floor of the Erasmus Building where the department grew further in expertise and employees.

2001 Started the PhD program.

After several years of working at the LECO Ann was seriously thinking of pursuing the university education she originally planned so many years before. However, the head of LECO, Dr. Timo ten Hagen, offered her the opportunity to start the PhD program in her department and she gratefully accepted.

2008 Present

Research work is never finished, but it is simply time to cut the cord and bundle the work into a thesis. Devoted to her work, Ann found that the pros out weighed the cons. Therefore, be assured that she will continue this promising work.

Addendum

Statement of appreciation

Het is bijna 13 jaar geleden dat ik vanuit Vlaanderen naar Nederland verhuisde en in de kelder van de hoogbouw terechtkwam. Naïef als ik was verwachte ik een gelijksoortige cultuur zoals ik die in België had ervaren. Groot was mijn verbazing dat men elkaar met de voornaam aansprak, iets wat in een Belgische ziekenhuis absoluut geen sprake van kon zijn. Aangezien we beiden Nederlands spreken had ik ook geen taalproblemen verwacht maar kwam bedrogen uit. De verschillen in taal zorgen (zelfs nu nog) voor hilarische momenten. Sjanse is in Vlaanderen gewoon geluk hebben, een uurwerk is een Vlaams horloge, in Vlaanderen leeft men in de voormiddag (vernoene) in een andere tijdzone, namelijk 's ochtends, wijsheidstanden zijn Vlaamse verstandskiezen, een tas is een Vlaamse mok en wanneer men met me afspreekt om tien over halfzeven kan men beter een afspraak met me maken om zes uur veertig. Kaassoufflés, vlammetjes, bitterballen, drop, hagelslag, gevulde koeken, stroopwafels, boerenkoolstamppot met een unox rookworst, heerlijk… Zelfs de buitenlandse keuken vind ik geweldig. Toen ik de eerste keer roti at in de Warum Mini was ik meteen verkocht. Wat ik niet over mijn Vlaamse hart kan krijgen is eten uit de muur. Het spijt me vreselijk, jongens. Oja en een broodje kroket, bah… Ik hou van Rotterdam. Mijn jeugd heb ik doorgebracht in een klein dorp waar iedereen elkaar kent. Toen ik een tiener werd had dit dorp me niets meer te bieden en ben ik in Brugge gaan studeren en wonen. De stap naar Rotterdam was de volgende. En ik was dolgelukkig me te kunnen verliezen in de anonimiteit van deze geweldige dynamische stad. Het is nooit saai in Rotterdam. Ik ben blij deze stap te hebben gezet en durf er niet aan te denken hoe mijn leven er nu zou hebben uitgezien indien ik dit niet had gedaan. IK HEB HIER GOEDE VRIENDEN, GEZELLIGE COLLEGA'S EN PRACHTIG WERK. AL WAT MIJ REST IS DEZE MENSEN TE BEDANKEN.

DANK!

Ha, jullie dachten toch niet dat het daarbij bleef.

Timo, de altijd aanwezige.

In 1995 kwam ik het lab binnen als nog niet eens afgestudeerd, bescheiden meisje en ik ben nooit meer weg gegaan. Nu ga ik nog eens afstuderen, de bescheidenheid is behoorlijk verdwenen maar ik ben niet weg te slaan. In die tijd is het lab gegroeid van 4 mensen tot wat het nu is en is nog steeds volop in ontwikkeling. Met recht een prestatie om trots op te zijn en ik ben blij het volledige proces te hebben meegemaakt. Omdat je me de kans hebt gegeven dit promotie traject te starten toen ik daar klaar voor was, ligt dit boekje er. Het project heeft iets langer geduurd dan bij "normale" promovendi maar ik had veel te leren. En ik zal nog veel moeten leren en ik ben blij dat je er bent om de schade te beperken. Dank voor al je steun en je toewijding.

Mijn promotor, Lex, de vliegeraar.

Als een orkaan reis je de wereld rond en bent daarom weinig op het werk aanwezig. Echter dat rondreizen werpt zijn vruchten af in het opzetten van klinische trials, financiering en verder onderzoek. Het feit dat je iedere keer weer met ons onderzoek kan meepraten als je er bent bewijst je betrokkenheid tot dit werk. Dank je hartelijk voor de mogelijkheid om bij jou te promoveren.

The developers

Kirsten, thank you for the massive amount of TNF. Without this, this research would have been financially impossible. Simon for the Cilengitide and the paper as a result of our collaboration.

Mijn commissieleden

Prof.dr.ir. de Jong, Prof.dr. Storm en Prof.dr. Looijenga, dank u. Marion voor het verbeteren van een flink aantal spelfouten. Voor mij geen tien voor taal. Beste Gert. Helaas kan je niet achter de tafel tijdens mijn verdediging zitten maar ik zal met plezier terugdenken aan het liposomen congres in Japan. Hopelijk volgen er nog van dat soort uitstapjes. Ook dank aan de leden van de grote commissie, Prof.dr. Löwik, Dr Sleijfer en Prof.dr. Brouckaert. Beste Peter, voor jou bewaren we met veel plezier een plek aan de commissietafel.

Mijn collega's, mijn analisten, ~~Mijn werknemers~~, mijn helpers, mijn uitvoerders *zodat ik lekker achter de computer kan gaan zitten en regelmatig kan gaan netwerken (lees: koffie drinken). Gisela, Dieuwertje, Debby, Thomas, Joost, Cindy.* ***Dank****, meer kan ik niet zeggen.* ***Dank*** *voor het werk dat jullie voor mij, maar ook voor anderen, uitvoeren.* ***Dank*** *voor het accepteren van mijn grillig bipolar karakter. Ik beloof hierbij plechtig jullie te zullen steunen bij moeilijkheden tot het beste van mijn capaciteit.* ***Dank*** *aan degene die er niet meer zijn; Sjoerd, Herma en, tevens een van mijn paranimf omdat ik dit jaren geleden had belooft, Sandra. Hierbij wil ook Kim* ***bedanken****, de PA van het lab, omdat zij nu alle administratie in het lab doet waardoor er voor ons meer tijd is vrijgekomen om te doen wat onderzoekers horen te doen; onderzoeken.*

De exen.

Tja dat zijn er ook zoveel. Mijn toenmalige nu reeds gepromoveerde mede AIO's, Remco, Saske, Flavia. Het waren leuke tijden toen we op een veel te klein kamertje zaten. Maar we mogen met recht allen zeggen dat we mooi werk hebben afgeleverd ondanks dat het pericyten paper nog steeds niet is gepubliceerd. Maar ook Eric Manusama, Alex van der Veen, Hans de Wilt, Marc van Ijken, Mark de Vries, Boudewijn, Titia, en Lucy.

Andere exen zijn de vele studenten en stagiaires die ik in de loop der jaren heb voorbij zien komen waarvan ik met velen nog steeds contact heb. Om er een aantal te noemen, Peter, Sanja, Sangeeta, Paul, Joyce, Tom, Yvette,... Dank voor jullie werk. Ze worden ook steeds jonger maar helaas lijkt dat maar zo. Ik ben degene die ouder wordt.

De huidige promovendi en de nieuwe lichting.

STEFAN, MARNA, JILL. JULLIE HEBBEN GENEESKUNDE GESTUDEERD EN HET LEF GEHAD OM DIT ONDERZOEK IN TE STAPPEN. MOGEN JULLIE DEZE PERIODE AFSLUITEN MET MOOIE PUBLICATIES EN JULLIE VERDER ONTWIKKELEN TOT GOEDE CHIRURGEN. DANK VOOR DE GESPREKKEN, ZOWEL WERK ALS PRIVÉ, HET LUISTEREN NAAR FRUSTRATIES EN DE GEZELLIGE BORRELS.

TO MY NEW COLLEAGUES, ASHA, LYLY AND BILYANA, I WOULD LIKE TO SAY. 'IT WAS THE BEST OF TIME, IT WAS THE WORST OF TIME'. ENJOY THE GOOD STUFF, LEARN FROM MISTAKES AND DON'T LET THE BAD THINGS GET YOU DOWN.

AND, LARS OUR LATEST ADDITION FROM GERMANY; AS AN ALREADY EXPERIENCED POSTDOC YOU KNOW THE UPS AND DOWNS OF RESEARCH. MAKE US PROUD.

The others. This research has also been done in collaboration with other groups. Ik wil vooral Prof.dr. Brouckaert bedanken voor het wederzijdse contact. Prof.dr. De Bruijn voor het uitvoeren van de melphalan bepalingen. Het duurt soms een tijd voor u wat van ons hoort maar we komen altijd terug. And also thanks to Prof.dr. Curzio Ruegg for the possibility to stay in your lab and your contribution especially in the Cilengitide paper.

Mijn familie.

Ik wil vooral mijn ouders bedanken voor hun steun toen ik mijn eerste jaar hoger onderwijs niet haalde. Door hen ben ik niet bij de pakken blijven zitten en dat jaar overgedaan op een andere school waar ik een hele leuke tijd heb gehad. Stiekem had mijn moeder gehoopt dat ik Nederland uit mijn hoofd zou zetten maar helaas. Nu vinden ze Rotterdam geweldig en er is altijd wel een reden (de winkels) om hierheen te komen. Aan mijn twee zusjes zou ik willen zeggen. Ga er voor...En merci aan mijn oma, al snapt ze niets van wat ik aan het doen ben.

Docenten maken het verschil. Tevens wil ik de docenten, Nicole Kellner en Luc Parmentier van de Hogeschool Simon Stevin te Brugge bedanken. Zij hebben me na een zware tijd mijn plezier en leergierigheid opnieuw aangewakkerd.

Vrienden,

Sandra, voor je jarenlange vriendschap, de uitjes, vakanties, of gewoon geklets. Will en Henk, dank u voor alle uitnodigingen voor feestjes en "zomaar" etentjes. Sjaak en Anky. Jullie energie en levenslust is een inspiratie. Dank dat ik jullie altijd kan inschakelen als er iets te beleven valt en jullie kan "lenen" om me ergens heen te brengen. Frans en Dirk. Mijn gesprekken met jullie hebben vaak een filosofisch kantje en zijn altijd heel prettig. Natasja, Sandra en Lieven, naast mijn familie, de reden om nog eens de Vlaamse kant op te gaan. Hopelijk krijg ik nu meer tijd om wat vaker langs te komen. Vera, voor de gesprekken aan de telefoon.

Is dat alles? Ik moet maar eens wat meer vrienden gaan maken.

Color Section

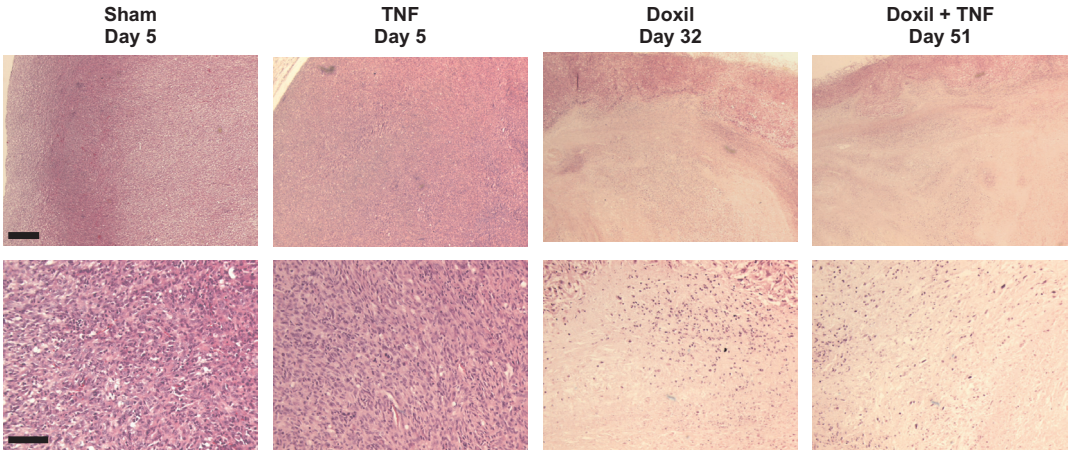

Figure 2. Massive necrosis is observed after Doxil treatment. Paraffin sections of the osteosarcoma after systemic treatment were stained with haematoxylin-eosin. Sham and TNF-treated tumors hardly showed any necrosis when the tumors reached a size of 17 mm. Necrosis was observed in Doxil treated tumors that was further enhanced with the addition of TNF. Scale bar apply for upper pictures, 500 µm. Scale bar apply for lower pictures, 100 µm.

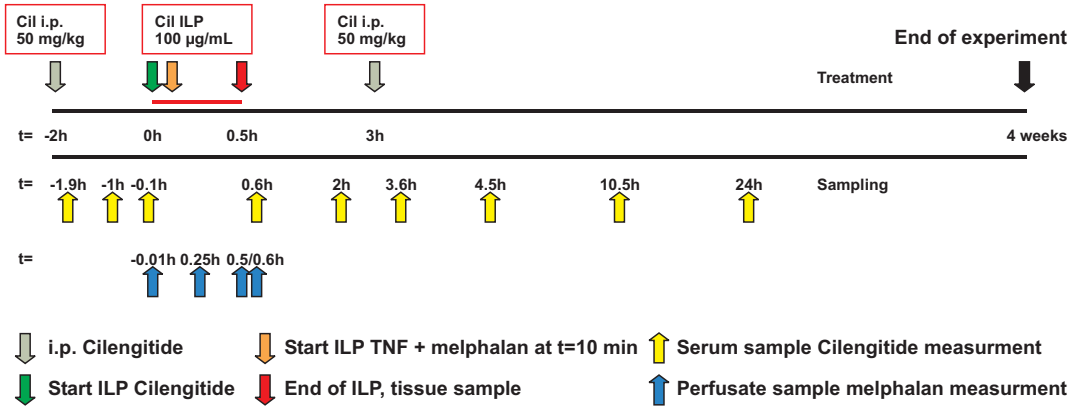

Figure 1. Time-line of Cilengitide treatment and sample collection.

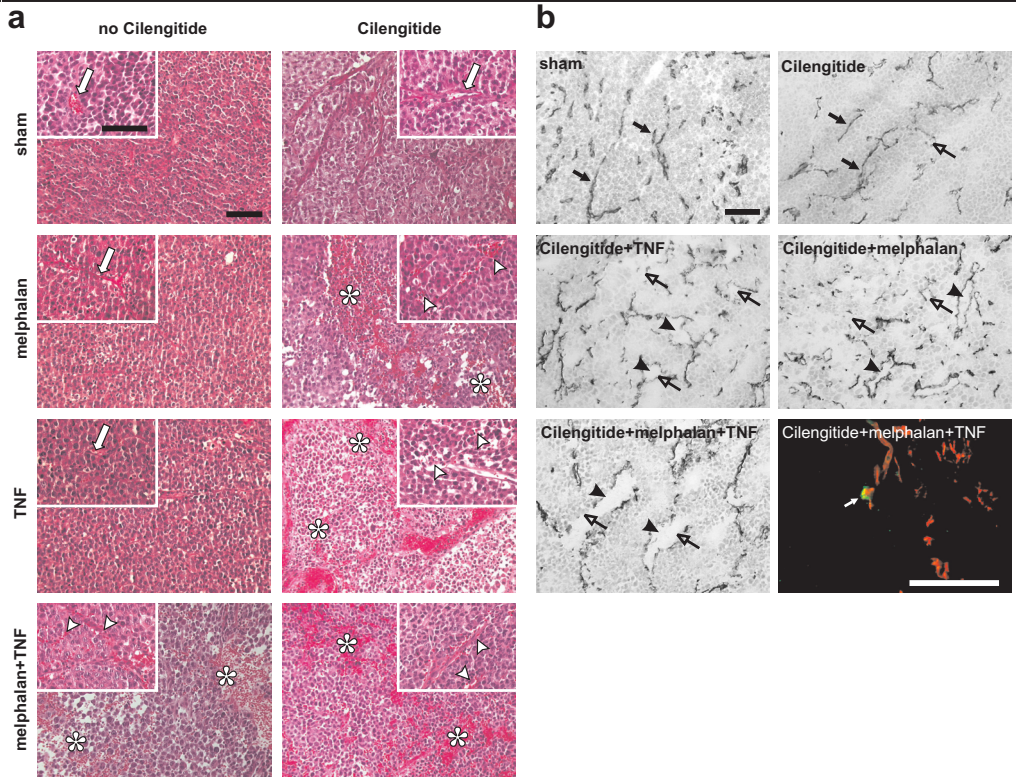

Figure 3. Histopathology of BN175 tumor after Cilengitide treatment in combination with a melphalan-based ILP. (**a**) Tumors were excised immediately after treatment for histological evaluation. Left panel, H&E staining was performed on tumors of all groups and showed no effect on tumor cells and tumor vasculature (open arrow) when animals were treated with sham, melphalan or TNF alone. Confirming previous results, ILP with melphalan plus TNF resulted in marked vascular damage (arrow head), which was accompanied by hemorrhage and edema (asterisk). Right panel, administration of Cilengitide alone had no noticeable effect on tumor histology or on tumor-associated vasculature (open arrow). However, when Cilengitide was combined with melphalan, TNF or melphalan plus TNF massive vascular destruction (open arrow) and hemorrhage (asterik) were observed. (**b**) Damage to the tumor-associated vasculature is visualized by CD31 staining. Tumors were removed at the end of the treatment, frozen and processed for immunohistochemistry as described in the experimental procedures. Perfusion with Cilengitide alone had marginal effect on tumor vessel integrity or diameter (closed arrow), while treatment with a combination of Cilengitide with melphalan, TNF or melphalan plus TNF resulted in profound loss of vascular integrity (open arrow) and widening of the vascular lumen (arrow head). Endothelial cell apoptosis is shown after treatment with Cilengitide plus melphalan and TNF by TUNEL staining. The photograph (lower right panel) demonstrates apoptotic tumor cells (green), endothelial cells (red) and apoptotic endothelial cells (yellow, arrow). Scale bar apply for all images, 100 µm.

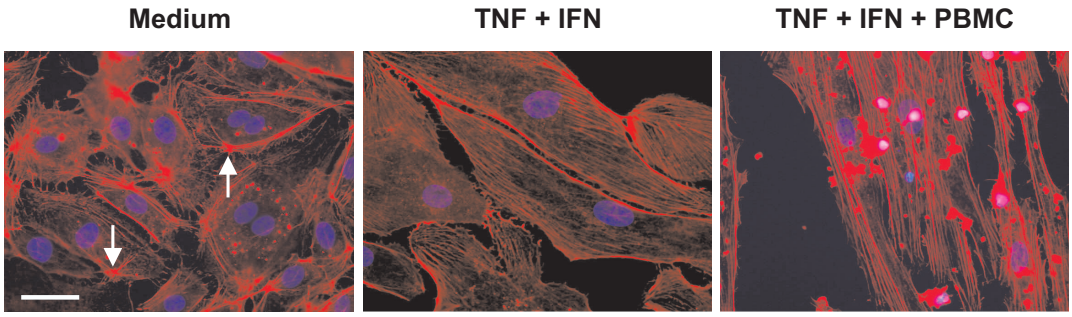

Figure 2. The cytoskeleton changes after incubation of primed PBMC. Staining for F-actin (red) and DAPI (blue) after incubation of HUVEC as described in the experimental procedures. Untreated cells revealed actin mainly localized at the periphery of the cell and clustering to form actin rich points (arrow). Cells treated with TNF (10 µg/ml) in combination with IFN (0.001 µg/ml) showed a decrease in peripheral actin and actin fibers oriented in the long axis of the cell. Cells treated with a combination of TNF, IFN and PBMC showed further elongation of actin fibers. Scale bar apply for all images, 50 µm.

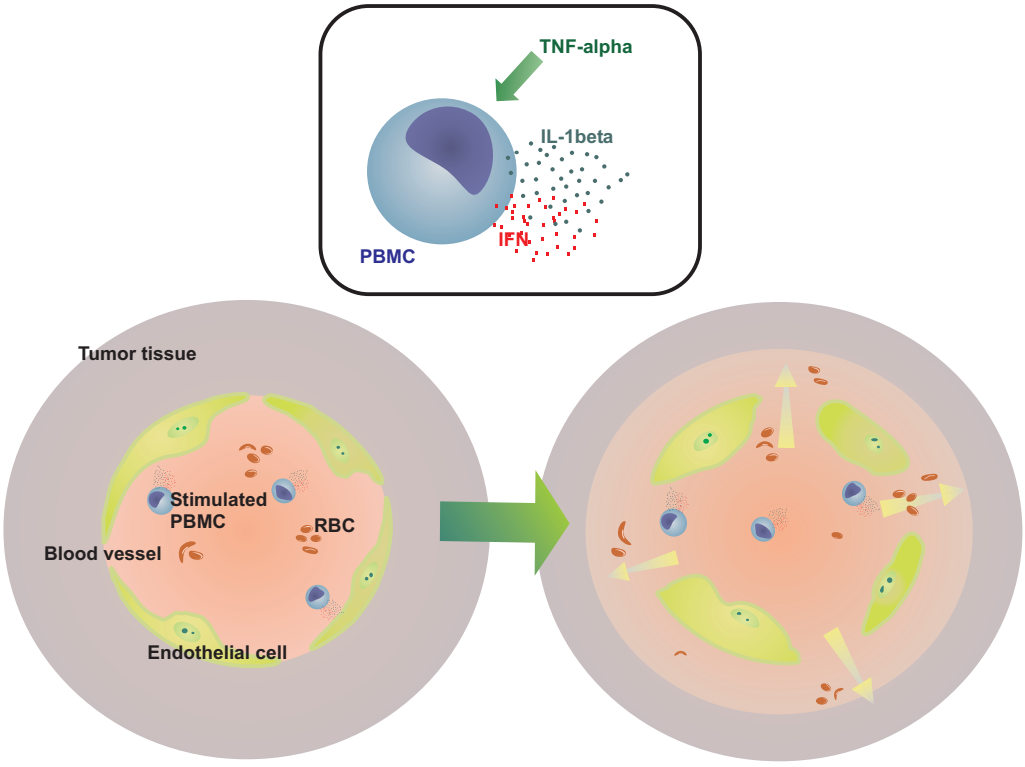

Figure 7. Proposed mechanism of TNF-mediated changes in tumor vascular permeability leading to augmented local drug accumulation in high-dose TNF combination therapy. Here we show that TNF, added in combination with cytotoxic agents, activate PBMC to produce IL-1ß and IFN. Mainly IFN and IL-1ß are responsible for the induction of morphological changes of the endothelial lining of the tumor-associated vasculature, thereby increasing vascular permeability. This enhances infiltration of blood cells and improves drug accumulation in the surrounding tumor tissue.

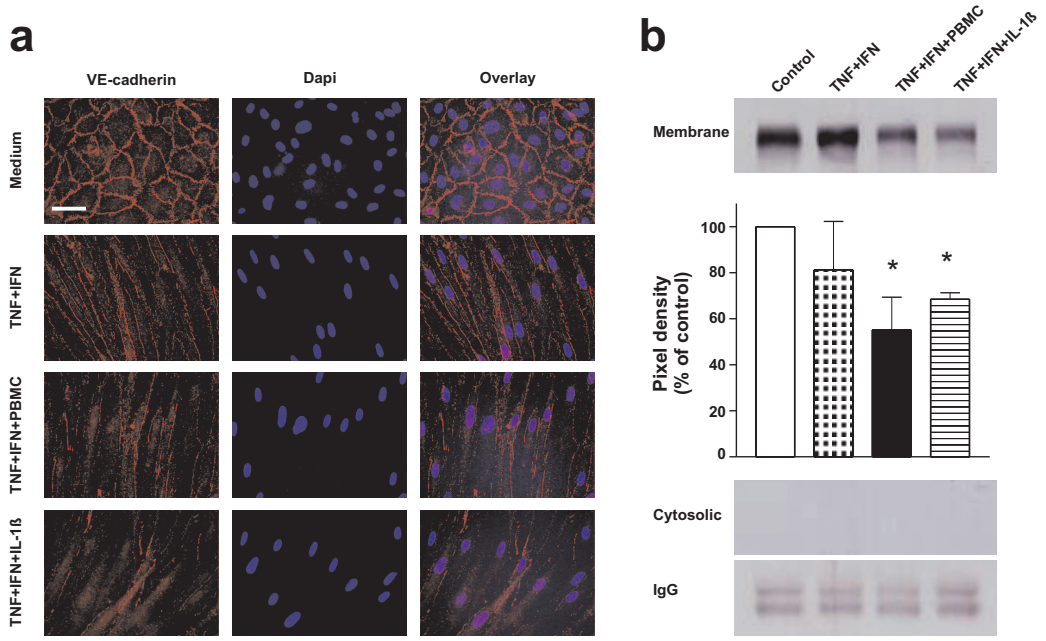

Figure 3. VE-cadherin is degraded at the cell membrane. (**a**) Staining for VE-cadherin and DAPI of HUVEC after incubation for 72 hours as described in the experimental procedures. Control treated cells show that VE-cadherin localized at cell-cell junctions between two cells. Incubating the cells with TNF and IFN resulted in a more speckled pattern of VE-cadherin. Addition of PBMC and IL-1ß further reduced VE-cadherin expression at the cell junctions. Scale bar apply for all images, 50 µm. (**b**) Western blotting show a significant decrease in the expression of VE-cadherin in the membrane fraction of HUVEC after incubation of TNF in combination with IFN and PBMC. Replacing PBMC with IL-1ß also significantly decreased the amount of VE-cadherin. Columns represent percentage pixel density compared to control ± SD of at least 4 individual experiments; *, $P < 0.05$ *versus* control treated cells.

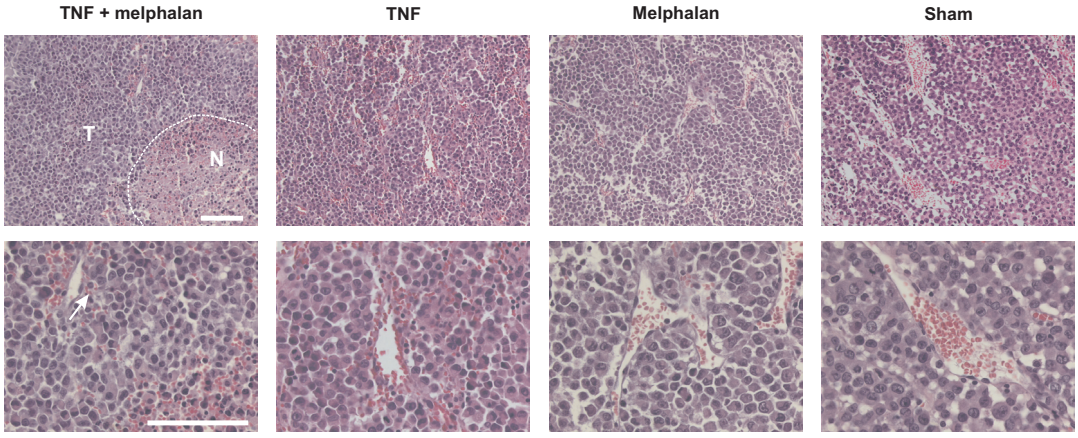

Figure 1. Effect of TNF on the histopathology of tumor tissue after ILP. HE staining directly after perfusion with melphalan in combination with TNF showed necrotic areas, destruction of the vascular lining and extravasation of erythrocytes (arrow). Perfusion with TNF alone also induced vascular damage and erythrocyte infiltration. In sham or melphalan-treated tumors the vessel lining was still intact. Dotted line denotes the boundary between normal tumor tissue (T) and necrotic tissue (N). Scale bar apply for all images, 100 µm.

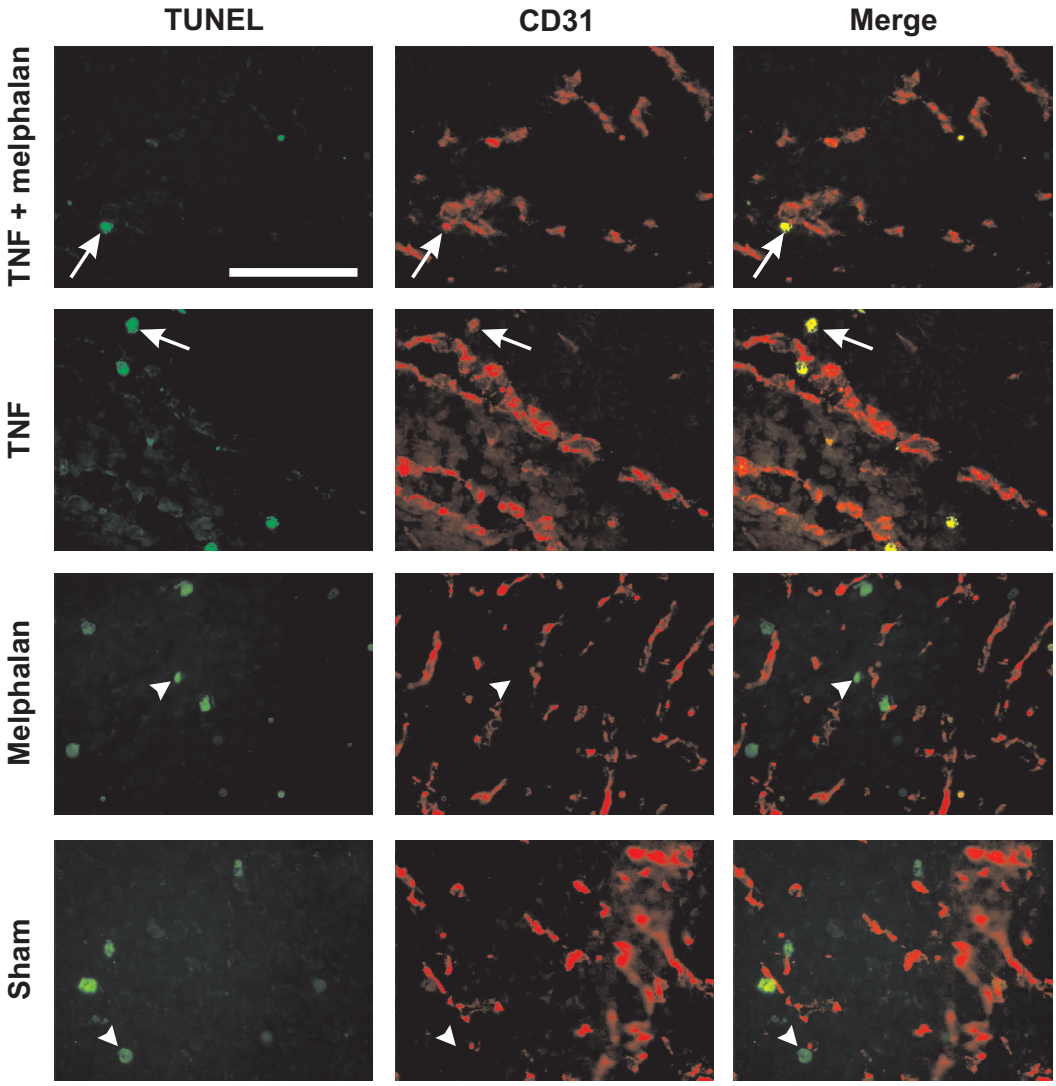

Figure 2. Effect of TNF on apoptosis of endothelial cells in tumor directly after ILP. Photographs demonstrating apoptotic tumor cells (green, arrowhead), endothelial cells (CD31, red) and apoptotic endothelial cells (yellow, arrow). Perfusion with melphalan in combination with TNF or with TNF alone induces apoptosis of endothelial cells whereas in the staining of tumor tissue after sham or melphalan perfusion no apoptotic endothelial cells were observed. Scale bar apply for all images, 100 µm.

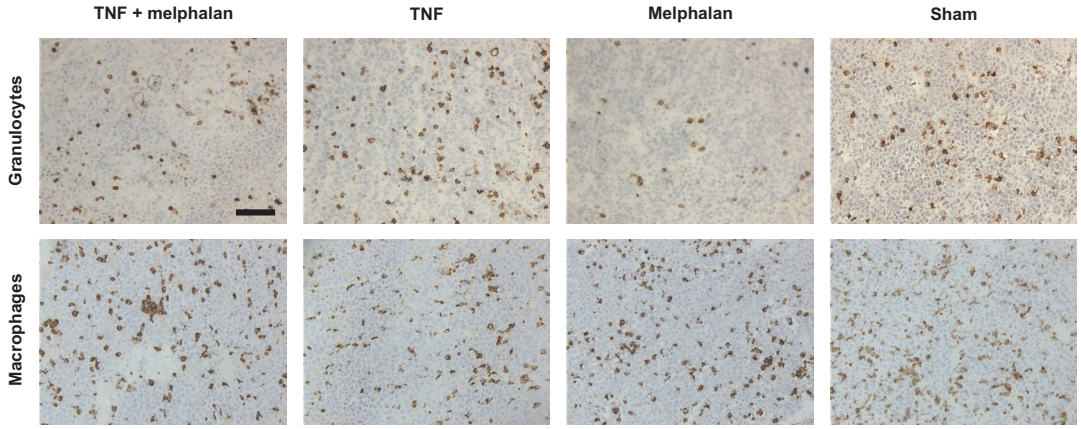

Figure 4. TNF has no effect on redistribution of granulocytes and macrophages. Directly after treatment tumors were excised and stained for granulocytes and macrophages. There was no change in the number or redistribution of the tumor infiltrating cells between the treatments. Scale bar apply for all images, 100 µm.

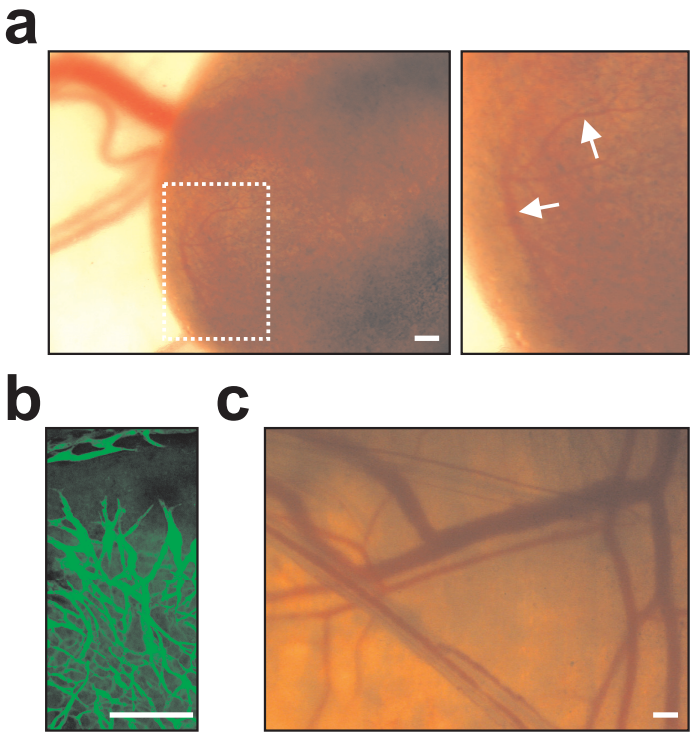

Supplementary Figure 1. Intravital microscopy reveals profound intratumoral vascularization in the B16BL6 model. Ten days after tumor implantation in the dorsal skin-fold chamber the tumor growth and vasculature were visualized. (**a**) While some newly formed blood vessels originating from the surrounding normal vasculature feed the B16BL6 tumor, abundant intratumoral branches were observed (magnification, arrow). (**b**) For a better visualization in the B16BL6 tumor, FITC-BSA was injected and a chaotic, branched tumor vasculature is observed in the tumor. (**c**) The pattern of the normal vasculature displayed minimal branching, even vessel diameter and a definable direction. Scale bar apply to all images, 250 µm.

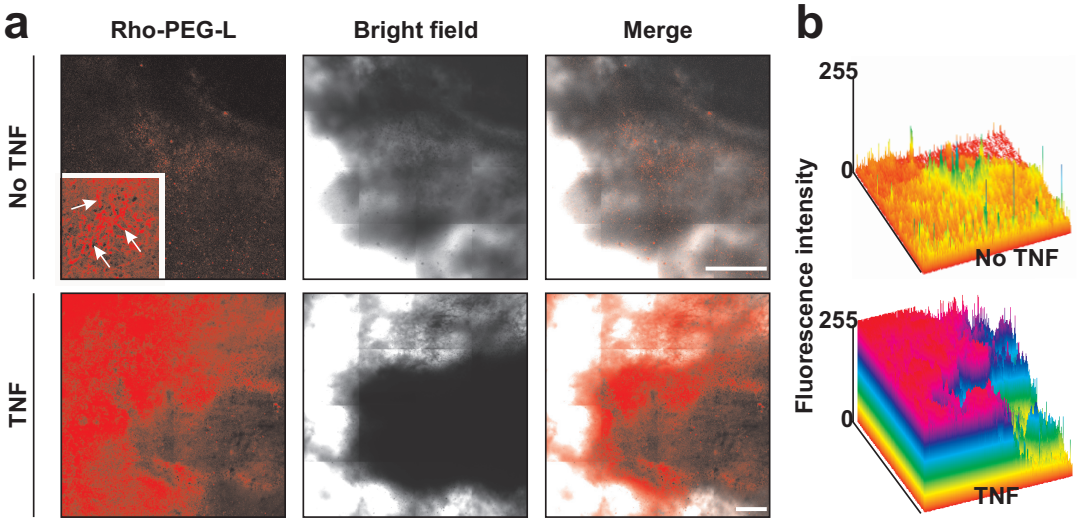

Supplementary Figure 2. Addition of TNF leads to an increased accumulation of long circulating liposomes (Rho-PEG-L) in the tumor tissue. Intravital microscopy scans of the B16BL6 melanoma were compared to illustrate the effect of mTNF on the liposomal uptake after systemic administration. (**a**) Hardly any liposomes were observed in the tumor tissue. Only in a few regions liposomes were seen intravascular (insert, arrow). Addition of mTNF clearly inflicted a homogenous intratumoral accumulation of liposomes. Scale bar apply to all images, 500 µm. (**b**) The increase in height of the fluorescence intensity peaks of the surface plots illustrates increased accumulation of liposomes when combined with mTNF.

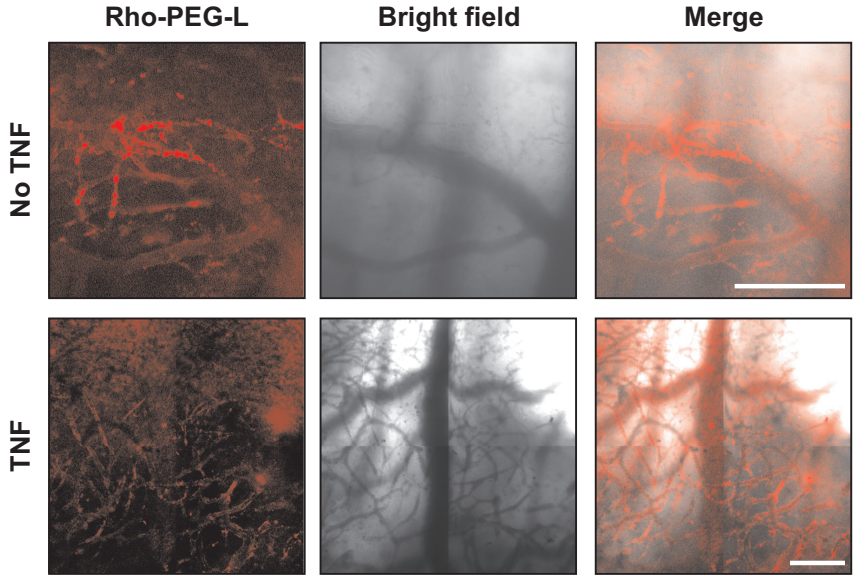

Supplementary Figure 3. Addition of TNF does not render the tumor blood vessels permeable for 400 nm liposomes. Tumor distribution of systemic injection with long circulating liposomes (Rho-PEG-L) of 400 nm in combination with saline or mTNF using intravital microscopy was studied. In mice injected with liposomes hardly any extravasation into the surrounding tumor tissue could be seen even with the addition of mTNF. The image overlay shows that obstruction of the 400 nm liposomes is found in the chaotic tumor related vessels. Scale bar apply to all images, 200 µm.

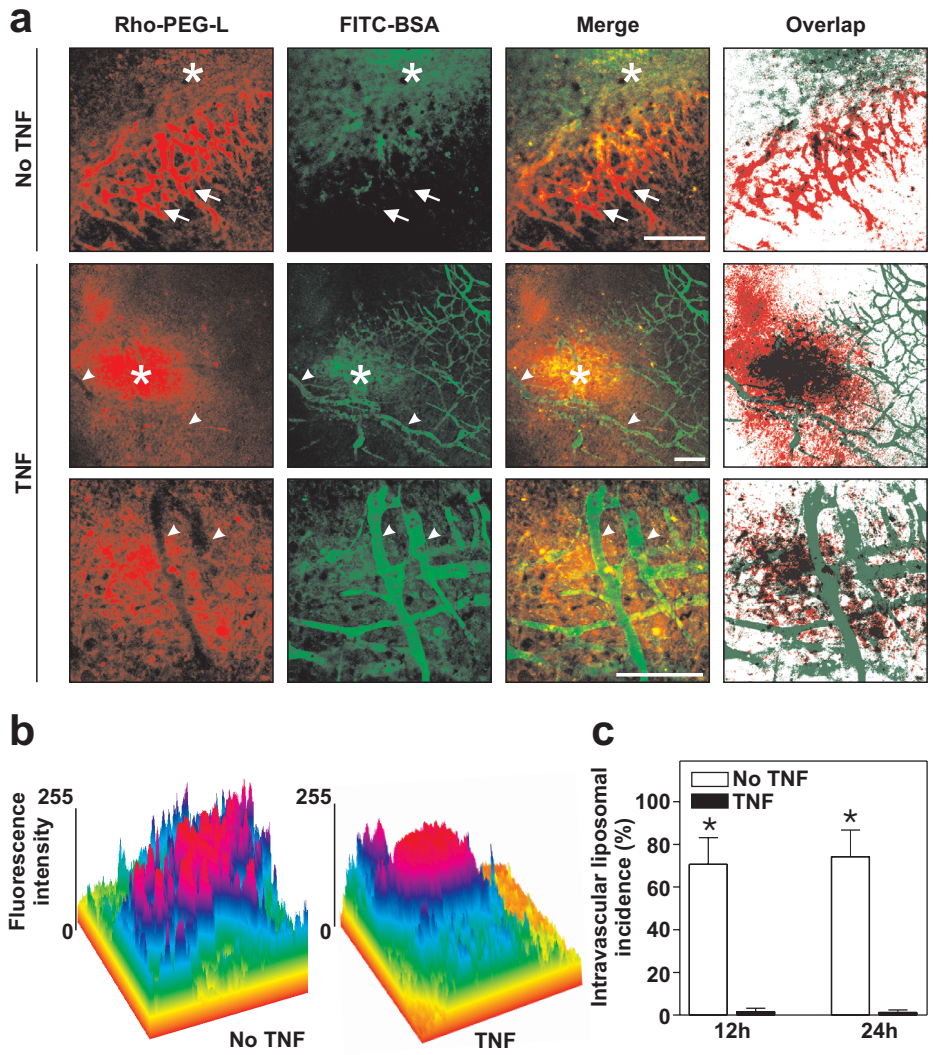

Figure 2. Addition of TNF promotes liposomal extravasation through hyperpermeable vessels. The effect of mTNF on tumor distribution of systemically injected long circulating liposomes (Rho-PEG-L) was studied by intravital microscopy. Twelve or 24 hours later mice were injected with FITC-BSA to visualize functional vessels. (**a**) In mice injected with Rho-PEG-L alone, some liposomes were seen in the surrounding tumor tissue (asterix), but predominantly in the blood vessels. In blood vessels filled with liposomes no green FITC-BSA fluorescence could be seen (arrow), indicating that these intravascular liposomes were obstructing the blood flow. When mTNF was added, liposomal extravasation was observed at sites were also FITC-BSA leaked out (asterix), indicating that mTNF rendered the vessels hyperpermeable for liposomes. FITC-BSA was seen in the tumor vessels (arrowhead) indicating intact functionality. These blood vessels seemed deprived of liposomes suggesting that all liposomes had extravasated into the surrounding tumor tissue. Scale bar apply to all images, 200 µm. (**b**) Surface plots show high intensity peaks in the tumor vessels when liposomes alone were given. Consistent with the confocal pictures, surface plot of images from mice injected with liposomes combined with mTNF show high fluorescence intensity at hyperpermeable sites in the tumor. (**c**) After calculation of the incidence that a liposome was found inside a vessel, a strong reduction in intravascular presence was found when mice were injected in combination with mTNF. Columns represent percentage liposomes found intravascular ± SEM of at least 6 scans of 5 individual animals; #, $P < 0.01$ *versus* no mTNF of the same time point.

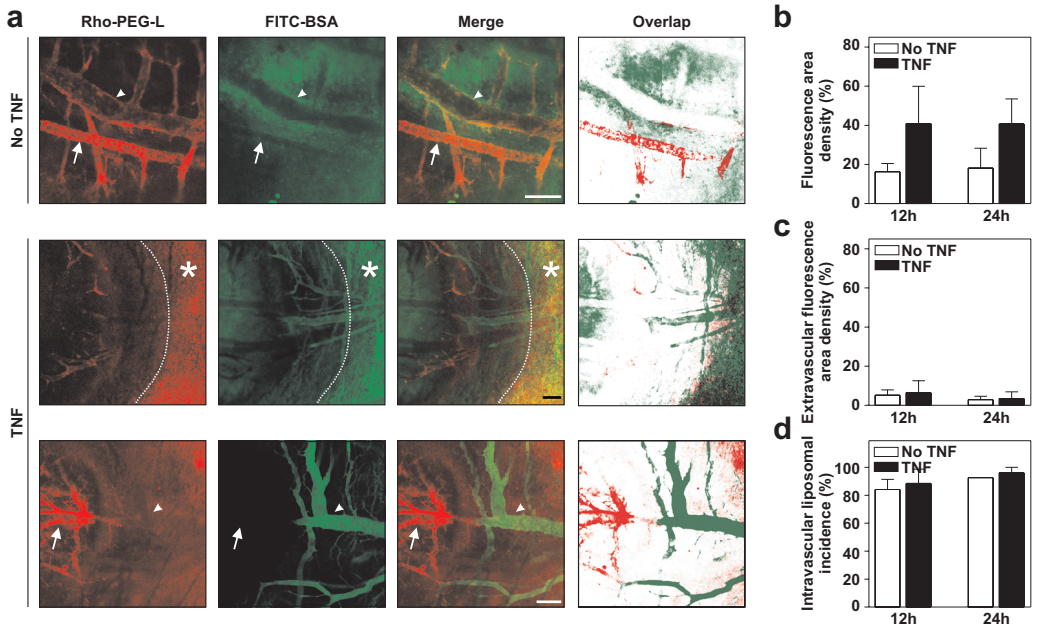

Figure 3. Addition of TNF does not render the tumor blood vessels permeable for 400 nm liposomes. Tumor distribution of systemic injection with long circulating liposomes (Rho-PEG-L) of 400 nm in combination with saline or mTNF using intravital microscopy was studied. Twelve or 24 hours later mice were injected with FITC-BSA to visualize functional vessels. (**a**) In mice injected with liposomes, even with the addition of mTNF, hardly any extravasation into the surrounding tumor tissue could be seen. Only at the rim of the tumor (dotted line) accumulation of liposomes could be observed (asterix). In some vessels liposomes were found to remain inside a FITC-BSA permeable tumor vessel (arrowhead). When vessels were filled with liposomes these vessel became non-functional (arrow). Scale bar apply to all images, 200 µm. (**b**) Although more 400 nm liposomes were found in the tumor with the addition of mTNF, levels were much lower compared to 100 nm liposomes. Columns represent percentage fluorescent area density ± SEM of at least 6 scans of 3 to 4 individual animals. (**c**) After calculation of the extravascular fluorescent intensity hardly any liposome could be measured outside the vessels, indicating that even with the addition of mTNF 400 nm liposomes remained trapped in the tumor vessels Columns represent percentage extravascular fluorescent area density ± SEM of at least 6 scans of 3 to 4 individual animals. (**d**) The incidence that a liposome was found inside the vessel no difference was found between the two treatment groups. Also when mTNF was co-administered liposomes were predominantly found inside the tumor vessels. Columns represent percentage liposomes found intravascular ± SEM of at least 6 scans of 3 individual animals.

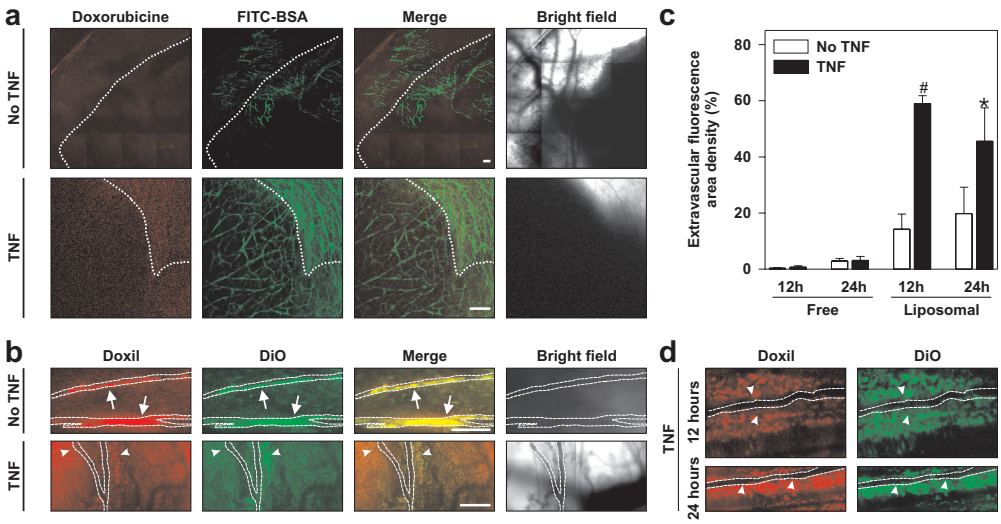

Figure 4. Addition of TNF provokes extravasation of long circulating liposomes. Tumor distribution of doxorubicin and Doxil was studied using intravital microscopy. Twelve hours after administration of doxorubicin, mice were injected with FITC-BSA to visualize functional vessels. In the case of Doxil, the liposomal component was labeled with a fluorescent marker DiO. B16BL6 melanoma-bearing mice were injected with doxorubicin or Doxil-DiO in combination with saline or mTNF. (**a**) In mice treated with doxorubicin, 12 hours later hardly any drug could be observed in the tumor tissue (dotted line = rim of the tumor) even in the presence of mTNF, although the vessels were functional. (**b**) When Doxil-DiO alone was administered, liposomes were observed in the vessels (arrows) and surrounding tissue. However, when Doxil-DiO was combined with mTNF massive extravasation of Doxil from the blood vessels (dotted line) into the tumor interstitium was observed (arrowheads). (**c**) After calculation of the extravascular fluorescent intensity a significant increase was found 12 hours and 24 hours after injection in combination with mTNF. Columns represent percentage extravascular fluorescent area density ± SEM of at least 6 scans of 5 individual animals; #, $P < 0.01$; *, $P < 0.05$ *versus* no mTNF at the same time point. (**d**) Twelve and 24 hours after administration of Doxil in combination with mTNF empty vessels (dotted line) were observed surrounded by extravasated liposomes (arrowheads). Scale bar apply to all images: 200 µm.

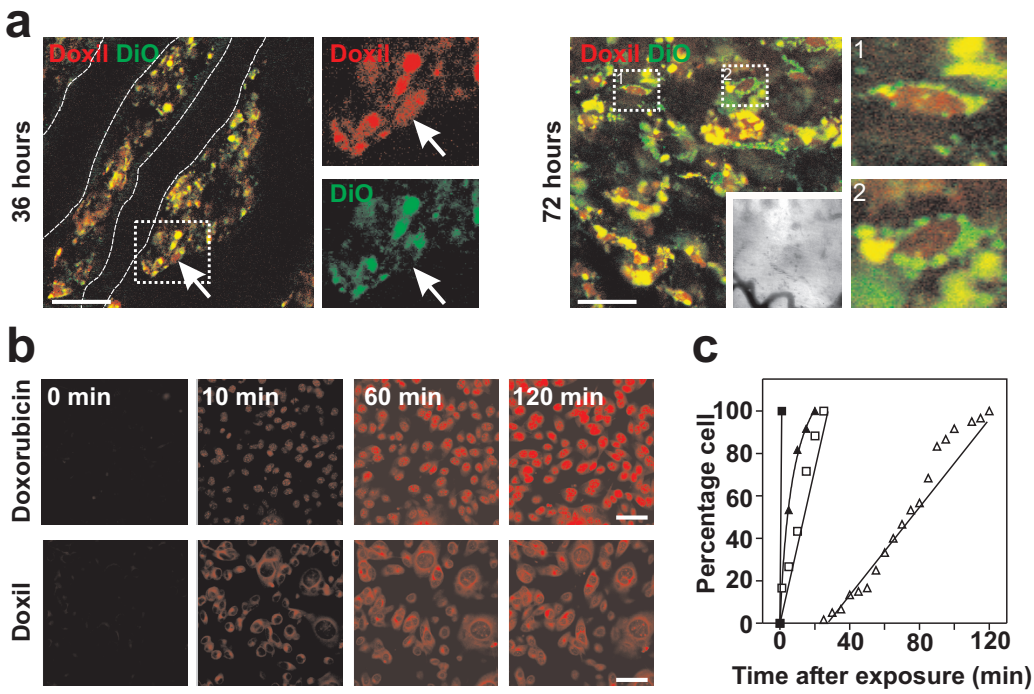

Figure 5. The complete liposome is taken up by the tumor cell and broken down in the cytoplasm. Using intravital microscopy the cellular uptake of Doxil was observed. (**a**) Thirty-six hours after systemic injection of Doxil-DiO, the liposomes (yellow) were seen in the cytoplasm of the tumor cell, whereas only doxorubicin (red) could be observed in the nucleus (arrow). At higher magnification, doxorubicin (red, arrow) was seen in the nucleus while the liposome (green, arrow) was only found in the cytoplasm. Also 72 hours after systemic injection the red fluorescent of doxorubicin in the nucleus of the tumor cell and the yellow fluorescent of the complete liposome inside the cytoplasm could still be observed. (**b**) For better understanding of the uptake of doxorubicin in the B16BL6 melanoma cell, cells were incubated with doxorubicin or Doxil and time-lapse microscopy was performed. Doxorubicin was immediately taken up by the cell and transported to the nucleus. On the other hand, Doxil took much longer to occur in the cytoplasm. Scale bar apply to all images; 200 µm. (**c**) The percentage B16BL6 cells positive for doxorubicin in the cytoplasm (■) and nucleus (▲) after incubation with free doxorubicin or in the cytoplasm (□) and nucleus (Δ) after incubation with Doxil were calculated. Very rapidly all cells had taken up the doxorubicin and stained positive for nuclear doxorubicin. In case of cells incubation with Doxil, doxorubicin was observed in the cytoplasm much later compared to the administration of free drug. Transport from the cytoplasm to the nucleus also took much longer. Data points represent the percentage cells that are positive for doxorubicin.

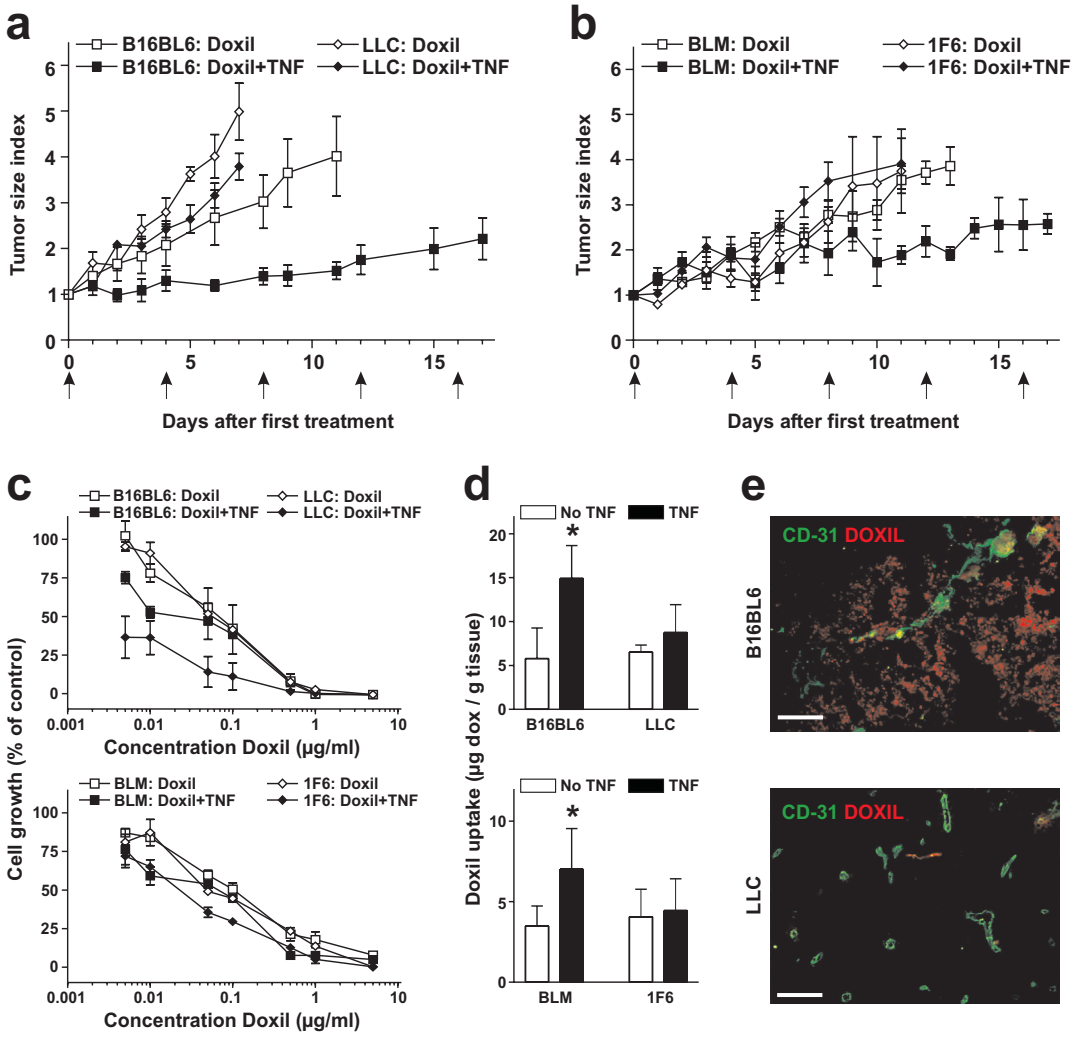

Figure 1. Addition of TNF improves tumor response and augments intratumoral drug uptake in B16BL6 and BLM. (**a**,**b**) Graphs show the tumor size index of subcutaneous implanted B16BL6 and LLC (**a**) and BLM and 1F6 (**b**) during systemic treatment with Doxil and low-dose mTNF. Mice were injected 5 times i.v. with an interval of 4 days (arrows). Addition of mTNF resulted in synergistic tumor response of the B16BL6 and BLM, but no effect of mTNF was observed in the LLC and 1F6. Data points represents tumor size index ± SD of 6 individual animals. (**c**) *In vitro* growth of tumor cells (B16BL6, LLC: upper graph; BLM, 1F6: lower graph) 72 hours following incubation with different concentration Doxil and 10 µg/ml TNF (mTNF for B16BL6, LLC and HuTNF for BLM and 1F6). Addition of TNF had no synergistic effect with Doxil on the tumor cells. Data points represent percentage cell growth of incubated cells compared to control treated cells at 0 hour ± SEM of 3 individual experiments in duplicate. (**d**) Doxil uptake in the tumors (B16BL6, LLC: upper graph; BLM, 1F6: lower graph) with or without addition of mTNF. Tumors were excised 24 hours following a single injection and the amount of doxorubicin was measured. Addition of mTNF to Doxil treatment enhanced drug accumulation in the B16BL6 and BLM tumors in contrast to LLC and 1F6. Columns represent µg doxorubicin per g tumor tissue ± SD of 3 to 5 individual animals; *, $P < 0.05$ TNF *versus* no TNF. (**e**) Representative immunofluorescent photographs of CD31 expression and Doxil accumulation in B16BL6 and LLC 12 hours following treatment with Doxil and TNF. In accordance with the Doxil uptake, accumulation of Doxil into the tumor intersititium was observed in the B16BL6 and hardly any Doxil was seen in the LLC. Scale bar apply to all images, 100 µm.

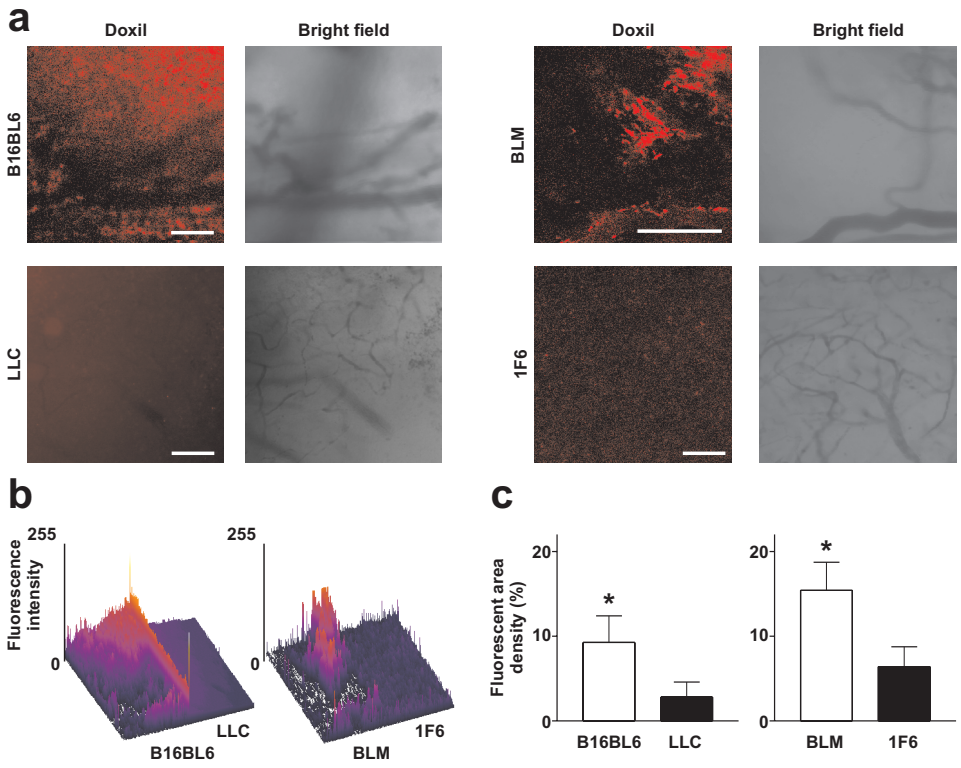

Figure 2. Addition of TNF strongly improves liposomal distribution in the tumor interstitium of the B16BL6 and BLM. (**a**) Representative intravital microscopy scans of the tumors were compared to illustrate the effect of mTNF on liposomal uptake following systemic administration. Addition of mTNF clearly inflicted an intratumoral accumulation of Doxil in the B16BL6 and BLM 24 hours after treatment. Scale bar apply to all images, 200 µm. (**b**) Increase in height of the fluorescence intensity peaks of the surface plots illustrates increased accumulation of liposomes when combined with mTNF in the B16BL6 and BLM. (**c**) After calculation of the extravascular fluorescent intensity a significant increase was found in the B16BL6 (left graph) and in BLM (right graph) 24 hours following injection of Doxil in combination with mTNF. Columns represent fluorescent area density ± SEM of at least 4 scans of 3 individual animals; *, $P < 0.05$ B16BL6 or BLM *versus* LLC or 1F6.

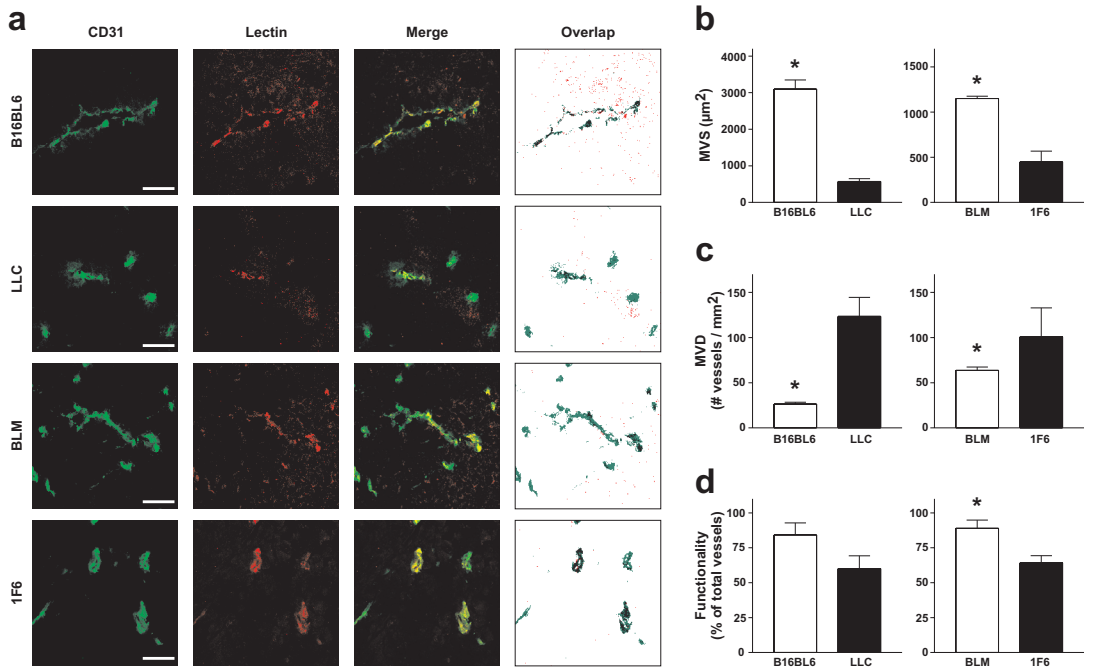

Figure 3. Structural differences in vasculature between TNF-sensitive and TNF-insensitive tumors. (**a**) Tumor-bearing mice were injected i.v. with lectin, 10 min later tumors were excised and histological sections were stained for endothelial cells (CD31, green) and functional blood vessels with an antibody against lectin (red). Scale bar apply to all images, 50 µm. (**b**) After measuring the microvessel size (MVS) significant larger blood vessels were found in the B16BL6 and BLM. (**c**) The microvessel density (MVD) was determined by counting the number of vessels per mm^2 and was found significant higher in the LLC and 1F6 (**d**) The percentage functional vessels was calculated and in spite of a significant difference in size and density, most of the tumor vessels were functional. Columns represent mean ± SEM of at least 6 scans from 3 sections of 3 individual tumors; *, $P < 0.05$ B16BL6 or BLM *versus* LLC or 1F6.

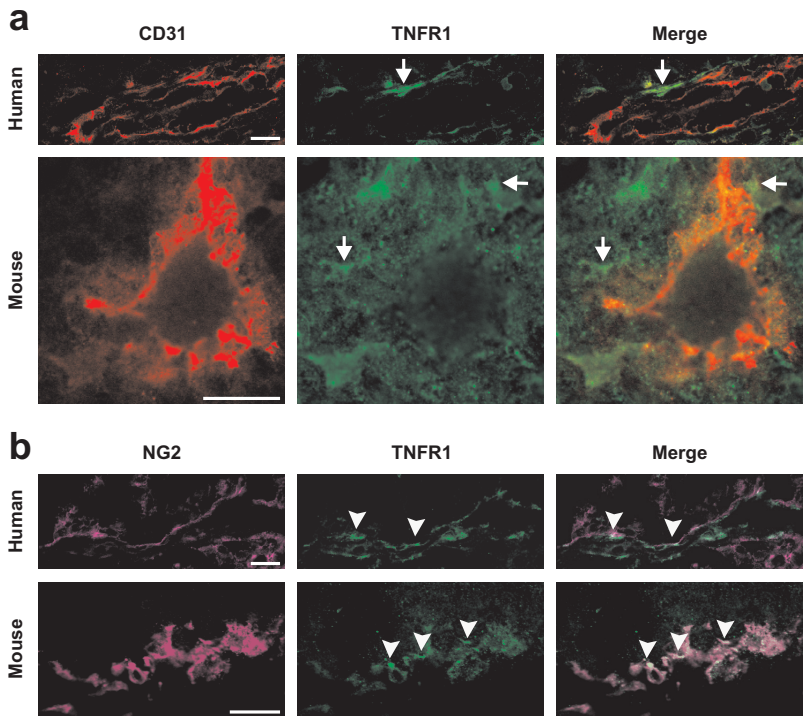

Figure 4. TNFR1 is expressed by pericytes of the tumor-associated vasculature. (**a**) Immunofluorescent staining for endothelial cells (CD31, red) and TNFR1 (green) in human (upper panels) and mouse (lower panels) tumor sections showed no co-localization (arrow). (**b**) Staining for pericytes (NG2, purple) and TNFR1 (green) showed TNFR1 expression by pericytes (arrowhead) of the tumor-associated vasculature of human (upper panels) and mouse (lower panels) tumor biopsies. Scale bar apply to all images, 20 μm.

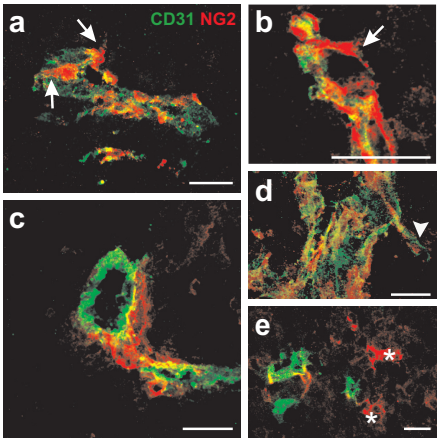

Figure 5. Morphology of the tumor-associated endothelial cells (CD31, green) and pericytes (NG2, red). (**a, b**) NG2 staining of pericytes show close association with endothelial cells, however multiple protrusions (arrows) into the tumor stroma were observed. (**c**) Some pericytes projected away from a vessel and connected neighboring vessels. (**d**) Endothelial cells migrating into the tumor parenchyma were found to be associated with pericytes at several occasions (arrowhead). (**e**) NG2 positive cells that were not associated with endothelial cells (asterix), designated as myofibroblasts, were found in the LLC. Scale bar applied to all images, 20 μm.

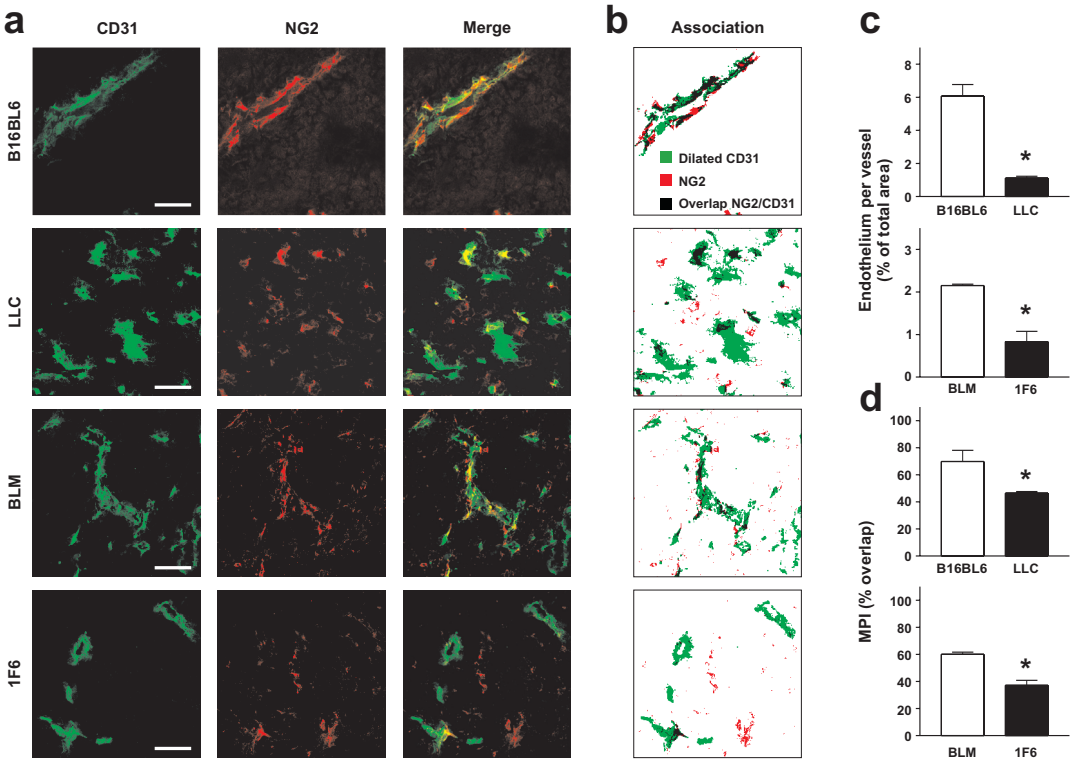

Figure 6. Difference in pericyte coverage is found between TNF-sensitive tumors and TNF-insensitive tumors. (**a**) Tumor sections were stained for endothelial cells (CD31, green) and pericytes (NG2, red). In the merge picture an intense association between endothelial cells and pericytes was seen in the B16BL6 and BLM. Scale bar apply to all images, 50 µm. (**b**) Analysis of the endothelial-pericyte association. Images of the endothelial cells (green) and pericytes (red) were binarized and the diameter of endothelial cells was dilated. The overlap of both cells is shown in black. (**c**) The percentage endothelial cells per vessel were calculated for B16BL6, LLC (left graph), BLM and 1F6 (right graph). In accordance with the MVS, B16BL6 and BLM contained significantly more endothelial cells per vessel then respectively the LLC and 1F6. Columns represent percentage area endothelium per vessel per field of interest ± SEM of at least 6 scans from 3 sections of 3 individual tumors; *, $P < 0.05$ B16BL6 or BLM *versus* LLC or 1F6. (**d**) Using the overlap images, microvessel pericyte coverage index (MPI) was measured in the B16BL6, LLC (left graph) and BLM, 1F6 (right graph). The MPI in tumor vessels of B16BL6 and BLM was significant higher compared to the MPI in LLC and 1F6. Columns represent percentage MPI of at least 6 scans from 3 sections of 3 individual tumors; *, $P < 0.05$ B16BL6 or BLM *versus* LLC or 1F6.

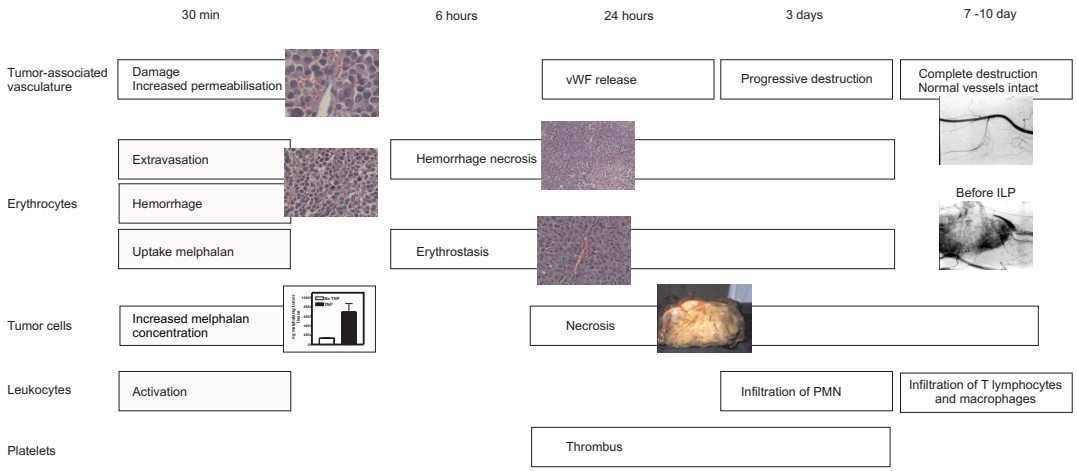

Figure 2. Schematic overview. Involvement of the different tumor compartments after TNF- based melphalan perfusion.

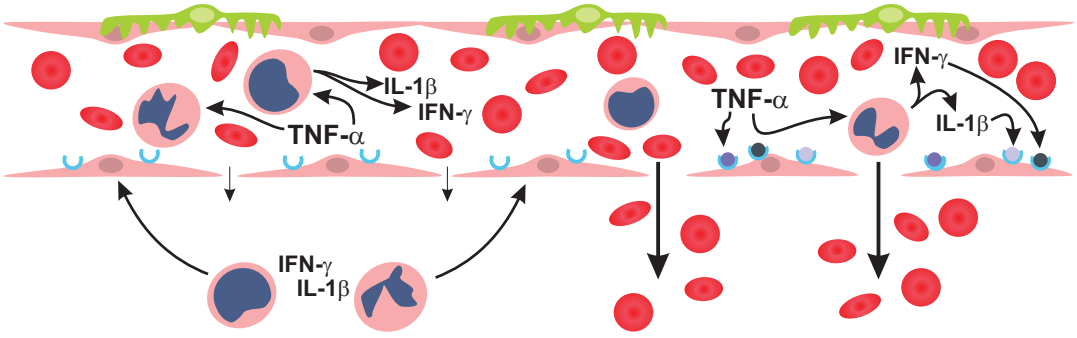

Figure 3. Action of TNF on the vascuar bed. The action of TNF on the tumor vascular bed involves at least two key leukocyte members: PMN and cells present in the PBMC pool. In particular cells producing IL-1ß and IFN are involved. TNF triggers the release of these cytokines and affects the endothelial cells directly. When interacting together TNF, IL-1ß and IFN resort endothelial gap formation, which is absent or less apparent when one of these cytokines is missing. We speculate that activated immune cells already present in the tumor contribute to the cytokine production as well.

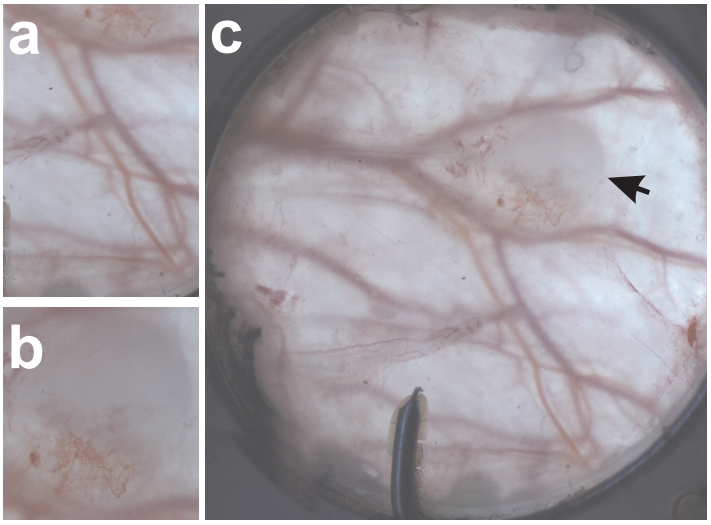

Figure 1. The difference in tumor-associated vasculature and normal vasculature. (**a**) Blood vessels deliver nutrients, oxygen and other molecules in the tissues it passes and removes toxins. This system is arranged in arteries, veins and capillaries with their own specific characteristics and phenotype. (**b**) In contrast to the structural organized blood vessels of the basic organs, the tumor-associated vasculature is "abnormal". It display a lack of hierarchical branching and organization in which the recognizable features of arterioles, capillaries and venules is lost. The vessels are tortuous and unevenly dilated. As a result, tumor blood flow is chaotic, might be stationary and can even change direction. This leads to hypoxia and acidosis in solid tumors. Due to these properties of the tumor-associated vasculature the intratumoral drug accumulation is very heterogeneous. (**c**) The complete overview of the dorsal skin-fold window with a lewis lung carcinoma (arrow) 6 days after tumor implantation.

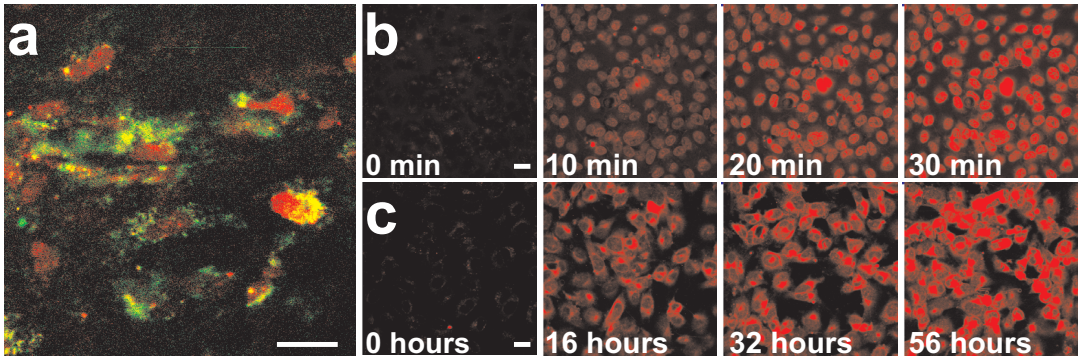

Figure 2. Intratumoral and intracellular fate of Doxil. Using the dorsal skin-fold chamber we observed that, with the addition of TNF, Doxil labeled with a green fluorescent marker extravasates from the tumor blood vessels into the tumor intersitium between 12 to 24 hours. (**a**) Seventy-two hours after systemic injection, the liposomes (green fluorescent) remained in the cytoplasm of the cell, while doxorubicin (red fluorescent) was found in the nucleus. No indications of Doxil or liposomes outside the cells in the interstitial space were found. This suggest that the liposome is taken up completely by the cells and is thereafter broken down. (**b**) Tumor cells were incubated with doxorubicin in a migration ring and the fate of the free drug was followed for several hours. Almost immediately after adding the drug, doxorubicin was taken up by the cells and transported to the nucleus. (**c**) In contrary to the free drug, when cells were incubated with Doxil hardly any drug was observed in the nucleus and most remained in the cytoplasm. Scale bar apply for all images, 20 µm.

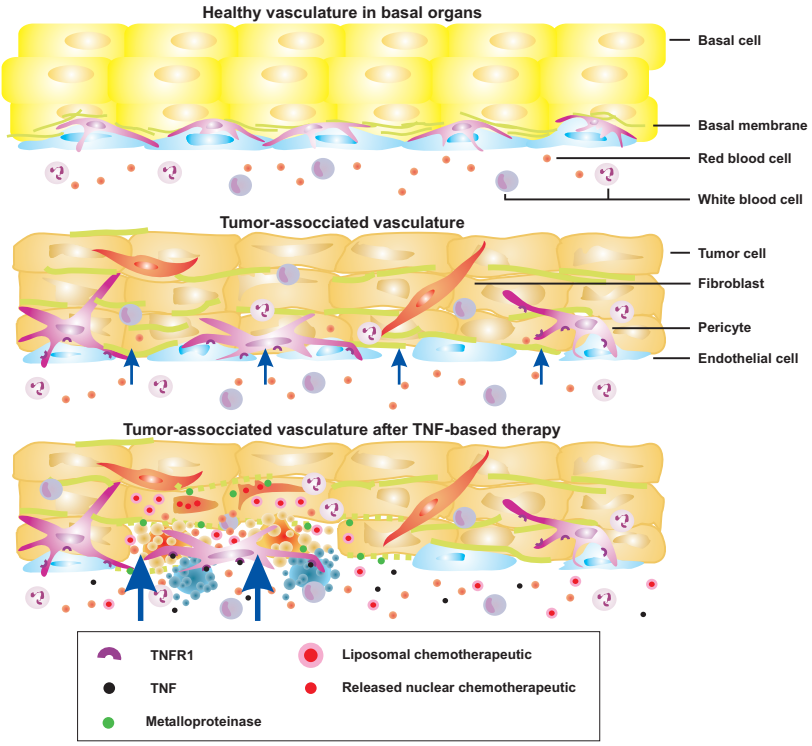

Figure 3. Abnormalization of the tumor-associated vasculature. In the vasculature of basic organs the endothelial cells forms a quiescent and tightly packed lining separating the blood and blood-born elements from the rest of the body. Mural cells (smooth muscle cells and pericytes) form the muscle of the blood vessel and have specific properties according to the type of blood vessel they can be found at. The tumor-associated vasculature has endothelial cells that are morphological different from these in the normal vessels. Because of the fast growing properties of most tumors they are highly active and have irregular shapes with openings between the cells making the vessel highly permeable. Also the pericytes are different, forming a loose association with the endothelial cells and displaying extensions into the intersitium. The basal membrane is irregular in size with a different protein composition and structure. After TNF-based therapy, TNF binds to the TNFR1 located on the pericytes. These cells produce to further elucidate endogenous factors that has its effect on endothelial cells. The permeability of the endothelial lining is further increased for the co-administered drug, melphalan (in free form this will have micromolecular properties however absorbed in erythrocytes melphalan will act as a macromolecule) or long-circulating liposomes Doxil. MMPs produced by the endothelial cells will degrade the underlying matrix providing a better entrance for the chemotherapeutic compound. The liposomal drug enters as a whole the tumor cell were it is slowly degraded releasing the active drug intracellulary that eventually kills the tumor cell.